agriculture

Special Issue Reprint

Plant–Soil–Microorganism Interaction in Grassland Agroecosystem

Edited by
Xingxu Zhang, Tingyu Duan and Xiangling Fang

mdpi.com/journal/agriculture

MDPI

Plant–Soil–Microorganism Interaction in Grassland Agroecosystem

Plant–Soil–Microorganism Interaction in Grassland Agroecosystem

Editors

Xingxu Zhang
Tingyu Duan
Xiangling Fang

MDPI

Basel • Beijing • Wuhan • Barcelona • Belgrade • Novi Sad • Cluj • Manchester

Editors

Xingxu Zhang
State Key Laboratory of Herbage Improvement and Grassland Agro-Ecosystems, Key Laboratory of Grassland Livestock Industry Innovation, Ministry of Agriculture and Rural Affairs, College of Pastoral Agriculture Science and Technology Lanzhou University Lanzhou China

Tingyu Duan
State Key Laboratory of Herbage Improvement and Grassland Agro-Ecosystems, Key Laboratory of Grassland Livestock Industry Innovation, Ministry of Agriculture and Rural Affairs, College of Pastoral Agriculture Science and Technology Lanzhou University Lanzhou China

Xiangling Fang
State Key Laboratory of Herbage Improvement and Grassland Agro-Ecosystems, Key Laboratory of Grassland Livestock Industry Innovation, Ministry of Agriculture and Rural Affairs, College of Pastoral Agriculture Science and Technology Lanzhou University Lanzhou China

Editorial Office
MDPI
St. Alban-Anlage 66
4052 Basel, Switzerland

This is a reprint of articles from the Special Issue published online in the open access journal *Agriculture* (ISSN 2077-0472) (available at: https://www.mdpi.com/journal/agriculture/special_issues/Plant_Soil_Microorganism).

For citation purposes, cite each article independently as indicated on the article page online and as indicated below:

Lastname, A.A.; Lastname, B.B. Article Title. *Journal Name* **Year**, *Volume Number*, Page Range.

ISBN 978-3-7258-1231-8 (Hbk)
ISBN 978-3-7258-1232-5 (PDF)
doi.org/10.3390/books978-3-7258-1232-5

Contents

About the Editors

Xingxu Zhang

Prof. Dr. Xingxu Zhang now works at the State Key Laboratory of Herbage Improvement and Grassland Agro-ecosystems, Key Laboratory of Grassland Livestock Industry Innovation, Ministry of Agriculture and Rural Affairs, College of Pastoral Agriculture Science and Technology, Lanzhou University, Lanzhou 730000, China. Prof. Dr. Xingxu Zhang's major interests include grass and endophyte; soil microbiology; and plant protection.

Tingyu Duan

Prof. Dr. Tingyu Duan now works at the State Key Laboratory of Herbage Improvement and Grassland Agro-ecosystems, Key Laboratory of Grassland Livestock Industry Innovation, Ministry of Agriculture and Rural Affairs, College of Pastoral Agriculture Science and Technology, Lanzhou University, Lanzhou 730000, China. Prof. Dr.Tingyu Duan's major interests include forage crop pathology; arbuscular mycorrhizal fungal; and disease control.

Xiangling Fang

Prof. Dr. Xiangling Fang now works at the State Key Laboratory of Herbage Improvement and Grassland Agro-ecosystems, Key Laboratory of Grassland Livestock Industry Innovation, Ministry of Agriculture and Rural Affairs, College of Pastoral Agriculture Science and Technology, Lanzhou University, Lanzhou 730000, China. Prof. Dr. Xiangling Fang's major interests include Forage Pathology; Soil-borne diseases in alfalfa; and Grassland Microbiology.

agriculture

MDPI

Article

ROS Regulate *NCF2*, Key Metabolic Enzymes and MDA Levels to Affect the Growth of *Fusarium solani*

Jie Li [1,2,*], Lidan Feng [3], Dong Li [1], Xianglin Liu [1], Yangyang Pan [4], Jing He [1,2] and Junxia Zhang [1]

[1] College of Forestry, Gansu Agricultural University, Lanzhou 730070, China
[2] Wolfberry Harmless Cultivation Engineering Research Center of Gansu Province, Lanzhou 730070, China
[3] College of Food Science and Engineering, Gansu Agricultural University, Lanzhou 730070, China
[4] College of Veterinary Medicine, Gansu Agricultural University, Lanzhou 730070, China
* Correspondence: lj81658@gsau.edu.cn

Abstract: *Fusarium solani* is the most significant pathogen that causes root rot in wolfberry, which has led to serious economic losses in terms of production. As an important enzyme in organisms, NADPH oxidase produces ROS. However, the mechanism of ROS mediated by NADPH oxidase in the growth of *F. solani* has not been studied. In this study, *F. solani* colonies were treated with 40 μmol/L DPI and 0.0012% H_2O_2. The growth rate in terms of colonies, number of spores, key gene expression levels, activity of key enzymes and the content of key products of ROS metabolic pathways were determined. The results showed that the growth rate of colonies treated by DPI decreased by 19.43%, the number of macroconidia increased by 231.03%, the IOD/area values of O_2^- and H_2O_2 decreased by 34.88% and 16.97%, respectively, the expression levels in terms of *NCF2*, *SOD1*, *CTA1* and *PXMP4* significantly decreased and the activities of SOD, CAT and POD decreased significantly, while the MDA content increased significantly. Additionally, in the case of the colonies treated with exogenous H_2O_2, the MDA content decreased significantly while the other indicators increased. Taken together, the *NCF2* gene is involved in regulating the activity of NADPH oxidase and regulates the products of O_2^- and ROS metabolism enzyme genes and their activities to affect colony growth in the *F. solani* growth process.

Keywords: NADPH oxidase; ROS; *Fusarium solani*; growth rate; DPI

Citation: Li, J.; Feng, L.; Li, D.; Liu, X.; Pan, Y.; He, J.; Zhang, J. ROS Regulate *NCF2*, Key Metabolic Enzymes and MDA Levels to Affect the Growth of *Fusarium solani*. *Agriculture* **2022**, *12*, 1840. https://doi.org/10.3390/agriculture12111840

Academic Editor: Alessandro Vitale

Received: 7 September 2022
Accepted: 31 October 2022
Published: 2 November 2022

1. Introduction

Root rot disease is the most serious disease in Wolfberry (*Lycium barbarum* L.) production, especially in those with a long planting period. According to statistics, the highest incidence rate reached 72.4% and occurred in all the main producing bases [1]. The main pathogens of wolfberry root rot contain *Fusarium solani*, *F. oxysporum*, *F. dimerum*, *F. moniliforme* and *Rhizoctonia solani* [2]. *F. solani* has a stronger pathogenicity compared to other root rot pathogens in the Gansu production area [3]. Recent studies have shown that ROS play an important physiological role in cell signal transduction and transcription. At the same time, ROS can react to a variety of ligands, including growth factors, cytokines and protein G-linked receptors [4]. At present, multiple studies have confirmed that the ROS produced by pathogens are positively correlated with their growth and pathogenicity [5,6].

NADPH oxidase can specifically produce superoxide anion, which is the most important kind of ROS, and its abnormal regulation affects the redox signal cascade that controls cell proliferation and death [7]. NADPH oxidase is located on the cell membrane [8] and is the key enzyme in terms of redox signals in eukaryotic cells [9]. ROS generation from NADPH oxidase requires the assembly of multi-subunit complexes [10,11]. Filamentous fungi include three different NADPH oxidase subfamilies, namely NoxA, NoxB and NoxC. Among them, *NoxA* and *NoxB* are homologous to the mammalian catalytic subunit $gp91^{phox}$, and *NoxC* contains the putative calcium-binding left-handed motif, which is homologous to human *Nox5* and plant *Nox*; it also contains the homologous regulatory subunit $p67^{phox}$

(*NoxR*, *NCF2*) and the small *GTPase Rac* gene [12]. The *NoxA* complex controls sporophore formation [13], the sclerotia [14,15] and germ tubes [16], toxicity [14,17] and cellulose degradation [18]. The *NoxB* complex is responsible for host tissue infiltration [19], ROS production [20] and ascospore germination [21].

However, the role of ROS mediated by NADPH oxidase in *F. solani* isolate growth remains unclear. The key subunit of the NADPH complex that restricts the growth of *F. solani* and its downstream genes needs to be explored. Additionally, the growth, spore number, gene expression and physiological recovery of *F. solani* by exogenous ROS need to be verified. In this study, *F. solani* was used as the test isolate, was cultured in PDA and was treated with the NADPH oxidase inhibitor DPI and a typical ROS such as H_2O_2. The changes in ROS production intensity and location, key differentially expressed genes and key antioxidant enzyme indices among treatments were measured to reveal the role of ROS mediated by NADPH oxidase in the growth of *F. solani* and provide a theoretical basis for the control of wolfberry root rot.

2. Materials and Methods

2.1. Fungi

The *F. solani* isolate was isolated from wolfberry root with root rot disease in Wuhe Township, Jingyuan County, Gansu Province, China (36.98° N, 105.21° E, 1700 m). The isolate was stored at −70 °C in a refrigerator at the Wolfberry Harmless Cultivation Engineering Research Center, College of Forestry, Gansu Agricultural University according to the method of Leslie and Summerell [22]. PDA medium was used to activate and culture the isolate at 25 °C for 8 days before use. After the second culture, the 5 mm plugs were taken out and used as inoculation material in the study.

2.2. Treatment and Sample Collection

Four treatments were set up in this study, and *F. solani* isolate was inoculated in PDA medium for S1 treatment. For S2 treatment, the isolate was inoculated in PDA medium containing 40 μmol/L DPI. For S3 treatment, the isolate was cultured in PDA medium containing 40 μmol/L DPI for 3 days, and 5 mL of 0.0012% H_2O_2 solution was added on the 4th day. For S4 treatment, the isolate was cultured in PDA medium for 3 days, and 5 mL 0.0012% H_2O_2 solution was added on the 4th day. There were three repetitions each treatment and fifteen dishes each repetition.

The colonies were observed at 10:00 a.m. every day. The transverse and longitudinal diameters of the colonies were measured by the cross method. The number of spores were determined on the 8th day by a hemocytometer [23]. When the S1, S2 and S3 had been cultured for 8 days, histochemical stained ROS were detected by using the NBT and DAB methods. At the same time, the samples were scraped, mixed, weighed, sub-packed and stored in liquid nitrogen to determine the O_2^- and H_2O_2 contents, the activities of major enzymes such as SOD, POD and CAT, the MDA content and the expression level of genes. Fifteen samples were collected for each treatment, 0.2 g each sample. In addition, when S4 had been cultured for 8 days, six mixed samples were collected for O_2^- and H_2O_2 determination.

2.3. Transcriptome Extraction, Sequencing, Comparison and Analysis

The total RNA was extracted from the S1, S2 and S3 treatments by employing the Trizol® kit method, and the genomic DNA was removed. After testing the concentration and quality of RNA and mRNA with poly-A tail, the RNA and mRNA were enriched by Oligo(dT) magnetic beads. The fragmented mRNA was used as templates, the random oligonucleotides were used as primers and the first strand of cDNA was synthesized in a reverse transcriptase system (Invitrogen, Waltham, MA, USA). The RNA strand was degraded with RNase H and the second strand of cDNA was synthesized from dNTPs in a DNA polymerase I system. The purified double stranded cDNA was used to repair the end, add the A tail and connect the sequencing connector. The length of cDNA, roughly

250–300 bp, was screened with AMPure XP beads and amplified by PCR and the PCR product was purified with ampure XP beads again, before the the library fragments were finally obtained. The library fragments were sequenced by Wuhan Frasergen Gene Information Co., Ltd. (Wuhan, China) on an Illumina PE150 sequencing platform to obtain raw reads. The splice sequences, low-quality (base number ≤ 5) reads and their paired ends and undetected reads (N content $\geq 10\%$) and their paired ends were filtered out to obtain clean reads. The contents of Q20, Q30 and GC and the sequence repeat levels were calculated to assess the quality of the sequencing data. The clean reads were compared with the reference genome and information on the differences between the reads and the original after the sequencing was assembled to determine the source genes of these reads by HISAT2 software. Finally, RSEM software was used to obtain the number of reads of each transcript in each sample and convert them in FPKM (fragments per kilobase per million bases) to obtain the expression levels of genes. The DEGs (differentially expressed genes) were calculated and screened by DESeq2 software, and when $|\log2\text{Fold Change}| > 2$ and p-adjust < 0.05, the genes were identified as the final differentially expressed genes. Referring to the FPKM value and the pathway map enriched by KEGG (Kyoto Encyclopedia of Genes and Genomes) and GO (Gene Ontology), the genes related to the ROS metabolism pathway were thoroughly analyzed to obtain the differentially expressed genes upstream and downstream [24].

2.4. Real-Time Quantitative PCR Expression Analysis

The RNA preparation and cDNA synthesis were performed in the same way as transcriptome sequencing. Primers were designed according to the DEG sequences, and the gene information and primers are shown in Table 1. The reaction system was 1 μL cDNA (500 ng/μL), 0.5 μL each of upstream and downstream primers (0.2 μmol/mL), 10 μL 2× SYBR Green Pro Taq HS Premix and 8 μL DDH_2O, for a total reaction volume of 20 μL. The specific reaction conditions were: predenaturation at 95 °C for 10 s, after denaturation at 95 °C for 10 s, annealing for 10 s and extension at 72 °C for 10 s; a total of 40 cycles were performed. A Light Cycler 96 SW 1.1 (Roch, Switzerland) was used for real-time quantitative PCR. The reference gene was β-actin, and the number of repeats was $n = 3$. The reaction specificity was determined according to the melting curve, and the CQ (cycle threshold) value of each sample was obtained. The relative expression level of the target gene was calculated by the $2^{-\Delta\Delta Ct}$ method [25,26].

Table 1. List of oligonucleotide primers used for RT-qPCR studies.

GeneID	Genename	Forward Primer Sequence	Reverse Primer Sequence
NECHADRAFT_57795	*CTA1*	AGCCAGACTACCATGTCAAAG	GGAGCCTTCTTGATCTCTTCAG
NECHADRAFT_74783	*PXMP4*	CGATTCGCCGTCATCTACAA	CCAAAGACAAAGTAGCCTCCA
NECHADRAFT_81761	*NCF2*	GGCTACACTGTCTTCTCCATTC	GTAGTCCTTGGTCTTGAGGTTTC
NECHADRAFT_59203	*SOD1*	CCCTCTTCAAGACTTGCTTCT	GAGGATTGGGTATCTGGTTTGT

2.5. Determination of MDA Content

MDA determination referred to the method of Hodges et al. [27].

2.6. The Superoxide Anion(O_2^-) and Hydrogen Peroxide (H_2O_2) Content Assay

The O_2^- content was determined according to Wang and Luo [28]. The H_2O_2 content was estimated by forming a titanium–hydroperoxide complex according to Prochazkova et al. [29] with modifications.

2.7. Enzyme Extraction

All enzyme extracts were conducted by homogenizing 0.3 g of frozen colonies in a mortar on ice, using the following extraction media: 10 mL of 50 mmol/L phosphate buffer (pH 7.8) for SOD and POD and 10 mL of 50 mM phosphate buffer (pH 7.5) containing

5 mmol/L dithiothreitol (DTT) and 2% PVPP (*w*/*v*) for CAT. The extracts were then centrifuged at 12,000× *g* for 20 min at 4 °C. The supernatants were used for enzyme assays.

2.8. Enzymatic Activity Assays

SOD activity was assayed by the method of Rao et al. [30] with modifications. CAT activity was assayed according to Wang et al. [31] with modifications. POD activity was assayed colorimetrically with guaiacol as the hydrogen donor according to the method of Venisse et al. [32] with modifications.

2.9. Histochemical Detection of ROS

O_2^- was visually detected by using the NBT (Nitro-blue tetrazolium chloride, Amresco, Dallas, TX, USA) staining method [33]. The pictures were taken with a Nikon D750 digital camera. The images were counted and analyzed by using Image Pro Plus 6.0, and the relative content of O_2^- was quantified by the ratio of integrated optical density (IOD) to the total colony area. H_2O_2 was visually detected by DAB (3,3′-diaminobenzidine; Sigma, St. Louis, MO, USA) staining as described previously [34]. The pictures were taken and treated by using the same method as in the case of O_2^-.

2.10. Statistical Analysis

All statistical analyses were performed by the GraphPad Prism9.0 analysis module. All the data were presented as the mean ± SD, and the significance of treatments were analyzed by the one-way ANOVA and Tukey's multiple comparisons test. A *p*-value less than 0.05 was considered statistically significant. The graphs were generated by GraphPad Prism9.0.

3. Results

3.1. Colony Growth and Spore Number

Figure 1a shows the colony growth of S1, S2 and S3 within 8 days. On the 8th day, the colony diameter of S1 was the largest, 15.22% and 8.47% larger than S2 and S3, respectively; S2 was 7.97% smaller than S3, and the differences between the three colonies were significant.

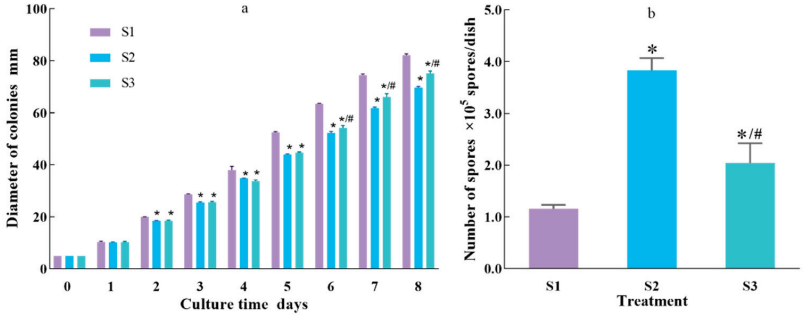

Figure 1. Colony growth and spore number after different treatments. (**a**) is the diameter of colonies and (**b**) is the number of spores (macroconidia). S1 group (n = 5): inoculation of *F. solani* on normal PDA; S2 group (n = 5): inoculation of *F. solani* on PDA containing 40 μmol/L DPI; S3 group (n = 5): inoculation of *F. solani* on PDA containing 40 μmol/L DPI. On the fourth day of cultivation, 5 mL of 0.0012% H_2O_2 was added to each dish. Data are expressed as the mean ± SD. * $p < 0.05$ S2 or S3 vs. S1, # $p < 0.05$ S3 vs. S2.

Within 8 days, the growth rates of S1, S2 and S3 were 9.65 mm d^{-1}, 8.08 mm d^{-1} and 8.78 mm d^{-1}, respectively. The growth rate of S2 was 19.43% lower than that of S1. From day 0 to 4, the growth rate of S1 was 8.24 mm d^{-1}, which was significantly higher

than that of S2 and S3 at 7.45 mm d^{-1} and 7.22 mm d^{-1}, respectively, with these being practically the same. From day 5 to 8, after adding H_2O_2, the growth rate of S3 reached 10.34 mm d^{-1}, which was significantly higher than that of S2 (8.72 mm d^{-1}) and close to S1 (11.06 mm d^{-1}). From the 5th day, the growth rate of S3 accelerated. On the 6th day, the diameter of S3 was significantly larger than that of S2, and the significant difference continued until the end of observation.

At the 8th day of culture, the number of spores of *F. solani* isolate were detected. The S1, S2 and S3 treatments produced macroconidia but the number of microconidia was low and chlamydospore was not observed. As shown Figure 1b, the macroconidia number of S1, S2 and S3 were $1.16 \pm 0.08 \times 10^5$, $3.83 \pm 0.24 \times 10^5$ and $2.05 \pm 0.38 \times 10^5$ spores per dish, respectively. Compared to S1, the macroconidia numbers of S2 and S3 were significantly higher, 231.03% and 76.92% higher, respectively. Compared with S3, the macroconidia number of S2 was 87.10% higher, with a significant upward trend.

3.2. Colony Histochemical Detection of ROS

As shown in Figure 2, the three treatments produced O_2^-, and the edge colonies were particularly rich. The counting results of the Image-Pro software showed that the IOD/area values of S1, S2 and S3 were 0.086 a.u., 0.056 a.u. and 0.078 a.u., respectively, and the O_2^- production decreased by 34.88% after NADPH was inhibited, with it recovering after the addition of 0.0012% H_2O_2, as shown in S3.

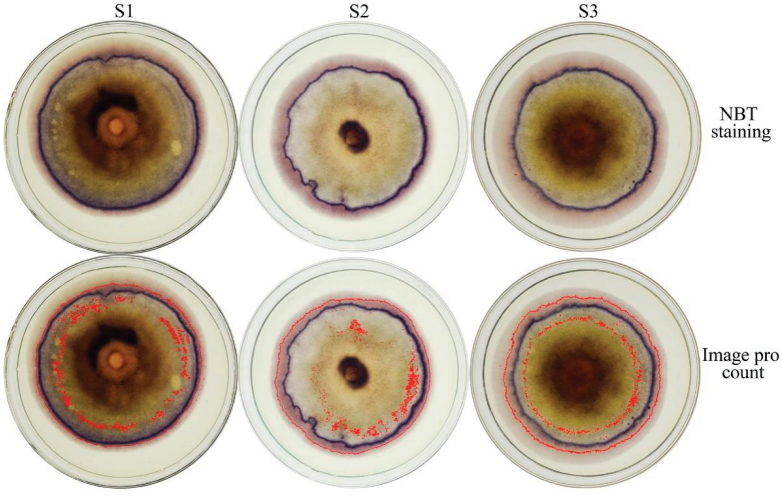

Figure 2. NBT staining photos of colony superoxide anion. The upper row is the shoot in the back light, and the lower row is the Image-pro software count picture. S1 group (n = 3): inoculation of *F. solani* on normal PDA; S2 group (n = 3): inoculation of *F. solani* on PDA containing 40 μmol/L DPI; S3 group (n = 3): inoculation of *F. solani* on PDA containing 40 μmol/L DPI. On the fourth day of cultivation, 5 mL of 0.0012% H_2O_2 was added to every dish.

As shown in Figure 3, the three colony treatments produced H_2O_2, which was distributed at 1/3 from the outer edge of the colonies. The counting results showed that the IOD/area value was 0.165 a.u., 0.193 a.u. and 0.285 a.u. for S1, S2 and S3, respectively.

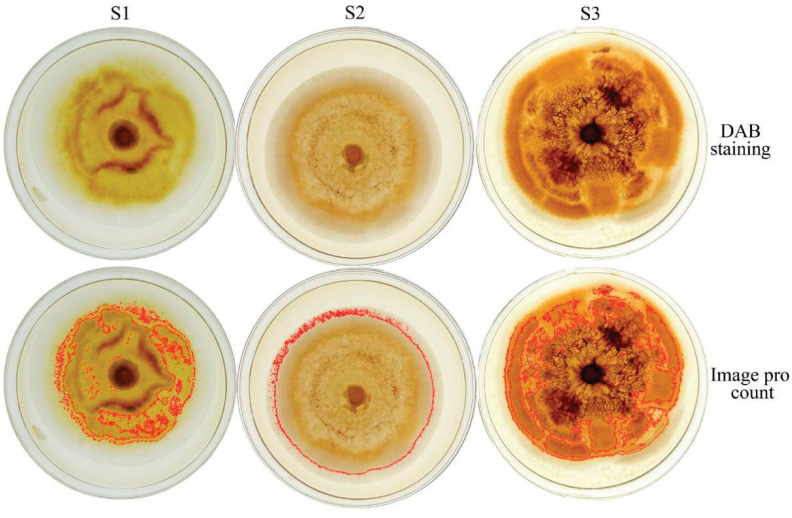

Figure 3. DAB staining photos of colony hydrogen peroxide. The upper row shoot in back light, the lower row is the Image-Pro software count picture. S1 group (n = 3): inoculation of *F. solani* on normal PDA; S2 group (n = 3): inoculation of *F. solani* on PDA containing 40 μmol/L DPI; S3 group (n = 3): inoculation of *F. solani* on PDA containing 40 μmol/L DPI. On the fourth day of cultivation, 5 mL of 0.0012% H_2O_2 was added to each dish.

3.3. mRNA Expression of NCF2, SOD1, CTA1 and PXMP4

As shown in Figure 4, the expression of key genes in the ROS metabolic pathway such as *NCF2*, *SOD1*, *CTA1* and *PXMP4* was greatly affected after treatment, and the results were verified by RT-qPCR.

The FPKM value of the *NCF2* gene in S2 was 49.95 ± 4.87, which was 25.34% lower than that of S1. The FPKM value of S3 increased significantly, with it being 153.23% higher than that of S1 and 239.16% higher than that of S2 (Figure 4a). The RT-qPCR results showed that variation trend was similar to that shown in Figure 4a. The relative expression value of S3 was 8.90 ± 0.55, which was 7.86 times higher than that of S1 and 15.33 times higher than that of S2. (Figure 4b).

The FPKM value of the *SOD1* gene in S2 was as low as 195.44 ± 28.10, 21.42% lower than that of S1, but the difference was not significant (p = 0.766); the S3 FPKM value increased to 343.98 ± 116.59, with this increasing by 38.31% and 76.00% compared with the S1 and S2 values, respectively (Figure 4c). The relative value of S2 significantly decreased to 0.49 ± 0.05 (p = 0.043), 53.22% lower than that of S1. The S3 relative expression value increased to 3.65 ± 0.47, 2.48 and 6.45 times higher that than S1 and S2, respectively (Figure 4d).

The FPKM values of the *CTA1* gene in S1, S2 and S3 were 28.67 ± 0.52, 11.43 ± 0.33, and 15.66 ± 3.95, respectively. The FPKM value in S2 was significantly low (p = 0.010) compared with S1. The same value in S3 was 26.99% higher than that of S2 (Figure 4e). Furthermore, the trend of the relative expression value was similar to that of the FPKM value. The relative expression values of S1 and S2 were 0.20 ± 0.11 and 1.28 ± 0.20, respectively. The S2 was significantly lower than S1. The S3 relative expression value was 0.57 ± 0.14, with this being a significant increase, 65.42% (p = 0.004), compared with S2 (Figure 4f).

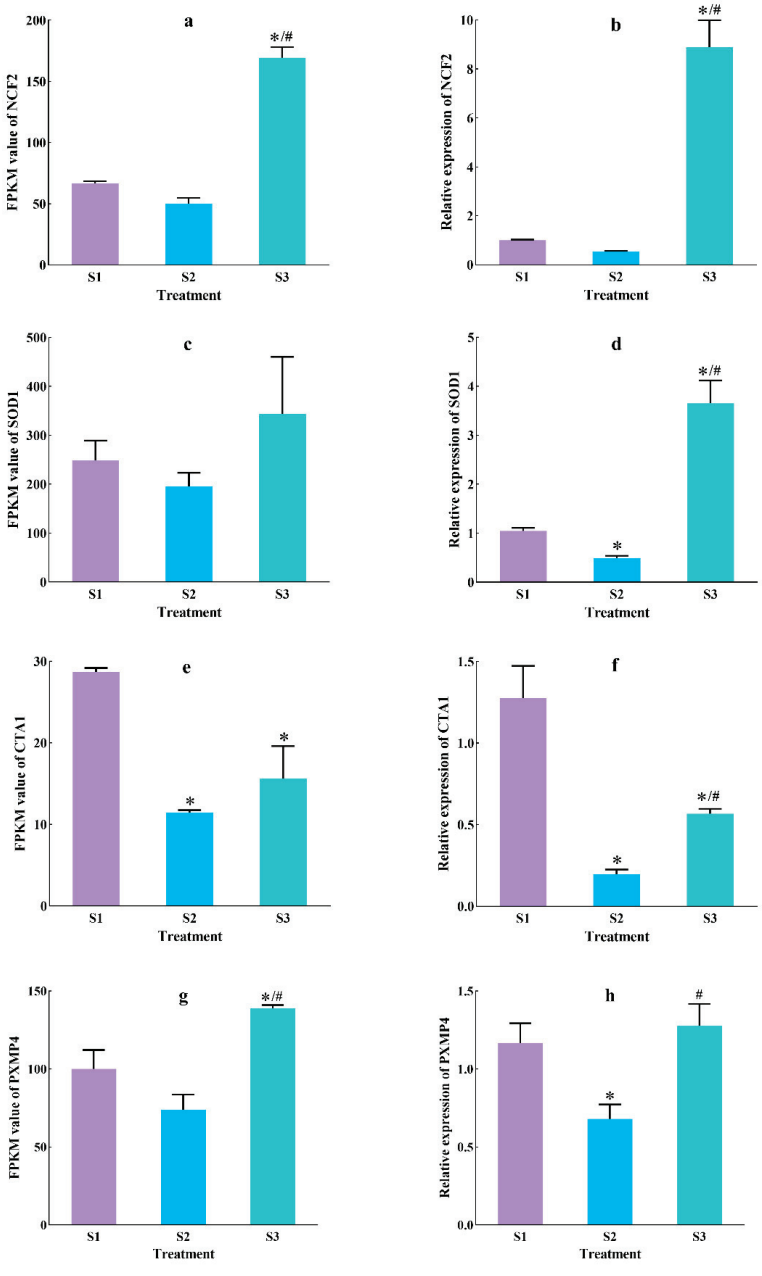

Figure 4. mRNA expression of *NCF2*, *SOD1*, *CTA1* and *PXMP4* in the *F. solani* colony. (**a**,**c**,**e**,**g**) are fragments per kilobase of exon model per million mapped fragments (FPKM) values from transcriptome sequencing data; (**b**,**d**,**f**,**h**) are relative expression values from RT-qPCR data. S1 group ($n = 3$): inoculation of *F. solani* on PDA; S2 group ($n = 3$): inoculation of *F. solani* on PDA containing 40 μmol/L DPI; S3 group ($n = 3$): inoculation of *F. solani* on PDA containing 40 μmol/L DPI. On the fourth day of cultivation, 5 mL of 0.0012% H_2O_2 was added to each dish. Data are expressed as mean ± SD. * $p < 0.05$ S2 or S3 vs. S1, # $p < 0.05$ S3 vs. S2.

The FPKM value of the PXMP4 gene in S3 was the highest among the three treatments, reaching 139.07 ± 1.97, with this being 38.90% ($p = 0.007$) higher and 88.13% ($p = 0.001$) higher than S1 (100.13 ± 12.12) and S2 (73.93 ± 9.72), respectively (Figure 4g). The change in the trend between the relative expression value and the FPKM value of the PXMP4 gene were practically the same. S3 was the highest among the three treatments, reaching 1.28 ± 0.14, which was significantly higher, 86.87%, than S2 (Figure 4h).

3.4. Colony ROS Level

As shown in Figure 5, the concentrations of O_2^- and H_2O_2 in four treatments were measured.

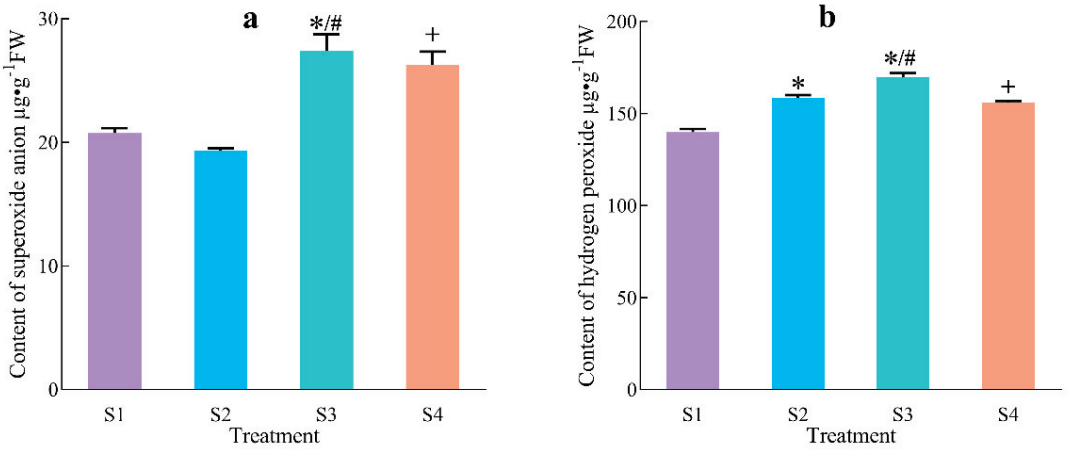

Figure 5. The main ROS content in the *F. solani* colony. (**a**) Superoxide anion (O_2^-); (**b**) hydrogen peroxide (H_2O_2). S1 group ($n = 3$): inoculation of *F. solani* on PDA; S2 group ($n = 3$): inoculation of *F. solani* on PDA containing 40 μmol/L DPI; S3 group ($n = 3$): inoculation of *F. solani* on PDA containing 40 μmol/L DPI; S4 group ($n = 3$): inoculation of F. solani on PDA and on the fourth day of cultivation, 5 mL of 0.0012% H2O2 was added to each dish. Data are expressed as mean ± SD. * $p < 0.05$ S2 or S3 vs. S1, # $p < 0.05$ S3 vs. S2, + $p < 0.05$ S4 vs. S1.

Figure 5a shows the change in O_2^- content in the colonies. The contents of S1, S2, S3 and S4 were 20.75 ± 0.41 μg g^{-1}FW, 19.35 ± 0.18 μg g^{-1}FW, 27.39 ± 1.34 μg g^{-1}FW and 26.28 ± 1.07 μg g^{-1}FW, respectively. The O_2^- content increased significantly after the addition of 0.0012% H_2O_2. Compared with S2, the O_2^- contents of S3 and S4 increased 5.53 μg g^{-1}FW and 8.04 μg g^{-1}FW, respectively.

As shown in Figure 5b, the H_2O_2 contents of S1, S2, S3 and S4 were 139.96 ± 1.71 μg g^{-1}FW,158.39 ± 1.64 μg g^{-1}FW, 169.84 ± 2.09 μg g^{-1}FW and 156.01 ± 0.87 μg g^{-1}FW, respectively. Compared with S1, the H_2O_2 content of S4 increased 16.05 μg g^{-1}FW. Compared with S2, the H_2O_2 content of S3 increased 11.45 μg g^{-1}FW, and the increment was less than that without inhibitor.

3.5. Colony Oxidant–Antioxidant Level

As shown in Figure 6, the activities of antioxidant enzymes such as SOD, CAT and POD and the MDA content, which indicates the level of cell membrane oxidation in the *F. solani* colony, were detected.

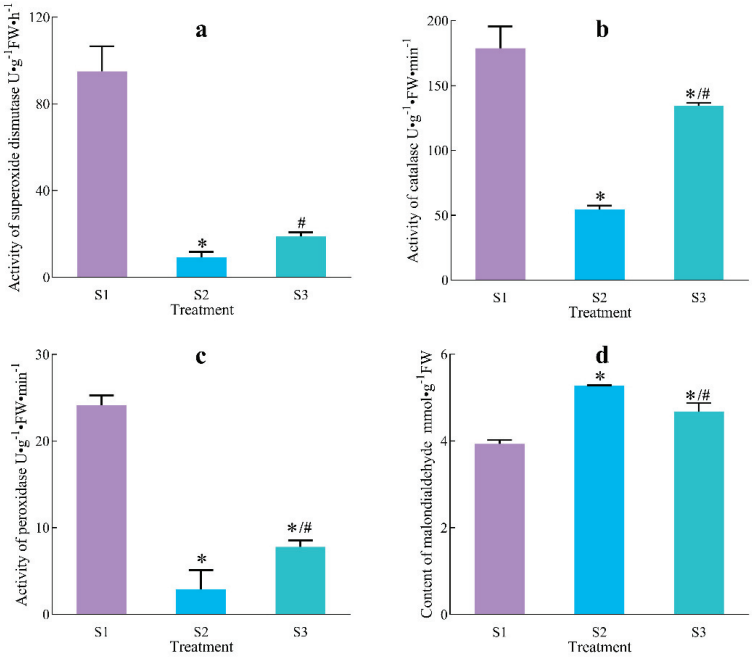

Figure 6. Oxidant-antioxidant parameters in the *F. solani* colony. (**a**) Superoxide dismutase (SOD). (**b**) Catalase (CAT). (**c**) Peroxidase (POD). (**d**) Malondialdehyde (MDA). S1 group (n = 3), inoculation of *F. solani* on PDA; S2 group (n = 3), inoculation of *F. solani* on PDA containing 40 μmol/L DPI; S3 group (n = 3), inoculation of *F. solani* on PDA containing 40 μmol/L DPI. On the fourth day of cultivation, 5 mL of 0.0012% H_2O_2 was added to each dish. Data are expressed as the mean ± SD. * $p < 0.05$ S2 or S3 vs. S1, # $p < 0.05$ S3 vs. S2.

The SOD activities of S1, S2 and S3 were 95.04 ± 11.53 U g^{-1}FW h^{-1}, 9.13 ± 1.68 U g^{-1}FW h^{-1} and 18.79 ± 1.52 U g^{-1}FW h^{-1}, respectively. Compared with S1, the SOD activities of S2 and S3 90.39% and 80.23% lower, respectively. Compared with S3, the SOD activity of S2 51.43% higher, but the upward trend was not significant (p = 0.53) (Figure 6a).

Compared with S1, the CAT activities of S2 and S3 were 69.51% and 24.91% lower, respectively. S3 was 59.40% higher than S2, with a significant upward trend (Figure 6b).

Compared with S1, the POD activities of S2 and S3 were 88.05% and 67.68% lower, respectively. Compared with S3, the POD activity of S2 was 63.02% higher (Figure 6c).

The change in trend in terms of MDA content in the colonies varied from that of the antioxidant enzymes such as SOD, CAT and POD. The MDA contents of S1, S2 and S3 were 3.93 ± 0.13 μg g^{-1}FW, 5.28 ± 0.02 μg g^{-1}FW and 4.68 ± 0.19 μg g^{-1}FW, respectively. Compared with S1, the MDA contents of S2 and S3 were 27.73% and 10.19% higher, respectively. Compared with S2, the MDA content of S3 was 11.48% lower, with a significant downward trend (Figure 6d).

4. Discussion

As the most important enzyme in the ROS production system and the key enzyme of redox signals in eukaryotic cells, NADPH oxidase is specially located on the cell membrane [8,9,35]. NADPH oxidase is composed of multiple subunits. $p47^{phox}$ subunit are phosphorylated to form cytoplasmic complexes when the cells are stimulated, before being adsorbed to the cell membrane and then combining with the two membrane structures to assemble into the NADPH complex to produce O_2^- [11]. Subsequently, the O_2^- is

decomposed into H_2O_2 under the action of iron-sulfur protein, and O_2^- as well as H_2O_2 are important ROS types.

ROS play a dual role in organisms, not only as by-products of cellular aerobic metabolism, cause cellular peroxidation [36,37], but also as signal molecules in cells to regulate cell proliferation and differentiation [38]. The content of ROS produced in the interaction process is related to the pathogenicity of fungi [5]. The pathogens may successfully infect and form interaction combinations or may fail and form plant immunity [39]. Therefore, changing the ROS content of a colony may convert the pathogenicity of the strain [6] and may affect the growth and macroconidia number of the isolate, as shown in this study. The addition of the NADPH oxidase inhibitor DPI can effectively reduce the extracellular O_2^- concentration of the marine diatom *Thalassiosira oceanica* and reduce the efficiency of PSII [40]. The knockout of key NADPH oxidase genes such as *Nox1* and *Nox2* in pathogenic bacteria can block the production of O_2^- and affect colony growth and expansion [41,42]. In this study, DPI was added to PDA medium, and, as a result, the O_2^- content of the *F. solani* decreased by 34.88% and 7.24%, respectively, as determined by NBT staining and the hydroxylamine hydrochloride method. The results of transcriptome sequencing and RT-qPCR showed that the mRNA expression of the *NCF2* (*p67^{phox}*) gene was inhibited, with the expression decreasing by 25.34% and 84.40%, respectively. Furthermore, the growth rate decreased by 19.43%, which indicates that by reducing O_2^- produced by colonies, NADPH oxidase can effectively inhibit colony growth, which is largely consistent with previous studies. The H_2O_2 content in the colonies was determined by the titanium sulfate precipitation method and DAB chemical staining after inhibition by DPI. The H_2O_2 content in the colonies did not decrease as reported above but increased by 13.17% and 16.97%, respectively, reaching a significant level in this study, which is inconsistent with most previous research results and was most likely due to the addition of DPI significantly inhibiting the gene expression and activities of antioxidant enzymes such as SOD, CAT and POD as well as greatly reducing the metabolic capability of H_2O_2, thus leading to the increase in H_2O_2 content. However, Libik-Konieczny et.al showed that adding DPI to the isolated vascular bundles of *Mesembryanthemum crystallinum* inhibited the activity of NADPH oxidase and reduced the H_2O_2 content [43], which is consistent with the results of this study. At the same time, the MDA content increased by 27.33% after the activity of NADPH oxidase was inhibited, resulting in higher values compared to the S1 treatment. Meanwhile, the oxidative stress on the cell membrane was intensified, which confirmed that the H_2O_2 content increased.

There are several enzymes that regulate the ROS balance and redox signals in organisms, such as NADPH oxidase, SOD, CAT, PRX and GPX [44,45], which can maintain the ROS content at a nontoxic level in cells [36]. When trying to break the balance between the production and clearance of reactive oxygen species, ROS-mediated redox reactions are usually initiated [46] to affect life processes. In this study, DPI inhibited the production of ROS, disrupted the redox balance of *F. solani* colonies and seriously affected the growth of the colonies. Previous studies have shown that DPI pretreatment of wild-type *Arabidopsis* or knockout of the *atrbohD/F* gene can reduce the activities of key enzymes, such as SOD, CAT, APX and GR, under salt stress, leading to a decline in long-term salt resistance [47]. Regarding the interaction between the pathogen *F. thiocyanum* and potato tubers, the activity of potato NADPH oxidase increased, the production rate of O_2^- increased significantly and the activities of CAT, POD, SOD, GR and APX rose steadily [48]. In this study, the relative expression of ROS metabolism and key genes such as *NCF2*, *SOD1*, *CTA1* and *PXMP4* decreased, which is consistent with previous research, confirming that the NADPH oxidase inhibitor DPI affected the activity of key ROS metabolism enzymes and the relative expression of genes.

In this study, H_2O_2 was added to *F. solani* colonies, and NADPH oxidase was inhibited by DPI. The O_2^- concentration increased to a high level, *NCF2* gene expression increased dramatically and the colony growth rate recovered, with these results being the same as those for *Arabidopsis* under salt stress. It was established that the H_2O_2 pro-

duced by NADPH oxidase under salt stress at the inception phase was likely used as a signal substance to trigger the antioxidant response of *Arabidopsis*, activate the activities of antioxidant enzymes such as CAT, APX and GR and reduce the damage caused by salt stress [47]. Meanwhile, the H_2O_2 concentration increased when exogenous H_2O_2 was added to the normal cultured colony (S4) and displayed higher values compared to the inhibition treatment, indicating that the colonies inhibited by NADPH oxidase could utilize more exogenous H_2O_2 and that supplementation with exogenous H_2O_2 could significantly reduce the MDA content in the colonies to alleviate the oxidative stress of the colonies' cell membranes. In *F. solani*, H_2O_2 is the key growth signal substance that can reverse regulate O_2^-.

There are some problems that need to be further researched arising from this study. First, the DPI inhibited the production of O_2^- by NADPH oxidase, but the O_2^- content only decreased by 7.24%, a nonsignificant level, indicating that there are still other ways to produce O_2^- in *F. solani*. The most likely reason for this is that DPI is a noncompetitive inhibitor of NADPH oxidase and only reacts with reducible NADPH oxidase [49], so other ROS production pathways and their physiological functions in *F. solani* need to be further studied. In addition, comparing the transcriptome sequencing of the three treatments, the expression of genes related to cytochrome P450 such as *cyp12*, *af510* and *gsfF-1* were strongly inhibited, and their mechanism and relationship with ROS metabolism also need to be studied.

5. Conclusions

The addition of DPI and H_2O_2 can change the level of ROS in colonies, regulate the expression of *NCF2* and its downstream genes *SOD1*, *CTA1* and *PXMP4* and change the activities of key metabolic enzymes such as SOD, CAT and POD and the level of MDA to change the degree of cell membrane oxidation and affect the growth of *F. solani* (Figure 7). In conclusion, the results provide a scientific breakthrough for further exploration of the interaction mechanism of NADPH oxidase, key ROS metabolic enzymes and MDA during the growth of *F. solani*.

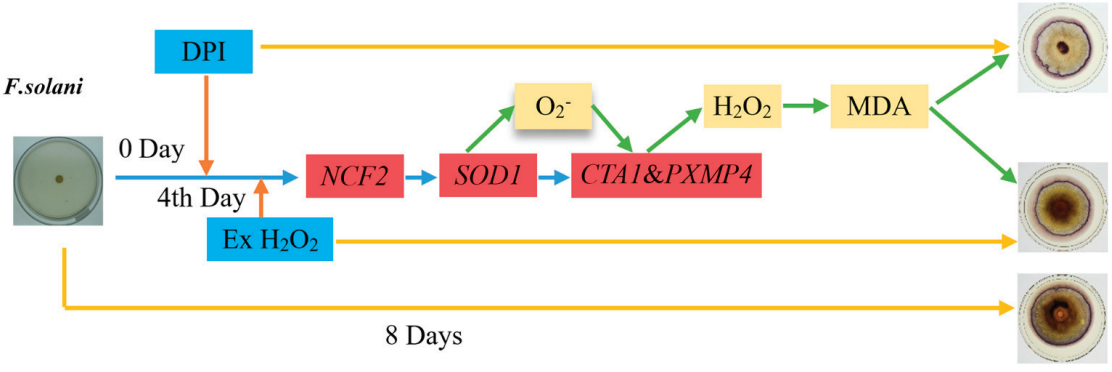

Figure 7. The mode diagram of ROS on *F. solani* growth.

Author Contributions: Conceptualization, J.L. and L.F.; methodology, D.L. and J.Z.; software, D.L.; validation, X.L., Y.P. and J.H.; formal analysis, X.L.; writing—original draft preparation, J.L.; writing—review and editing, J.L.; visualization, D.L. and J.L.; supervision, J.L.; project administration, J.L. All authors have read and agreed to the published version of the manuscript.

Funding: This research was funded by the Gansu Natural Science Foundation of China (18JR3RA177) and the Gansu University Innovation Fund Project of China (2020A-055). The funders had no role in the study design, data collection and analysis, decision to publish or preparation of the manuscript.

Institutional Review Board Statement: Not applicable.

Informed Consent Statement: Not applicable.

Data Availability Statement: We have uploaded the metadata spreadsheet, processed datafiles and raw datafiles to the GEO database and acquired the accession number GSE208534. We have created the reviewers link: https://www.ncbi.nlm.nih.gov/geo/query/acc.cgi?acc=GSE208534 (accessed on 19 July 2022).

Acknowledgments: The authors would like to acknowledge the technical support of Chengde Yang from the Plant Protection College of Gansu Agricultural University.

Conflicts of Interest: The authors declare no conflict of interest.

Abbreviations

APX: ascorbate peroxidase; CAT: catalase; DAB: 3,3′-diaminobenzidine; DPI: diphenyleneiodonium chloride; FPKM: fragments per kilobase of exon model per million mapped fragments; GPX: glutathione peroxidase; GR: glutathione reductase; MDA: malondialdehyde; NADPH: nicotinamide adenine dinucleotide phosphate; NBT: nitro-blue tetrazolium chloride; PDA: potato dextrose agar; POD: peroxidase; PRX: peroxiredoxin; ROS: reactive oxygen species; SOD: superoxide dismutase.

References

1. Li, H.; Li, G.Y.; Fu, J.H. Identification of the causing agent of wolfberry root rot in Xinjiang. *J. Plant Protect.* **1998**, *25*, 253–257.
2. Lu, Z.K.; Yang, J.N. Occurrence and control of wolfberry root rot. *J. Plant Protect.* **1994**, *21*, 249–254.
3. Li, J.; Feng, L.D.; Wang, Y.K.; He, J.; Chen, X.R. Identification and biological characteristics of dominant pathogens of *Lycium bararum* root rot in Gansu Province. *Arid Zone Res.* **2017**, *34*, 1093–1100.
4. Poljak, B.; Jamnik, P.; Raspor, P.; Miklós, P. *Oxidation-Antioxidation-Reduction Processes in the Cell: Impacts of Environmental Pollution*, 2nd ed.; Elsevier: Amsterdam, The Netherlands, 2019; pp. 831–837.
5. Taheri, P.; Irannejad, A.; Goldani, M.; Tarighi, S. Oxidative burst and enzymatic antioxidant systems in rice plants during interaction with *Alternaria alternata*. *Eur. J. Plant Pathol.* **2014**, *140*, 829–839. [CrossRef]
6. Segmüller, N.; Kokkelink, L.; Giesbert, S.; Kan, J.V.; Tudzynski, P. NADPH oxidases are involved in differentiation and pathogenicity in *Botrytis cinerea*. *Mol. Plant-Microbe Interact.* **2008**, *21*, 808–819. [CrossRef] [PubMed]
7. Magnani, F.; Nenci, S.; Fananas, E.M.; Ceccon, M.; Romero, E.; Fraaije, M.W. Crystal structures and atomic model of NADPH oxidase. *Proc. Natl. Acad. Sci. USA* **2017**, *114*, 6764–6769. [CrossRef]
8. Babior, B.M.; Lambeth, J.D.; Nauseef, W. The Neutrophil NADPH Oxidase. *Arch. Biochem. Biophys.* **2002**, *397*, 342–344. [CrossRef]
9. Rossi, D.C.P.; Gleason, J.E.; Sanchez, H.; Mcnees, C.; Schatzman, S.; Culbertson, E. 294—*Candida albicans* FRE8 encodes a member of the NADPH oxidase family that produces a burst of ROS during fungal morphogenesis. *Free Radic. Biol. Med.* **2017**, *112*, 194–195.
10. Grissa, I.; Frédérique, B.; Grognet, P.; Grossetete, S.; Silar, P. The Nox/Ferric reductase/Ferric reductase-like families of Eumycetes. *Fungal Biol.* **2010**, *114*, 766–777. [CrossRef]
11. Heller, J.; Tudzynski, P. Reactive oxygen species in phytopathogenic fungi: Signaling, development, and disease. *Annu. Rev. Phytopathol.* **2011**, *49*, 369–390. [CrossRef]
12. Takemoto, D.; Scott, T.B. A $p67^{phox}$-like regulator is recruited to control hyphal branching in a fungal-grass mutualistic symbiosis. *Plant Cell* **2006**, *18*, 2807–2821. [CrossRef] [PubMed]
13. Donofrio, N.M.; Wilson, R.A. Redox and rice blast: New tools for dissecting molecular fungala-plant interactions. *New Phytol.* **2014**, *201*, 367–369. [CrossRef] [PubMed]
14. Schuermann, J.; Buttermann, D.; Herrmann, A.; Giesbert, S.; Tudzynski, P. Molecular characterization of the NADPH oxidase complex in the ergot fungus *Claviceps purpurea*: *CpNox2* and *CpPls1* are important for a balanced host-pathogen interaction. *Mol. Plant-Microbe Interact.* **2013**, *26*, 1151–1164. [CrossRef]
15. Cudejkova, M.M.; Vojta, P.; Josef, V.; Galuszka, P. Quantitative and qualitative transcriptome analysis of four industrial strains of *Claviceps purpurea* with respect to ergot alkaloid production. *New Biotechnol.* **2016**, *33*, 743–754. [CrossRef] [PubMed]
16. Roca, M.G.; Weichert, M.; Siegmund, U.; Tudzynski, P.; Fleissner, A. Germling fusion via conidial anastomosis tubes in the grey mould *Botrytis cinerea* requires NADPH oxidase activity. *Fungal Biol.* **2012**, *116*, 380–387. [CrossRef]
17. Kim, H.J.; Chen, C.; Kabbage, M.; Dickman, M.B. Identification and characterization of *Sclerotinia sclerotiorum* NADPH Oxidases. *Appl. Environ. Microb.* **2011**, *77*, 7721–7729. [CrossRef]
18. Brun, S.; Malagnac, F.; Bidard, F.; Lalucque, H.; Silar, P. Functions and regulation of the *Nox* family in the filamentous fungus *Podospora anserina*: A new role in cellulose degradation. *Mol. Microbiol.* **2010**, *74*, 480–496. [CrossRef]
19. Egan, M.J.; Wang, Z.Y.; Jones, M.A.; Smirnoff, N.; Talbot, N.J. Generation of reactive oxygen species by fungal NADPH oxidases is required for rice blast disease. *Proc. Natl. Acad. Sci. USA* **2008**, *104*, 11772–11777. [CrossRef]

20. Marschall, R.; Schumacher, J.; Siegmund, U.; Tudzynski, P. Chasing stress signals-exposure to extracellular stimuli differentially affects the redox state of cell compartments in the wild type and signaling mutants of *Botrytis cinerea*. *Fungal Genet. Biol.* **2016**, *90*, 12–22. [CrossRef]
21. Nallely, C.D.; Karen, A.D.; Hansberg, W.; Jesús, A. NADPH oxidases *NOX-1* and *NOX-2* require the regulatory subunit *NOR-1* to control cell differentiation and growth in *Neurospora crassa*. *Eukaryot. Cell.* **2008**, *7*, 1352–1361.
22. Leslie, J.; Summerell, B. *The Fusarium Laboratory Manual*; Blackwell Publishing: Ames, IA, USA, 2016; pp. 28–29.
23. Thakur, A.; Singh, V.; Kaur, A.; Kaur, S. Suppression of Cellular Immune Response in *Spodoptera litura* (Lepidoptera: Noctuidae) Larvae by Endophytic Fungi *Nigrospora oryzae* and *Cladosporium uredinicola*. *Ann. Entomol. Soc. Am.* **2014**, *107*, 674–679. [CrossRef]
24. Yang, I.S.; Kim, S. Analysis of Whole Transcriptome Sequencing Data: Workflow and Software. *Genom. Inform.* **2015**, *13*, 119–125. [CrossRef] [PubMed]
25. Livak, K.J.; Schmittgen, T.D. Analysis of relative gene expression data using real-time quantitative PCR. *Methods* **2002**, *25*, 402–408. [CrossRef] [PubMed]
26. Tao, Y.; Van, P.A.F.; Huang, Q.; Shao, Y.; Zhang, L.; Xie, B. Identification of novel and robust internal control genes from *Volvariella volvacea* that are suitable for RT-qPCR in filamentous fungi. *Sci. Rep.* **2016**, *6*, 29236. [CrossRef]
27. Hodges, D.M.; Delong, J.M.; Forney, C.F. Improving the thiobarbituric acid-reactive-substance assay for estimating lipid peroxidation in plant tissues containing anthocyanin and other interfering compounds. *Planta* **1999**, *207*, 604–611. [CrossRef]
28. Wang, A.G.; Luo, G.H. Quantitative relation between the reaction of hydroxylamine and superoxide anion radicals in plants. *Plant Physiol. Commun.* **1990**, *84*, 2895–2898.
29. Prochazkova, D.; Sairam, R.K.; Srivastava, G.C.; Singh, D.V. Oxidative stress and antioxidant activity as the basis of senescence in maize leaves. *Plant Sci.* **2001**, *161*, 765–771. [CrossRef]
30. Rao, M.V.; Paliyath, G.; Ormrod, D.P. Ultraviolet-B- and ozone-induced biochemical changes in antioxidant enzymes of *Arabidopsis thaliana*. *Plant Physiol.* **2001**, *110*, 125e36. [CrossRef]
31. Wang, Y.S.; Tian, S.P.; Xu, Y. Effects of high oxygen concentration on pro- and anti-oxidant enzymes in peach fruits during postharvest periods. *Food Chem.* **2005**, *91*, 99–104. [CrossRef]
32. Venisse, J.S.; Gullner, G.; Brisset, M.N. Evidence for the involvement of an oxidative stress in the initiation of infection of pear by *Erwinia amylovora*. *Plant Physiol.* **2001**, *125*, 2164–2172. [CrossRef]
33. Barceló, A.R. Hydrogen peroxide production is a general property of the lignifying xylem from vascular plants. *Ann. Bot.* **1998**, *82*, 97–103. [CrossRef]
34. Shinogi, T.; Suzuki, T.; Kurihara, T.; Narusaka, Y.; Park, P. Microscopic detection of reactive oxygen species generation in the compatible and incompatible interactions of *Alternaria alternata* Japanese pear pathotype and host plants. *J. Gen. Plant Pathol.* **2003**, *69*, 7–16. [CrossRef]
35. Lambeth, J.D.; Neish, A.S. Nox enzymes and new thinking on reactive oxygen: A double-edged sword revisited. *Annu. Rev. Pathol.* **2014**, *9*, 119–145. [CrossRef] [PubMed]
36. Mittler, R.; Vanderauwera, S.; Gollery, M.; Van, B.F. Reactive oxygen gene network of plants. *Trends Plant Sci.* **2004**, *9*, 490–498. [CrossRef]
37. Foyer, C.H.; Noctor, G. Redox Signaling in Plants. *Antioxid. Redox Sign.* **2013**, *18*, 2087–2090. [CrossRef] [PubMed]
38. Mittler, R.; Vanderauwera, S.; Suzuki, N.; Miller, G.; Tognetti, V.B.; Vandepoele, K. ROS signaling: The new wave? *Trends Plant Sci.* **2011**, *16*, 300–309. [CrossRef]
39. Ekanayake, G.; LaMontagne, E.D.; Heese, A. Never walk alone: Clathrin-coated vesicle components in plant immunity. *Annu. Rev. Phytopathol.* **2019**, *57*, 387–409. [CrossRef]
40. Diaz, J.M.; Plummer, S.; Hansel, C.M.; Andeer, P.F.; Saito, M.A.; McIlvin, M.R. NADPH-dependent extracellular superoxide production is vital to photophysiology in the marine diatom *Thalassiosira oceanica*. *Proc. Natl. Acad. Sci. USA* **2019**, *116*, 201821233. [CrossRef]
41. Malagnac, F.; Lalucque, H.; Lepère, G.; Silar, P. Two NADPH oxidase isoforms are required for sexual reproduction and ascospore germination in the filamentous fungus *Podospora anserina*. *Fungal Genet. Biol.* **2004**, *41*, 982–997. [CrossRef]
42. Li, W.; Christopher, M.; Sean, W.; Joshi, M.; Subramaniam, R. Characterization of NADPH oxidase genes *NoxA* and *NoxB* in *Fusarium graminearum*. *Can. J. Plant Pathol.* **2014**, *36*, 12–21.
43. Libik-Konieczny, M.; Kozieradzka-Kiszkurno, M.; Desel, C.; Michalec-Warzecha, Ż.; Miszalski, Z.; Konieczny, R. The localization of NADPH oxidase and reactive oxygen species in in vitro-cultured *Mesembryanthemum crystallinum* L. hypocotyls discloses their differing roles in rhizogenesis. *Protoplasma* **2015**, *252*, 477–487. [CrossRef] [PubMed]
44. Passaia, G.; Margis-Pinheiro, M. Glutathione peroxidases as redox sensor proteins in plant cells. *Plant Sci.* **2015**, *234*, 22–26. [CrossRef]
45. Mittler, R. ROS Are Good. *Trends Plant Sci.* **2016**, *22*, 11–19. [CrossRef] [PubMed]
46. Vanderauwera, S.; Suzuki, N.; Miller, G.; van de Cotte, B.; Morsa, S.; Ravanat, J.-L.; Hegie, A.; Triantaphylidès, C.; Shulaev, V.; van Montagu, M.C.E.; et al. Extranuclear protection of chromosomal DNA from oxidative stress. *Proc. Natl. Acad. Sci. USA* **2011**, *108*, 1711–1716. [CrossRef]
47. Ben, R.K.; Benzarti, M.; Debez, A.; Bailly, C.; Savouré, A.; Abdelly, C. NADPH oxidase-dependent H_2O_2 production is required for salt-induced antioxidant defense in *Arabidopsis thaliana*. *J. Plant Physiol.* **2015**, *174*, 5–15.

48. Bao, G.H.; Bi, Y.; Li, Y.C.; Kou, Z.; Hu, L.; Ge, Y. Overproduction of reactive oxygen species involved in the pathogenicity of *Fusarium* in potato tubers. *Physiol. Mol. Plant Pathol.* **2014**, *86*, 35–42. [CrossRef]
49. O'Donnell, B.V.; Tew, D.G.; Jones, O.T.; England, P.J. Studies on the inhibitory mechanism of iodonium compounds with special reference to neutrophil NADPH oxidase. *Biochem. J.* **1993**, *290*, 41–49. [CrossRef]

agriculture

MDPI

Article

Allelopathic Effects of Foliar *Epichloë* Endophytes on Belowground Arbuscular Mycorrhizal Fungi: A Meta-Analysis

Rui Zhong [1,2,*], Lin Zhang [1,*] and Xingxu Zhang [2]

[1] College of Resources and Environmental Sciences, National Academy of Agriculture Green Development, Key Laboratory of Plant-Soil Interactions, Ministry of Education, China Agricultural University, Beijing 100193, China
[2] State Key Laboratory of Grassland Agro-Ecosystems, College of Pastoral Agriculture Science and Technology, Lanzhou University, Lanzhou 730020, China
* Correspondence: ruizhong@cau.edu.cn (R.Z.); linzhang@cau.edu.cn (L.Z.)

Abstract: Many grasses are simultaneously symbiotic with *Epichloë* fungal endophytes and arbuscular mycorrhizal fungi (AMF). *Epichloë* endophytes are a group of filamentous fungi that colonize and grow within aerial plant tissues, such as leaves and stems. Infection and hyphal growth of *Epichloë* endophytes confer fitness advantages to the host plants. In addition to producing fungal alkaloids and altering host metabolic/genetic profiles, it is proven that symbiosis of plants with root/foliar endophytes affects the plant–soil relationship. We propose that the *Epichloë* presence/infection results in variations of soil and root AMF through allelopathic effects. We performed a meta-analysis that integrated the allelopathic effects of *Epichloë* endophytes on grass–AMF development. In the pre-symbiotic phase of grass–AMF symbiosis, root exudation from *Epichloë*-infected plants positively affected AMF growth, whereas the shoot exudates of *Epichloë*-infected plants inhibited AMF growth. In the symbiotic phase of grass–AMF symbiosis, the *Epichloë* infection was found to reduce root mycorrhizal colonization in plants. No pattern in the response of soil AMF to *Epichloë* presence was found. This study should improve our understanding of the impact of *Epichloë* endophytes on belowground microbial symbionts within the same host plant. Grass–*Epichloë*–AMF symbiosis may become an important model for studying above–belowground interactions.

Keywords: *Epichloë* endophytes; allelopathy; arbuscular mycorrhizal fungus; host grass

Citation: Zhong, R.; Zhang, L.; Zhang, X. Allelopathic Effects of Foliar *Epichloë* Endophytes on Belowground Arbuscular Mycorrhizal Fungi: A Meta-Analysis. *Agriculture* **2022**, *12*, 1768. https://doi.org/10.3390/agriculture12111768

Academic Editor: Nadia Massa

Received: 6 September 2022
Accepted: 20 October 2022
Published: 25 October 2022

1. Introduction

Above–belowground (ABG) interaction is one of the frontiers in studying and understanding the key biochemical and ecological processes in agricultural and natural ecosystems [1,2]. Plants interact with a wide range of microbes—both above- and belowground—that influence plant fitness through nutrient cycling and a wide array of signaling compounds [3–6]. Grass species are the main components of grassland and agricultural ecosystems, and their fungal symbionts may exert an important effect on plant fitness and biological processes [7–10]. Many types of grass in Poaceae are symbiotic with *Epichloë* (Ascomycota, Clavicipitaceae) fungal endophytes [7,9,10]. *Epichloë* fungal endophytes grow asymptomatically within the intercellular spaces of the aerial tissues of the grass hosts and vertically transmit their progeny through seeds. *Epichloë* endophytes are a source of secondary metabolites [4,6,11], such as protective fungal alkaloids that are toxic to herbivores and inhibit pathogen colonization, including lolines, indole diterpenes, ergot alkaloids, and peramines. The infection and growth of *Epichloë* endophytes modify plant immune and metabolic profiles to establish a hyphal network within aerial tissues to promote plant persistence and fitness [10,12].

Epichloë-infected grass plants may offer a competitive advantage to non-infected grass by influencing the root-associated (bulk soil, rhizosphere soil, and root endosphere) microbes [13–15]. A previous study suggested that aboveground *Epichloë* endophytes also

generate shifts and variations in belowground biochemical processes and components [8]. Arbuscular mycorrhizal fungi (AMF), belonging to the subphylum Glomeromycotina, can form complex associations with host plants and play important roles in promoting plant fitness and productivity [5]. The symbiosis of AMF with roots begins with spore germination, and the development processes of pre-symbiotic and symbiotic phases are also determined by the host plants. Previous studies on *Epichloë*-infected grass plants reported shifts in the soil AMF community structure and root AMF colonization [15,16]. Some studies have assessed the potential pathways of *Epichloë* infection/presence on the developmental status of grass–AMF symbiosis, including root/*Epichloë* exudation and shoot litter [17–19]. *Epichloë* infection also changed the root exudation profiles [20,21] and shoot decomposition. However, the *Epichloë*-facilitated soil microbial processes and the subsequent soil microbial responses that contribute to greater tolerance or resistance to grass hosts are unknown. Determining this may carry significant economic and ecological importance in the development of sustainable agricultural practices [13,22].

Understanding the influences of grass–*Epichloë* interactions on the plant–soil–microbe interactions is of ecological and agricultural importance in grassland and agricultural ecosystems. Based on the transmission of *Epichloë* endophytes and AMF, we propose a model that integrates the effects of grass–*Epichloë*-AMF association. Here, we took complementary approaches to validate the multiple tripartite interactions and the predictions of our model. We reviewed the literature related to the interactions between *Epichloë* endophytes and AMF. A meta-analysis critically analyzed the potential pathways of *Epichloë* infection on pre-symbiotic and symbiotic phases of grass–AMF development, including (1) exploring the allelopathic effects of *Epichloë* endophytes on the pre-symbiotic phase of grass–AMF symbiosis, and (2) accessing the effects of *Epichloë* infection on the symbiotic phase of belowground grass–AMF symbiosis.

2. Material and Methods

We performed a quantitative analysis of published results about the effects of *Epichloë* endophyte infection on the pre-symbiotic and symbiotic phases of grass–AMF symbiosis. We obtained and reviewed the related literature reporting the multiple interactions between *Epichloë* and AMF, and performed a standard meta-analysis. Papers in journals were collected from the Web of Science and the China National Knowledge Infrastructure (CNKI) databases using the keywords "*Epichloë*/*Neotyphodium* and mycorrhiza" in May 2022.

These papers were screened based on the following criteria: (1) these fungal endophytes belong to the *Epichloë* (formerly *Neotyphodium*) genus, and the host plants of *Epichloë* endophytes are the cool-season grass species; (2) the experiments had to examine the effects of *Epichloë* endophyte infection/presence on growth and/or colonization of AMF; (3) the references of these selected papers were also checked to search for further appropriate papers; (4) the selected papers had to include the means of AMF growth and colonization for both the endophyte-infected and endophyte-free grasses. Here a total of 32 papers (21 papers in English and 11 papers in Chinese) were obtained from the databases and references of the selected papers for the subsequent meta-analysis.

The extracted values were obtained from the graphs using GetData Graph Digitizer 2.22 and tables in the selected papers. The mean and standard deviations (= standard errors $\times \sqrt{n}$ or the unreported standard deviations were estimated at 10% of the mean), and the number of repetitions (n) of *Epichloë*-infected (experimental group) and non-infected (control group) grass plants were extracted from the selected papers. The data were grouped into the following categories: (1) exudation resources (shoot, root, and *Epichloë* strains) or AMF growth (spore germination and hyphal growth) indices in the pre-symbiotic phase of grass–AMF development, and (2) grass classification (grass genus level) or root/soil AMF (root AMF colonization, root AMF concentration, and length of the extraradical hyphae of soil AMF) in the symbiotic phase of grass–AMF symbiosis. For each group as a categorical variable, this group had to be reported in at least five cases. The AMF growth indices in the pre-symbiotic phase of grass–AMF symbiosis were determined by laboratory experiments,

and the root/soil AMF indices in the symbiotic phase of grass–AMF symbiosis were determined by controlled pot and field experiments. The meta-analysis was performed using MetaWin software (version 2.1, an intellectual property of Michael S. Rosenberg, Dean C. Adams and Jessica Gurevitch), and these effects were calculated using the log of the response ratio (*lnR*) using the following Equation according to a study [23].

$$lnR = \ln\left(\frac{\overline{X_e}}{\overline{X_C}}) = \ln(\overline{X_e}) \ - \ \ln(\overline{X_c}\right)$$

where $\overline{X_e}$ and $\overline{X_c}$ represent the mean AMF growth and colonization of the experimental and control groups, respectively.

The variance of the natural logarithm of the response ratio (*lnR* (*v*)) was approximated using the following Equation according to a study [24].

$$lnR(v) = \frac{S_e^2}{n_e\overline{X}_e^2} + \frac{S_c^2}{n_c\overline{X}_c^2}$$

where n_e and n_c indicate the repetitions of the experimental and control groups, respectively, and S_e and S_c indicate the standard deviations of the experimental and control groups, respectively [24]. The *lnR* means of the effects of *Epichloë* infection/presence on AMF growth and root/soil AMF were calculated using the combination of *lnR* and *lnR(v)*, and *lnR(v)* was weighted by the inverse variance of *lnR* for each observation. The 95% bootstrap confidence intervals (95% CI) for the mean *lnR* were calculated using 9999 iterations of bootstrapping, according to a previous study [24].

3. Results

From 142 articles obtained from the Web of Science (124 articles) and CNKI (18 articles) databases, only 32 articles were selected and included in the meta-analysis. A total of 198 cases were obtained from these selected references, including: (1) allelopathic effects of *Epichloë* fungal endophytes on AMF growth (78 cases in 5 studies), and (2) *Epichloë* infection on soil and root AMF colonization in plants (120 cases of 31 studies). The present meta-analysis aimed to access whether foliar *Epichloë* presence/infection could result in some changes to the belowground AMF components (spore germination, hyphal growth, root AMF colonization/concentration, and soil AMF length in pre-symbiotic and symbiotic phases of grass–AMF development) of the grass hosts.

3.1. Does Epichloë Presence Affect the Pre-Symbiotic Phase of Grass-Arbuscular Mycorrhizal Fungi Development?

The results of this present meta-analysis showed there were significant (Q_t = 89.88, p = 0.009, df = 75) and negative (effect size = −0.025, 95% CI = −0.129 to 0.008) effects of *Epichloë* fungal endophytes on the pre-symbiotic phase of grass–AMF development within a grass plant (Figure 1A,B). Exudates of *Epichloë* fungal strains had a weakly negative (effect size = −0.024, 95% CI = −0.154 to 0.106) effect on AMF growth (spore germination, hyphal length, and branch numbers) compared to the control (equal volume of medium) group (Figure 1A). Meanwhile, the shoot exudation from *Epichloë*-infected grass plants negatively (effect size = −0.351, 95% CI = −0.1655 to −0.048) affected the AMF growth in the pre-symbiotic phase of grass–AMF development than that of non-infected grass plants (Figure 1A). However, root exudation of *Epichloë*-infected grass plants stimulated (effect size = 0.250, 95% CI = −0.007 to 0.508) AMF growth compared to that of non-infected plants (Figure 1A).

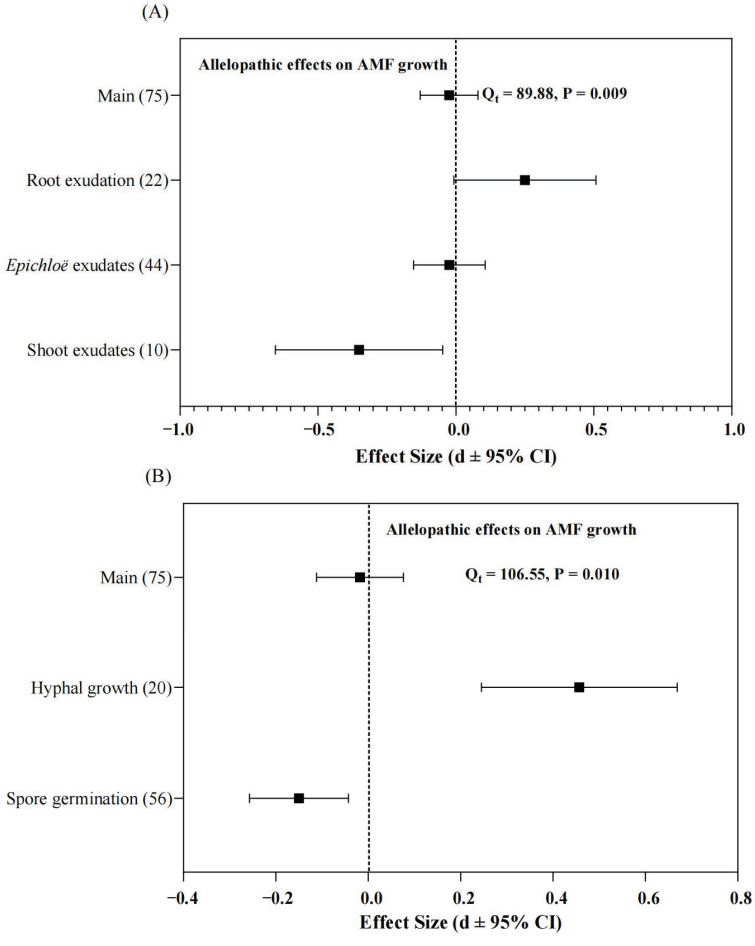

Figure 1. The cumulative effect size of allelopathic effects of *Epichloë* endophytes on the pre-symbiotic phase of the grass and arbuscular mycorrhizal fungi (AMF) development among (**A**) different allelopathic (exudates from root, shoot, and *Epichloë* strains) effects, or (**B**) AMF germination and hyphal growth. Squares indicate the mean values and bars denote the 95% confidence interval (CI).

The present meta-analysis indicated there was an overall negative effect (Q_t = 106.55, p = 0.010, df = 75, effect size = 0.018, 95% CI = −0.112 to 0.076) of *Epichloë*-associated (shoot, root and *Epichloë* strains) exudates on the spore germination and hyphal growth of AMF (Figure 1B). The *Epichloë*-associated exudates reduced (effect size = 0.150, 95% CI = −0.256 to −0.043) the spore germination of AMF (Figure 1B). However, the *Epichloë*-associated exudates increased (effect size = 0.457, 95% CI = 0.245 to 0.669) the hyphal growth of AMF (Figure 1B).

3.2. Does Epichloë Infection Affect the Symbiotic Phase of Grass–Arbuscular Mycorrhizal Fungi Development?

The present meta-analysis showed an overall negative effect of *Epichloë* infection on belowground AMF (Q_t = 203.69, p = 0.000, df = 119, effect size = −0.075, 95% CI = −0.128 to −0.022) and root AMF colonization (Q_t = 173.21, p = 0.000, df = 102, effect size = −0.087, 95% CI = −0.143 to −0.030) of grass plants (Figure 2A,B). The *Epichloë* infection reduced root AMF colonization (effect size = −0.088, 95% CI = −0.151 to −0.025) and root AMF concentration (effect size = −0.082, 95% CI = −0.232 to 0.067) of grass plants (Figure 2A). In line with the results of allelopathic effects on AMF growth via root exudations and shoot

litter, there was no change (effect size = 0.005, 95% CI = −0.151 to 0.161) in the length of extraradical AMF hyphae in the growing soil of *Epichloë*-infected versus non-infected plants (Figure 2A).

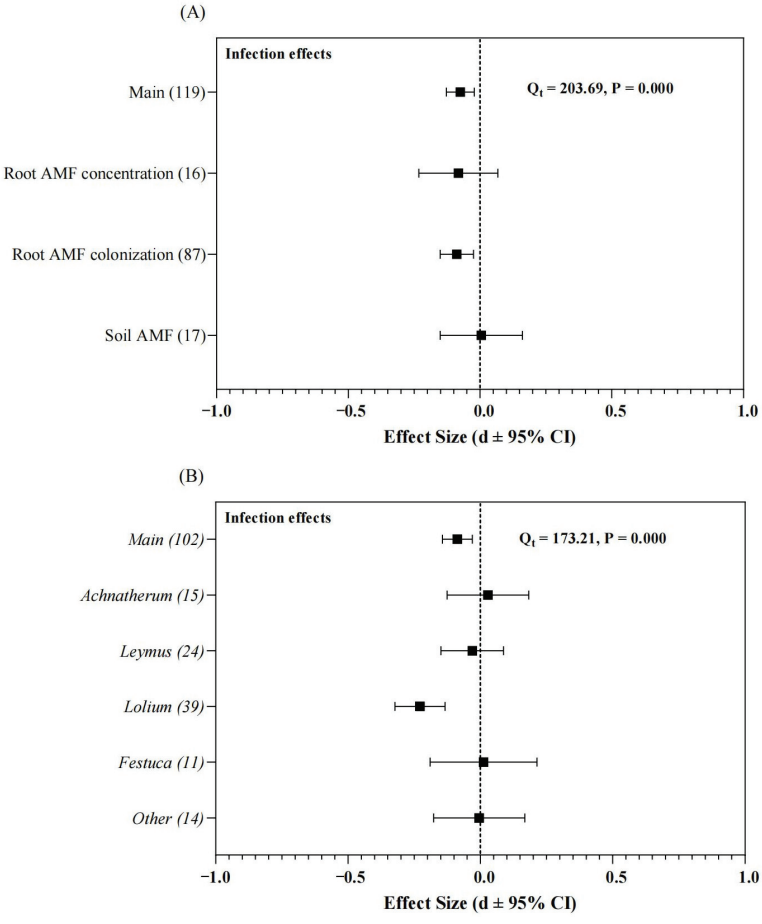

Figure 2. The cumulative effect size of *Epichloë* endophytes infection on the symbiotic phase of the grass and arbuscular mycorrhizal fungi (AMF) development among (**A**) soil and root AMF effects or (**B**) root AMF colonization of different plant genera. The squares indicate the mean values and the bars denote the 95% confidence interval (CI).

The present meta-analysis also indicated that the root AMF colonization was significantly (Q_t = 203.69, p = 0.000, df = 119) decreased (effect size = −0.087, 95% CI = −0.143 to −0.030) in the roots of *Epichloë*-infected versus non-infected plants (Figure 2B). In line with the main effects, the same effects were observed in the *Lolium* (effect size = −0.228, 95% CI = −0.322 to −0.133) and *Leymus* (effect size = −0.031, 95% CI = −0.149 to 0.088) grass plants (Figure 2B). However, the opposite results were found in *Festuca* (effect size = 0.012, 95% CI = −0.190 to 0.214) and *Achnatherum* (effect size = 0.029, 95% CI = −0.126 to 0.183) grass plants (Figure 2B).

3.3. Synthesis of Epichloë Effects on the Development of Grass and Arbuscular Mycorrhizal Fungi

We addressed two perspectives to understand or explain the effects of *Epichloë*-infection on AMF from changes of root exudation and shoot litter mediated by *Epichloë*

endophytes, and these variations of AMF in root and soil could contribute to the improvement of plant growth and resistance (Figure 3). The root exudation and shoot litter from the *Epichloë* infected grass plants positively and negatively affected the growth of AMF in the pre-symbiotic phase of grass AMF development compared with the non-infected grass plants (Figure 3). Therefore, there were no obvious changes in the growing soil of *Epichloë* infected versus non-infected grass plants (Figure 3). Collectively, the presence of foliar *Epichloë* reduced root colonization by AMF (Figure 3).

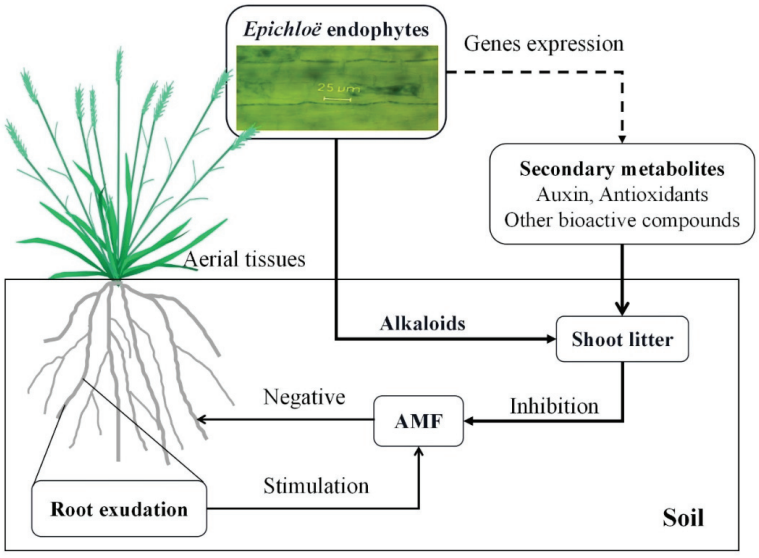

Figure 3. The synthesis of potential mechanisms for the effects of *Epichloë* endophytes infection/presence on the developmental processes of grass roots and soil arbuscular mycorrhizal fungi (AMF).

4. Discussion

The ABG interaction considers the spatiotemporal scales involved in the interactions between aboveground *Epichloë* fungal endophytes and belowground AMF within a plant [25]. The spatiotemporal scales could help to understand the coexistence interactions between foliar *Epichloë* endophyte and root AMF in a plant [25]. *Epichloë* systemic endophytes are found in the aerial tissues of 20% ~ 30% of all grasses [7], and AMF colonizes the roots of 80% of angiosperms [26], suggesting that these three-way plant–fungal interactions are ecologically common. Based on the transmission modes of *Epichloë* (vertically transmitted through seeds) and AMF (horizontally colonized grass roots), *Epichloë* endophytes had higher spatiotemporal priority to modify host metabolic and genetic profiles than co-infected AMF [25]. Here, we addressed two perspectives to investigate how foliar *Epichloë* endophyte presence/infection affects AMF growth and the development of grass–AMF symbiosis by altering (1) root exudates and (2) shoot litter decomposition (Figure 3).

4.1. The Effects of Epichloë Presence on the Pre-Symbiotic Phase of Grass–AMF Development

The development of AMF symbiosis with plants begins with spore germination, and the related developmental processes depend on the host plants, such as root exudation and plant litter. Root exudates provide chemical signaling to regulate rhizosphere microbial biomass and diversity [3]. Previous meta-analysis and experiment cases showed that the presence of *Epichloë* endophytes stimulated root exudation [8] and altered the composition of root exudates of the host grass [20,21]. For example, *Epichloë*-infected grass roots release more carbon (in the form of phenolic compounds and amines) into the rhizosphere through root exudation and volatiles than non-infected grasses [20,27]. Some secondary metabolites (such

as lipids, flavonoids, and phenolic compounds) could regulate the pre-symbiotic phase of plant-AMF symbiosis [28,29] at the start of the connection of AMF initial mycelium with plant roots [30]. Our meta-analysis showed that root exudation of *Epichloë*-infected plants stimulated AMF growth (Figure 1). Additionally, higher AMF diversity in the rhizosphere has been reported in *Achnatherum inebrians* plants hosting the endophyte *Epichloë gansuensis* in field experiments under drought stress [14]. However, the shoot litter of *Epichloë*-infected plants also affected soil microbes compared to non-infected plants [25,31]. Shoot exudates of *Epichloë*-infected grasses inhibited AMF growth in the present meta-analysis (Figure 1). There was a reasonable explanation that *Epichloë* fungal alkaloids were present in the litter of *Epichloë*-infected plants [32,33] and the soil for more than 50 days [34]. Additionally, flavonoids (recognized as inhibitors of AMF [35]) were higher in the roots of *Epichloë*-infected than in non-infected *Lolium multiflorum* plants [36]. This study showed that shoot and root exudation had opposite effects on AMF growth; therefore, there was no obvious change in soil AMF in *Epichloë*-infected versus non-infected grasses (Figures 1–3). This is in line with a study showing that aboveground *Epichloë*-grass associations do not affect belowground AMF symbionts [37]. The shifts of root-associated soil fungal and bacterial community structures in the *Epichloë*-infected versus non-infected grass plants had been reported in many field and pot cases [8,38–41]. There were different *Epichloë*-associated effects on the AMF growth—*Epichloë* presence reduced the spore germination of AMF strains while promoting the hyphal growth of AMF (Figure 1). This could help explain the variations of soil AMF associated with the presence of an *Epichloë* endophyte. However, the response mechanism of the root-associated microbiome of grass plants to the infection of *Epichloë* endophyte is still unclear. Further research should consider the potential mechanisms underlying these selections of soil microbiome by the infection of *Epichloë* endophytes.

4.2. The Effects of Epichloë Infection on the Symbiotic Phase of Grass–AMF Development

The symbiotic phase in which the AMF mycelium contacts and starts to grow along the root surface and enters the root endosphere is determined by the plant's nutritional status and defenses [30]. Root mycorrhizal colonization was lower in *Epichloë*-infected plants than in non-infected plants (Figure 2). In line with two meta-studies, AMF negatively colonized the grass roots of *Epichloë*-infected plants [8,13]. *Epichloë* infection promotes auxin content [42], nutrients [42,43], and biomass accumulation [4,44] in the roots of grass hosts. Therefore, we propose that the presence of *Epichloë* may reduce the beneficial effects of AMF in grass hosts. A previous study supports our suggestion that *Epichloë* endophytes facilitate the invasion of grass hosts by reducing the benefits derived from other mutualisms [13]. Additionally, the hyphal growth of *Epichloë* endophytes in aerial tissues also modified the metabolic profiles (promoting the accumulation of flavonoids, benzoic acids, and cinnamic acids) of the roots of grass hosts [36,45], which may inhibit root colonization by AMF. We proposed that the decrease of AMF colonization in the roots of *Epichloë*-infected versus non-infected grass plants was partly explained by the higher bioactive compounds in the roots of plants infected with *Epichloë* fungal endophytes. Some indirect evidence has been reported that *Epichloë* infection altered the root exudation [20,21], root metabolic profiles [36,42], and root/rhizosphere AMF community [14,37], while whether the relationship among root exudation, root metabolic profiles and root/rhizosphere AMF are shifted in the root–soil relations of *Epichloë*-infected versus non-infected grass plants were sill not clear. Generally, the aboveground *Epichloë* endophytes could result in changes to belowground AMF, especially AMF growth and root colonization. This meta-analysis also provides insight into the connection between chemical changes in root exudates and shoot litter for plant–soil interactions in ecosystem processes.

5. Conclusions and Further Perspectives

In conclusion, we propose that the presence/infection and hyphal growth of *Epichloë* endophytes in aboveground tissues negatively affected belowground AMF. Root exudation

of *Epichloë*-infected plants stimulated AMF growth in the pre-symbiotic phase, whereas shoot exudates of *Epichloë*-infected grass plants inhibited AMF growth. Additionally, AMF negatively colonized grass hosts hosting an *Epichloë* endophyte. There were no obvious changes in soil AMF. This study should help improve the understanding of the multiple plant–microbe interactions in ABG interactions. This study provides insights and evidence of the capability of the belowground plant and soil processes to be altered by aboveground *Epichloë* endophytes. There was a positive relationship between the AMF colonization rate and the *Epichloë* infection rate of the *Poa bonariensis* population [46]. The *Epichloë*-infected *Hordeum comosum* population had greater AMF colonization than non-infected plants [47]. The concentration of aboveground *Epichloë* endophyte is positively related to AMF concentration in the individual plant [48]. This means that the concentration of both *Epichloë* fungal endophytes and AMF within a grass plant was decreased compared with grass plants infected with either *Epichloë* endophytes or AMF. Some studies also reported that AMF colonization also reduced the concentration of *Epichloë* endophytes and their fungal alkaloid production [49]. Future research should consider (1) how variations in belowground processes from the *Epichloë* endophytes present feedback to the *Epichloë*–grass associations; (2) genetic and metabolic profiles of grass hosts to respond to simultaneous infections and environmental stresses; and (3) simultaneous infections on plant growth and defenses and the applications of multiple plant–microbe interactions in sustainable agriculture.

Author Contributions: R.Z. and L.Z. developed the concept; R.Z. collected and analyzed the data, R.Z., L.Z. and X.Z. wrote this manuscript, and all authors revised this manuscript. All authors have read and agreed to the published version of the manuscript.

Funding: This study was financially supported by the China Postdoctoral Science Foundation (2021M703515) and the Fundamental Research Funds for the Central Universities (lzujbky-2022-ey21), Lanzhou University.

Institutional Review Board Statement: Not applicable.

Data Availability Statement: Data is contained within the article.

Acknowledgments: Thanks to Michael Christensen from AgResearch Ltd., Grasslands Research Centre, New Zealand, for his valuable suggestions.

Conflicts of Interest: The authors declare no conflict of interest.

References

1. Wardle, D.A.; Bardgett, R.D.; Klironomos, J.N.; Setälä, H.; van der Putten, W.H.; Wall, D.H. Ecological linkages between aboveground and belowground biota. *Science* **2004**, *304*, 1629–1633. [CrossRef] [PubMed]
2. Ramirez, K.S.; Geisen, S.; Morriën, E.; Snoek, B.L.; van der Putten, W. Network analyses can advance above-belowground ecology. *Trends Plant Sci.* **2018**, *23*, 759–768. [CrossRef] [PubMed]
3. Bais, H.P.; Weir, T.L.; Perry, L.G.; Gilroy, S.; Vivanco, J.M. The role of root exudates in rhizosphere interactions with plants and other organisms. *Annu. Rev. Plant Biol.* **2006**, *57*, 233–266. [CrossRef]
4. Bastias, D.A.; Martínez-Ghersa, M.A.; Ballaré, C.L.; Gundel, P.E. *Epichloë* fungal endophytes and plant defenses: Not just alkaloids. *Trends Plant Sci.* **2017**, *22*, 939–948. [CrossRef]
5. De Vries, F.T.; Griffiths, R.I.; Knight, C.G.; Nicolitch, O.; Williams, A. Harnessing rhizosphere microbiomes for drought-resilient crop production. *Science* **2020**, *368*, 270–274. [CrossRef]
6. Schardl, C.L.; Florea, S.; Pan, J.; Nagabhyru, P.; Bec, S.; Calie, P.J. The epichloae: Alkaloid diversity and roles in symbiosis with grasses. *Curr. Opin. Plant Biol.* **2013**, *16*, 480–488. [CrossRef] [PubMed]
7. Leuchtmann, A. Systematics, distribution, and host specificity of grass endophytes. *Nat. Toxins* **1992**, *1*, 150–162. [CrossRef] [PubMed]
8. Omacini, M.; Semmartin, M.; Perez, L.I.; Gundel, P.E. Grass-endophyte symbiosis: A neglected aboveground interaction with multiple belowground consequences. *Appl. Soil Ecol.* **2012**, *61*, 273–279. [CrossRef]
9. Kauppinen, M.; Saikkonen, K.; Helander, M.; Pirttilä, A.M.; Wäli, P.R. *Epichloë* grass endophytes in sustainable agriculture. *Nat. Plants* **2016**, *2*, 15224. [CrossRef]
10. Schardl, C.L.; Leuchtmann, A.; Spiering, M.J. Symbioses of grasses with seedborne fungal endophytes. *Annu. Rev. Plant Biol.* **2004**, *55*, 315–340. [CrossRef]
11. Ju, Y.; Sacalis, J.N.; Still, C.C. Bioactive flavonoids from endophyte-infected blue grass (*Poa ampla*). *J. Agric. Food Chem.* **1998**, *46*, 3785–3788. [CrossRef]

12. Scott, B.; Green, K.; Berry, D. The fine balance between mutualism and antagonism in the *Epichloë festucae*-grass symbiotic interaction. *Curr. Opin. Plant Biol.* **2018**, *44*, 32–38. [CrossRef] [PubMed]
13. Perez, L.I.; Gundel, P.E.; Parisi, P.A.G.; Moyano, J.; Fiorenza, J.E.; Omacini, M.; Nunez, M.A. Can seed-borne endophytes promote grass invasion by reducing host dependence on mycorrhizas? *Fungal Ecol.* **2021**, *52*, 101077. [CrossRef]
14. Zhong, R.; Xia, C.; Ju, Y.W.; Zhang, X.X.; Duan, T.Y.; Nan, Z.B.; Li, C.J. A foliar *Epichloë* endophyte and soil moisture modified belowground arbuscular mycorrhizal fungal biodiversity associated with *Achnatherum inebrians*. *Plant Soil* **2021**, *458*, 105–122. [CrossRef]
15. Arrieta, A.M.; Iannone, L.J.; Scervino, J.M.; Vignale, M.V.; Novas, M.V. A foliar endophyte increases the diversity of phosphorus-solubilizing rhizospheric fungi and mycorrhizal colonization in the wild grass Bromus auleticus. *Fungal Ecol.* **2015**, *17*, 146–154. [CrossRef]
16. Johnson, L.J.; de Bonth, A.C.M.; Briggs, L.R.; Caradus, J.R.; Finch, S.C.; Fleetwood, D.J.; Fletcher, L.R.; Hume, D.E.; Johnson, R.D.; Popay, A.J.; et al. The exploitation of epichloae endophytes for agricultural benefit. *Fungal Divers.* **2013**, *60*, 171–188. [CrossRef]
17. Wu, R.H.; Liu, H.; Wu, M.; Ren, A.Z.; Gao, Y.B. Effects of *Epichloë* endophytes of *Achnatherum sibiricum* on spore germination of arbuscular mycorrhizal fungi. *Chin. J. Appl. Ecol.* **2018**, *29*, 4145–4151, (In Chinese with English Abstract).
18. Novas, M.V.; Iannone, L.J.; Godeas, A.M.; Scervino, J.M. Evidence for leaf endophyte regulation of root symbionts: Effect of Neotyphodium endophytes on the pre-infective state of mycorrhizal fungi. *Symbiosis* **2011**, *55*, 19–28. [CrossRef]
19. Vignale, M.V.; Iannone, L.J.; Scervino, J.M.; Novas, M.V. *Epichloë* exudates promote in vitro and in vivo arbuscular mycorrhizal fungi development and plant growth. *Plant Soil* **2018**, *422*, 267–281. [CrossRef]
20. Guo, J.Q.; Rebecca, M.; McNear, D.H. Tall fescue cultivar and fungal endophyte combinations influence plant growth and root exudate composition. *Front. Plant Sci.* **2015**, *6*, 183. [CrossRef]
21. Patchett, A.; Newman, J.A. Comparison of plant metabolites in root exudates of *Lolium perenne* infected with different strains of the fungal endophyte *Epichloë festucae* var. *lolii*. *J. Fungi* **2021**, *7*, 148. [CrossRef] [PubMed]
22. Hager, H.; Gailis, M.; Newman, J. Allelopathic effects of *Epichloë* fungal endophytes: Experiment and meta-analysis. *Plant Soil* **2022**, 1–16. [CrossRef]
23. Hedges, L.V.; Gurevitch, J.; Curtis, P.S. The meta-analysis of response ratios in experimental ecology. *Ecology* **1999**, *80*, 1150–1156. [CrossRef]
24. Gurevitch, J.; Curtis, P.S.; Jones, M.H. Meta-analysis in ecology. *Adv. Ecol. Res.* **2001**, *32*, 199–247.
25. Mack, K.M.L.; Rudgers, J.A. Balancing multiple mutualists: Asymmetric interactions among plants, arbuscular mycorrhizal fungi, and fungal endophytes. *Oikos* **2008**, *117*, 310–320. [CrossRef]
26. Brundrett, M.C. Coevolution of roots and mycorrhizas of land plants. *New Phytol.* **2002**, *154*, 275–304. [CrossRef] [PubMed]
27. Rostás, M.; Cripps, M.G.; Silcock, P. Aboveground endophyte affects root volatile emission and host plant selection of a belowground insect. *Oecologia* **2015**, *177*, 487–497. [CrossRef]
28. Scervino, J.M.; Ponce, M.A.; Erra-Bassells, R.; Vierheilig, H.; Ocampo, J.A.; Godeas, A. Flavonoids exhibit fungal species and genus specific effects on the presymbiotic growth of *Gigaspora* and *Glomus*. *Mycol. Res.* **2005**, *109*, 789–794. [CrossRef]
29. Jiang, Y.N.; Wang, W.X.; Xie, Q.J.; Liu, N.; Liu, L.X.; Wang, D.P.; Zhang, X.W.; Yang, C.; Chen, X.Y.; Tang, D.Z.; et al. Plants transfer lipids to sustain colonization by mutualistic mycorrhizal and parasitic fungi. *Science* **2017**, *356*, 1172–1175. [CrossRef]
30. Souza, T. *Handbook of Arbuscular Mycorrhizal Fungi*; Springer International Publishing: Cham, Switzerland, 2015.
31. Antunes, P.M.; Miller, J.; Carvalho, L.M.; Klironomos, J.N.; Newman, J.A. Even after death the endophytic fungus of *Schedonorus phoenix* reduces the arbuscular mycorrhizas of other plants. *Funct. Ecol.* **2008**, *22*, 912–918. [CrossRef]
32. Siegrist, J.; McCulley, R.; Bush, L.; Phillips, T. Alkaloids may not be responsible for endophyte-associated reductions in tall fescue decomposition rates. *Funct. Ecol.* **2010**, *24*, 460–468. [CrossRef]
33. Gundel, P.E.; Helander, M.; Garibaldi, L.A.; Vázquez-de-Aldana, B.R.; Zabalgogeazcoa, I.; Saikkonen, K. Direct and indirect effects of the fungal endophyte *Epichloë uncinatum* on litter decomposition of the host grass, *Schedonorus pratensis*. *Plant Ecol.* **2017**, *218*, 1107–1115. [CrossRef]
34. Franzluebbers, A.J.; Hill, N.S. Soil carbon, nitrogen, and ergot alkaloids with short- and long-term exposure to endophyte-infected and endophyte-free tall fescue. *Soil Sci. Soc. Am. J.* **2005**, *69*, 404–412. [CrossRef]
35. de Carvalho, P.L.N.; Silva, E.O.; Chagas-Paula, D.A.; Hortolan Luiz, J.H.; Ikegaki, M. Importance and implications of the production of phenolic secondary metabolites by endophytic fungi: A mini-review. *Mini Rev. Med. Chem.* **2016**, *16*, 259–271. [CrossRef] [PubMed]
36. Ponce, M.A.; Bompadre, M.J.; Scervino, J.M.; Ocampo, J.A.; Chaneton, E.J.; Godeas, A.M. Flavonoids, benzoic acids and cinnamic acids isolated from shoots and roots of Italian rye grass (*Lolium multiflorum* Lam.) with and without endophyte association and arbuscular mycorrhizal fungus. *Biochem. Syst. Ecol.* **2009**, *37*, 245–253. [CrossRef]
37. Slaughter, L.C.; McCulley, R.L. Aboveground *Epichloë coenophiala*-grass associations do not affect belowground fungal symbionts or associated plant, soil parameters. *Microb. Ecol.* **2016**, *72*, 682–691. [CrossRef]
38. Bell-Dereske, L.; Takacs-Vesbach, C.; Kivlin, S.N.; Emery, S.M.; Rudgers, J.A. Leaf endophytic fungus interacts with precipitation to alter belowground microbial communities in primary successional dunes. *FEMS Microb. Ecol.* **2017**, *93*, fix036. [CrossRef]
39. Ding, N.; Guo, H.; Kupper, J.V.; McNear, D.H. Phosphorus source and *Epichloe coenophiala* strain interact over time to modify tall fescue rhizosphere microbial community structure and function. *Soil Biol. Biochem.* **2021**, *154*, 208125. [CrossRef]

40. van Hecke, M.M.; Treonis, A.M.; Kaufman, J.R. How does the fungal endophyte *Neotyphodium coenophialum* affect tall fescue (*Festuca arundinacea*) rhizodeposition and soil microorganisms? *Plant Soil* **2005**, *275*, 101–109. [CrossRef]
41. Chen, J.; Deng, Y.K.; Yu, X.H.; Wu, G.H.; Gao, Y.B.; Ren, A.Z. *Epichloë* endophyte infection changes the root endosphere microbial community composition of *Leymus chinensis* under both potted and field growth conditions. *Microb. Ecol.* **2022**, 1–13. [CrossRef]
42. Cui, X.L.; Zhang, X.X.; Shi, L.; Christensen, M.J.; Nan, Z.B.; Xia, C. Effects of *Epichloë* endophyte and transgenerational effects on physiology of *Achnatherum inebrians* under drought stress. *Agriculture* **2022**, *12*, 761. [CrossRef]
43. Xia, C.; Christensen, M.J.; Zhang, X.X.; Nan, Z.B. Effect of *Epichloë gansuensis* endophyte and transgenerational effects on the water use efficiency, nutrient and biomass accumulation of *Achnatherum inebrians* under soil water deficit. *Plant Soil* **2018**, *424*, 555–571. [CrossRef]
44. Zhong, R.; Bastías, D.A.; Zhang, X.X.; Li, C.J.; Nan, Z.B. Vertically transmitted *Epichloë* systemic endophyte enhances drought tolerance of *Achnatherum inebrians* host plants through promoting photosynthesis and biomass accumulation. *J. Fungi* **2022**, *8*, 512. [CrossRef] [PubMed]
45. Malinowski, D.P.; Alloush, G.A.; Belesky, D.P. Evidence for chemical changes on the root surface of tall fescue in response to infection with the fungal endophyte *Neotyphodium coenophialum*. *Plant Soil* **1998**, *205*, 1–12. [CrossRef]
46. Novas, M.V.; Iannone, L.J.; Godeas, A.M.; Cabral, D. Positive association between mycorrhiza and foliar endophytes in *Poa bonariensis*, a native grass. *Mycol. Progress* **2008**, *8*, 75. [CrossRef]
47. Casas, C.; Gundel, P.E.; Deliens, E.; Iannone, L.J.; Martinez, G.G.; Vignale, M.V.; Schnyder, H. Loss of fungal symbionts at the arid limit of the distribution range in a native Patagonian grass-Resource eco-physiological relations. *Funct. Ecol.* **2022**, *36*, 583–594. [CrossRef]
48. Liu, H.; Wu, M.; Liu, J.M.; Qu, Y.B.; Gao, Y.B.; Ren, A.Z. Tripartite interactions between endophytic fungi, arbuscular mycorrhizal fungi, and *Leymus chinensis*. *Microb. Ecol.* **2020**, *79*, 98–109. [CrossRef]
49. Liu, Q.H.; Parsons, A.J.; Xue, H.; Fraser, K.; Ryan, G.D.; Newman, J.A.; Rasmussen, S. Competition between foliar *Neotyphodium lolii* endophytes and mycorrhizal *Glomus* spp. fungi in *Lolium perenne* depends on resource supply and host carbohydrate content. *Funct. Ecol.* **2011**, *25*, 910–920. [CrossRef]

agriculture

MDPI

Article

Growth, Sporulation, Conidial Germination and Lethal Temperature of *Paraphoma radicina*, A Fungal Pathogen of Alfalfa (*Medicago sativa*) Root Rot

Shi Cao [1,*] and Yan-Zhong Li [2,*]

[1] Biocontrol Engineering Laboratory of Crop Diseases and Pests of Gansu Province, College of Plant Protection, Gansu Agricultural University, Lanzhou 730070, China
[2] State Key Laboratory of Grassland Agro-Ecosystems, Key Laboratory of Grassland Livestock Industry Innovation, Ministry of Agriculture and Rural Affairs, Engineering Research Center of Grassland Industry, Ministry of Education, College of Pastoral Agriculture Science and Technology, Lanzhou University, Lanzhou 730020, China
* Correspondence: caosh15@lzu.edu.cn (S.C.); liyzh@lzu.edu.cn (Y.-Z.L.); Tel.: +86-153-4931-2372 (Y.-Z.L.)

Abstract: In 2020, alfalfa root rot, a disease caused by *Paraphoma radicina*, was identified in Inner Mongolia, China, where it seriously affected alfalfa crop yields. Conditions for in vitro growth, sporulation and conidial germination of *P. radicina* are poorly understood, limiting further studies. In this contribution, we evaluated the suitability of different media, carbon and nitrogen sources, as well as temperature and pH for *P. radicina* in vitro growth and germination. In addition, the temperature sensitivity of these cultures was assessed. *Paraphoma radicina* growth and sporulation were most vigorous on the ARDA medium, reaching the maximum growth and sporulation rates after 4 weeks of incubation. All carbon and nitrogen sources supported growth, but none induced sporulation. The best carbon and nitrogen sources for growth were mannitol and peptone, respectively. Conidial germination was observed in the 4 to 35 °C temperature range, with an optimum temperature of 25 °C. The germination rate was highest at pH 7, and more than 50% of conidia germinated after 38 h of incubation at 25 °C. On the other hand, temperatures above 55 °C (10 min) and 41 °C (10 min) proved lethal for the mycelial and conidial forms of the pathogen, respectively. These results can provide clues to the environmental conditions amenable for *P. radicina* infection of alfalfa crops and, on the whole, a better understanding of pathogenicity.

Keywords: *Paraphoma radicina*; growth; sporulation; conidial germination; lethal temperature

Citation: Cao, S.; Li, Y.-Z. Growth, Sporulation, Conidial Germination and Lethal Temperature of *Paraphoma radicina*, A Fungal Pathogen of Alfalfa (*Medicago sativa*) Root Rot. *Agriculture* **2022**, *12*, 1501. https://doi.org/10.3390/agriculture12091501

Academic Editor: Alessandro Vitale

Received: 17 August 2022
Accepted: 16 September 2022
Published: 19 September 2022

1. Introduction

Fungal root rot is a common disease in alfalfa crops in several areas of the world, including the USA, Canada, Australia, Iran and China [1–5]. Root rot induces discoloration of the infected tissues and subsequent development of black and necrotic areas, often leading to alfalfa plant death. A variety of plant pathogenic fungi has been reported to induce root rot in alfalfa, such as *Fusarium* spp. [1,6], *Pythium* sp. [7,8], *Phytophthora* sp. [9,10], *Mycoleptodiscus terrestris* [11,12], *Microdochium tabacinum* [13], *Rhizoctonia solani* [14] and *Phoma sclerotioides* [2]. *Paraphoma radicina* was reported to be a new pathogen causing alfalfa root rot in Inner Mongolia, China, and pathogenicity experiments showed that *P. radicina* is significantly detrimental to alfalfa growth [15].

Paraphoma radicina is the type species of the genus *Paraphoma*, although it was originally named *Phoma radicina* [16]. The fungus was initially described in isolates obtained from cysts of *Heterodera glycines* in North Carolina, USA, in soybean field soils [17]. Subsequently, it was also recorded on *H. glycines* in Shenyang, China [18]. *Paraphoma radicina* was previously reported as a saprophytic species on the roots of herbaceous and woody plants [16]. However, in a previous publication, we showed this species to be able to infect

alfalfa roots and cause severe root rot [15]. Pycnidia of *P. radicina* are commonly present on black necrotic root tissue of diseased alfalfa. Pycnidia formed on the diseased plant tissue were found to contain many viable conidia, which are believed to serve as inocula in alfalfa infection. Since the teleomorph of the fungus is still unknown [19], it is considered that conidia play an important role in the spread of the disease and, therefore, conidial germination may be an important factor for successful infection.

Conidial germination, sporulation, colonization and mycelial growth of fungi are greatly influenced by nutritional and environmental factors [20–22]. However, information on the influence of these factors on the biological and physiological characteristics of *P. radicina* is currently limited. The effects of temperature and pH on mycelial growth have been previously evaluated [15], where it was found difficult to induce conidiation of *P. radicina* in vitro, which may limit further studies on effective disease control. In the present study, our objectives were to determine the effect of (i) culture media on mycelial growth and conidial production, (ii) carbon and nitrogen sources on growth and (iii) temperature and pH on conidial germination, and to determine the lethal temperature of *P. radicina*. The outcome of the research described here will contribute to a greater understanding of the etiological agent of the alfalfa root rot epidemic to guide strategies for preventing the spread of this disease and mitigate potential crop yield losses in China.

2. Materials and Methods

2.1. Biological Material

Isolates of *P. radicina* were obtained from root tissues of diseased alfalfa plants in Chifeng city, Inner Mongolia, China. The type isolate of *P. radicina* (LYZ187) used in all experiments was that previously obtained [15]. Pure cultures of *P. radicina* were grown on potato dextrose agar (PDA) at 25 °C and L:D 0:24 h for four weeks for later use as inocula. Mycelial plugs (5 mm diameter) were aseptically cut from the margins of actively growing colonies with a sterile cork borer and transferred to a new PDA Petri dish. Plates were inoculated by placing plugs face down on each dish, with five replicates per treatment. The dishes were sealed with laboratory film (Parafilm^{TM}, Oshkosh, WI, USA) and randomly arranged in a 25 °C incubator.

2.2. Mycelial Growth and Sporulation of P. Radicina on Different Agar Media

The growth of *P. radicina* was assessed on eight different media (Table 1). All agar media were autoclaved at 121 °C for 20 min prior to being poured into individual Petri dishes. Colony shape and color were observed in the first week either by the eye or under a dissecting microscope. Photographs were taken with a Handheld Canon DS126391 camera and colony features were recorded. Colony diameters were measured weekly for four weeks, and growth rates were calculated as the colony diameter with less than five millimeters of mycelial plugs. After one week of incubation, five milliliters of sterilized distilled water were added to each plate, and the colony surface was gently scraped with a sterilized glass spreader to dislodge conidia. The resulting suspension was filtered through sterile gauze, and the procedure was repeated with another five milliliters of water. The combined conidial suspension volume was measured, and the concentration of conidiospores was estimated with a hemacytometer. The collection of conidiospores was repeated after four weeks of incubation [23].

Table 1. Test media and the preparation method.

Media Name	Ingredients and Preparation Method [1,2]
Potato dextrose agar (PDA)	200 g fresh potato, 20 g dextrose, distilled water 1000 mL
Oatmeal agar (OA)	30 g oatmeal (boiled in distilled water for 1 h, then filtered through 2-layer gauze), distilled water 1000 mL
Pine needle agar (PNA)	100 g fresh pine needle (take the filtrate after boiling for 1 h), 10 g dextrose, 5 g peptone, 1 g K_2HPO_4, 0.5 g $MgSO_4 \cdot 7H_2O$, distilled water 200 mL
Malt extract agar (MEA)	30 g malt extract, 3 g peptone, distilled water 1000 mL
Potato carrot agar (PCA)	20 g fresh potato, 20 g fresh carrot, distilled water 1000 mL
Cherry decoction agar (CHA)	200 g fresh cherry (extract the juice with a juicer, and boiled in distilled water for 30 min, then filtered through 2-layer gauze), distilled water 1000 mL
V-8 juice agar (V8A)	3 g $CaCO_3$, 200 mL V-8 juice
Alfalfa root decoction agar (ARDA)	100 g clean alfalfa root (cut the root into small pieces, boiled for 30 min and filtered), distilled water 1000 mL

[1] Each 1000 mL media contained 17 g agar. [2] PDA, OA, MEA, CHA and V8A were prepared as described by Crous et al. [24]. PNA as defined by Wu [25]. PCA was prepared according to the method of Li and Nan [26]. ARDA was self-prepared.

2.3. Effects of Carbon and Nitrogen Sources on Growth

For carbon source suitability experiments, nine carbon compounds were assessed for their ability to support mycelial growth. The basal medium consisted of 20 g of dextrose, 5 g of KNO_3, 2 g of Na_3PO_4, 1 g of $MgSO_4$, 17 g of agar and up to 1000 mL of distilled water; the other eight carbon sources were sucrose, mannitol, fructose, D-xylose, lactose, soluble starch, maltose and cellulose. Dextrose in the basal medium was replaced with 20 g of each carbon source to prepare individual formulations to be tested [26]. Growth rates, measured as the colony diameter, were monitored for four weeks.

Seven nitrogen compounds were assessed for their ability to support mycelial growth: Peptone, urea, ammonium nitrate, ammonium chloride, glycine, sodium nitrate and ammonium sulfate. Five grams of each nitrogen source were added to the basal media (20 g of dextrose, 2 g of Na_3PO_4, 1 g of $MgSO_4$, 17 g of agar and up to 1000 mL of distilled water) to prepare individual formulations to be tested. Inoculated media were incubated in the dark at 25 °C.

2.4. Effect of Temperature and pH on Conidial Germination

To determine the optimal temperature for conidial germination of *P. radicina*, conidial suspensions in sterile distilled water were adjusted to 1.0×10^6 spores/mL with a hemacytometer. Using the slide technique [27], a 10 µL drop of a conidial suspension was placed in a cavity slide using a micropipette. The slide was then placed onto the well of a 90 mm plastic Petri plate on top of a moist filter paper to maintain the humidity level. The plates were sealed with parafilm and incubated (L:D 0:24 h) at 4, 10, 15, 20, 25, 28, 30 or 35 °C, respectively. Treatments were replicated three times. Conidial germination was monitored every four hours through microscopic observation at ×400 magnification using an Olympus CX31 microscope (Olympus, Tokyo, Japan). Samples were observed continuously for 38 h until there were no new conidia germinating. The conidial germination rate was determined by counting conidia in 30 randomly selected fields on each plate. A conidium was considered germinated if the germ tube was at least one-half the length of the conidium.

To assess the effect of pH on conidial germination, sterile water was adjusted to pH 4, 5, 6, 7, 8, 9 or 10 by the addition of 0.1 M NaOH or HCl prior to the preparation of conidial suspensions. These suspensions were allowed to germinate while being kept moist using the slide technique described above. All Petri dishes were incubated at 25 °C in the dark. Observation and evaluation of the conidial germination were carried out as described above.

2.5. Lethal Temperature of Mycelium and Conidia

Mycelial plugs (5 mm diameter) were placed in a sterilized test tube, and then the tubes were placed in a thermostat water bath at 40–55 °C (temperature gradient: 1 °C) for 10 min (preheating: One minute). After cooling, the plugs were taken out and placed face down on PDA media dishes. All plates were incubated for one week at 25 °C in the dark to evaluate mycelial growth capability.

To determine the lethal temperature for conidia, 2 mL of a conidial suspension was taken into sterilized test tubes and subjected to heat treatment as described above. Conidial viability was determined by measuring the germination rate after 34 h in cavity slides as described [28].

2.6. Data Analysis

Growth rate, sporulation and conidial germination rate data were subjected to analysis using SPSS Statistics 21 analysis software (SPSS Inc., Chicago, IL, USA) using descriptive statistics, one-way ANOVA and the Duncan test with $p \leq 0.05$ as the significance threshold. The effects of carbon and nitrogen sources on growth were statistically analyzed by the least significant difference (LSD) and Duncan tests ($p \leq 0.05$).

3. Results

3.1. Suitability of Media for Growth and Sporulation

P. radicina was able to grow on all media. Aerial mycelia were compact, floccose or cottony after one week of cultivation on PDA, PNA, MEA, CHA and V8A. Conversely, marginal hyphae were sparse on OA, PCA and ARDA, where they were concentrated at the center of the colonies, and the hyphae grew first vertically and then horizontally. On OA, the colony color appeared pale luteous, with a pale olivaceous grey mycelium (Figure S1).

After four weeks of incubation on PDA, OA, PNA, MEA, PCA, CHA, V8A and ARDA media dishes, growth rates ranged from 0.21 to 0.30 cm/d, with the largest growth rate observed on ARDA. Growth rates were in the order ARDA > OA > V8A > CHA > MEA > PCA > PNA > PDA, where the growth rates on ARDA, OA and V8A were significantly greater than those measured in other media ($p \leq 0.05$) (Table 2).

Table 2. Mean (±SEM) growth rates and sporulation of *Paraphoma radicina* on eight different media grown at L:D 0:24 h and 25 °C and measured one and four weeks after inoculation.

Media	4 Weeks Growth Rate (cm/d)	Sporulation (10^6 Conidia/mL)	
		1 Week	4 Weeks
PDA	0.21 ± 0.08 c [1]	/ [2]	1.18 ± 0.48 b
OA	0.29 ± 0.01 a	/	/
PNA	0.23 ± 0.01 bc	/	/
MEA	0.24 ± 0.03 b	/	/
PCA	0.23 ± 0.00 b	/	/
CHA	0.25 ± 0.00 b	/	/
V8A	0.28 ± 0.01 a	/	/
ARDA	0.30 ± 0.01 a	1.20 ± 0.37	17.85 ± 7.35 a

[1] The growth rate on each media was calculated by dividing the colony diameter by the number of days. Means with different letters in the same column are significantly different according to Duncan's test at $p \leq 0.05$. [2] / = No sporulation.

The fungus produced no conidia on OA, PNA, MEA, PCA, CHA and V8A after four weeks, but did sporulate on PDA and ARDA. On ARDA, the sporulation was 1.20×10^6 conidia/mL after one week and 17.85×10^6 conidia/mL after four weeks. On the other hand, no conidia were produced on PDA after one week, but 1.18×10^6 conidia/mL were recorded after four weeks. The sporulation was significantly greater on ARDA than PDA after four weeks of incubation ($p \leq 0.05$) (Table 2).

3.2. Effects of Carbon and Nitrogen Sources on Growth

All carbon sources supported the growth of *P. radicina,* but vigor varied substantially between media with different carbon sources. From one to four weeks, the colony diameter increased significantly with the incubation time in all carbon sources tested (Table 3). The diameter of the *P. radicina* colonies was the largest on the lactose medium after one week; this was significantly greater when compared with other carbon sources. After four weeks, this fungus exhibited the largest colony diameter on mannitol, soluble starch, lactose and sucrose, and the least vigorous growth on cellulose. Growth on cellulose was the least vigorous. After four weeks, *P. radicina* growth on mannitol, soluble starch, lactose, sucrose and D-xylose was significantly greater than on the other media. Out of the nine compounds tested, the carbon source best supporting *P. radicina* growth was mannitol, while cellulose was barely utilized by this fungus (Table 3).

Table 3. Mean (±SEM) colony diameter (cm) of *Paraphoma radicina* measured weekly for four weeks on different carbon sources and at L:D 0:24 h and 25 °C.

Carbon Source	Colony Diameter (cm)			
	1 Week	2 Weeks	3 Weeks	4 Weeks
Dextrose	2.47 ± 0.06 d [1]	4.33 ± 0.35 c	6.43 ± 0.32 b	7.27 ± 0.06 a
Sucrose	3.00 ± 0.00 c	5.40 ± 0.20 b	7.47 ± 0.06 a	7.73 ± 0.21 a
Mannitol	2.97 ± 0.06 d	5.80 ± 0.10 c	7.50 ± 0.20 b	7.83 ± 0.15 a
Fructose	2.67 ± 0.12 c	4.93 ± 0.60 b	7.03 ± 0.06 a	7.47 ± 0.15 a
D-Xylose	2.83 ± 0.15 d	5.53 ± 0.21 c	7.10 ± 0.53 b	7.70 ± 0.10 a
Lactose	3.23 ± 0.21 c	5.80 ± 0.52 b	7.30 ± 0.26 a	7.77 ± 0.06 a
Soluble starch	3.00 ± 0.00 d	5.50 ± 0.10 c	7.53 ± 0.06 b	7.77 ± 0.06 a
Maltose	2.87 ± 0.06 d	4.87 ± 0.21 c	6.47 ± 0.15 b	7.10 ± 0.10 a
Cellulose	2.40 ± 0.10 d	4.47 ± 0.06 c	6.37 ± 0.12 b	6.93 ± 0.15 a
LSD $_{(p<0.05)}$ [2]	0.181	0.544	0.420	0.216

[1] Treatment means with different letters across the four assessment periods are significantly different according to Duncan's test at $p \leq 0.05$. [2] Data in the same column are separated by the least significant different (LSD) ($p \leq 0.05$).

The ability of *P. radicina* to grow on media with different nitrogen sources was variable. Growth on the peptone medium was significantly greater than those on other nitrogen sources after one week. The colony diameter of *P. radicina* was also the largest on the peptone medium after four weeks of incubation, and was significantly greater than on glycine and urea, but not significantly different from other nitrogen sources (Table 4). The nitrogen source best supporting the growth of *P. radicina* was peptone, while glycine and urea were deficient sources for fungal growth.

Table 4. Mean (±SEM) colony diameter of *Paraphoma radicina* on seven different nitrogen sources grown at L:D 0:24 h and 25 °C, measured one and four weeks after inoculation.

Nitrogen Sources	Colony Diameter (cm)	
	1 Week	4 Weeks
Peptone	3.00 ± 0.00 c [1]	7.07 ± 0.15 a
Urea	1.67 ± 0.06 d	6.23 ± 0.15 a
Ammonium nitrate	2.67 ± 0.06 c	6.73 ± 0.12 a
Ammonium chloride	2.53 ± 0.06 c	6.77 ± 0.06 a
Glycine	3.00 ± 0.10 b	5.17 ± 0.81 a
Sodium nitrate	2.77 ± 0.06 c	6.70 ± 0.17 a
Ammonium sulfate	2.60 ± 0.10 c	6.70 ± 0.20 a
LSD$_{(p<0.05)}$ [2]	0.121	0.591

[1] Treatment means with different letters across the two assessment periods are significantly different according to Duncan's test at $p \leq 0.05$. [2] Data in the same column are separated by the least significant different (LSD) ($p \leq 0.05$).

The fungus produced no conidia on either of the nine carbon sources media or on the seven nitrogen source media tested in our experiments.

3.3. Effect of Temperature and pH on Conidial Germination

Conidia of *P. radicina* were able to germinate in the range of 4–35 °C, but the time of the onset of germination varied with temperature. Regardless, conidial germination onset was not observed earlier than 14 h at any temperature tested. Indeed, conidial germination was initiated at 18 h after incubation at 20, 25 and 28 °C, while the onset of germination was at 22 h, 26 h and 30 h at 30, 15 and 35 °C, respectively; lastly, initial germination was observed after 34 h at 4 °C and 10 °C. The conidial germination rate reached a maximum after 34 h at all temperature treatments and remained constant afterward (Table 5). When compared within any set time, percentages of conidial germination increased in the 4 to 25 °C range, where a maximum was observed, and then decreased with increasing temperature. After incubation for 38 h at 25 °C, germination reached a maximum of 52.36%, which was significantly greater than that observed at other temperatures. In contrast, germination rates at 4 and 35 °C were 1.14% and 1.92%, respectively, significantly smaller than those observed in other treatments (Table 5). Therefore, the observed optimum temperature for conidial germination of *P. radicina* was determined as 25 °C.

Table 5. Conidial germination rate (%) of *Paraphoma radicina* at varying temperatures and measured across seven time intervals.

Temperature (°C)	Incubation Time (h)						
	14	18	22	26	30	34	38
4	0.00 ± 0.00 a [1]	0.00 ± 0.00 c	0.00 ± 0.00 d	0.00 ± 0.00 e	0.00 ± 0.00 d	1.14 ± 0.89 e	1.14 ± 0.89 e
10	0.00 ± 0.00 a	0.00 ± 0.00 c	0.00 ± 0.00 d	0.00 ± 0.00 e	0.00 ± 0.00 d	8.22 ± 3.11 d	8.22 ± 3.11 d
15	0.00 ± 0.00 a	0.00 ± 0.00 c	0.00 ± 0.00 d	1.98 ± 1.73 de	4.36 ± 2.28 d	14.30 ± 2.42 c	14.30 ± 2.42 c
20	0.00 ± 0.00 a	4.13 ± 2.03 b	6.50 ± 4.18 c	11.31 ± 5.13 c	17.07 ± 5.22 bc	25.71 ± 2.75 b	25.71 ± 2.75 b
25	0.00 ± 0.00 a	14.27 ± 3.81 a	22.48 ± 4.51 a	34.32 ± 6.66 a	44.25 ± 12.72 a	52.36 ± 4.74 a	52.36 ± 4.74 a
28	0.00 ± 0.00 a	6.77 ± 3.64 b	14.49 ± 4.81 b	18.88 ± 2.13 b	21.93 ± 6.19 b	24.88 ± 5.03 b	24.88 ± 5.03 b
30	0.00 ± 0.00 a	0.00 ± 0.00 c	4.85 ± 3.57 c	6.86 ± 1.96 cd	12.88 ± 6.27 c	17.16 ± 2.07 c	17.16 ± 2.07 c
35	0.00 ± 0.00 a	0.00 ± 0.00 c	0.00 ± 0.00 d	0.00 ± 0.00 e	1.65 ± 1.42 d	1.92 ± 1.50 e	1.92 ± 1.50 e

[1] Means with different letters in the same column are significantly different according to Duncan's test at $p \leq 0.05$.

Conidia of *P. radicina* had the highest germination rate at 25 °C, with the onset of germination at 18 h. On the other hand, the germination rate displayed no changes after 38 h, compared with the previous time set. Therefore, those conditions were chosen to assess the effect of pH on the conidial germination rate. Conidia of *P. radicina* were able to germinate across all pH levels tested. Both after 18 h or 38 h of incubation in sterile water at different pH, the germination rate increased as pH values increased from pH 4 to pH 7, with a maximum rate observed at pH 7. The germination rate then decreased as the pH increased from pH 7 to pH 10. Furthermore, at their maxima, after 18 h and 38 h of incubation, the values observed (43.83 % and 57.92 %, respectively) were significantly greater than those found at any other pH (Table 6). Therefore, the optimum pH value for conidial germination of *P. radicina* was determined to be pH 7.

Table 6. Conidial germination rate (%) of *Paraphoma radicina* at seven pH values at 18 and 38 h. Grown at 25°C and L:D 0:24.

pH	Incubation Time (h)	
	18	38
4	19.78 ± 4.92 b [1]	21.96 ± 3.44 c
5	20.58 ± 1.69 b	22.41 ± 3.33 c
6	20.93 ± 1.99 b	24.13 ± 5.36 c
7	43.83 ± 6.03 a	57.92 ± 5.90 a
8	6.25 ± 1.59 c	36.24 ± 1.97 b
9	3.14 ± 0.53 cd	28.35 ± 7.55 c
10	1.54 ± 0.44 d	26.03 ± 10.05 c

[1] Means with different letters in the same column are significantly different according to Duncan's test at $p \leq 0.05$.

3.4. Lethal Temperature of Mycelium and Conidia

Mycelia of *P. radicina* were able to grow after 10 min of heat treatment at temperatures in the range of 35 to 54 °C. Nevertheless, mycelia were found to be unable to grow at temperatures greater than or equal to 55 °C (Table S1). On the other hand, conidia were found to be able to germinate after 10 min of heat treatment in a water bath at 35 and 40 °C only, with observed germination rates of 15.12% and 6.77%, respectively. However, in our hands, conidia no longer germinated when the temperature was greater than or equal to 41 °C (Table S1). Thus, the lethal temperatures for *P. radicina* mycelial growth and conidial germination determined were 55 °C (10 min) and 41 °C (10 min), respectively.

4. Discussion

The establishment of a successful parasitic relationship between fungal pathogens and their hosts is influenced to varying degrees by environmental conditions [20,29]. Therefore, the elucidation of the factors influencing fungal growth, sporulation and conidial germination is of practical importance to devise better disease control strategies.

In earlier research, the aerial mycelium of *P. radicina* was described as pale olivaceous on OA medium and the colony color as pale luteous due to the production of a diffusible pigment [16]. Our initial results after evaluating the colony characteristics of *P. radicina* on various media agreed with those previously reported. In the present study, we evaluated the effects of eight media on conidia production of *P. radicina* and demonstrated that it was able to produce pycnidia and conidia only on PDA and ARDA media, while few conidia were generated on PDA. This is in agreement with earlier studies where it was also reported that pycnidia and conidia of *P. radicina* were not produced abundantly on the PDA medium [17]. Furthermore, in this study, we found that conidia of *P. radicina* were not produced on OA. Conversely, previous authors mentioned that the fungus produced abundant pycnidia on OA [16]. This discrepancy is likely due to differences in culture conditions. Our research showed that *P. radicina* displayed the greatest growth rate and sporulation on the ARDA medium, indicating that ARDA is the optimal medium for *P. radicina* culture.

This research also showed that *P. radicina* was able to use all tested carbon and nitrogen sources. After four weeks of incubation, the fungus showed significantly that the most vigorous growth was attained when mannitol was used as a carbon source, and when peptone was used as a nitrogen source. These attributes have been found in other fungal pathogens. For example, the growth rate of *Embellisia astragali* was reported to be greatest on mannitol and peptone after four weeks [26]. External nutrients can promote conidia production in some pathogenic fungi. Thus, *Verticillium alfalfa* displayed excellent sporulation on lactose and starch, and the greatest sporulation rate on peptone [30]. Furthermore, when the carbon nutritional requirements of *Phoma medicaginis* were studied, it was found that monosaccharides and disaccharides were nearly equivalent in the production of pycnidia, but superior to polysaccharides [31]. The same study reported that the formation of pycnidia and conidia was favored on nitrate more than ammonium nitrogen sources in

P. medicaginis. However, we found no conidia production by *P. radicina* on any of the tested carbon and nitrogen sources. This may indicate that conditions required for sporulation are more demanding compared to other fungi.

Our research showed that the optimal temperature for conidial germination of *P. radicina* was 25 °C. There was little germination at temperatures below 5 °C or above 35 °C. These results were similar to those in earlier reports where other species of fungi from alfalfa were studied [30,32]. In comparison, *P. radicina* mycelia can grow across a wide range of temperatures from 5 to 35 °C, with an optimal temperature in the range of 25 to 30 °C [15]. This finding suggests that *P. radicina* temperature requirements for conidial germination are in general agreement with those for mycelial growth. Of interest was the result showing that the lethal temperature for mycelial growth was greater than that of the conidia. This may be due to the formation of chlamydospores within the mycelium during incubation.

Fungal conidial germination was found early to be influenced by the hydrogen ion concentration in the growth medium [33]. In the present study, we observed that *P. radicina* conidia germinated at pHs ranging from pH 4 to pH 10, with the optimal at pH 7. In a previous report, we found that the optimal pH for mycelial growth of this fungus was within the range of pH 8 to pH 9, and that the growth was slow when the pH of the culture medium was <pH 4 or >pH 10 [15]. Despite this difference in the optimal pH for conidial germination versus mycelial growth, these results indicate that both excessive acidity and alkalinity are detrimental to the growth and conidial germination of *P. radicina*.

5. Conclusions

Our study has identified several factors that affect the growth, sporulation, and conidial germination of *P. radicina* and further defined the lethal temperature for mycelial growth and conidial germination of the fungus. The results indicated that ARDA was the most suitable medium for the growth and sporulation of *P. radicina*. Mannitol and peptone were the best sources of carbon and nitrogen, respectively. The optimal temperature for conidial germination was 25 °C, and the germination rate showed the maximum at pH 7. The lethal temperatures for *P. radicina* mycelial growth and conidial germination were 55 °C (10 min) and 41 °C (10 min), respectively. We believe our findings will contribute to the knowledge of the biological and physiological characteristics of *P. radicina* and assist in the development of disease control measures to mitigate alfalfa crop losses.

Supplementary Materials: The following supporting information can be downloaded at: https://www.mdpi.com/article/10.3390/agriculture12091501/s1. Figure S1: Morphology and characters of *P. radicina* after one week of cultivation on eight media; Table S1: Effect of temperature on *P. radicina* germination and mycelium growth.

Author Contributions: Conceptualization, S.C. and Y.-Z.L.; methodology, S.C. and Y.-Z.L.; software, S.C.; formal analysis, S.C.; investigation, S.C.; resources, Y.-Z.L.; data curation, S.C.; writing—original draft preparation, S.C.; writing—review and editing, Y.-Z.L.; visualization, S.C. and Y.-Z.L.; supervision, Y.-Z.L.; project administration, Y.-Z.L.; funding acquisition, S.C. All authors have read and agreed to the published version of the manuscript.

Funding: This research was financially supported by openly recruited Doctors of Gansu Agricultural University [GAU-KYQD-2020-32].

Institutional Review Board Statement: Not applicable.

Informed Consent Statement: Not applicable.

Data Availability Statement: Not applicable.

Acknowledgments: We thank Clement Nzabanita for his valuable technical assistance during this study. We would like to express gratitude to EditSprings for the expert linguistic services provided. The authors would like to thank the editors and all the reviewers who participated in the review.

Conflicts of Interest: The authors declare no conflict of interest.

References

1. Berg, L.E.; Miller, S.S.; Dornbusch, M.R.; Samac, D.A. Seed rot and damping-off of alfalfa in Minnesota caused by *Pythium* and *Fusarium* species. *Plant Dis.* **2017**, *101*, 1860–1867. [CrossRef] [PubMed]
2. Hollingsworth, C.R.; Gray, F.A.; Groose, R.W. Evidence for the heritability of resistance to brown root rot of alfalfa, caused by *Phoma sclerotioides*. *Can. J. Plant Pathol.* **2005**, *27*, 64–70. [CrossRef]
3. Musial, J.M.; Aitken, K.S.; Mackie, J.M.; Irwin, J.A.G. A genetic linkage map in autotetraploid lucerne adapted to northern Australia, and use of the map to identify DNA markers linked to resistance to *Phytophthora medicaginis*. *Aust. J. Agr Res.* **2005**, *56*, 333–344. [CrossRef]
4. Fatemi, J. Fungi associated with alfalfa root rot in Iran. *Phytopathol. Mediterr.* **1972**, *11*, 163–165. Available online: https://www.jstor.org/stable/42684143 (accessed on 1 June 2022).
5. Fang, X.L.; Zhang, C.X.; Nan, Z.B. Research advances in *Fusarium* root rot of alfalfa (*Medicago sativa*). *Acta Prataculturae Sin.* **2019**, *28*, 169–183.
6. Jiang, D.; Xu, C.Z.; Han, W.B.; Harris-Shultz, K.; Ji, P.S.; Li, Y.G.; Zhao, T.X. Identification of fungal pathogens and analysis of genetic diversity of *Fusarium tricinctum* causing root rots of alfalfa in north-east China. *Plant Pathol.* **2021**, *70*, 804–814. [CrossRef]
7. Basu, P.K. Survey of eastern Ontario alfalfa fields to determine common fungal diseases and predominant soil-borne species of *Pythium* and *Fusarium*. *Can. Plant Dis. Surv.* **1983**, *63*, 51–54.
8. Zhang, C.X.; Wang, Z.N.; Fang, X.L.; Nan, Z.B. Occurrence of root rot on alfalfa (*Medicago sativa*) caused by *Pythium coloratum* in China. *Plant Dis.* **2020**, *104*, 3269–3269. [CrossRef]
9. Kuan, T.L.; Erwin, D.C. Predisposition effect of water saturation of soil on *Phytophthora* root rot of alfalfa. *Phytopathology* **1980**, *70*, 981–986. [CrossRef]
10. Cai, W.; Tian, H.; Liu, J.R.; Fang, X.L.; Nan, Z.B. *Phytophthora cactorum* as a pathogen associated with root rot on alfalfa (*Medicago sativa*) in China. *Plant Dis.* **2021**, *105*, 231. [CrossRef]
11. Smith, R.R.; Grau, C.R.; Gray, L.E. First report of *Mycoleptodiscus terrestris* infecting forage legumes and soybeans in Wisconsin. *Plant Dis.* **1998**, *82*, 126–126. [CrossRef] [PubMed]
12. Živanov, D.; Živanov, S.T.; Samac, D. First Report of *Mycoleptodiscus terrestris* Causing Crown and Root Rot of Alfalfa (*Medicago sativa*) in Minnesota. *Plant Dis.* **2021**, *105*, 214. [CrossRef] [PubMed]
13. Wen, Z.H.; Duan, T.Y.; Christensen, M.J.; Nan, Z.B. *Microdochium tabacinum*, confirmed as a pathogen of alfalfa in Gansu Province, China. *Plant Dis.* **2015**, *99*, 87–92. [CrossRef] [PubMed]
14. Zhang, C.X.; Yu, S.T.; Tian, H.; Wang, Z.; Yu, B.H.; Ma, L.S.; Nan, Z.B.; Fang, X.L. Varieties with a high level of resistance provide an opportunity to manage root rot caused by *Rhizoctonia solani* in alfalfa. *Eur. J. Plant Pathol.* **2021**, *160*, 983–989. [CrossRef]
15. Cao, S.; Liang, Q.W.; Nzabanita, C.; Li, Y.Z. *Paraphoma* root rot of alfalfa (*Medicago sativa*) in Inner Mongolia, China. *Plant Pathol.* **2020**, *69*, 231–239. [CrossRef]
16. Boerema, G.H.; de Gruyter, J.; Noordeloos, M.E.; Hamers, M.E.C. *Phoma Identification Manual: Differentiation of Specific and Infra-specific Taxa in Culture*; CABI Publishing: Wallingford, UK, 2004; pp. 158–159.
17. Morgan-Jones, G.; White, J.F. Studies in the genus *Phoma* III *Paraphoma*, a new genus to accommodate *Phoma radicina*. *Mycotaxon* **1983**, *81*, 57–65.
18. Wang, K.N.; Liu, W.Z.; Duan, Y.X.; Liu, Y. A new recorded genus for China—*Paraphoma*. *Acta Mycol. Sin.* **1996**, *15*, 309–310.
19. De Gruyter, J.; Woudenberg, J.H.C.; Aveskamp, M.M.; Verkley, G.J.M.; Groenewald, J.Z.; Crous, P.W. Systematic reappraisal of species in *Phoma* section *Paraphoma*, *Pyrenochaeta* and *Pleurophoma*. *Mycologia* **2010**, *102*, 1066–1081. [CrossRef]
20. Wang, N.Y.; Dewdney, M.M. The effects of nutrition and environmental factors on conidial germination and appressorium formation of *Phyllosticta citricarpa*, the causal agent of citrus black spot. *Phytopathology* **2019**, *109*, 650–658. [CrossRef]
21. Li, X.; Li, B.H.; Lian, S.; Dong, X.L.; Wang, C.X.; Liang, W.X. Effects of temperature, moisture and nutrition on conidial germination, survival, colonization and sporulation of *Trichothecium roseum*. *Eur. J. Plant Pathol.* **2019**, *153*, 557–570. [CrossRef]
22. Li, C.J.; Nan, Z.B.; Li, F. Biological and physiological characteristics of *Neotyphodium gansuense* symbiotic with *Achnatherum inebrians*. *Microbiol. Res.* **2008**, *163*, 431–440. [CrossRef] [PubMed]
23. Fang, Z.D. *Methodology for Plant Pathology*; China Agricultural Press: Beijing, China, 1998.
24. Crous, P.W.; Verkley, G.J.M.; Groenewald, J.Z.; Samson, R.A. *Fungal Biodiversity. CBS Laboratory Manual Series 1*; CBS-KNAW Fungal Biodiversity Centre: Utrecht, The Netherlands, 2009.
25. Wu, J.W. The oxidized pine needle extract culture medium—A fungal selective culture medium. *Acta Microbiol. Sin.* **1975**, *15*, 37–41.
26. Li, Y.Z.; Nan, Z.B. Nutritional study on *Embellisia astragali*, a fungal pathogen of milk vetch (*Astragalus adsurgens*). *Anton Leeuw.* **2009**, *95*, 275–284. [CrossRef]
27. Zeng, C.Y.; Zhu, X.Y.; Cui, Z.; Li, Y.Z. Antifungal activity of plant extracts against *Embellisia astragali*, the fungal causal agent of yellow dwarf and root-rot disease of standing milkvetch. *Crop Pasture Sci.* **2015**, *66*, 735–739. [CrossRef]
28. Tang, S.S.; Liu, Z.H.; Yu, C.G.; Zheng, C.; An, X.; Li, J.B.; Zhao, T.C. Identification and biological characteristics of watermelon anthracnose caused by *Colletotrichum orbiculare* in Liaoning Province. *Plant Prot.* **2014**, *40*, 38–44.
29. Agrios, G.N. *Plant Pathology*, 5th ed.; Elsevier Academic Press: Amsterdam, The Netherlands, 2005.
30. Li, F.; Matloob, M.; Nzabanita, C.; Li, Y.Z. Growth, sporulation and germination of *Verticillium alfalfae* on media. *Eur. J. Plant Pathol.* **2021**, *161*, 383–395. [CrossRef]

31. Chung, H.S.; Wilcoxson, R.D. Effects of temperature, light, carbon and nitrogen nutrition on reproduction in *Phoma medicaginis*. *Mycopathologia* **1971**, *44*, 297–308. [CrossRef]
32. Zhang, L.; Pan, L.Q.; Wang, S.R.; Yuan, Q.H.; Wang, Y.; Miao, L.H. Study on the biological characteristics of the alfalfa phoma leaf spot pathogen. *J. China Agric. Univ.* **2015**, *20*, 158–166.
33. Gottlieb, D. The physiology of spore germination in fungi. *Bot. Rev.* **1950**, *16*, 229–257. [CrossRef]

agriculture

MDPI

Article

Physicochemical Properties and Antibiosis Activity of the Pink Pigment of *Erwinia persicina* Cp2

Yujuan Zhang, Xiaoni Liu, Xiangyang Li, Liang Zhao, Hong Zhang, Qianying Jia, Bo Yao and Zhenfen Zhang *

Key Laboratory of Grassland Ecosystem, Ministry of Education, College of Grassland Science, Gansu Agricultural University, Lanzhou 730070, China
* Correspondence: zhangzf@gsau.edu.cn

Abstract: The control and management of fungal diseases is a worldwide problem. A variety of microbial pigments have excellent antibacterial effects, and naturally occurring bacterial pigments may help in tackling fungal diseases. In order to explore the basic properties and biological functions of the pink pigment produced by *Erwinia persicina* Cp2, we used organic solvents to extract the pink pigment, analyzed the physicochemical properties of the pigment, determined the chemical composition using ultra-high performance liquid chromatography-tandem mass spectrometry (UPLC-MS/MS), and selected five pathogenic fungi to study the inhibitory effects of the pink pigment. The results showed that the main component of the pink pigment was usambarensine, which had a good light stability and a good temperature stability at room temperature (<40 °C), but the influence of the oxidant on its activity was greater than that of the reductant; simultaneously, we found that strong acids, strong alkalis, Cu^{2+}, and Zn^{2+} all greatly affect the stability of the pink pigment, while Fe^{2+} and Fe^{3+} made the pigment darker. Meanwhile, the pigment could exert a good inhibitory effect against four plant pathogenic fungi: *Alternaria solani*, *Sclerotinia sclerotiorum*, *Rhizoctonia solani*, and *Fusarium proliferatum*. However, the inhibition of *Fusarium oxysporum*. f. sp *cucumerinum* decreased significantly in the later stages. This study had detected the purification process and antifungal activity on five fungi of the pink pigment of *Erwinia persicina* Cp2. It lays a theoretical and practical foundation for the production of related biological agents.

Keywords: bacterial pigment; chemical composition; stability; fungi inhibition

Citation: Zhang, Y.; Liu, X.; Li, X.; Zhao, L.; Zhang, H.; Jia, Q.; Yao, B.; Zhang, Z. Physicochemical Properties and Antibiosis Activity of the Pink Pigment of *Erwinia persicina* Cp2. *Agriculture* **2022**, *12*, 1641. https://doi.org/10.3390/agriculture12101641

Academic Editor: Aocheng Cao

Received: 15 August 2022
Accepted: 3 October 2022
Published: 8 October 2022

1. Introduction

A total of 40% of the world's arable land is used for agriculture, but only 1.5% of this area is used for organic agriculture [1,2]. Soil-borne diseases are an important constraint on green agricultural production and result in the reduced productivity and lower yields. Common soil-borne pathogens include *Fusarium oxysporum*, *Rhizoctonia solani*, *Phytophthora* spp., *Pythium* spp., and *Verticillium dahliae* [3]. These pathogens are widely found in areas of intensively planted soil and cause devastating diseases such as fusarium wilt, root rot, early blight, and bacterial wilt, which affect maize, cotton, wheat, and other food crops, reducing yields by 50–75% or even wiping out crops entirely [4]. To prevent and control such diseases, the most widely used methods in traditional agricultural production are the cultivation of disease-resistant crop varieties and the use of chemical fungicides [5,6]. However, disease-resistant crop varieties have a long cultivation cycle and remain vulnerable to pathogens enriched in the soil. Fungicides are typically inexpensive and convenient to use, but because of the restrictions on the types of agricultural chemicals used in green and organic agriculture, as well as increasing concerns for food safety and the environment in recent years, greener and environmentally friendly biological control methods without chemical residues have become a hot spot for research at home and abroad [7].

Researchers have found that using biological control measures to inoculate artificially selected antagonistic bacteria in the soil, or applying the fermentation products or secondary

metabolites of certain strains to plants, could effectively reduce the incidence of soil-borne diseases and increase crop yields [8,9]. Secondary metabolites of bacteria mainly include lipopolysaccharide (LPS), extracellular polysaccharide (EPS), bacterial pigment, and protease [10,11]. As one of the secondary metabolites of bacteria, pigments have been widely used in industries such as dyes [12], food additives [13], and medicine [14]. The biological functions of pigments used in such applications include the interference in the electron transfer of host cells [15], regulation of immune mechanisms [16], bactericidal effects [17] and bacteriostatic effects [18]. However, due to the different characteristics of various bacteria, the chemical components of the bacterial pigments produced are also different. Some chemical substances found in bacterial pigments, including phenazine carboxylic acid, pyocyanin, pyoluteorin, and pyrrolnitrin, may exhibit better biocontrol effects than others [19,20]. Ohmori et al. [21] also reported that the bacterial pigment pyoluteorin could be used as a new type of biological pesticide for the control of wilt disease in cotton.

Erwinia persicina is a Gram-negative rod-shaped bacterium of the *Enterobacteriaceae* family. Hao et al. [22] first reported and named this new pathogen isolated from cucumber, banana, and tomato plants in 1990. Since then, researchers have found that *Erwinia persicina* can cause diseases in plants [23,24], animals [25], and edible fungi [26] at certain levels. The pathogen is milky white on the NA medium, with glossy edges and a diameter of 1–4 mm. However, it grows rapidly on many nutrient media and produces a pink water-soluble pigment after it is connected into a piece, and it also causes a trend of the pink pigment spreading in the roots, stems, leaves, and other tissues of the invaded plants, including onion and parsley [27,28]. However, the recent study [29] pointed out that *Erwinia persicina* also exhibits the potential as a biological control agent, as an inhibitor of Salmonella pollution in the industrial cultivation of sprouts.

We also observed, during the experiment. that *Erwinia persicina* Cp2 produced a large amount of pink pigment under aging and extreme environmental conditions, and had certain antibacterial properties. Therefore, *Erwinia persicina* Cp2 was used as the tested strain, the bacterial pink pigment was extracted with organic solvents, the physicochemical properties and chemical composition of the pink pigment were studied, and the typical disease pathogens included: *Alternaria solani*, *Sclerotinia sclerotiorum*, *Rhizoctonia solani*, *Fusarium oxysporum*. f. sp *cucumerinum*, and *Fusarium proliferatum* were used as representative strains to verify the antibacterial activity of the pink pigment, to explore the particularity and potential biocontrol function of the pigment material, and to lay the foundation for further research into pesticides with biocontrol functions obtained from microorganisms.

2. Materials and Methods

2.1. Test Strains

The tested bacteria was *Erwinia persicina* Cp2 (ID: 756944) isolated from alfalfa seeds [30]. *Alternaria solani* (ID: 3106919), *Sclerotinia sclerotiorum* (ID: 17372726), *Rhizoctonia solani* (ID: 14572378), *Fusarium oxysporum*. f. sp *cucumerinum* (ID: 306247), and *Fusarium proliferatum* (ID: 17735672) were donated by the College of Plant Protection of Gansu Agricultural University. All strains were stored in the Pasture Pathology Laboratory of Gansu Agricultural University, at a temperature of −80 °C (LanZhou, China).

2.2. Test Agars

We used a nutrient agar (NA) for the cultivation and short-term storage of the Cp2 strains, and used King's B medium for the cultivation and enrichment of the pink pigment of Cp2. In addition, we used a potato dextrose agar (PDA) for the cultivation of pathogenic fungi and the control of antibacterial tests. To the PDA base, we added pink pigment to a level of 20% of the total volume (the absorbance of the pink pigment was 0.785) to make pink pigment PDA (PPPDA), then used this PPPDA to study the antibacterial activity of the five kinds of pathogenic fungi.

2.3. Preparation of the Pink Pigment of Erwinia persicina Cp2

We used an inoculating loop to scrape the bacteria from the NA, then inoculated these bacteria in King's B medium using the single-line method and left them to culture in the dark at 28 °C for about 72 h until they contained a large amount of pigment. Then, we took bacterial samples for experimental use using medicine spoons.

2.4. Extraction and Purification of the Pink Pigment

For the crude extraction and purification of the pink pigment, we used organic solvent extraction methods [31]. We collected bacteria in a culture plate, scraped a sample of 1.0 g and placed it in a 10 mL centrifuge tube. Then, we added 5 mL of distilled water, chloroform, ethyl acetate, isoamyl alcohol, petroleum ether, glacial acetic acid, n-butanol, and absolute ethanol, respectively, to the centrifuge tube with bacteria and soaked it for 2 h (During this process, the tube was shaken with a vortex oscillator for 1 min every 30 min). Following the centrifugation at 12,000 rpm for 15 min, the supernatant was collected [31]. Finally, we observed the dissolution status of the pink pigment in various solvents and selected the best leaching agent and extraction solution to obtain a pure pigment.

2.5. The Absorbance Spectrum of the Pink Pigment

Following the method used by Venil et al. [32], we used the spectral scanning mode of the UV spectrophotometer (Thermo Fisher Scientific, Waltham, MA, USA) to scan the wavelengths of 200–800 nm at the interval of 1 nm in the pure pink pigment at room temperature in order to determine the maximum wavelength.

2.6. Components Detection of the Pink Pigment

2.6.1. Collection and Processing of the Pink Pigment Sample

We removed the sample from the −80 °C refrigerator, left it to thaw on ice, and then shook it with the vortex for 10 s. We mixed 50 µL of the sample and 150 µL of a 20% acetonitrile methanol internal standard extractant. We vortexed the mixture for 3 min and centrifuged it (12,000 rpm, 4 °C) for 10 min. Then we transferred 150 µL of the supernatant and left it to stand at −20 °C for 30 min. Finally, we centrifuged it again for 3 min (12,000 rpm, 4 °C) and removed the supernatant for analysis.

2.6.2. Analysis of the Metabolites of the Pink Pigment

The sample extracts were analyzed using an LC-ESI-MS/MS system (UHPLC, ExionLC AD, https://sciex.com.cn/ (accessed on 15 November 2021); MS, QTRAP® System, https://sciex.com/cn/ (accessed on 25 November 2021)). The analytical conditions were as follows: for the UPLC, the column was Waters ACQUITY UPLC HSS T3 C18 (1.8 µm, 2.1 mm × 100 mm); the column temperature was 40 °C; the flow rate was 0.35 mL/min; the injection volume was 5 µL; the solvent system was water (0.1% formic acid): acetonitrile (0.1% formic acid); and the gradient program was 95:5 *v*/*v* at 0 min, 10:90 *v*/*v* at 10.0 min, 10:90 *v*/*v* at 11.0 min, 95:5 *v*/*v* at 11.1 min, and 95:5 *v*/*v* at 14.0 min.

The Quadrupole Time-of-Flight mass spectrometer was used for its ability to acquire MS/MS spectra on an information-dependent basis (IDA) during an LC/MS experiment. In this mode, the acquisition software (TripleTOF 6600, AB SCIEX) continuously evaluated the full scan survey MS data as it collected and triggered the acquisition of the MS/MS spectra depending on the preselected criteria. For each cycle, 12 precursor ions whose intensity was greater than 100 were chosen for the fragmentation at a collision energy of 30 V (12 MS/MS events with the product ion accumulation time of 50 msec each). The electron spray ion (ESI) source conditions were set as the following: the ion source gas I (GSI) as 50 Psi; the ion source gas II (GSII) as 50 Psi; the curtain gas as 25 Psi; the source temperature 500 °C; the ion spray voltage floating (ISVF) was 5500 V or −4500 V in the positive or negative modes, respectively.

Linear ion trap (LIT) and triple quadrupole (QQQ) scans were acquired on a triple quadrupole-linear ion trap mass spectrometer (QTRAP), QTRAP® LC-MS/MS System,

equipped with an ESI Turbo ion-spray interface, operating in the positive and negative ion modes and controlled by Analyst 1.6.3 software (Lincoln, Dearborn, MI, USA). The ESI source operation parameters were as follows: the source temperature was 500 °C; the ISVF was 5500 V (positive), −4500 V (negative); the ion source GSI, GSII, curtain gas were set at 50, 50, and 25.0 Psi, respectively; and the collision gas was high. Instrument tuning and mass calibration were performed with 10 and 100 μmol/L polypropylene glycol solutions in QQQ and LIT modes, respectively. For each period, we monitored a specific set of multiple reaction monitoring (MRM) transitions, according to the metabolites eluted within the period concerned.

2.7. The Stability of the Pink Pigment

2.7.1. The Light Stability of the Pink Pigment

The pigment solutions were taken and placed under natural light and dark conditions at room temperature, and the samples were taken after 0, 2, 4, 6, and 8 h of treatment to determine their absorbance at the characteristic wavelengths. Three experimental replicates were performed.

2.7.2. The Temperature Stability of the Pink Pigment

The method was referenced from Zhang et al. [33] and further improved. The pigment solutions were taken and placed at temperatures of 4, 20, 40, 60, 80, 100, and 120 °C for 2 h. The absorbance of the pink pigments after 2 h were also measured using 0 h as a control. Three experimental replicates were performed.

2.7.3. The pH Stability of the Pink Pigment

The method of Ugwu et al. [34] was referred to and further improved. Specifically, the pH value of the deionized water to levels between 1 and 14 using HCl and NaOH. For each pH level, we took 4 mL of deionized water, added 1 mL of the pigment solution, and then mixed to observe how the pigment color changed at the different pH conditions. We separately measured the absorbance after standing periods of 0 h and 2 h. Three experimental replicates were performed.

2.7.4. The Metal Ions Stability of the Pink Pigment

We adopted and improved upon the method used by Li et al. [35]. That is, we prepared 100 mmol/L solutions of Na^+, K^+, Ca^{2+}, Mg^{2+}, Mn^{2+}, Cu^{2+}, Zn^{2+}, Fe^{2+}, and Fe^{3+}, we took 0.5 mL of each ion solution and separately added this to 4.5 mL of the pigment solution to give a final concentration of 10 mmol/L. Once it was mixed uniformly, we measured the absorbance after standing for 0 h and 2 h, then calculated the preservation rate. Three experimental replicates were performed.

$$\text{Preservation Rate (\%)} = A_2/A_0 \times 100\%;$$

A_0 and A_2 were the absorbance of the pigment at 0 h and 2 h with metal ions, respectively.

2.7.5. The Redox Stability of the Pink Pigment

We took 4 mL of the pink pigment solution and added 2%, 4%, 6%, 8%, and 10% H_2O_2 solution (10% v/v) or Na_2SO_3 solution (100 g/L), separately. Once it was uniformly mixed, we determined the absorbance after standing for 0 h and 2 h. Three experimental replicates were performed.

2.8. The Inhibitory Effect of the Pink Pigment on the Soil-Borne Pathogenic Fungi

We referred to the research method of You et al. [36], and we used agar punch with a diameter of 0.5 cm to punch mycelial cakes on the same circumference as the edge of the cultured colony, and connected it to the center of the PDA (control) and the PPPDA medium. Three replicates were set up for each group of treatments. All were incubated in

the dark at a constant 25 °C maintained by means of a thermostat. We took the time when the edge of the colony of the control group was close to the wall of the dish as the time point. During this period, the diameter of the colony of each treatment was measured using the cross method continuously every day, and the growth rate, and the growth inhibition rate were calculated simultaneously. Three experimental replicates were performed.

$$\text{Growth inhibition rate (\%)} = (\text{Diameter of control colony} - \text{Diameter of treated colony})/(\text{Diameter of control colony} - \text{Diameter of mycelial cake}) \times 100\%.$$

2.9. Statistical Analysis

All experiments were carried out at least three times while the results were expressed and presented in tables as mean, with error bars expressed in the form of ±standard error (SE). One-way ANOVA, Duncan's new multiple range method and an independent sample *t*-test were used for the significant analysis of variance. The software we used was Analyst 1.6.3 (Lincoln, Dearborn, MI, USA) to process the metabolomic data.

3. Results

3.1. The Extraction and Purification of the Pink Pigment

The results showed that the pink pigment was extremely soluble in glacial acetic acid, followed by anhydrous ethanol and distilled water. This phenomenon made the pink pigment water-soluble. We also found that the pigment was soluble in n-butanol and slightly soluble in ethyl acetate; however, it was insoluble in chloroform, isoamyl alcohol and petroleum ether (Table 1). Therefore, after a thorough consideration of the solubility and characteristics of the solvents, we chose ethanol as the leaching agent and chloroform as the extractant for our experiment.

Table 1. The solubility of the pink pigment in organic solvents.

Solvent Type	Distilled Water	Chloroform	Ethyl Acetate	Isoamyl Alcohol	Petroleum Ether	Glacial Acetic Acid	N-Butanol	Anhydrous Ethanol
Solubility	+++	-	+	-	-	++++	++	+++

Note: "-" means insoluble in the solution; "+" means soluble in the solution, the higher the quantity, the greater the solubility.

The pink pigment could be dissolved under various ethanol concentration gradients, with a maximum solubility at an ethanol concentration of 75% (Table 2).

Table 2. The solubility of the pink pigment in ethanol solutions.

Solvent Type	Distilled Water	25% Ethanol	50% Ethanol	75% Ethanol	Anhydrous Ethanol
Solubility	++	+	++	+++	++

Note: "+" means soluble in the solution, the higher the quantity, the greater the solubility.

The leaching agent was 75% ethanol and the extractant chloroform were selected to extract and purify the pink pigment. In this process, there would be three situations due to the change of the ratio of the two solvents. A, B, and C were the diagrams of the chloroform and anhydrous ethanol ratios set as close to 1:1, greater than 1:1, and less than 1:1, respectively (Figure 1). In this test, chloroform was added to the crude pigment extract containing 75% ethanol and left to stand for a few moments until the effect of A was achieved and then collected the "pigment + water" phase.

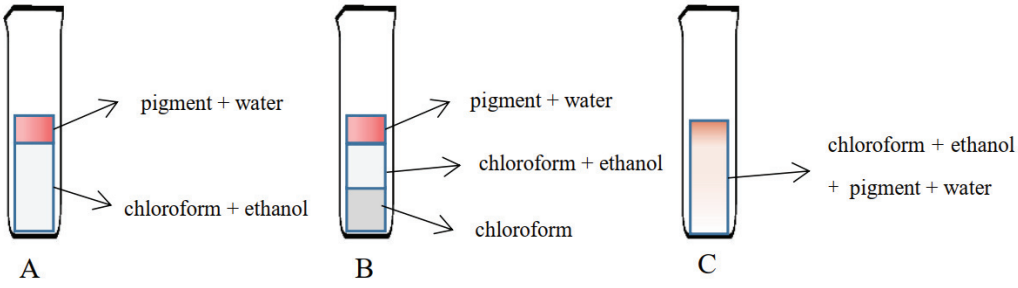

Figure 1. Schematic diagram of the purifying pink pigment with different ratios of the leaching agent and extractant. (**A**) indicates chloroform and anhydrous ethanol ratios close to 1:1; (**B**) indicates chloroform and anhydrous ethanol ratios greater than 1:1; (**C**) indicates chloroform and anhydrous ethanol ratios less than 1:1.

3.2. The Wavelength Scanning of the Pink Pigment

We scanned the wavelength of the pure pigment under 200–800 nm and found that the maximum absorbance of 0.943 was achieved when the wavelength was 340 nm (Supplementary Materials Figure S1).

3.3. Results of the Composition Test of the Pink Pigment

We used Analyst 1.6.3 software to process the mass spectrometry data, we obtained the total ions current (TIC) of the pink pigment sample (Figure 2), and used the multiple reaction monitoring (MRM) to collect the pink pigment sample date (Supplementary Materials Figure S2). At the same time, the MRM scanning was used to obtain the peak area of each compound. In order to compare the material content difference of each metabolite in the sample among all of the detected metabolites, we corrected the mass spectrum peaks according to the information of the metabolites retention time and peak type. By such means, we ensured the accuracy of the qualitative quantification (Supplementary Materials Figure S3) and obtained a final figure for the metabolites detected in the pink pigment solution (Supplementary Materials Table S1).

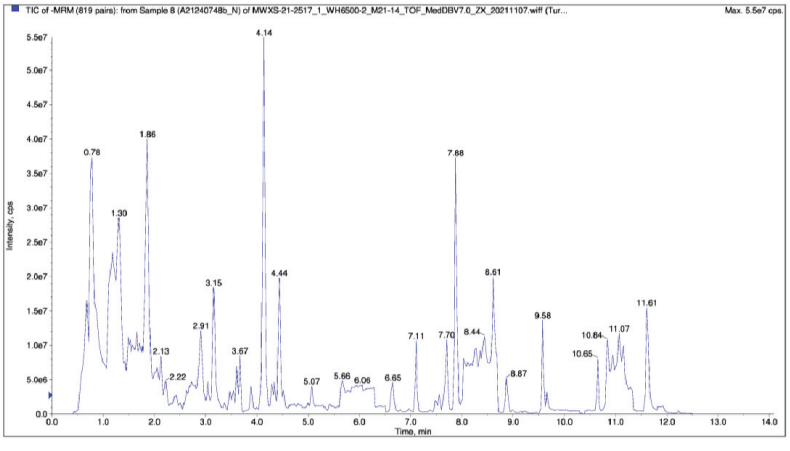

Figure 2. The total ions current (TIC) for the sample mass spectrometry. The abscissa was the retention time of the metabolite detection, and the ordinate was the ion current intensity of the ion detection (the intensity unit is count per second, cps).

According to the MRM scan results, the ten substances most prevalent in the pink pigment samples were usambarensine, isopentenyl pyrophosphate, eicosanoyl EA, and various small molecule substances and polypeptides (Table 3).

Table 3. Top ten compounds of the pink pigment.

Number	Compounds	Precursor	Score	ID Source
1	Usambarensine	450.3	0.524	2-Insilico
2	Isopentenyl pyrophosphate	515.0	0.785	2-MedDB2.0
3	Eicosanoyl-EA	356.4	0.673	2-mHK6.0
4	Glu-Pro-Lys	414.2	0.665	2-mHK6.0
5	2(1H)-Pyridinone	191.1	0.880	2-MetDNA
6	2,3,4,5-Tetrahydrodipicolinate	189.1	0.764	2-MetDNA
7	Pro-Ser-Val	343.2	0.644	2-mHK6.0
8	Ser-Pro-Asp	318.1	0.644	2-mHK6.0
9	Val-Val-His-Ala-Glu	554.3	0.780	2-mHK6.0
10	Dimethyl sulfoxide	79.0	0.679	2-mHK6.0

3.4. The Stability of the Pink Pigment

3.4.1. Effect of the Light on the Stability of the Pink Pigment

The results showed no significant differences in the absorbance of the pink pigment between light and dark conditions (Figure 3A).

3.4.2. Effect of the Temperature on the Stability of the Pink Pigment

At 0 h, there was no significant difference in absorbance of the pink pigment under the eight temperature treatments. With the increase in temperature, the absorbance values showed an overall increasing trend after 2 h, but there was no significant difference in the absorbance of the pink pigment under the temperature conditions between 4 and 30 °C; after 40 °C, the difference was significant under each temperature treatment ($p < 0.05$); at 120 °C, the maximum value was reached but only 1.01 times that of 4 °C (Figure 3B).

3.4.3. Effect of Oxidants on the Stability of the Pink Pigment

With the increase of the 10% H_2O_2 content, the absorbance of the pink pigment decreased to varying degrees at 0 h and 2 h. At 0 h, the absorbance of the pink pigment was significantly different from the control (10% H_2O_2 content was 0) when the content was between 2 and 10% ($p < 0.05$). At 2 h, when the content was 2%, the absorbance of the pink pigment was 80% of the control, afterwards, although the absorbance continued to decrease, the overall trend did not change much (Figure 3C).

3.4.4. Effect of the Reducing Agent on the Stability of the Pink Pigment

With the increased percentage of the 100 g/L Na_2SO_3 content, at 0 h, the absorbance of the pink pigment first increased and then decreased, and reached the maximum value when the Na_2SO_3 content was 2%. At 8%, it reached the minimum value of 0.98 times that of the control. At 2 h, with the increasing percentages of the reducing agent, the absorbance of the pink pigment gradually increased, but with no significant difference between 4% and 10% (Figure 3D).

3.4.5. Effect of the pH on the Stability of the Pink Pigment

When the pH value was between 1 and 10, the absorbance of the pink pigment showed a downward trend at 0 and 2 h, but the difference was not significant at the pH values between 5 and 9. However, the absorbance of the pink pigment significantly increased under acidic conditions at pH 1. Under alkaline conditions, the pH value showed a downward trend at 0 h, but at 2 h, it first decreased and then increased, with a pH value of 14 at 0 h, the absorbance levels were 80% of those recorded at 2 h (Figure 3E).

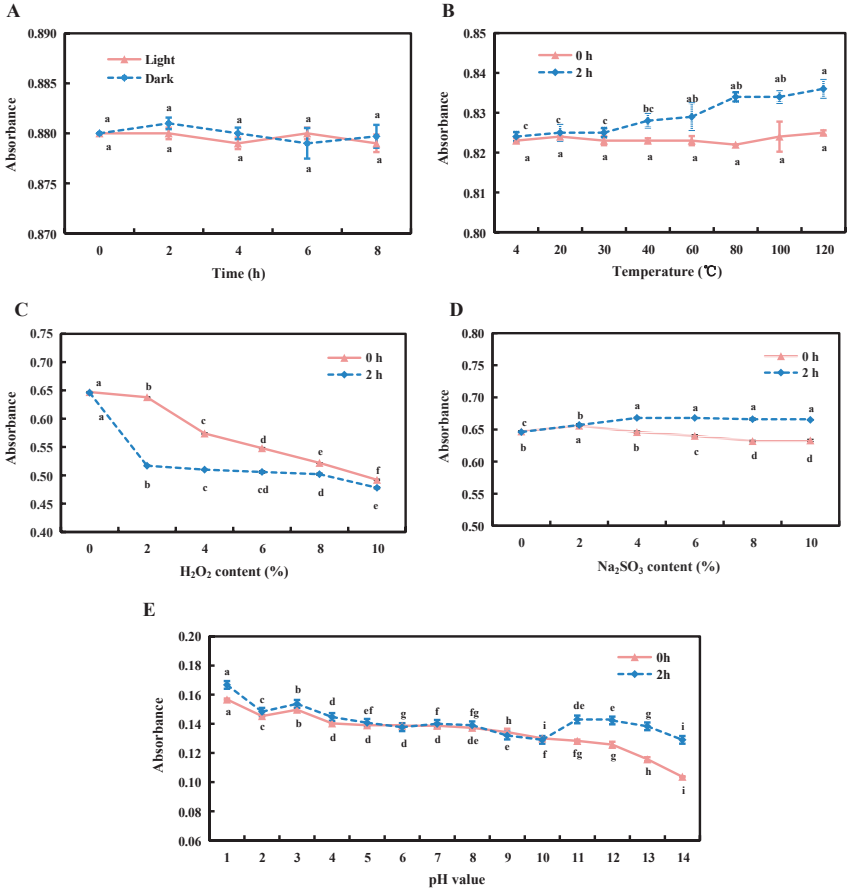

Figure 3. Effects of the different conditions on the stability of the pink pigment. The pink solid line and the blue dotted line in the figure indicate the changing trends of the absorbance of the pink pigment at 0 h and 2 h treatment, respectively. Light stability (**A**), temperature stability (**B**), oxidants stability (**C**), reducing agent on the stability (**D**) and pH stability (**E**) were measured. Different letters indicate significant differences in the pink pigment under different durations of the treatment at $p < 0.05$, and the error bars were expressed in the form of ±standard error (SE).

3.4.6. Effect of the Metal Ions on the Stability of the Pink Pigment

The nine metal ions had little effect on the absorbance of the pink pigment at 0 h, compared to the control (CK), but after 2 h, the pink pigment changed color in some of the metal ions and there were differences in the same absorbance. Among them, the absorbance of the pink pigment added with Na^+, K^+, Mn^{2+}, and Ca^{2+} decreased after 2 h, but the reduction was only small, observation of the pink pigment solution revealed that the color only slightly lightened. Mg^{2+} produced a certain decolorizing effect on the pink pigment, both Fe^{2+} and Fe^{3+} deepened the color, and the color enhancement effect of Fe^{2+} ions was more than 1.86 times that of CK. Fe^{3+} ions deepened the color of the pink pigment while also producing a flocculent precipitation. Cu^{2+} and Zn^{2+} ions caused the pink pigment to turn grassy green and light green, respectively after 2 h (Table 4).

Table 4. Effect of the metal ions on the stability of the pink pigment.

Ion Species	Absorbance		Preservation Rate/%	Color
	0 h	2 h		
CK	0.853 bc	0.854 c	100.12 c	pink
Na^{+}	0.851 c	0.850 d	99.88 c	pink
K^{+}	0.838 f	0.789 g	94.15 f	pink
Fe^{2+}	0.836 f	1.553 a	185.77 a	dark pink
Fe^{3+}	0.847 d	1.067 b	125.97 b	pink (flocculent precipitation)
Mn^{2+}	0.856 a	0.813 f	94.98 e	pink
Mg^{2+}	0.845 d	0.655 h	77.51 g	light pink
Ca^{2+}	0.842 e	0.836 e	99.29 d	pink
Cu^{2+}	0.829 g	—	—	grassy green
Zn^{2+}	0.855 ab	—	—	light green

Note: Different letters indicate significant differences in the pink pigment under different durations of treatment at $p < 0.05$.

3.5. Inhibition of the Soil-Borne Pathogenic Fungi by the Pink Pigment

3.5.1. The Inhibition of *Alternaria solani* by the Pink Pigment

On the 8th day, the colony of the CK control group was close to the wall of the dish (Figure 4A). The growth rate of the CK colony showed an upward trend with the increase in treatment time from the 1st to 8th day, and the difference was extremely significant at different times ($p < 0.05$). The growth inhibition rate of the treatment group PM against *Alternaria solani*, reached 100% on the 1st to 3rd days, and the growth inhibition rate was still above 90% on the 4th to the 5th day. Subsequently, the inhibitory effect of PM decreased significantly, but on the 8th day, the growth rate of the bacterial circle was only 0.45 times that of the CK control group, and the growth inhibition rate was as high as 58.29% (Figure 4B).

3.5.2. The Inhibition of *Sclerotinia sclerotiorum* by the Pink Pigment

On the 6th day, the colony of the CK control group was close to the wall of the dish (Figure 4C). The growth rate for both the CK control and PM treatment groups exhibited an upward trend from the 1st to the 6th day. However, the growth rate of the colonies on the PM treatment had no significant difference between the 1st–2nd day and the 3rd–5th day. The growth inhibition rate of the PM treatment group on *Sclerotinia sclerotiorum* showed a trend of first a decline and then an increase, and reached the minimum value of 83.14% on the 3rd day, the growth inhibition rate was over 90% on the 4th to the 5th day, and the growth inhibition rate was as high as 87.36% on the 6th day and the colony growth rate was only 0.19 times that of the control group (Figure 4D).

3.5.3. The Inhibition of *Rhizoctonia solani* by the Pink Pigment

On the 4th day, the colony on the CK control group was close to the wall of the dish, but the mycelial cake on the PM treatment group did not grow further (Figure 4E). The growth rate of the colony on the control group CK showed a gradual increase to 7.76 cm on the 4th day, but the colony on the PM treatment did not grow any further and the inhibition of the growth of *Rhizoctonia solani* remained at 100% during this period (Figure 4F).

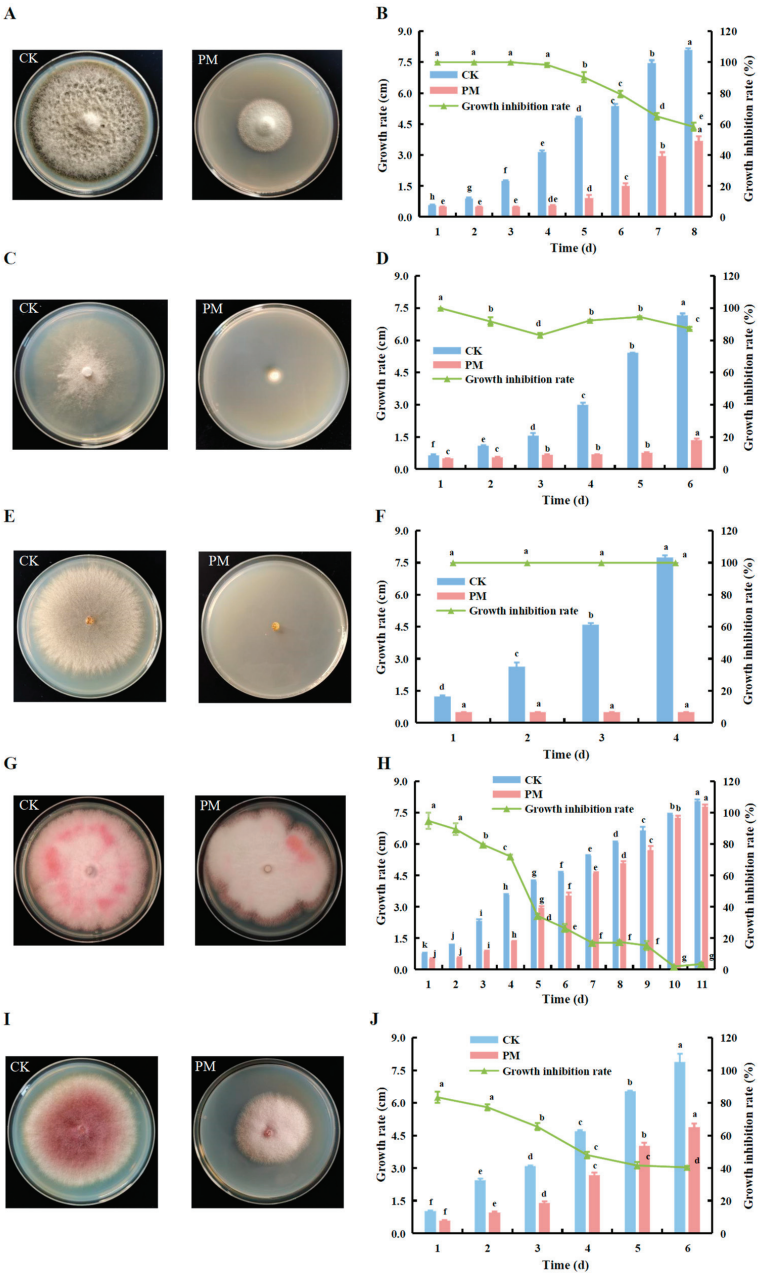

Figure 4. Inhibition of the soil-borne pathogenic fungi by the pink pigment. The inhibition rates of the pink pigment on *Alternaria solani* (**A**,**B**), *Sclerotinia sclerotiorum* (**C**,**D**), *Rhizoctonia solani* (**E**,**F**), *Fusarium oxysporum*. f. sp *cucumerinum* (**G**,**H**), and *Fusarium proliferatum* (**I**,**J**) were determined. CK is the control group without pink pigment; PM is the treatment group with pink pigment. Different letters indicate significant differences in the pink pigment under different treatments at $p < 0.05$, and error bars were expressed in the form of ±standard error (SE).

3.5.4. The Inhibition of *Fusarium oxysporum*. f. sp *cucumerinum* by the Pink Pigment

On the 11th day, the colonies in the CK control group and the PM treatment group were close to the wall of the dish, but the colony in the PM treatment was smaller in diameter and lighter in color than the CK group (Figure 4G). From the 1st to 11th days, the growth rate of the CK control and PM treatment groups showed an upward trend, and the difference at each time was extremely significant ($p < 0.05$). On the 1st day, the maximum growth inhibition rate of the treatment group PM on *Fusarium oxysporum*. f.sp *cucumerinum* was 89.45%, and the growth inhibition rate was as high as 70% in the first 4 days, and the growth inhibition rate continued to decline after the 4th day (Figure 4H).

3.5.5. The Inhibition of *Fusarium proliferatum* by the Pink Pigment

On the 6th day, the colony of the CK control group was close to the dish wall (Figure 4I). The growth rate of the colonies in both the CK control and the PM treatment group showed an increasing trend from the 1st to 6th days, with highly significant differences at all times ($p < 0.05$). The growth inhibition rate of the colony in PM, remained above 60% from 1st to 3rd days, then decreased but remained above 40%. On the 6th day, the growth inhibition rate reached a minimum of 40.46% and the growth rate of the colony in the PM treatment group was 0.62 times higher than that of the CK control group (Figure 4J).

4. Discussion

Bacterial pigments offer new potential solutions for the biological control of plant diseases. For the extraction of pigments, a common method is to use organic solvents to extract the crude pigments, and then use other organic solvents to prepare the mobile phases according to a certain ratio to separate and obtain the purified pigments [32], because the carrier involves at least three or four kinds of organic solvents, the process of removing organic solvents is cumbersome and various organic solvents may affect the activity of the pigment. Therefore, this experiment was based on a review study on the extraction process of the bacterial pigments by Muhammad et al. [31]. We measured the solubility of the pigment-containing bacteria in several organic solvents, then used a 75% ethanol solution as a leaching agent to obtain a crude pigment solution, and we used chloroform as an extractant for purification purposes, thereby ensuring the pink pigment of the highest activity and quality. In this study, we found the maximum absorption wavelength of the pink pigment to be 340 nm. However, previous studies of the maximum absorption wavelengths of the bacterial pigments prodigiosin, carotenoids and pyocyanin were around 530 nm [37], 480 nm [38], and 250 nm [39], respectively. These findings may be closely related to the specific compounds of bacterial pigments. In our study, after analyzing the compounds of the pink pigment, we found that usambarensine, isopentenyl pyrophosphate, eicosanoyl EA were included. Among them, Dassonneville et al. [40] showed that usambarensine, as a bis-indole compound, displayed potent antiamoebic activities and showed antigardial, antimalarial, and cytotoxic effects. Therefore, the antifungal activity of the pink pigment in this study may be closely related to this substance.

The antibacterial substances contained in the fermentation broth of the strains include alkaloids, anthraquinones, phenazines, and lipoic acids [41–44]. Chang et al. [39] identified the most important pigment components of *Pseudomonas aeruginosa* as three phenazine substances: dihydroxyphenazine-1-carboxylic acid, phenazine-1-carboxylic acid, and oxychloroquinoline. Therefore, the antibacterial activity of the fermentation broth is likely to be related to the bacterial pigment produced by the strain during the cultivation process. Tanya et al. [45] also found that prodigiosin had an inhibitory effect on crop pathogens. This study found that the growth inhibition rate of the pink pigment on *Alternaria solanacearum* was as high as 100% in early stages. Samen et al. [46] used PDA plates containing the commonly used fungicides difenocarb and chlorothalonil, similar to those used in this study, for susceptibility testing against *Alternaria solanacearum* in tomato plants and found that these fungicides inhibited some pathogens by only about 30%. Rapeseed sclerotinia is a fungal disease caused by *Sclerotinia sclerotiorum* [47]. In this experiment, we found that

the growth inhibition rate of the pink pigment against *Sclerotinia sclerotiorum* reached more than 80% between the 1st and 6th days. Potato sclerotia, also known as mole disease or rhizoctonia canker, is a globally occurring soil disease caused by *Rhizoctonia solani* [48], which causes disease mainly by infesting plants through secreted proteins, effectors, secondary metabolites, and cell wall degrading enzymes [49]. In this study, we found that the growth inhibition rate of the plate containing the pink pigment on *Rhizoctonia solani* reached 100% between the 1st and 4th days. Cucumber wilt is a type of fungal disease caused by *Fusarium oxysporum*. f. sp *cucumerinum* invading the vascular bundles of melons, it is particularly serious during the flowering and fruiting stages [50]. Our study found that the pink pigment exhibited good antibacterial activity against *Fusarium oxysporum*. f. sp *cucumerinum* in the early stages, but its effectiveness decreased with time. Tuli et al. [51] pointed out that the bacterial pigments were biodegradable and thus completely non-toxic in the environment. In addition, this study found that the growth inhibition rate of the pink pigment against the pathogen of alfalfa root rot (*Fusarium oxysporum*) was higher than 40% from the 1st to 6th days, which was higher than the corresponding inhabitation rate against *Fusarium oxysporum*. f. sp *cucumerinum* for the same period.

In summary, the water-soluble pink pigment of *Erwinia persicina* Cp2 showed a good inhibition of a variety of soil-borne pathogens. Although the pink pigment showed a reduced growth inhibition rate of some strains in the later stage, it further showed that the biological activity of the pink pigment can be reduced in the environment with the increase of time. Moreover, the study reported that the bacterial pigments could promote plant development and inhibit the growth of pathogenic fungi [52]. Therefore, the sensitivity of the five pathogenic fungi to the pink pigment in this study proved that pink pigment has the potential as a biocontrol agent, or a new biological agent and may be less polluting to the environment as a new bioreagent. However, the effect of the pink pigment on plants still needs further research.

5. Conclusions

In this study, we studied the physical and chemical properties of the pink pigment of *Erwinia persicina* Cp2 and found that the best leaching agent solvent for the pink pigment was 75% ethanol, while the best extractant was chloroform. We determined the maximum absorption wavelength was 340 nm; and the main component of the pink pigment was usambarensine. In addition, we study found that the pink pigment exerted a good inhibitory effect on four types of soil-borne disease pathogens: *Alternaria solani*, *Sclerotinia sclerotiorum*, *Rhizoctonia solani*, and *Fusarium proliferatum*. Among them, the inhibitory effect of *R. solani* was most notable, however, the inhibition of *Fusarium oxysporum*. f. sp *cucumerinum* decreased significantly with time.

Supplementary Materials: The following supporting information can be downloaded at: https://www.mdpi.com/article/10.3390/agriculture12101641/s1, Figure S1: The wavelength scanning map of pink pigment; Figure S2: Multimodal Plot for Multiple reaction monitoring (MRM) metabolite detection; Figure S3: Integral correction diagram for metabolite quantitative analysis; Table S1: Data for metabolites detected in the pink pigment solution.

Author Contributions: Y.Z. performed the experiments, analyzed the data. X.L. (Xiaoni Liu), X.L. (Xiangyang Li), L.Z., H.Z., Q.J. and B.Y. made helpful comments on our work and manuscript. Z.Z. conceived and supervised the project. All authors have read and agreed to the published version of the manuscript.

Funding: This research was funded by the National Natural Science Foundation of China (32060396), Natural Science Foundation of Gansu Province, China (20JR10RA562), Science and Technology Planning Project of Lanzhou City (2019-RC-116), Youth Tutor Fund of Gansu Agricultural University (GAU-QDFC-2019-08), and Key Laboratory of Grassland Ecosystem of the Ministry of Education (KLGE202203).

Institutional Review Board Statement: Not applicable.

Informed Consent Statement: Not applicable.

Data Availability Statement: Not applicable.

Conflicts of Interest: The authors declare no conflict of interest.

References

1. Foley, J.A.; Ramankutty, N.; Brauman, K.A.; Cassidy, E.S.; Gerber, J.S.; Johnston, M.; Mueller, N.D.; O'Connell, C.; Ray, D.K.; West, P.C.; et al. Solutions for a cultivated planet. *Nature.* **2011**, *478*, 337–342. [CrossRef] [PubMed]
2. Larsen, A.E.; Powers, L.C.; Mccomb, S. Identifying and characterizing pesticide use on 9000 fields of organic agriculture. *Nat. Commun.* **2021**, *12*, 5461. [CrossRef] [PubMed]
3. Daguerre, Y.; Siegel, K.; Edel-Hermann, V.; Steinberg, C. Fungal proteins and genes associated with biocontrol mechanisms of soil-borne pathogens: A review. *Fungal Biol. Rev.* **2014**, *28*, 97–125. [CrossRef]
4. Mihajlovic, M.; Rekanovic, E.; Hrustic, J.; Grahovac, M.; Tanovic, B. Methods for management of soilborne plant pathogens. *Pestic. I Fitomedicina.* **2017**, *32*, 9–24. [CrossRef]
5. Mowlick, S.; Inoue, T.; Takehara, T.; Kaku, N.; Ueki, K.; Uekiet, A. Changes and recovery of soil bacterial communities influenced by biological soil disinfestation as compared with chloropicrin-treatment. *AMB Express.* **2013**, *3*, 46. [CrossRef] [PubMed]
6. Fang, X.; Phillips, D.; Verheyen, G.; Li, H.; Barbetti, M.J. Yields and resistance of strawberry cultivars to crown and root diseases in the field, and cultivar responses to pathogens under controlled environment conditions. *Phytopathol. Mediterr.* **2012**, *51*, 69–84. [CrossRef]
7. Shim, M.Y.; Starr, J.L.; Keller, N.P.; Woodard, K.E.; Lee, T.A., Jr. Distribution of isolates of *Sclerotium rolfsii* tolerant to pentachloronitrobenzene in texas peanut fields. *Plant Dis.* **1998**, *82*, 103–106. [CrossRef]
8. Xu, T.; Li, Y.; Zeng, X.D.; Yang, X.L.; Yang, Y.Z.; Yuan, S.S.; Hu, X.C.; Zeng, J.R.; Wang, Z.Z.; Liu, Q.; et al. Isolation and evaluation of endophytic *Streptomyces endus* OsiSh-2 with potential application for biocontrol of rice blast disease. *J. Sci. Food Agric.* **2017**, *97*, 1149–1157. [CrossRef] [PubMed]
9. Liu, J.J.; Hagberg, I.; Novitsky, L.; Hadj-Moussa, H.; Avis, T.J. Interaction of antimicrobial cyclic lipopeptides from *Bacillus subtilis* influences their effect on spore germination and membrane permeability in fungal plant pathogens. *Fungal Biol.* **2014**, *118*, 855–861. [CrossRef] [PubMed]
10. Davies, J.C. Pseudomonas aeruginosa in cystic fibrosis: Pathogenesis and persistence. *Paediatr. Respir. Rev.* **2002**, *3*, 128–134. [CrossRef]
11. Ali, J.; Rafiq, Q.A.; Ratcliffe, E. Antimicrobial resistance mechanisms and potential synthetic treatments. *Future Sci. OA* **2018**, *4*, FSO290. [CrossRef] [PubMed]
12. Wong, H.; Koehler, P.E. Production of red water-soluble *Monascus* pigments. *J. Food Sci.* **2010**, *48*, 1200–1203. [CrossRef]
13. Dufossé, L. Microbial production of food grade pigments. *Food Technol. Biotechnol.* **2006**, *44*, 313–321.
14. Prince, L.R.; Bianchi, S.M.; Vaughan, K.M.; Bewley, M.A.; Marriott, H.M.; Walmsley, S.R.; Taylor, G.W.; Buttle, D.J.; Sabroe, I.; Dockrell, D.H.; et al. Subversion of a lysosomal pathway regulating neutrophil apoptosis by a major bacterial toxin, pyocyanin. *J. Immunol.* **2008**, *180*, 3502–3511. [CrossRef] [PubMed]
15. Kaufmann, G.F.; Sartorio, R.; Lee, S.H.; Rogers, C.J.; Meijler, M.M.; Moss, J.A.; Clapham, B.; Brogan, A.P.; Dickerson, T.J.; Janda, K.D. Revisiting quorum sensing: Discovery of additional chemical and biological functions for 3-Oxo-*N*-acylhomoserine lactones. *Proc. Natl. Acad. Sci. USA* **2005**, *102*, 309–314. [CrossRef] [PubMed]
16. Rada, B.; Gardina, P.; Myers, T.G.; Leto, T.L. Reactive oxygen species mediate inflammatory cytokine release and EGFR-dependent mucin secretion in airway epithelial cells exposed to *Pseudomonas pyocyanin*. *Mucosal Immunol.* **2011**, *4*, 158–171. [CrossRef]
17. Ge, P.; Scholl, D.; Prokhorov, N.S.; Avaylon, J.; Shneider, M.M.; Browning, C.; Buth, S.A.; Plattner, M.; Chakraborty, U.; Ding, K.; et al. Action of a minimal contractile bactericidal nanomachine. *Nature.* **2020**, *580*, 1–5. [CrossRef] [PubMed]
18. Toohey, J.I.; Nelson, C.D.; Krotkov, G. Toxicity of phenazine carboxylic acid to some bacteria, algae, higher plants, and animals. *Can. J. Bot.* **2011**, *43*, 1151–1155. [CrossRef]
19. Maurhofer, M.; Keel, C.; Haas, D.; Défago, G. Influence of plant species on disease suppression by *Pseudomonas fluorescens* strain CHAO with enhanced antibiotic production. *Plant Pathol.* **1995**, *44*, 40–50. [CrossRef]
20. Jiang, G.C.; Lin, Y.C.; Zhou, S.N.; Vrijmoed, L.; Jones, E. Studies on the secondary metabolites of mangrove fungus No.1403 from the South China Sea. *Acta Sci. Nat. Univ. Sunyatseni.* **2000**, *39*, 68–72. [CrossRef]
21. Ohmori, T.; Hagiwara, S.I.; Ueda, A.; Minoda, Y.; Yamada, K. Production of pyoluteorin and its derivatives from n-paraffin by *Pseudomonas aeruginosa* S10B2. *Agric. Biol. Chem.* **2014**, *42*, 2031–2036. [CrossRef]
22. Hao, M.V.; Brenner, D.J.; Steigerwalt, A.G.; Kosako, Y.; Komagata, K. *Erwinia persicinus*, a new species isolated from plants. *Int. J. Syst. Evol. Microbiol.* **1990**, *40*, 379–383. [CrossRef]
23. Zhang, Z.F.; Nan, Z.B. *Erwinia persicina*, a possible new necrosis and wilt threat to forage or grain legumes production. *Eur. J. Plant Pathol.* **2014**, *139*, 349–358. [CrossRef]
24. Orel, D.C. *Erwinia persicina* as the new causal agent of lettuce soft rot. *Eur. J. Plant Pathol.* **2020**, *158*, 223–235. [CrossRef]
25. Walaa, I.M.; Zhang, Z.F.; Ibrahim, M.H.; Shi, S.L. Experimental infection in mice with *Erwinia persicina*. *Microb. Pathog.* **2019**, *130*, 38–43. [CrossRef]

26. Yan, J.J.; Lin, Z.Y.; Wang, R.Q.; Liu, F.; Tong, Z.J.; Jiang, Y.J.; Mukhtar, I.; Xie, B.G. First report of *Erwinia persicina* causing pink disease in *Flammulina velutipes* (Enoki Mushroom) in China. *Plant Dis.* **2018**, *103*, 1–5. [CrossRef]
27. Cho, H.; Park, J.Y.; Kim, Y.K.; Sohn, S.H.; Park, D.S.; Kwon, Y.S.; Kim, C.W.; Back, C.G. Whole-genome sequence of *Erwinia persicina* B64, which causes pink soft rot in onions. *Microbiol. Resour. Announc.* **2019**, *8*, 1–3. [CrossRef]
28. Nechwatal, J.; Theil, S. *Erwinia persicina* associated with a pink rot of parsley root in Germany. *J. Plant Dis. Prot.* **2019**, *126*, 161–167. [CrossRef]
29. Kim, W.; Choi, S.Y.; Han, I.; Cho, S.K.; Lee, Y.; Kim, S.; Kang, B.; Choi, O.; Kim, J. Inhibition of *Salmonella enterica* growth by competitive exclusion during early alfalfa sprout development using a seed-dwelling *Erwinia persicina* strain EUS78. *Int. J. Food Microbiol.* **2020**, *312*, 1–7. [CrossRef]
30. Zhang, Z.F.; Nan, Z.B. First report of *Erwinia persicinus* causing wilting of *Medicago sativa* sprouts in China. *Plant Dis.* **2012**, *96*, 454. [CrossRef]
31. Numan, M.; Bashir, S.; Mumtaz, R.; Tayyab, S.; Rehman, N.U.; Khan, A.L.; Shinwari, Z.K.; Al-Harrasi, A. Therapeutic applications of bacterial pigments: A review of current status and future opportunities. *Biotech.* **2018**, *8*, 1–15. [CrossRef] [PubMed]
32. Venil, C.K.; Zakaria, Z.A.; Usha, R.; Ahmad, V.A. Isolation and characterization of flexirubin type pigment from *Chryseobacterium* sp. UTM-3 T. *Biocatal. Agric. Biotechnol.* **2014**, *3*, 103–107. [CrossRef]
33. Zhang, Y.Q.; Zhao, X.Y.; Ma, Y.; Jiang, Y.; Wang, D.; Liang, H. Comparison of blue discoloration in radish root among different varieties and blue pigment stability analysis. *Food Chem.* **2021**, *340*, 1–9. [CrossRef] [PubMed]
34. Ugwu, C.T.; Ogbonna, C.N.; Ogbonna, J.C.; Aoyagi, H. Production and stability of pigments by *Talaromyces purpurogenus* LC128689 in an alternating air phase-liquid phase cultivation system. *Biotechnol. Appl. Biochem.* **2021**, *69*, 1–10. [CrossRef]
35. Li, S.H.; Li, T.P.; Fu, W.N.; Yu, X.J.; Zhao, Z.S.; Jia, Y.F. Effects of metal ions on the stability of purple sweet potato pigment. *Adv. Mater. Res.* **2011**, *396-398*, 1325–1328. [CrossRef]
36. You, C.; Zhang, C.; Feng, C.; Wang, J.; Kong, F. *Myroides odoratimimus*, a biocontrol agent from the rhizosphere of tobacco with potential to control *Alternaria alternata*. *BioControl* **2015**, *60*, 555–564. [CrossRef]
37. Kang, S.G.; Jin, W.; Bibb, M.; Lee, K.J. Actinorhodin and undecylprodigiosin production in wild-type and relA mutant strains of *Streptomyces coelicolor* A3 (2) grown in continuous culture. *FEMS Microbiol. Lett.* **1998**, *168*, 221–226. [CrossRef]
38. Deli, J.; Molnár, P.; Matus, Z.; Tóth, G.; Steck, A. Reisolation of carotenoid 3,6-epoxides from red paprika (*Capsicum annuum*). *Helv. Chim. Acta* **1996**, *79*, 1435–1443. [CrossRef]
39. Chang, P.C.; Blackwood, A.C. Simultaneous production of three phenazine pigments by Pseudomonas aeruginosa Mac 436. *Can. J. Microbiol.* **1969**, *15*, 439–444. [CrossRef]
40. Dassonneville, L.; Wattez, N.; Mahieu, C.; Colson, P.; Houssier, C.; Frederich, M.; Tits, M.; Angenot, L.; Bailly, C. The plant alkaloid usambarensine intercalates into DNA and induces apoptosis in human HL60 leukemia cells. *Anticancer Res.* **1999**, *19*, 5245–5250.
41. Han, J.H.; Shim, H.; Shin, J.H.; Kim, K.S. Antagonistic activities of *Bacillus* spp. strains isolated from tidal flat sediment towards anthracnose pathogens *Colletotrichum acutatum* and *C. gloeosporioides* in south Korea. *Plant Pathol. J.* **2015**, *31*, 165–175. [CrossRef]
42. Abriouel, H.; Franz, C.; Omar, N.B.; Gálvez, A. Diversity and applications of *Bacillus* bacteriocins. *FEMS Microbiol. Rev.* **2011**, *35*, 201–232. [CrossRef]
43. El-Beih, A.A.; Kato, H.; Ohta, T.T. CYP3A4 inhibitors isolated from a marine derived fungus *Penicillium* species. *J. Nat. Med.* **2007**, *61*, 175–177. [CrossRef]
44. Isabel, M.; Jordi, C.; Emilio, M. Cyclic lipopeptide biosynthetic genes and products, and inhibitory activity of plant-associated bacillus against phytopathogenic bacteria. *PLoS ONE* **2015**, *10*, 1–21. [CrossRef]
45. Tanya, C.; Marina, R.; Thando, N.; Sehaam, K.; Wesaal, K. A Metabolomics and molecular networking approach to elucidate the structures of secondary metabolites produced by *Serratia marcescens* strains. *Front. Chem.* **2021**, *72*, 633870. [CrossRef]
46. Samen, F.A.E.; Goussous, S.J.; Al-Shudifat, A.; Makhadmeh, I. Reduced sensitivity of tomato early blight pathogen (*Alternaria solani*) isolates to protectant fungicides, and implication on disease control. *Arch. Phytopathol. Plant Prot.* **2016**, *49*, 1–17. [CrossRef]
47. Kirkegaard, J.A.; Robertson, M.J.; Hamblin, P.; Sprague, S.J. Effect of blackleg and sclerotinia stem rot on canola yield in the high rainfall zone of southern New South Wales, Australia. *Aust. J. Agric. Res.* **2006**, *57*, 201–212. [CrossRef]
48. Suwannarach, N.; Kumla, J.; Bussaban, B.; Lumyong, S. Biocontrol of *Rhizoctonia solani* AG-2, the causal agent of damping-off by *Muscodor cinnamomi* CMU-Cib 461. *World J. Microbiol. Biotechnol.* **2012**, *28*, 3171–3177. [CrossRef]
49. Li, D.Y.; Li, S.A.; Wei, S.H.; Sun, W.X. Strategies to manage rice sheath blight: Lessons from interactions between rice and *Rhizoctonia solani*. *Rice* **2021**, *14*, 21. [CrossRef]
50. Chen, F.; Wang, M.; Zheng, Y.; Luo, J.M.; Yang, X.R.; Wang, X.L. Quantitative changes of plant defense enzymes and phytohormone in biocontrol of cucumber fusarium wilt by *Bacillus subtilis* B579. *World J. Microbiol. Biotechnol.* **2010**, *26*, 675–684. [CrossRef]
51. Tuli, H.S.; Chaudhary, P.; Beniwal, V.; Sharma, A.K. Microbial pigments as natural color sources: Current trends and future perspectives. *J. Food Sci. Technol.* **2015**, *52*, 1–10. [CrossRef] [PubMed]
52. Levy, E.; Eyal, Z.; Chet, I.; Hochman, A. Resistance mechanisms of *Septoria tritici* to antifungal products of *Pseudomonas*. *Physiol. Mol. Plant Pathol.* **1992**, *40*, 163–171. [CrossRef]

agriculture

MDPI

Article

Switchgrass Establishment Can Ameliorate Soil Properties of the Abandoned Cropland in Northern China

Chunqiao Zhao [1], Xincun Hou [1], Qiang Guo [1], Yuesen Yue [1], Juying Wu [1], Yawei Cao [1], Qinghai Wang [1], Cui Li [1], Zhengang Wang [2] and Xifeng Fan [1,*]

[1] Institute of Grassland, Flowers and Ecology, Beijing Academy of Agricultural and Forestry Sciences, No. 9, Shuguanghuayuan Middle Road, Haidian District, Beijing 100097, China; zhaochunqiao@grass-env.com (C.Z.); houxincun@grass-env.com (X.H.); guoqiang@grass-env.com (Q.G.); yueyuesen@grass-env.com (Y.Y.); wujuying@grass-env.com (J.W.); mscaoyw@163.com (Y.C.); wqh@grass-env.com (Q.W.); biolicui@163.com (C.L.)

[2] China Environmental Protection Foundation, No. 16, Guangqumennei Street, Chongwen District, Beijing 100062, China; wangzhengang2022@163.com

* Correspondence: xifengfan_bj@163.com; Tel.: +86-10-5150-3408

Abstract: The bioenergy crop switchgrass (*Panicum virgatum* L.) has been recognized as friendly to the soil of cultivated land depending on the previous land use types and management practices. However, the effects of switchgrass establishment on soil properties at a broader depth when it is harvested annually without any fertilization in northern China largely remain unknown. To explore the impacts of unfertilized switchgrass on soil physical and chemical properties, 0–100 cm soil samples were collected from 7-year cropland-to-switchgrass conversion and the bare land (control). The results showed that switchgrass establishment increased soil total and capillary porosity, CFU numbers of the microbial communities (fungi, bacteria, and actinomycetes), contents of microbial biomass (carbon, nitrogen, and phosphorus), and water-soluble organic carbon, and decreased soil bulk density, mostly at 0–60 cm depths, compared to the control values. Notably, the annual harvest of switchgrass insignificantly increased soil total and available nitrogen contents and slightly reduced available phosphorus and potassium contents. In conclusion, long-term cropland conversion to unfertilized switchgrass could ameliorate soil properties and does not cause soil depletion. The output of this study could inspire governments and farmers to make large-scale use of switchgrass in the ecological restoration of abandoned cropland in north China.

Keywords: *Switchgrass*; abandoned cropland; soil organic carbon; soil nitrogen; soil microbial biomass; soil microbial communities

Citation: Zhao, C.; Hou, X.; Guo, Q.; Yue, Y.; Wu, J.; Cao, Y.; Wang, Q.; Li, C.; Wang, Z.; Fan, X. Switchgrass Establishment Can Ameliorate Soil Properties of the Abandoned Cropland in Northern China. *Agriculture* **2022**, *12*, 1138. https://doi.org/10.3390/agriculture12081138

Academic Editors: Xingxu Zhang, Tingyu Duan, Xiangling Fang and Gaowen Yang

Received: 18 July 2022
Accepted: 28 July 2022
Published: 1 August 2022

1. Introduction

The pursuit of crop production in the last 60 years has forced vast areas of land that were unsuitable for agricultural production, including 8×10^6 hm^2 of grassland, to be reclaimed for farming in China [1,2]. Many severe ecological problems, such as soil degradation and acidification, soil erosion by wind and water, and agricultural non-point source pollution have already emerged and severely affected the safety of the ecological environment in these areas [1,3]. Conversion of cropland to grassland or forests in these areas has been evidenced as a profitable strategy for such environmental problems that has been implemented in many other countries worldwide and adopted by Chinese governments recently [4,5]. Meanwhile, the conversion of cropland, especially the marginal cropland in these areas, provides enormous opportunity for the large-scale use of switchgrass due to its great potential in bioenergy and multiple ecological services.

Switchgrass (*Panicum virgatum* L.) is a C_4, warm season, deeply rooted perennial grass native to North America [6]. It has a wide range of ecological adaptations due to its high tolerance to various stresses and high nutrient- and water-use efficiencies [7,8].

Switchgrass, as one of the most photosynthetically efficient crops, can generate a large quantity of lignocellulosic biomass with adequate nutrient and high-quality fibers, and therefore has been proposed as a model feedstock crop to generate both forage and non-food bioethanol [9]. Moreover, switchgrass is of great interest due to its multiple ecological services such as soil erosion control, wildlife habitats, ornamental purposes, and nitrogen leakage prevention [10]. Recently switchgrass has been successfully introduced in northern China and shows good ecological adaptability [11]. Thus, switchgrass has been considered a good candidate for environmental restoration of marginal cropland, which is a promising solution to address the increasing demand for bioenergy feedstock, as well as to mitigate the environmental problems there, such as by its amelioration effects on degraded soil.

In addition to the biomass yield potential of switchgrass, the effects of its long-term cultivation on the soil micro-environment are also significant concerns. Several publications have revealed that soil physical properties were distinctively ameliorated after switchgrass establishment, e.g., decreased soil bulk density (BD) and increased soil porosity and aggregates [12–14], but this was mostly confined to a shallow soil layer (0–40 cm). For soil chemical properties, a plethora of papers have reported carbon sequestration effects after the cultivation of switchgrass independent of the establishment years, soil types, climate characteristics, and management practices. However, the quantity of the sequestrated carbon differs under those different conditions [15–20]. In contrast, Kasanke et al. (2020) reported that the long-term carbon accrual in soils under switchgrass production depends mainly on the initial site selection [21]. Soil nutrient levels after switchgrass establishment is another research focus worldwide. The annual harvest of switchgrass biomass indicates the long-term export of element nutrients from the cultivated land, which implies soil depletion risk if there is not any fertilization, primarily when harvested at a high frequency [22] and at an earlier time [23,24]. However, the removal rate of switchgrass was much lower than the annual crops [25]. The positive effects of fertilization on switchgrass yield have been proved. However, soil heath status after the annual harvest of switchgrass without fertilization compensation is greatly ignored. The uses of fertilization for switchgrass in many field experiments complicates soil nutrient variations, impeding people's understanding of this question. Hence, the long-term nutrient removal by biomass harvest in unfertilized switchgrass land greatly challenges soil health [14,22–24,26]. To date, the effects of switchgrass establishment on soil properties in the absence of any fertilization have not been addressed, which remarkably prevents the large-scale uses of switchgrass in northern China.

Soil microbial activity usually reflects microbiological processes of soil microorganisms and is a potential indicator of soil quality, as plants rely on soil microorganisms to mineralize organic nutrient for growth and development [27]. Soil microbial communities play a critical role in the cycling of soil nutrient materials, which is usually affected by crop cover, management practices, soil types, and soil depths. Switchgrass establishment has been evidenced to increase soil bacteria and fungi communities and their activities [28–30], while lacking exploration at a deeper soil depth. It's worth noting that switchgrass establishment might promote soil microbial nitrogen fixation, especially under low nitrogen levels, which accounts for a nonnegligible amount of nitrogen for the growth and development of switchgrass [31–33]. Hence, it is attractive to detect soil nitrogen levels after switchgrass establishment, especially when fertilization is not applied. It is necessary to uncover the microbial alterations after the conversion of cropland to unfertilized switchgrass.

We hypothesized that long-term switchgrass cultivation could dramatically ameliorate soil properties, but may generate some adverse effects on soil nutrient levels due to the annual export of element materials from the field. The objectives of this study were to (1) evaluate the effects of 7-year switchgrass establishment on soil physical and chemical properties; (2) to illustrate changes in soil nutrient levels after switchgrass cultivation compared to the bare land; and (3) to reveal the alterations in soil microbial communities including the quantity of soil bacteria, fungi, and actinomycetes as well as the contents of microbial carbon, nitrogen, and phosphorus.

2. Materials and Methods

2.1. Study Site Description and Management

The experiment site was located at the experimental base of the Institute of Grassland, Flowers and Ecology, Beijing Academy of Agricultural and Forestry Sciences (40°23′ N, 116°28′ E) at Town in Beijing, China (Figure S1). The soil type, climate characteristics, and the initial soil properties were well described in our previously published paper [34]. The experiment was based on a long-term yield evaluation test platform for switchgrass, which was built in 2006. There were two types of land in this study, switchgrass-cultivated land (switchgrass plot) and the bare land (bare land plot). We set five 4 × 5 m subplots for each type of land; these five subplots were not adjacent and were distributed randomly in the experiment field. We considered the five subplots of each plot to be five replicates in this study.

Before switchgrass plantation, rotary tillage was conducted at around 30 cm depth, and then about 150 kg/ha compound fertilizer (N:P:K = 20:12.5:10) was spread evenly over the whole experiment area. In mid-April 2006, we planted switchgrass seedlings (four leaf stage) with 80 cm plant spacing. Then, about 200 m^3/ha irrigation was provided by sprinkler irrigation after plantation to ensure the expected growth of switchgrass according to our previous experience. Beyond that, there was just natural rainfall during the whole experiment period. The weeds in the switchgrass and bare land were manually prevented. In early November of each year, the above-ground biomass, including all the litter, was harvested, leaving around 10 cm stubble height. Beyond that, there were not any other management practices in this experiment. The amount of rainfall ranged from 318.00 mm to 733.20 mm, and the average temperature was 13.29 during the 2006 to 2012 period in this area.

2.2. Soil Sampling and Properties Determination

Soil samples were collected in mid-November 2012 from the two plots. Before sampling, the apparent litter and small rocks were carefully removed. We dug a quadrat pit layer by layer (20 cm for each layer to 100 cm) in each subplot of the two plots. The exact location of the quadrat is displayed in Figure S2. Soil from the layers 0–20, 20–40, 40–60, 60–80, and 80–100 cm was thoroughly mixed using the soil cone method, and then ten random subsamples were acquired from the cone to form one composed replicate. Hence, there were five soil replicates for each layer of the two plots. Undisturbed soil cores at different soil layers of each quadrate were taken by a cylindrical steel ring of 100 cm^3 volume with five replicates for soil physical property analysis. The visible rocks were removed from soil samples and all soil samples were passed through a 2 mm sieve. Each soil replicate was divided into two parts; one part was transported back to the laboratory in a 4 °C incubator and then stored in a 4 °C refrigerator for the determination of microbial indicators. The other part was naturally air-dried and crushed by a micro-mill (Tianjin TEST Instrument Co., LTD, Tianjin, China) for the determination of soil organic carbon (SOC), total nitrogen (TN), total phosphorous (TP), total potassium (TK), available nitrogen (AN), available phosphorus (AP), available potassium (AK), and soil pH.

Soil capillary porosity (CP) was determined by the core method [35]. Soil total porosity (TPO) was calculated as the difference between the saturated soil weight and the dry soil weight divided by the sample volume [35]. Soil bulk density (BD) and soil water contents were determined based on the oven-dried cutting ring-acquired soil samples. Soil pH was measured using a 1:2.5 ratio of 0.01 M $CaCl_2$ solution/soil suspension according to the professional standard of China (LY/T 1239-1999) by a Nahita pH meter, model ST 5000 (Ohaus International Trading (Shanghai) Co., LTD, Shanghai, China). A Vario Macro CHNS instrument (Elementar Analys ensysteme GmbH, Hanau, Germany) was used to determine soil TN [34]. We determined soil AN, AP, and AK contents using the alkaline $KMnO_4$ oxidation method, Olsen's extract method, and the NH_4OAc extract method, respectively [36]. About 10 g of fresh soil samples were used to determine microbial C and N contents using the chloroform fumigation-K_2SO_4 extraction and potassium persulfate digestion methods,

respectively [37]. Soil microbial phosphorus (MP) contents were determined by chloroform fumigation method coupled with phosphorus detection by molybdate colorimetry [38]. The values were corrected for phosphate sorption to the soil during the extraction and for microbial phosphorus not recovered by fumigation [38]. The potassium dichromate oxidation method coupled with ferrous sulfate titrimetry was used to determine SOC and water-soluble organic carbon (WSOC) contents. Digestion and colorimetric methods were used to determine soil TP content [39]. The atomic absorption method was used to determine soil total K (TK) contents [40]. Soil actinomycete is the third most abundant community and plays crucial roles in the mineralization process of soil organic materials, e.g., the degradation of cellulosic materials, and hence participates primarily in soil element cycling and soil amelioration. Hence, we herein analyzed these three dominant microbial communities. We used the solid medium made from beef extract, Martin's medium [41], and Gause I Medium [42] to culture soil bacteria, fungi, and actinomycetes, respectively. The medium was invertedly cultured at 2 °C in a constant temperature incubator for one week. The CFU numbers were calculated according to the following formula,

$$\mathrm{CFU} = \frac{\mathrm{C} \times \mathrm{n}}{\mathrm{m}} \quad (1)$$

where CFU indicates the CFU numbers of soil bacteria, fungi, and actinomycetes. C, n, and m represented the average community number, dilution ratio, and soil dry weights, respectively.

2.3. Statistical Analysis

The experiment data were organized and prepared using Microsoft Office Excel 2010. Shapiro–Wilk and Levene tests were performed to check the data distribution and homoscedasticity before the analysis, respectively. A Wilcoxon rank-sum test corrected by the "Bonferroni" method was carried out to verify the significant differences in soil indexes of the paired groups at $p < 0.05$ and 0.01. The correlation analysis based on Pearson's method at $p < 0.05$ (*) and 0.01 (**) levels in this work were carried out using the "psych" package in R software (3.5.2). The figures were created using Origin (2019b, OriginLab Corporation, Northampton, MA, USA) and R software (Bell Laboratories, Inc., Windsor, ON, Canada).

3. Results

3.1. Soil Physical Properties of the Bare Land and Switchgrass Land

Figure 1 showed the great changes in soil physical properties after switchgrass establishment compared to the bare land. The switchgrass establishment significantly ($p < 0.05$, 0.01, or 0.001) increased 0–60 cm soil CP by 40.51%, 16.92%, and 14.33% sequentially from the top to the bottom (Figure 1a). Soil CP from 60–100 cm exhibited a slight ($p > 0.05$) decrease by 5.89% and 10.92% sequentially compared to the bare land (Figure 1a). Soil TP at 0–100 cm depth of switchgrass land was significantly ($p < 0.05$, 0.01, or 0.001) higher by 30.98%, 24.05%, 7.90%, 18.34, and 11.96% sequentially compared to the bare land (Figure 1b). For soil BD, 0–60 cm soil of switchgrass land significantly ($p < 0.05$ or 0.01) decreased by 6.37%, 4.58%, and 2.17% sequentially compared to the bare land (Figure 1c), while BD of 60–100 cm soil of the two land types seemed to be similar (Figure 1c). The water contents of 0–100 cm soil all showed an increased trend compared to the bare land, and the increase percentages reached 38.26%, 16.08%, 9.63%, 10.09%, and 5.13%, sequentially, though the difference at 80–100 cm was not statistically significant ($p > 0.05$, Figure 1d).

As is shown in Figure 2, no significant difference in SOC was observed at 0–100 cm soil between the two types of land. The WSOC of switchgrass land soil at 0–40 cm showed significant ($p < 0.05$) increases by 86.79% and 23.97%, respectively, compared to the bare land (Figure 2b). Soil WSOC at 40–100 cm depths of switchgrass cultivated land all exhibited an increasing trend compared to the bare land, but the differences were not significant (Figure 2b).

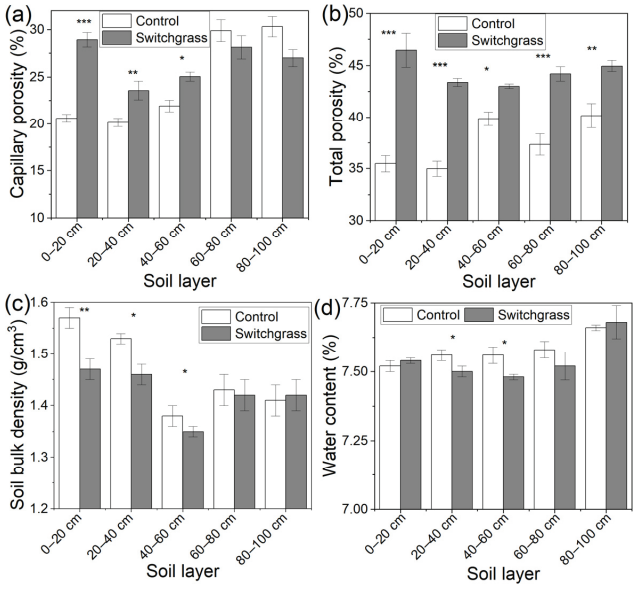

Figure 1. Soil (**a**) capillary porosity, (**b**) total porosity, (**c**) bulk density, and (**d**) water contents in the bare land (control) and switchgrass-cultivated land. Error bars (standard deviation) were correctly added at the top of the mean columns. A Wilcoxon rank-sum test was used to analyze the significant differences in each soil index between control and switchgrass land at $p < 0.05$ (*), 0.01 (**), and 0.001 (***) levels.

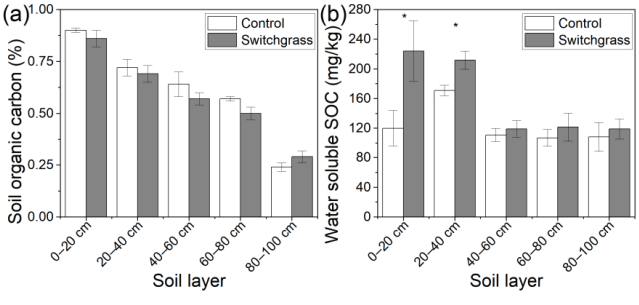

Figure 2. Soil (**a**) organic carbon and (**b**) water-soluble carbon content in bare land (control) and switchgrass-cultivated land. Error bars (standard deviation) were correctly added at the top of the mean columns. A Wilcoxon rank-sum test was used to analyze the significant differences between the bare land and switchgrass cultivated land at $p < 0.05$ (*).

3.2. Soil Chemical Properties of the Bare Land and Switchgrass Land

Soil nutrient levels after switchgrass establishment showed some differences compared to the bare land (Figure 3). Soil TN, TP, and AN content all showed a gradual decreasing trend with soil depths, while TP and AK showed the opposite trend (Figure 3). We found significant ($p < 0.05$ or 0.01) increases in soil TN at 0–40 and 60–80 cm by 7.92%, 30.67%, and 20.34%, sequentially, compared to the bare land (Figure 3a). In contrast, no significant difference was observed in soil TN between switchgrass and bare land (Figure 3a). The decreasing trend is presented in Figure 3b in soil TP at 0–100 cm (except for 20–40 cm) of switchgrass land compared to the bare land, though the differences were insignificant in some layers. For 0–20 cm and 80–100 cm soil, the decreasing percentages reached 2.78% and 9.68%, respectively, whereas the increasing percentage in 20–40 cm was 3.03%

(Figure 3b). For soil TK, 0–40 cm and 80–100 cm soil of switchgrass land exhibited significant ($p < 0.01$) increases by 3.80%, 4.30%, and 5.69%, sequentially, compared to the bare land, and 40–80 cm soil showed a similar value (Figure 3c). Soil AN of 0–80 cm in switchgrass land was significantly ($p < 0.01$ or 0.001) higher by 27.97%, 47.19%, 21.68%, and 59.16%, sequentially, than the values in the bare land (Figure 3d). The 80–100 cm soil exhibited no significant difference (Figure 3d). For AP, we did not observe a significant difference in 0–20 cm soil between the two types of land (Figure 3e), and a significant ($p < 0.05$) increase of 7.51% was found in 20–40 cm soil (Figure 3e). On the contrary, AP of 40–100 cm soil in switchgrass land increased significantly ($p < 0.05$) by 5.70%, 13.00%, and 9.50%, sequentially, compared to the bare land (Figure 3e). Soil AK contents of the two types of land showed different changes in different soil depths (Figure 3f). A significant ($p < 0.05$) increase by 11.73% at 0–20 cm and significant decreases ($p < 0.05$) by 13.31% and 13.56% at 40–80 cm, respectively, were observed in switchgrass land compared to the bare land (Figure 3f). No significant differences were found in other soil depths (Figure 3f).

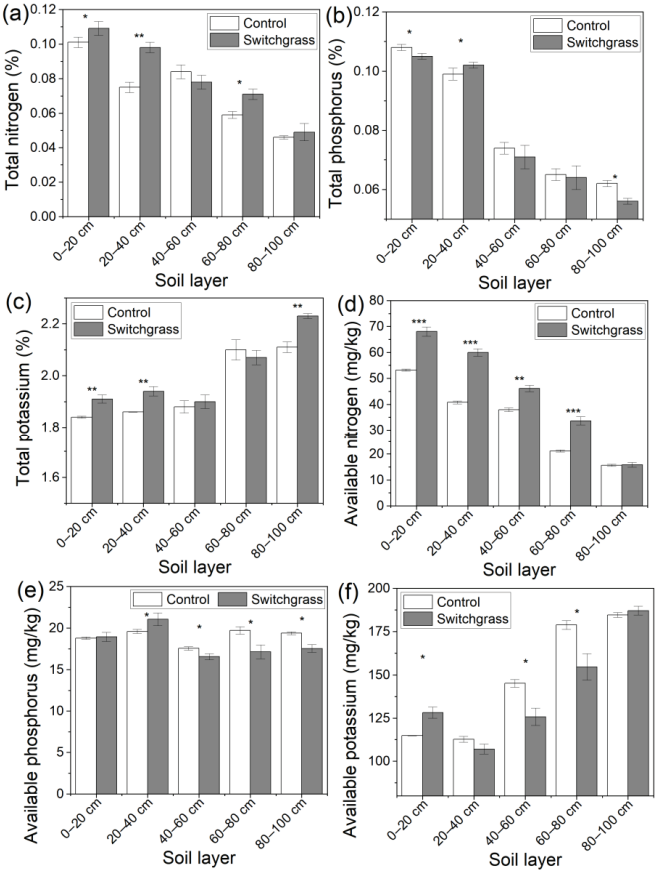

Figure 3. Soil total (**a**) nitrogen, (**b**) phosphorus, (**c**) potassium, and available (**d**) nitrogen, (**e**) phosphorus, (**f**) potassium in the bare land and switchgrass-cultivated land. Error bars (standard deviation) were correctly added at the top of the mean columns. A Wilcoxon rank-sum test was used to analyze the significant differences between the bare land and switchgrass cultivated land at $p < 0.05$ (*), 0.01 (**), and 0.001 (***) levels.

3.3. Soil Microbial Indicators and Correlations with Soil Other Properties

Soil microbial communities are primarily distributed in 0–40 cm soil (Figure 4). The large differences in the CFU number of fungi, bacteria, and actinomycetes occurred mainly in 0–40 cm soil depths between the two types of land (Figure 4). At 0–20 cm soil depth, the CFU numbers of fungi, bacteria, and actinomycetes in switchgrass land were significantly ($p < 0.05$, 0.01 or 0.001) higher by 149.27%, 37.60%, and 56.40% than the bare land (Figure 4a–c), and, in 20–40 cm soil, the increase percentages reached 775.37%, 70.80%, and 338%, respectively (Figure 4a–c). In 40–60 cm soil, only the CFU number of actinomycetes in switchgrass land increased significantly ($p < 0.001$), by 152% compared with the bare land (Figure 4c). Few differences were observed at other soil depths in the CFU number of the three microbial communities, but they mostly exhibited an increase (Figure 4).

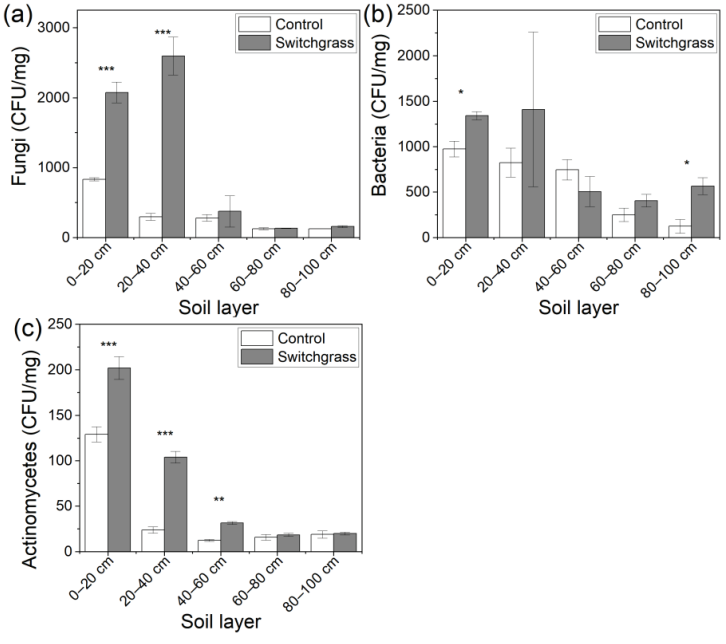

Figure 4. CFU numbers of (**a**) fungi, (**b**) bacteria, and (**c**) actinomycetes in the bare land and switchgrass-cultivated land. Error bars (standard deviation) were correctly added at the top of the mean columns. A Wilcoxon rank-sum test was used to analyze the significant differences between the bare land and switchgrass cultivated land at $p < 0.05$ (*), 0.01 (**), and 0.001 (***) levels.

Soil MC, MN, and MP at all five soil depths showed an increase in switchgrass land compared to the bare land (Figure 5). The significant ($p < 0.001$) increase percentages of soil MC in 0–40 cm soil in switchgrass land were large, reaching 117.42% and 57.58%, respectively, and at 40–100 cm soil depths, they reached 18.30%, 11.34%, and 37.87%, sequentially, when compared to the bare land (Figure 5a). For soil MN, the increase percentages reached 20.48% ($p > 0.05$), 41.01% ($p < 0.05$), 12.45% ($p > 0.05$), 42.20% ($p < 0.05$), and 11.45% ($p > 0.05$), sequentially, in switchgrass land (Figure 5b). The significant ($p < 0.05$ or 0.01) increases in soil MP mainly happened at 60–100 cm depths, and the increase percentages were 67.57% and 103.03%, sequentially; at the other soil depths, slight increases were observed (Figure 5c).

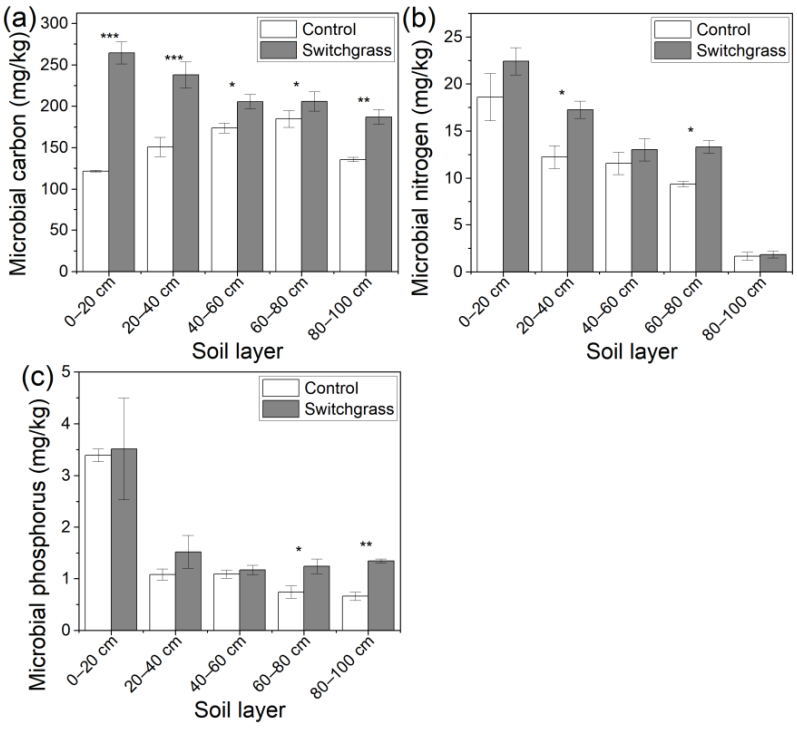

Figure 5. Soil microbial (**a**) carbon, (**b**) nitrogen, and (**c**) phosphorus contents in bare land and switchgrass-cultivated land. Error bars (standard deviation) were correctly added at the top of the mean columns. A Wilcoxon rank-sum test was used to analyze the significant differences between the bare land and switchgrass cultivated land at $p < 0.05$ (*), 0.01 (**), and 0.001 (***) levels.

According to the heatmap results, the microbial indicators, including the CFU numbers of the bacteria, fungi, and actinomycetes as well as MC, MN, and MP contents, were all positively correlated with WSOC, TP, SOC, TN, and AN (Figure 6). The microbial indicators (excluding MC) were negatively correlated with soil pH, TK, and AK. Soil AK showed significantly ($p < 0.05$ or 0.01) negative correlations with the CFU numbers of three microbial communities and MN (Figure 6). Soil pH, as an important soil indicator, was also included into the correlation analysis although few differences were observed in this study (the data was not shown). Soil MN exhibited significantly ($p < 0.01$) negative correlations with soil pH, TK, and AK (Figure 6). Soil MC only had significant ($p < 0.01$) positive correlations with soil TPO (Figure 6).

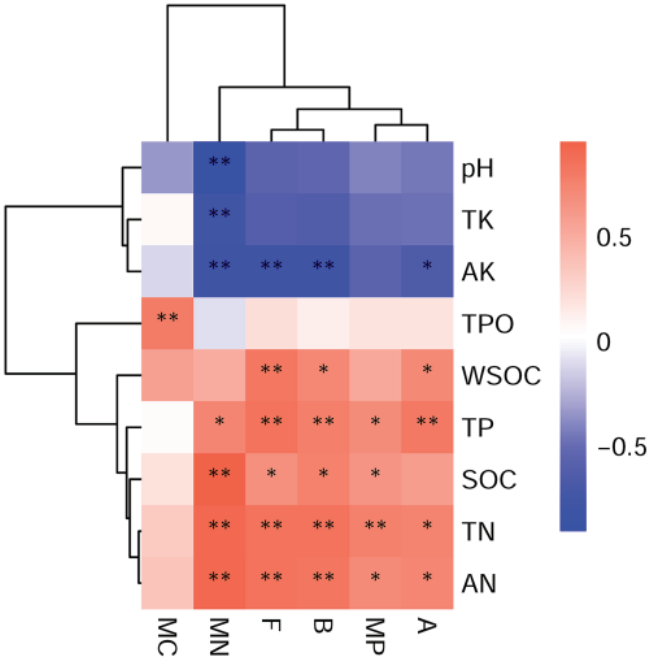

Figure 6. Pearson correlation analysis between soil microbial communities and properties. A, B, and F represent the actinomycetes, bacteria, and fungi. MN, MP, and MC indicate microbial nitrogen, phosphorus, and carbon. TN, TP, TK, TPO, AK, AN, SOC, and WSOC indicate soil total nitrogen, total phosphorus, total potassium, total porosity, and water-soluble organic carbon, respectively. The symbol * and ** indicate significant correlations at $p < 0.05$ and 0.01, respectively. The colored bar from white to red and blue shows the gradual increasing R^2 value of the positive and negative correlations, respectively.

4. Discussion

Switchgrass shows excellent potential as bioenergy raw material. It provides multiple ecological services, but the effects of its establishment without any fertilization on soil properties in abandoned cropland are unclear, which proposes the necessity of this work. To address these questions, we determined the main soil physical and chemical properties and CFU numbers of microbial communities, as well as the microbial biomass based on 7-year cropland to switchgrass conversion.

4.1. Effects of 7-Year Switchgrass Establishment on Soil Physical Properties

Potential improvements in soil physical properties are significant should switchgrass be cultivated on abandoned cropland, as it has a very developed root system. The increased soil porosity can promote soil aeration and water entry, which is an important indicator of soil quality [43]. Several studies have evidenced the increased soil CP and TPO in marginal cropland after switchgrass cultivation, which was mainly due to switchgrass developing root systems in deep soil and stalk residues on the land surface [14,44,45]. However, the effects of long-term (7-year) production of unfertilized switchgrass on soil physical properties in cropland in northern China are still ambiguous. In this study, the significantly ($p < 0.05$, 0.01, or 0.001) increased soil TPO (Figure 1b) indicates the dramatical amelioration effects of switchgrass on soil physical structure. However, the increases of soil CP seemed more pronounced at 0–60 cm depths than at 60–100 cm (Figure 1a), which implies that the amelioration effects primarily exist within a limited range of soil depth. Due to the changes in soil CP, the capacity of soil to absorb water was dramatically

enhanced, which led to a significantly ($p < 0.05$, 0.01, or 0.001) higher water content in 0–80 cm soil of switchgrass land (Figure 1d). We speculate that root residues contributed significantly to the improved soil porosity at deeper soil depths. The stubble residue after annual harvest was the predominant factor influencing the surface soil porosity [44,45].

Soil BD, which is also a critical soil property and indicates soil quality, represents the mass of dry soil per unit volume and essentially measures soil porosity, as a high number of soil pores results in low bulk density values [43]. A plethora of papers have reported decreased soil BD after switchgrass establishment, and the surface soil usually shows a more extensive range of variation than soil at deeper depths [14,43,46–48]. Consistent with the conclusion of the increased soil porosity in switchgrass land, the 0–60 cm soil BD was significantly ($p < 0.05$ or 0.01) decreased in the range of 0.03 to 0.1 g/cm^3 compared with the cropland (Figure 1c), which was consistent with most of the previous studies [14,43,46–48]. The minor sensitivity of soil BD at 60–100 cm was probably attributable to the predominant influences of clay content rather than switchgrass establishment [48]. In addition, the relatively rare root distribution in deeper soil was also another factor that should be considered. As we hypothesized, all these results evidenced the distinct amelioration effects of switchgrass establishment on soil physical structures, though there was no fertilization applied over a 7-year biomass harvest.

4.2. Effects of 7-Year Unfertilized Switchgrass on Soil Nutrient Levels

SOC, which is another important indicator of soil quality [49], has a large pool size and plays a vital role in global carbon cycling because of its slower turnover rate than atmospheric carbon [50]. The carbon sequestration potential of switchgrass establishment has been a great concern worldwide, and its carbon accrual effect has been widely evidenced [15–20]. However, there have been some particular case indicating experiment-site-dependent conclusions [21]. Unlike most studies, we herein observed similar SOC contents in 0–100 cm soil in switchgrass land compared to the bare land (Figure 2a). It is hard for us to provide reasonable explanations, but this was probably due to soil carbon priming effects, which should be explored further over a continuous time scale. Soil WSOC usually indicates carbon resources that could be directly used by the soil microbial communities. In this work, the significantly increased WSOC contents in switchgrass land imply relatively abundant carbon resources, which could benefit the enrichment of soil microbial communities, especially at 0–40 cm depths (Figure 2b).

Besides carbon accrual after switchgrass cultivation, the primary nutrients levels, such as those of nitrogen, phosphorus, and potassium, are also significant concerns for most people, especially in China. It is unrealistic for Chinese farmers to input any fertilization during switchgrass production due to the uncertain economic benefits that could be derived from the plantation system. Hence, there is a significant doubt about whether the soil quality was sustainable in the absence of any fertilization over a long-term period. However, the net element exports of switchgrass were much lower than those of cereal crops [25]. In this study, it is interesting that soil TN contents exhibited a significant increase instead of sharp decreases (Figure 3a). Several papers have evidenced the existence of non-symbiotic nitrogen-fixing bacteria and remarkable contributions to nitrogen requirements during the growth and development of switchgrass [31–33,51,52], which was the critical reason for the higher TN and AN (Figure 3a,d) in the switchgrass land. Moreover, the prevention of soil nitrogen leaching by the developed switchgrass root system [53] and decreased nitrogen emissions [54] are two factors that should not be ignored for nitrogen accumulation in switchgrass land.

The decreased soil TP and AP contents were reported in both 5-year and 9-year unfertilized switchgrass field experiments [14,17]. In this work, the significantly reduced soil TP and AP contents in deeper soil depths (40–100 cm, Figure 3b,e) imply soil phosphorus consumption through annual biomass harvest, which requires appropriate phosphorus compensation. The degradation of the stubble residues after annual harvest of switchgrass might contribute to the similar AP levels between the switchgrass and control group, but

it cannot change the decreasing trend of soil TP in surface soil (0–20 cm). Switchgrass roots were mainly distributed within 0–40 cm soil and were more dispersive in 20–40 cm soil. We speculated that the activation effects by the more abundant capillary roots on soil phosphorus, together with more root turnover, induced the significant increase in soil TP and AP contents in switchgrass land. The accrual of soil potassium caused by the degradation of switchgrass stubbles after biomass harvest accounted mainly for the significantly increased soil TK and AK levels in surface soil (0–40 cm), while it hardly changed the results of the significantly reduced AK contents in deeper soils, although the TK contents were similar.

4.3. Effects of 7-Year Unfertilized Switchgrass on Soil Microbial Indicators

The soil microbial community performs many pivotal ecological functions in soil nutrient and energy cycles [55]. Land-use changes have been widely evidenced to affect soil physical and chemical properties drastically and thus reshape soil microbial communities [56]. Several studies have reported increased numbers of soil bacteria, fungi, and actinomycetes, as well as microbial biomass [28–30,37]. However, a large knowledge gap exists in the current understanding of changes in the soil microbial communities and N cycling after the long-term cropland conversion to switchgrass in a temperate continental monsoon climate. In this work, consistent with the previous conclusions, significantly increased numbers of soil bacteria, fungi, and actinomycetes were observed predominantly in 0–40 cm soil after switchgrass establishment, which led to significantly increased microbial carbon, nitrogen, and phosphorus contents. These results are consistent with the significantly increased WSOC (Figure 2b) contents in this study. The increased microbial C/N (data not shown) usually indicate the shift of soil bacterial communities to fungi communities [57], which was also evidenced by the increased fungal and bacterial CFU ratio in this study (data not shown here).

5. Conclusions

In conclusion, we showed that switchgrass establishment can ameliorate soil physical properties, and the nutrient levels did not seem to be depleted except for the slight decrease of soil TP level, even when the biomass was annually harvested without any fertilization. The alterations of soil physical properties, such as increased soil porosity and decreased BD, and chemical properties, such as increased WSOC, TN, and AN, drove the shift of soil bacteria, fungi, and actinomycetes from the bare land pattern to the switchgrass land pattern. Outputs of this study could firmly dispel anxiety that soil nutrients might be exhausted under such a model over a long-term period, which could inspire the government and farmers to large-scale use of switchgrass on abandoned cropland in northern China. Based on our findings, it is exciting and of great significance to explore the mechanisms of the increased TN levels over the long-term switchgrass production without any nitrogen compensation through high-throughput sequencing and metagenomic strategies.

Supplementary Materials: The following supporting information can be downloaded at: https://www.mdpi.com/article/10.3390/agriculture12081138/s1. Figure S1: Schematic diagram of the experiment site location. Figure S2: Schematic diagram of the location of the plot pit.

Author Contributions: Conceptualization, C.Z., X.F. and X.H.; methodology, C.Z., Q.G. and Y.Y.; software, C.Z., Y.Y., X.H. and Y.C.; validation, C.Z., J.W., Q.G. and X.H.; formal analysis, C.Z., X.H., Z.W. and Y.Y.; investigation, C.Z., X.F. and X.H.; resources, X.F. and J.W.; data curation, C.Z., X.F., X.H. and Z.W.; writing—original draft preparation, C.Z., Y.C., Z.W., Q.W. and C.L., writing—review and editing, C.Z., X.H., Q.G., Y.Y., J.W., Q.W. and C.L., visualization, C.Z., Y.C., Q.W., C.L. and Z.W., supervision, X.F., X.H. and Y.Y.; project administration, X.F. and J.W.; funding acquisition, X.F. and J.W. All authors have read and agreed to the published version of the manuscript.

Funding: This research was funded by the Special Project for Capacity of the Scientific and Technological Innovation, grant numbers KJCX20210419 and KJCX20200210, and The National Natural Science Foundation of China (31971752). This study was also supported by the Lush Mountains Project Special Fund of China Environmental Protection Foundation 'Carbon sequestration and ecological restoration potential of switchgrass and its demonstration in saline-alkali land of the Yellow River Delta', grant number CEPFQS202169-16.

Institutional Review Board Statement: Not applicable.

Informed Consent Statement: Not applicable.

Data Availability Statement: The datasets used and analyzed during the current study are available from the corresponding author on reasonable request.

Acknowledgments: We thank researcher Wenjun Teng and others who contributed significantly to the establishment and maintenance of the experimental site. This research was funded by the Special Project for Capacity of the Scientific and Technological Innovation, grant numbers KJCX20210419 and KJCX20200210, and The National Natural Science Foundation of China (31971752). This study was also supported by the Lush Mountains Project Special Fund of China Environmental Protection Foundation, 'Carbon sequestration and ecological restoration potential of switchgrass and its demonstration in saline-alkali land of the Yellow River Delta', grant number CEPFQS202169-16.

Conflicts of Interest: The authors declare no conflict of interest.

References

1. Xu, Z.; Li, Y. Effects of grassland degradation on soil and water loss. *Arid. Land Res. Manag.* **2003**, *17*, 65–68.
2. Li, B.; Tang, H.; Wu, L.; Li, Q.; Zhou, C. Relationships between the soil organic carbon density of surface soils and the influencing factors in differing land uses in Inner Mongolia. *Environ. Earth Sci.* **2012**, *65*, 195–202. [CrossRef]
3. Ongley, E.D.; Xiaolan, Z.; Tao, Y. Current status of agricultural and rural non-point source pollution assessment in China. *Environ. Pollut.* **2010**, *158*, 1159–1168. [CrossRef]
4. Bullock, A.; King, B. Evaluating China's Slope Land Conversion Program as sustainable management in Tianquan and Wuqi Counties. *J. Environ. Manag.* **2011**, *92*, 1916–1922. [CrossRef]
5. Wei, H.; Zhang, K.; Zhang, J.; Li, D.; Zhang, Y.; Xiang, H. Grass cultivation alters soil organic carbon fractions in a subtropical orchard of southern China. *Soil Tillage Res.* **2018**, *181*, 110–116. [CrossRef]
6. Slessarev, E.W.; Nuccio, E.E.; McFarlane, K.J.; Ramon, C.E.; Saha, M.; Firestone, M.K.; Pett-Ridge, J. Quantifying the effects of switchgrass (*Panicum virgatum*) on deep organic C stocks using natural abundance ^{14}C in three marginal soils. *GCB Bioenergy* **2020**, *12*, 834–847. [CrossRef]
7. Berti, M.T.; Johnson, B.L. Switchgrass establishment as affected by seeding depth and soil type. *Ind. Crop. Prod.* **2013**, *41*, 289–293. [CrossRef]
8. McLaughlin, S.B.; Kszos, L.A. Development of switchgrass (*Panicum virgatum*) as a bioenergy feedstock in the United States. *Biomass-Bioenergy* **2005**, *28*, 515–535. [CrossRef]
9. Guretzky, J.A.; Biermacher, J.T.; Cook, B.J.; Kering, M.K.; Mosali, J. Switchgrass for forage and bioenergy: Harvest and nitrogen rate effects on biomass yields and nutrient composition. *Plant Soil* **2011**, *339*, 69–81. [CrossRef]
10. Phouthavong-Murphy, J.C.; Merrill, A.K.; Zamule, S.; Giacherio, D.; Brown, B.; Roote, C.; Das, P. Phytoremediation potential of switchgrass (*Panicum virgatum*), two United States native varieties, to remove bisphenol-A (BPA) from aqueous media. *Sci. Rep.* **2020**, *10*, 835. [CrossRef]
11. Yue, Y.; Hou, X.; Fan, X.; Zhu, Y.; Zhao, C.; Wu, J. Biomass yield components for 12 switchgrass cultivars grown in Northern China. *Biomass-Bioenergy* **2017**, *102*, 44–51. [CrossRef]
12. He, H.; Wu, N.; Liu, J.; Chen, J.; Liu, X.; Chang, W. Effects of planting years of *Panicum virgatum* on soil physical and chemical properties. *Ecol. Environ. Sci.* **2020**, *29*, 285–292. (In Chinese)
13. He, H.; Wu, N.; Liu, J.; Xu, X. Effects of different fertilization treatments on soil chemical properties and bacterial diversity in switchgrass field. *Soil Fertil. Sci. China* **2022**, *3*, 164–172. (In Chinese)
14. Stewart, C.E.; Follett, R.F.; Pruessner, E.G.; Varvel, G.E.; Vogel, K.P.; Mitchell, R.B. Nitrogen and harvest effects on soil properties under rainfed switchgrass and no-till corn over 9 years: Implications for soil quality. *GCB Bioenergy* **2015**, *7*, 288–301. [CrossRef]
15. Lemus, R.; Lal, R. Bioenergy Crops and Carbon Sequestration. *Crit. Rev. Plant Sci.* **2005**, *24*, 1–21. [CrossRef]
16. Liebig, M.; Johnson, H.; Hanson, J.; Frank, A. Soil carbon under switchgrass stands and cultivated cropland. *Biomass-Bioenergy* **2005**, *28*, 347–354. [CrossRef]
17. Lai, L.; Kumar, S.; Osborne, S.; Owens, V.N. Switchgrass impact on selected soil parameters, including soil organic carbon, within six years of establishment. *Catena* **2018**, *163*, 288–296. [CrossRef]
18. Chatterjee, A.; Long, D.S.; Pierce, F.J. Switchgrass influences on soil biogeochemical processes in the dryland region of the Pacific Northwest. *Commun. Soil Sci. Plant Anal.* **2013**, *44*, 2314–2326. [CrossRef]

19. Martinez-Feria, R.; Basso, B. Predicting soil carbon changes in switchgrass grown on marginal lands under climate change and adaptation strategies. *GCB Bioenergy* **2020**, *12*, 742–755. [CrossRef]
20. Ledo, A.; Smith, P.; Zerihun, A.; Whitaker, J.; Vicente-Vicente, J.L.; Qin, Z.; McNamara, N.P.; Zinn, Y.L.; Llorente, M.; Liebig, M.; et al. Changes in soil organic carbon under perennial crops. *Glob. Chang. Biol.* **2020**, *26*, 4158–4168. [CrossRef]
21. Kasanke, C.P.; Zhao, Q.; Bell, S.; Thompson, A.M.; Hofmockel, K.S. Can switchgrass increase carbon accrual in marginal soils? The importance of site selection. *GCB Bioenergy* **2021**, *13*, 320–335. [CrossRef]
22. Zhao, F.; Yang, W.; Zeng, Z.; Li, H.; Yang, X.; He, Z.; Gu, B.; Rafiq, M.T.; Peng, H. Nutrient removal efficiency and biomass production of different bioenergy plants in hypereutrophic water. *Biomass-Bioenergy* **2012**, *42*, 212–218. [CrossRef]
23. Kering, M.K.; Guretzky, J.A.; Interrante, S.M.; Butler, T.J.; Biermacher, J.T.; Mosali, J. Harvest timing affects switchgrass production, forage nutritive value, and nutrient removal. *Crop Sci.* **2013**, *53*, 1809–1817. [CrossRef]
24. Kimura, E.; Collins, H.P.; Fransen, S. Biomass production and nutrient removal by switchgrass under irrigation. *Agron. J.* **2015**, *107*, 204–210. [CrossRef]
25. Propheter, J.L.; Staggenborg, S. Performance of annual and perennial biofuel crops: Nutrient removal during the first two years. *Agron. J.* **2010**, *102*, 798–805. [CrossRef]
26. Kumar, P.; Lai, L.; Battaglia, M.L.; Kumar, S.; Owens, V.; Fike, J.; Galbraith, J.; Hong, C.O.; Farris, R.; Crawford, R.; et al. Impacts of nitrogen fertilization rate and landscape position on select soil properties in switchgrass field at four sites in the USA. *Catena* **2019**, *180*, 183–193. [CrossRef]
27. Chen, G.; Zhu, H.; Zhang, Y. Soil microbial activities and carbon and nitrogen fixation. *Res. Microbiol.* **2003**, *154*, 393–398. [CrossRef]
28. Liang, C.; Jesus, E.D.C.; Duncan, D.; Jackson, R.D.; Tiedje, J.M.; Balser, T.C. Soil microbial communities under model biofuel cropping systems in southern Wisconsin, USA: Impact of crop species and soil properties. *Appl. Soil Ecol.* **2012**, *54*, 24–31. [CrossRef]
29. Mafa-Attoye, T.G.; Thevathasan, N.V.; Dunfield, K.E. Indications of shifting microbial communities associated with growing biomass crops on marginal lands in Southern Ontario. *Agrofor. Syst.* **2019**, *94*, 735–746. [CrossRef]
30. Sekaran, U.; McCoy, C.; Kumar, S.; Subramanian, S. Soil microbial community structure and enzymatic activity responses to nitrogen management and landscape positions in switchgrass (*Panicum virgatum* L.). *GCB Bioenergy* **2019**, *11*, 836–851. [CrossRef]
31. Roley, S.S.; Ulbrich, T.C.; Robertson, G.P. Nitrogen fixation and resorption efficiency differences among twelve upland and lowland switchgrass cultivars. *Phytobiomes J.* **2021**, *5*, 97–107. [CrossRef]
32. Wewalwela, J.J.; Tian, Y.; Donaldson, J.R.; Baldwin, B.S.; Varco, J.J.; Rushing, B.; Lu, H.; Williams, M.A. Associative nitrogen fixation linked with three perennial bioenergy grasses in field and greenhouse experiments. *GCB Bioenergy* **2020**, *12*, 1104–1117. [CrossRef]
33. Roley, S.S.; Xue, C.; Hamilton, S.K.; Tiedje, J.M.; Robertson, G.P. Isotopic evidence for episodic nitrogen fixation in switchgrass (*Panicum virgatum* L.). *Soil Biol. Biochem.* **2019**, *129*, 90–98. [CrossRef]
34. Zhao, C.; Fan, X.; Li, X.; Hou, X.; Zhang, W.; Yue, Y.; Zhu, Y.; Wang, C.; Zuo, Y.; Wu, J. *Miscanthus sacchriflorus* exhibits sustainable yields and ameliorates soil properties but potassium stocks without any input over a 12-year period in China. *GCB Bioenergy* **2020**, *12*, 556–570. [CrossRef]
35. Huang, Y.; Wang, S.L.; Feng, Z.W.; Wang, H.; Huang, H. Comparative study of selected soil properties following introduction of broad-leaf trees into clear-felled Chinese fir forest. *Commun. Soil Sci. Plant Anal.* **2005**, *36*, 1385–1403. [CrossRef]
36. Dhillon, N.; Dev, G. Changes in available nitrogen, phosphorus and potassium in soils of different fertility status as affected by groundnut-wheat rotation. *J. Indian Soc. Soil Sci.* **1979**, *27*, 138–141.
37. Li, J.; Guo, C.; Jian, S.; Deng, Q.; Yu, C.-L.; Dzantor, K.E.; Hui, D. Nitrogen fertilization elevated spatial heterogeneity of soil microbial biomass carbon and nitrogen in switchgrass and gamagrass croplands. *Sci. Rep.* **2018**, *8*, 1734. [CrossRef]
38. Brookes, P.C.; Powlson, D.S.; Jenkinson, D.S. Measurement of microbial biomass phosphorus in soil. *Soil Biol. Biochem.* **1982**, *14*, 319–329. [CrossRef]
39. Bertheux, M.H. A modified procedure for the fractionation and determination of soil phosphorus. *J. Sci. Food Agric.* **1958**, *9*, 177–181. [CrossRef]
40. Khreish, E.A.; Boltz, D.F. Indirect spectrophotometric and atomic absorption spectrometric methods for the determination of potassium. *Mikrochim. Acta* **1970**, *58*, 1174–1180. [CrossRef]
41. Martin, J.P. Use of acid, rose-bengal and streptomycin in the plate method for estimating soil fungi. *Soil Sci.* **1950**, *69*, 215–232. [CrossRef]
42. Atlas, R.M.; Park, L.C. *Handbook of Microbiological Media*; CRC Press, Inc.: Boca Raton, FL, USA, 2000.
43. Murphy, C.A.; Foster, B.L.; Ramspott, M.E.; Price, K.P. Grassland management effects on soil bulk density. *Trans. Kans. Acad. Sci.* **2004**, *107*, 45–54. [CrossRef]
44. Singh, N.; Dhaliwal, J.K.; Sekaran, U.; Kumar, S. Soil hydrological properties as influenced by long-term nitrogen application and landscape positions under switchgrass seeded to a marginal cropland. *GCB Bioenergy* **2019**, *11*, 1026–1040. [CrossRef]
45. Blanco-Canqui, H.; Gilley, J.E.; Eisenhauer, D.E.; Jasa, P.J.; Boldt, A. Soil carbon accumulation under switchgrass barriers. *Agron. J.* **2014**, *106*, 2185–2192. [CrossRef]
46. Schmer, M.R.; Liebig, M.A.; Vogel, K.P.; Mitchell, R.B. Field-scale soil property changes under switchgrass managed for bioenergy. *GCB Bioenergy* **2011**, *3*, 439–448. [CrossRef]

47. Burylo, M.; Hudek, C.; Rey, F. Soil reinforcement by the roots of six dominant species on eroded mountainous marly slopes (Southern Alps, France). *Catena* **2011**, *84*, 70–78. [CrossRef]
48. Mudgal, A.; Anderson, S.H.; Baffaut, C.; Kitchen, N.R.; Sadler, E. Effects of long-term soil and crop management on soil hydraulic properties for claypan soils. *J. Soil Water Conserv.* **2010**, *65*, 393–403. [CrossRef]
49. Andrews, S.S.; Karlen, D.L.; Cambardella, C.A. The soil management assessment framework: A quantitative soil quality evaluation method. *Soil Sci. Soc. Am. J.* **2004**, *68*, 1945–1962. [CrossRef]
50. Dou, F.; Hons, F.; Ocumpaugh, W.; Read, J.; Hussey, M.; Muir, J. Soil organic carbon pools under switchgrass grown as a bioenergy crop compared to other conventional crops. *Pedosphere* **2013**, *23*, 409–416. [CrossRef]
51. Bahulikar, R.A.; Chaluvadi, S.R.; Torres-Jerez, I.; Mosali, J.; Bennetzen, J.L.; Udvardi, M. Nitrogen fertilization reduces nitrogen fixation activity of diverse diazotrophs in switchgrass roots. *Phytobiomes J.* **2021**, *5*, 80–87. [CrossRef]
52. Roley, S.S.; Duncan, D.S.; Liang, D.; Garoutte, A.; Jackson, R.D.; Tiedje, J.M.; Robertson, G.P. Associative nitrogen fixation (ANF) in switchgrass (*Panicum virgatum*) across a nitrogen input gradient. *PLoS ONE* **2018**, *13*, e0197320. [CrossRef] [PubMed]
53. Vadas, P.A.; Barnett, K.H.; Undersander, D.J. Economics and energy of ethanol production from alfalfa, corn, and switchgrass in the Upper Midwest, USA. *BioEnergy Res.* **2008**, *1*, 44–55. [CrossRef]
54. Monti, A.; Barbanti, L.; Zatta, A.; Zegada-Lizarazu, W. The contribution of switchgrass in reducing GHG emissions. *GCB Bioenergy* **2012**, *4*, 420–434. [CrossRef]
55. Philippot, L.; Raaijmakers, J.M.; Lemanceau, P.; van der Putten, W.H. Going back to the roots: The microbial ecology of the rhizosphere. *Nat. Rev. Microbiol.* **2013**, *11*, 789–799. [CrossRef]
56. van Delden, L.; Rowlings, D.W.; Scheer, C.; Grace, P.R. Urbanisation-related land use change from forest and pasture into turf grass modifies soil nitrogen cycling and increases N_2O emissions. *Biogeosciences* **2016**, *13*, 6095–6106. [CrossRef]
57. Marschner, P.; Kandeler, E.; Marschner, B. Structure and function of the soil microbial community in a long-term fertilizer experiment. *Soil Biol. Biochem.* **2003**, *35*, 453–461. [CrossRef]

agriculture

MDPI

Article

Occurrence and Nutrition Indicators of Alfalfa with *Leptosphaerulina* in Chifeng, Inner Mongolia

Lili Zhang and Yanzhong Li *

Key Laboratory of Grassland Livestock Industry Innovation, Ministry of Agriculture and Rural Affairs, Engineering Research Center of Grassland Industry, Ministry of Education, State Key Laboratory of Grassland Agro-Ecosystems, College of Pastoral Agriculture Science and Technology, Lanzhou University, Lanzhou 730020, China
* Correspondence: liyzh@lzu.edu.cn

Abstract: Alfalfa *Leptosphaerulina* leaf spot is a common disease of alfalfa, while its effect on alfalfa quality has not been reported. The present study aimed to investigate the alfalfa *Leptosphaerulina* leaf spot in Chifeng City, Inner Mongolia, China and determine the quality of alfalfa plants and leaves with different scales. The incidence and disease index of nine alfalfa cultivars ranged from 12.1% to 59.8% and 10.0 to 51.0, respectively. The incidence of the Optimus cultivar and the disease index of the WL168 cultivar were significantly higher than those of the other cultivars. Therefore, different scales (0–4) of the alfalfa WL168 plant and leaves were used to determine their nutritional levels. Compared with healthy plants and leaves, the severity of alfalfa leaf spot on a scale of 4 decreased by 3.7% to 29.4% or 1.7% to 40.7%, respectively, in 18 nutrients; and increased by 12.0% to 14.5% or 17.8% to 26.9% in the Rumen protein (RUP), acid detergent fiber (ADF) and neutral detergent fiber (NDF), respectively. In addition, the crude protein (CP) content of alfalfa plants or leaves based on a severity scale of 4 decreased by 16.7% and 6.2%, respectively. Correlation analysis revealed a strong negative correlation between 18 nutritional contents and disease severity, except for NDF, ADF and RUP. Conclusively, alfalfa *Leptosphaerulina* leaf spot strongly influences the plant and the leaves' nutrient content in the plant.

Keywords: alfalfa *Leptosphaerulina* leaf spot; incidence; disease index; nutrition

Citation: Zhang, L.; Li, Y. Occurrence and Nutrition Indicators of Alfalfa with *Leptosphaerulina* in Chifeng, Inner Mongolia. *Agriculture* **2022**, *12*, 1465. https://doi.org/10.3390/agriculture12091465

Academic Editor: Zhenfei Guo

Received: 15 July 2022
Accepted: 12 September 2022
Published: 14 September 2022

1. Introduction

Alfalfa is a highly nutritious perennial legume plant with a long history of use as a forage crop [1]. Compared with grasses, legumes such as alfalfa have a lower neutral detergent fiber (NDF) content but contain higher protein, energy and calcium concentrations [2–5]. Alfalfa is a high-quality forage crop that is also used to restore pastures owing to its deep root system and its ability to reduce soil erosion [6,7]. Alfalfa is widely cultivated in China as animal feed [8]. Alukhorqin Banner in Chifeng City, Inner Mongolia, China, is one of the important regions for alfalfa farming [9]. Alfalfa farming in China is restricted to certain regions because of alfalfa diseases [10].

The disease caused by *Leptosphaerulina australis* was found in Inner Mongolia in 2019 [11]. Alfalfa *Leptosphaerulina* leaf spot is a common disease of alfalfa leaves in humid areas [12]. The hyphae and ascocarps of *Leptosphaerulina* fungi overwinter in diseased tissues, and the ascospores are transmitted through the air [13]. This disease is primarily caused by fungi in the *Leptosphaerulina* sp., which typically infect members of *Agrostis*, *Festuca*, *Lolium* and *Poa* [14–16], while it can also infect *Setaria*, *Phleum pratense*, *Pisum sativum*, *Trifolium* and *Vicia faba* [17]. Five *Leptosphaerulina* species have been reported to be associated with *Leptosphaerulina* leaf blight. *Leptosphaerulina americana* has been isolated from the dead leaves of *Phleum pretense*, while it can also infect *Pisum*, *Trifolium* and *Vicia* [17]. *Leptosphaerulina argentinensis* infects creeping bentgrass (*Agrostis stolonifera* L.) [18], whereas *Leptosphaerulina australis* has been isolated from members of *Agrostis*, *Festuca*, *Lolium* and

Poa [14]. *Leptosphaerulina trifolii* has been isolated from *Poa* and *Medicago sativa* and other members of the non-turfgrass genera [19,20]. *Leptosphaerulina briosiana* has been isolated from alfalfa [21]. In China, alfalfa *Leptosphaerulina* leaf spot with *L. briosiana* was first reported in the Gongzhuling area, Jilin Province [13]. *L. trifolii* was then isolated from alfalfa in Heilongjiang Province, whereas *L. australis*on (alfalfa) in Inner Mongolia has also been reported [11,20,22]. In 2021, *Leptosphaerulina* species, including *L. americana, L. argentinensis*, *L. australis* and *L. trifolii,* were isolated from golf turfgrass in Beijing and Hainan [12].

Alfalfa disease seriously affects the yield and quality of alfalfa [23]. Previous studies have shown that leaf spot diseases reduced yield by 6% to 7% in Alberta, Canada [24], 16% in New Zealand [25], 40% in Australia [26] and 19% in the United States [27]. Leaf spot injuries caused by different pathogens can reduce the CP content in alfalfa leaves by up to 22% [28]. Lucerne common leaf spot and alfalfa *Stemphylium* leaf spot losses in alfalfa can be as high as 40–60% [29]. Anthracnose caused the yield reduction of 7% to 37% in alfalfa, but the NDF and ADF contents increased by 21% and 16%, respectively, and the crude fat and CP decreased by 35% and 17%, respectively [30]. *Phoma medicaginis* can reduce alfalfa yields about 50% [31]. *Pseudopeziza medicaginis* infection increased the ash, ADF, NDF, calcium (Ca), tannin and total phenol contents in diseased leaves by 20%, 71%, 40%, 136%, 22% and 51%, respectively, relative to the healthy leaves [32].

Previous research has shown that diseases can reduce alfalfa yield and quality to different degrees [30–32]. A hypothesis was proposed as to whether alfalfa *Leptosphaerulina* Leaf spot could affect alfalfa quality, alfalfa production and livestock health. Only a few studies have reported alfalfa *Leptosphaerulina* leaf spot in the past five years. Therefore, we systematically investigated the *Leptosphaerulina* leaf spot disease in nine (alfalfa) cultivars in Chifeng City Inner Mongolia to determine whether this disease was the most important alfalfa plant disease. Then, the cultivars with the highest disease index were selected to explore the relationship between the disease severity and nutrient content in alfalfa using a near-infrared detection method. Our findings will provide a theoretical basis for alfalfa *Leptosphaerulina* leaf spot disease indexing and control and the effect of this disease on livestock health and production.

2. Materials and Methods

2.1. Sample Cultivation

The nine diseased alfalfa cultivars used in this study were sampled from Aluhorqin Banner, Chifeng City, Inner Mongolia autonomous region of northeast China. The cultivars for the Gansu Yasheng Pastoral Company were planted in 2018, 2019 and 2020, respectively. The longitude of the field is between 120°13′13″ and 120°29′14″, the latitude is between 43°27′52″ and 43°34′54″ and the altitude is between 308.89 m and 357.18 m (Table 1). The sowing was broadcast. Irrigation was sprinkler. Fertilizer was used five times a year. Fertilizer kinds and dosage are shown in Supplementary Table S1.

Table 1. Field cultivars and survey times.

Planting Site No.	Cultivars	Proportion (hm^2)	Planting Years	Survey Years	Longitude	Latitude	Altitude
4	WL525	13.33	2020	2020	120°26′16″	43°32′5″	324.59
52	SW5909	35.07	2020	2020	120°29′14″	43°27′52″	315.13
26	Xinmu No.3	4.53	2019	2020	120°15′20″	43°34′0″	342.95
33	WL440	74.20	2020	2020	120°26′51″	43°29′45″	333.42
50	WL440	43.87	2020	2020	120°28′34″	43°27′56″	281.71
5	WL168HQ	35.07	2018	2019, 2020	120°19′3″	43°32′0″	331.28
35	Optimus Prime	40.80	2018	2019, 2020	120°26′43″	43°29′16″	333.15
2	Zhongmu No.5	37.13	2019	2019	120°18′58″	43°31′56″	340.11
38	Zhongmu No.5	69.20	2019	2019	120°19′3″	43°32′0″	331.28
5	Bright clover	35.07	2019	2019, 2020	120°19′3″	43°32′0″	331.28
20	Bright clover	24.60	2019	2020	120°19′22″	43°34′48″	324.49
25	Bright clover	43.87	2019	2020	120°14′44″	43°34′5″	356.64

Table 1. *Cont.*

Planting Site No.	Cultivars	Proportion (hm^2)	Planting Years	Survey Years	Longitude	Latitude	Altitude
27	Bright clover	5.80	2019	2020	120°15′21″	43°33′56″	349.83
46	Bright clover	54.73	2019	2020	120°13′13″	43°34′54″	350.72
47	Bright clover	59.67	2019	2020	120°13′23″	43°34′34″	343.48
76	Bright clover	38.60	2019	2019	120°18′49″	43°32′23″	360.13
18	Adina	42.40	2019	2020	120°29′10″	43°32′38″	321.18
19	Adina	83.47	2019	2020	120°26′34″	43°30′19″	323.24
25	Adina	43.87	2018	2020	120°13′43″	43°34′6″	356.51
35	Adina	36.33	2019	2019	120°13′43″	43°34′7″	357.18
37	Adina	10.27	2019	2020	120°26′39″	43°29′5″	319.44
41	Adina	35.67	2019	2020	120°26′40″	43°29′6″	331.19
42	Adina	35.40	2019	2020	120°27′52″	43°28′40″	308.89
56	Adina	47.33	2018	2019, 2020	120°13′43″	43°34′6″	356.51
57	Adina	30.27	2019	2020	120°13′43″	43°34′6″	356.51

2.2. Soil Characteristics

The soil type is sandy loam. Soil organic matter content was 5.9 $g \cdot kg^{-1}$. Total nitrogen was 0.5 $g \cdot kg^{-1}$. The content of available phosphorus was 10.17 $g \cdot kg^{-1}$. The available potassium content was 200 $g \cdot kg^{-1}$.

2.3. Climate Information

The climate information (rainfall and the air temperature) of the region during the experimental periods from mid-March to October in 2018, 2019 and 2020 is shown in Supplementary Table S2.

2.4. Alfalfa Leptosphaerulina Leaf Spot Disease Survey

Planting site, cultivars, proportion, planting years, survey years, longitude, latitude and altitude data are shown in Tables 1 and S3. In each field, five locations of approximately 25 m^2 (5 m×5 m) were randomly selected to assess the disease incidence. The plants were visually assessed for foliar alfalfa *Leptosphaerulina* leaf spot symptoms. The disease incidence was the proportion of the diseased plants in a given field. The disease severity index was the proportion of diseased leaves on each plant. The severity scale ranged 0–4, where0was a healthy plant; 1 was lesions covering 0–25% of the leaf; 2 was lesions covering 26–50% of the leaf; 3 was lesions covering 51–75% of the leaf; and 4 was lesions covering 76–100% of the leaf.

$$\text{Disease severity index (DSI)} = [\sum(\text{no. of plants/scale} \times \text{scale value})/(\text{highest scale value} \times \text{total no. of plants})] \times 100$$

2.5. Nutrient Sampling and Extraction

The nutrient content in the alfalfa plants and leaves with different disease severity in June 2019 was determined using WL168. A total of 10 alfalfa plants and 500 alfalfa leaves were selected for each severity scale. The samples were dried naturally, crushed and analyzed at the Quality Testing Laboratory of LandLakes Feed and Forage Testing Laboratory (China). For each severity scale, 10 alfalfa plants or 500 leaves were mixed and then divided into 3 samples for nutrient determination, respectively. A total of 21 nutrients were measured using rapid near-infrared (NIR) spectroscopy, and this equipment had been producted by FOSS in Denmark (FOSS DS2500, Hilleroed, Denmark). Crude protein (CP) was calculated by CP% = 6.25 N (%) [33]. Details of this process are shown in the Supplementary Table S4.

2.6. Statistical Analysis

The incidence data, disease index, and nutrition indices were analyzed using IBM SPSS Statistics 25 (Version 25.0; SPSS Inc, Chicago, IL, USA). Differences between groups were analyzed using one-way analysis of variance (ANOVA) and Duncan's test. Statistical significance was set at 0.05 or at 0.01.

3. Results

3.1. Incidence and Disease Index

We found significant differences in disease incidence among the cultivars ($p < 0.05$). The alfalfa *Leptosphaerulina* leaf spot incidence in nine alfalfa cultivars ranged from 12.1% to 59.8%. The highest incidence was observed on the Optimus Prime cultivar, whereas the lowest was on Adina. There was a significant difference in the disease incidence on Adina, which ranged from 12.1% to 52.5%. The index ranged from 10.0% to 51.0% ($p < 0.05$). The highest index was observed on cultivar WL168HQ. Thus, WL168HQ was used to measure the nutritional index (Table 2).

Table 2. The incidence and disease index of alfalfa *Leptosphaerulina* leaf spot.

Planting Site No.	Cultivar	Incidence (%)	Index
4	WL525	49.19 ± 3.97^{bc}	32.58 ± 2.05^{bc}
52	SW5909	43.77 ± 2.40^{cd}	27.79 ± 2.85^{bcd}
26	Xinmu No.3	36.44 ± 2.41^{e}	27.89 ± 1.04^{bcd}
33	WL440	42.87 ± 2.63^{d}	22.51 ± 1.91^{cde}
50	WL440	43.35 ± 2.67^{d}	33.64 ± 2.44^{b}
5	WL168HQ	24.73 ± 1.59^{hij}	51.00 ± 6.99^{a}
35	Optimus Prime	59.76 ± 2.07^{a}	16.50 ± 1.84^{ef}
2	Zhongmu No.5	29.04 ± 1.77^{fghi}	18.49 ± 1.82^{def}
38	Zhongmu No.5	21.11 ± 1.06^{jkl}	15.76 ± 0.96^{ef}
5	Bright clover	30.92 ± 1.88^{efgh}	17.51 ± 3.03^{def}
20	Bright clover	33.42 ± 1.59^{ef}	18.15 ± 1.52^{def}
25	Bright clover	25.31 ± 2.15^{ghij}	17.21 ± 1.30^{def}
27	Bright clover	25.30 ± 1.33^{ghij}	20.52 ± 3.29^{def}
46	Bright clover	26.21 ± 1.78^{ghij}	18.54 ± 1.36^{def}
47	Bright clover	23.57 ± 2.65^{ijk}	17.92 ± 1.31^{def}
76	Bright clover	31.38 ± 2.09^{efg}	14.86 ± 1.94^{ef}
18	Adina	35.45 ± 1.71^{e}	17.98 ± 2.35^{def}
19	Adina	18.02 ± 0.84^{klm}	14.74 ± 6.30^{ef}
25	Adina	15.10 ± 1.34^{lm}	22.73 ± 4.60^{cde}
35	Adina	23.74 ± 1.33^{ijk}	16.33 ± 1.74^{ef}
37	Adina	52.54 ± 2.32^{b}	18.81 ± 5.95^{ef}
41	Adina	17.28 ± 0.771^{m}	21.64 ± 4.09^{de}
42	Adina	17.08 ± 0.94^{lm}	19.41 ± 4.71^{def}
56	Adina	15.44 ± 1.10^{lm}	14.46 ± 3.48^{def}
57	Adina	12.13 ± 0.89^{m}	9.94 ± 1.08^{f}
		$p < 0.05$	$p < 0.05$

Different letters in the column indicate a significant difference ($p < 0.05$; Duncan's test).

3.2. Plant Nutrients

Alfalfa *Leptosphaerulina* leaf spot disease significantly affected the nutrient levels in the plants (Table 3) ($p < 0.05$). Compared with healthy plants, except for ADF, NDF and RUP, the nutrient content in alfalfa with scale 4 alfalfa *Leptosphaerulina* leaf spot decreased by 3.7% to 29.4%. The calcium (Ca), phosphorus (P), potassium (K), magnesium (Mg), ash, fat, CP, lignin, net milk production, maintenance net energy, net weight gain, relative feeding value, relative forage quality, total digestible nutrients, milk production,30h NDF digestible rate,48h NDF digestible rate and nonfibrous carbohydrate decreased by 29.4%, 25.0%, 2.5%, 20.0%, 7.2%,18.8%,16.7%, 9.0%, 5.0%, 7.0%, 14.3%, 10.3%,16.3%, 6.2%, 8.0%, 11.1%, 8.9% and 3.7%, respectively. However, the decrease in the 18 nutrients did not decrease continuously with the disease severity. For example, the P content was the same in grade 2 and grade 3 alfalfa *Leptosphaerulina* leaf spot, and Mg content was the same in grade 3 and grade 4 alfalfa *Leptosphaerulina* leaf spot. The highest disease severity in cultivar ash was grade 2.

Table 3. Nutrients in alfalfa plants with different severity levels.

Nutrient	Disease Severity Index				
	0	1	2	3	4
Calcium (Ca %)	1.7 ± 0.01 ^{a}	1.5 ± 0.01 ^{b}	1.5 ± 0.00 ^{c}	1.3 ± 0.01 ^{d}	1.2 ± 0.00 ^{e}
Phosphorus (P %)	0.4 ± 0.00 ^{a}	0.3 ± 0.00 ^{b}	0.3 ± 0.00 ^{b}	0.3 ± 0.00 ^{b}	0.3 ± 0.00 ^{c}
Potassium (K %)	2.4 ± 0.01 ^{ab}	2.4 ± 0.01 ^{a}	2.3 ± 0.03 ^{ab}	2.3 ± 0.02 ^{c}	2.3 ± 0.04 ^{bc}
Magnesium (Mg %)	0.4 ± 0.00 ^{a}	0.3 ± 0.00 ^{b}	0.3 ± 0.00 ^{b}	0.3 ± 0.00 ^{c}	0.3 ± 0.00 ^{c}
Ash (%)	7.8 ± 0.06 ^{c}	7.6 ± 0.04 ^{c}	8.4 ± 0.03 ^{a}	8.0 ± 0.05 ^{b}	7.2 ± 0.03 ^{d}
Fat (%)	1.8 ± 0.01 ^{a}	1.6 ± 0.01 ^{b}	1.6 ± 0.00 ^{c}	1.5 ± 0.01 ^{d}	1.5 ± 0.00 ^{d}
Crude protein (CP %)	21.5 ± 0.07 ^{a}	20.0 ± 0.14 ^{b}	19.1 ± 0.08 ^{c}	18.4 ± 0.07 ^{d}	17.9 ± 0.05 ^{e}
Lignin (%)	6.6 ± 0.01 ^{a}	6.6 ± 0.07 ^{a}	6.4 ± 0.02 ^{b}	6.3 ± 0.03 ^{c}	6.0 ± 0.02 ^{d}
Rumen protein (RUP %)	17.9 ± 0.07 ^{c}	18.0 ± 0.27 ^{c}	19.9 ± 0.22 ^{ab}	19.3 ± 0.21 ^{b}	20.5 ± 0.32 ^{a}
Acid washing fiber (ADF %)	30.2 ± 0.01 ^{d}	30.9 ± 0.32 ^{c}	33.0 ± 0.25 ^{b}	32.3 ± 0.17 ^{b}	33.9 ± 0.16 ^{a}
Neutral detergent fiber (NDF %)	39.1 ± 0.07 ^{c}	40.0 ± 0.34 ^{c}	42.4 ± 0.27 ^{b}	42.4 ± 0.28 ^{b}	43.8 ± 0.16 ^{a}
Net milk production (NEL %)	1.4 ± 0.00 ^{a}	1.4 ± 0.01 ^{b}	1.3 ± 0.01 ^{c}	1.3 ± 0.00 ^{c}	1.3 ± 0.01 ^{c}
Maintain net energy (NEM %)	1.4 ± 0.00 ^{a}	1.4 ± 0.01 ^{b}	1.3 ± 0.01 ^{c}	1.3 ± 0.01 ^{c}	1.3 ± 0.01 ^{c}
Net weight gain (NEG %)	0.7 ± 0.00 ^{a}	0.6 ± 0.01 ^{b}	0.6 ± 0.01 ^{c}	0.6 ± 0.00 ^{c}	0.6 ± 0.01 ^{c}
Relative feeding value (RFV %)	155.7 ± 0.33 ^{a}	150.7 ± 1.67 ^{b}	138.3 ± 1.45 ^{c}	132.7 ± 0.88 ^{d}	139.7 ± 1.20 ^{c}
Relative forage quality (RFQ %)	141.3 ± 0.33 ^{a}	128.3 ± 2.33 ^{b}	118.0 ± 1.53 ^{c}	114.3 ± 0.67 ^{c}	118.3 ± 1.45 ^{c}
Total digestible nutrients (TDN %)	59.0 ± 0.00 ^{a}	56.3 ± 0.33 ^{b}	55.3 ± 0.33 ^{c}	55.0 ± 0.00 ^{c}	55.3 ± 0.33 ^{c}
Milk production (kg/milk) (MT DM %)	1415.0 ± 1.53 ^{a}	1324.0 ± 9.00 ^{b}	1279.7 ± 6.77 ^{c}	1284.7 ± 2.85 ^{c}	1289.3 ± 6.84 ^{c}
30 h NDF digestible rate (NDF30 %)	14.9 ± 0.08 ^{a}	14.5 ± 0.10 ^{b}	14.0 ± 0.04 ^{c}	14.0 ± 0.05 ^{c}	13.2 ± 0.13 ^{d}
48 h NDF digestible rate (NDF48 %)	16.6 ± 0.08 ^{a}	16.1 ± 0.03 ^{b}	15.9 ± 0.07 ^{bc}	15.8 ± 0.06 ^{c}	15.1 ± 0.05 ^{d}
Nonfibrous carbohydrate (NFC %)	32.4 ± 0.20 ^{a}	31.9 ± 0.04 ^{b}	31.9 ± 0.17 ^{b}	30.8 ± 0.19 ^{c}	31.2 ± 0.08 ^{c}

Different letters in the line indicate a significant difference ($p < 0.05$; Duncan's test).

In addition, the RUP, ADF and NDF contents increased with the disease severity. They increased significantly because of the change in the severity of the alfalfa *Leptosphaerulina* leaf spot from grade 2 to 3.

3.3. Leaves Nutrients

Alfalfa *Leptosphaerulina* leaf spot affected the nutrient in leaves (Table 4). The content of 18 nutrients, including Ca, P, K, ash, fat, CP, lignin, net milk production and the net energy, among others, decreased significantly ($p < 0.05$). When the alfalfa *Leptosphaerulina* leaf spot severity 4 decreased by 1.7% to 40.7%, the Ca, P, ash, lignin and relative forage quality decreased by more than 20%. These findings demonstrate that several nutritional indices varied significantly at any of the alfalfa *Leptosphaerulina* leaf spot severities(0–4), but the degree of variation in the nutrient concentration was smaller in the 0–3 scales. The difference in the Ca, K, fat, net milk production, net weight gain and relative feeding value was larger, at disease scale 3–4.

Table 4. Nutrients in alfalfa leaves with different severity levels.

Nutrient	Disease Severity Index				
	0	1	2	3	4
Calcium (Ca %)	2.7 ± 0.01 ^{a}	2.5 ± 0.00 ^{b}	2.2 ± 0.01 ^{c}	2.0 ± 0.00 ^{d}	1.6 ± 0.01 ^{e}
Phosphorus (P %)	0.4 ± 0.00 ^{a}	0.4 ± 0.00 ^{b}	0.4 ± 0.00 ^{c}	0.4 ± 0.00 ^{d}	0.3 ± 0.00 ^{e}
Potassium (K %)	2.4 ± 0.02 ^{a}	2.2 ± 0.01 ^{b}	2.1 ± 0.01 ^{c}	1.9 ± 0.02 ^{e}	2.0 ± 0.01 ^{d}
Magnesium (Mg %)	0.6 ± 0.00 ^{a}	0.6 ± 0.00 ^{b}	0.5 ± 0.00 ^{c}	0.5 ± 0.00 ^{d}	0.5 ± 0.00 ^{e}
Ash (%)	12.3 ± 0.03 ^{a}	10.5 ± 0.12 ^{b}	10.3 ± 0.01 ^{bc}	10.2 ± 0.04 ^{c}	9.5 ± 0.05 ^{d}
Fat (%)	2.4 ± 0.01 ^{a}	2.4 ± 0.01 ^{a}	2.3 ± 0.01 ^{b}	2.3 ± 0.01 ^{c}	2.1 ± 0.00 ^{d}
Crude protein (CP %)	27.4 ± 0.01 ^{a}	26. 5 ± 0.01 ^{bc}	26.5 ± 0.08 ^{b}	26.3 ± 0.07 ^{c}	25.7 ± 0.10 ^{d}
Lignin (%)	4.2 ± 0.02 ^{a}	3.8 ± 0.01 ^{b}	3.1 ± 0.01 ^{c}	2.9 ± 0.03 ^{d}	2.7 ± 0.04 ^{e}
Rumen protein (RUP %)	13.0 ± 0.04 ^{c}	12.4 ± 0.12 ^{d}	13.4 ± 0.23 ^{c}	14.1 ± 0.22 ^{b}	16.5 ± 0.26 ^{a}
Acid washing fiber (ADF %)	16.1 ± 0.03 ^{d}	16.2 ± 0.13 ^{d}	16.6 ± 0.10 ^{c}	17.2 ± 0.12 ^{b}	19.8 ± 0.10 ^{a}
Neutral detergent fiber (NDF %)	21.4 ± 0.03 ^{d}	21.6 ± 0.19 ^{d}	22.1 ± 0.12 ^{c}	22.6 ± 0.10 ^{b}	25.2 ± 0.06 ^{a}
Net milk production (NEL %)	1.7 ± 0.00 ^{a}	1.6 ± 0.00 ^{b}	1.6 ± 0.00 ^{c}	1.6 ± 0.00 ^{d}	1.5 ± 0.00 ^{e}
Maintain net energy (NEM %)	1.7 ± 0.00 ^{a}	1.7 ± 0.00 ^{b}	1.7 ± 0.00 ^{c}	1.7 ± 0.00 ^{d}	1.6 ± 0.00 ^{e}
Net weight gain (NEG %)	1.0 ± 0.00 ^{a}	1.0 ± 0.00 ^{b}	1.0 ± 0.00 ^{c}	0.9 ± 0.00 ^{d}	0.9 ± 0.00 ^{e}

Table 4. *Cont.*

Nutrient	Disease Severity Index				
	0	1	2	3	4
Relative feeding value (RFV %)	332.7 ± 0.33 [a]	328.3 ± 3.18 [a]	319.3 ± 2.03 [b]	310.3 ± 1.76 [c]	271.0 ± 1.00 [d]
Relative forage quality (RFQ %)	326.0 ± 3.46 [a]	317.0 ± 0.58 [b]	305.0 ± 1.73 [c]	289.0 ± 2.08 [d]	255.7 ± 0.67 [e]
Total digestible nutrients (TDN %)	70.0 ± 0.00 [a]	69.0 ± 0.00 [b]	68.3 ± 0.33 [c]	67.0 ± 0.00 [d]	65.0 ± 0.00 [e]
Milk production (kg/milk) (MT DM %)	1830.0 ± 3.79 [a]	1783. 7 ± 0.88 [b]	1768.3 ± 4.41 [c]	1727.7 ± 2.60 [d]	1616.0 ± 2.08 [e]
30 h NDF digestible rate (NDF30 %)	11.3 ± 0.10 [a]	10.9 ± 0.02 [b]	10.4 ± 0.05 [c]	9.9 ± 0.03 [d]	9.7 ± 0.04 [e]
48 h NDF digestible rate (NDF48 %)	12.3 ± 0.03 [a]	11.2 ± 0.05 [b]	10.4 ± 0.07 [c]	10.0 ± 0.03 [d]	10.0 ± 0.06 [d]
Nonfibrous carbohydrate (NFC %)	42.6 ± 0.06 [a]	41.0 ± 0.07 [b]	40.7 ± 0.09 [c]	39.6 ± 0.02 [d]	34.3 ± 0.07 [e]

Different letters in the line indicate a significant difference ($p < 0.05$; Duncan's test).

In addition, the RUP, ADF and NDF contents increased gradually with the alfalfa *Leptosphaerulina* leaf spot severity. The increases ranged from 17.8% to 26.9%. However, the RUP content was significantly lower in grade 1 disease leaves than in healthy leaves ($p < 0.05$).

3.4. The Relationship between Disease Severity and Nutritional Content

We found a negative correlation between the alfalfa *Leptosphaerulina* leaf spot severity and the nutritional index, except for RUP, ADF and NDF. The alfalfa *Leptosphaerulina* leaf spot severity showed a strong negative correlation with the Ca, CP, NDF and 30h NDF digestible rate ($p < 0.01$) and a moderate correlation with Mg, fat, lignin and 48h NDF digestible rate (Table 5).

Table 5. Correlation between the severity of alfalfa *Leptosphaerulina* leaf spot and alfalfa plant nutrient content.

Nutrient	Pearson	Decision Coefficient	Regression Equation
Calcium (Ca %)	−0.986 **	$R^2 = 0.970$	y = −0.115x + 1.645
Phosphorus (P %)	−0.866	$R^2 = 0.677$	y = −0.012x + 0.348
Potassium (K %)	−0.747	$R^2 = 0.586$	y = −0.028x + 2.386
Magnesium (Mg %)	−0.933 *	$R^2 = 0.916$	y = −0.016x + 0.337
Ash(%)	−0.247	$R^2 = 0.061$	y = −0.073x + 7.952
Fat(%)	−0.906 *	$R^2 = 0.821$	y = −0.077x + 1.738
Crude protein(CP %)	−0.976 **	$R^2 = 0.952$	y = −0.883x + 21.160
Lignin(%)	−0.939 *	$R^2 = 0.880$	y = −0.156x + 6.691
Rumen protein(RUP %)	0.876	$R^2 = 0.769$	y = 0.618x + 17.850
Acid washing fiber(ADF %)	0.925 *	$R^2 = 0.855$	y = 0.882x + 30.270
Neutral detergent fiber(NDF %)	0.960 **	$R^2 = 0.921$	y = 1.177x + 39.220
Net milk production(NEL %)	−0.800	$R^2 = 0.650$	y = −0.018x + 1.379
Maintain net energy(NEM %)	−0.839	$R^2 = 0.690$	y = −0.023x + 1.391
Net weight gain(NEG %)	−0.839	$R^2 = 0.673$	y = −0.023x + 0.670
Relative feeding value(RFV %)	−0.835	$R^2 = 0.698$	y = −5.000x + 153.400
Relative forage quality(RFQ %)	−0.865	$R^2 = 0.748$	y = −6.000x + 136.000
Total digestible nutrients(TDN %)	−0.834	$R^2 = 0.695$	y = −0.866x + 57.930
Milk production(kg/milk) (MT DM %)	−0.811	$R^2 = 0.657$	y = −29.060x + 1376.000
30 h NDF digestible rate(NDF30 %)	−0.976 **	$R^2 = 0.950$	y = −0.386x + 14.890
48 h NDF digestible rate(NDF48 %)	−0.951 *	$R^2 = 0.903$	y = −0.320x + 16.550
Nonfibrous carbohydrate(NFC %)	−0.877	$R^2 = 0.769$	y = −0.371x + 32.380

"Pearson" means Pearson product–moment correlation coefficient, the correlation coefficient for *Leptosphaerulina* leaf spot severity and nutritional contents in the plant. "*" indicates significance at 5% ($p < 0.05$; Duncan's test). "**" indicates very significance at 1% ($p < 0.01$; Duncan's test).

The contents of 21 nutrients strongly or moderately correlated with the severity of alfalfa *Leptosphaerulina* leaf spot, except for RUP, ADF and net milk production (Table 6).

Table 6. Correlation between the severity of alfalfa *Leptosphaerulina* leaf spot and alfalfa leaf nutrient content.

Nutrient	Pearson	Decision Coefficient	Regression Equation
Calcium (Ca %)	−0.987 **	R^2 = 0.972	y = −0.273x + 2.728
Phosphorus (P %)	−0.926 *	R^2 = 0.859	y = −0.026x + 0.422
Potassium (K %)	−0.913 *	R^2 = 0.834	y = −0.118x + 2.349
Magnesium (Mg %)	−0.994 **	R^2 = 0.986	y = −0.030x + 0.572
Ash(%)	−0.899 *	R^2 = 0.806	y = −0.583x + 11.710
Fat(%)	−0.895 *	R^2 = 0.802	y = −0.078x + 2.437
Crude protein(CP %)	−0.925 *	R^2 = 0.853	y = −0.354x + 27.170
Lignin(%)	−0.969 **	R^2 = 0.937	y = −0.376x + 4.104
Rumen protein(RUP %)	0.895	R^2 = 0.738	y = 0.857x + 12.170
Acid washing fiber(ADF %)	0.861	R^2 = 0.741	y = 0.821x + 15.520
Neutral detergent fiber(NDF %)	0.891 *	R^2 = 0.793	y = 0.876x + 20.830
Net milk production(NEL %)	−0.874	R^2 = 0.799	y = −0.030x + 1.670
Maintain net energy(NEM %)	−0.940 *	R^2 = 0.916	y = −0.034x + 1.750
Net weight gain(NEG %)	−0.956 *	R^2 = 0.901	y = −0.033x + 1.026
Relative feeding value(RFV %)	−0.907 *	R^2 = 0.821	y = −14.130x + 340.600
Relative forage quality(RFQ %)	−0.963 **	R^2 = 0.928	y = −16.860x + 332.200
Total digestible nutrients(TDN %)	−0.979 **	R^2 = 0.958	y = −1.200x + 70.260
Milk production(kg/milk) (MT DM %)	−0.945 *	R^2 = 0.893	y = −48.400x + 1841.000
30 h NDF digestible rate(NDF30 %)	−0.993 **	R^2 = 0.986	y = −0.431x + 11.290
48 h NDF digestible rate(NDF48 %)	−0.947 *	R^2 = 0.894	y = −0.580x + 11.930
Nonfibrous carbohydrate(NFC %)	−0.900 *	R^2 = 0.810	y = −1.801x + 43.210

"Pearson" means Pearson product–moment correlation coefficient, the correlation coefficient for *Leptosphaerulina* leaf spot severity and nutritional contents in the plant. "*" indicates significance at 5% ($p < 0.05$; Duncan's test). "**" indicates very significance at 1% ($p < 0.01$; Duncan's test).

4. Discussion

4.1. Occurrence of Leptosphaerulina Leaf Spot

Previous studies showed that from June to September, alfalfa anthracnose [23], alfalfa downy mildew, alfalfa spring black stem, alfalfa *Stemphyllium* leaf spot and alfalfa rust occurred in Inner Mongolia, and their incidences were 34%, 26%, 23%, 22% and 28%, respectively [30]. In this study, the incidence of *Leptosphaerulina* leaf spot is about 60%, which is much higher than other diseases. In addition, this disease also occurred in alfalfa Heilongjiang province in 2015 [20]. Therefore, we must pay attention to prevention and control of this disease, especially in cultivation areas.

4.2. Quality of Alfalfa with Leptosphaerulina sp.

The quality of hay directly affects the feed intake and production in livestock, and nutrient content and digestibility of feeds can indicate the quality of hay [34,35]. The quality standard of alfalfa hay is mainly based on the national standard of alfalfa hay guidelines set by the United States market. Parameters analyzed include CP, NDF, ADF and relative feeding value (RFV) among others [35,36]. In this study, the CP content of healthy alfalfa and alfalfa with grade 1 and 2 alfalfa *Leptosphaerulina* leaf spot was higher than 19%. In addition, the alfalfa belonged to super-grade grass. For grade 3 and grade 4 disease, the CP content was 17–19%, and the fodder belonged to grade 1 grass. The ADF and NDF content in both healthy and diseased alfalfa plants was less than 31% and less than 40%, respectively, to which alfalfa belonged to the super-grade grass category. RFV is an important forage quality index [37]. In this study, the RFV of diseased alfalfa plants and leaves was reduced by 3% to 15% and 1% to 18%, respectively. The RFV of alfalfa plants in this research was 133–156%, and thus was classified into the first-grade grass category. In conclusion, based on different nutritional indicators, alfalfa grass with alfalfa *Leptosphaerulina* leaf spot still belonged to the grade 1 grass or super-grade grass category, consistent with export alfalfa hay quality. Alfalfa is an important livestock fodder in China [8]. Agricultural industry standards (NY/T1170-2006) for alfalfa hay quality grading based on CP, NDF and ash

content have been formulated in China [35].In this study, according to the protein content, the disease severity of the sampled alfalfa *Leptosphaerulina* leaf spot was grade 1, grade 2 and grade 3, whereas the corresponding alfalfa hay belonged to grade 1, grade 2 and grade 3, respectively. Therefore, alfalfa *Leptosphaerulina* leaf spot may affect alfalfa pricing in China, and livestock growth, especially for severity, is grade 4. Previous studies have shown that diseased forage grass has poor nutritional quality and is not suitable for the healthy growth of livestock [38].

4.3. Nutrition of Alfalfa with Leptosphaerulina sp.

Alfalfa is the primary livestock feed, owing to its considerable CP [39]. However, high crude fiber negatively affects the digestibility of CP [40]. Alfalfa anthracnose, alfalfa brown spot and alfalfa *Verticillium* wilt decreased the CP of alfalfa by 17%, 16% and 41%, respectively [30,32,41]. Here, the CP of alfalfa with *Leptosphaerulina* sp. decreased by about 17%, which was similar to that of alfalfa anthracnose and alfalfa brown spot, but lower than that of alfalfa *Verticillium* wilt. ADF and NDF increased by 21% and 16% in alfalfa anthracnose [30] and increased by 71% and 40% in alfalfa brown spot, respectively [32]. In this research, the ADF and NDF increased by about 12% in plant, but 18% and 23% in leaves, respectively, and this result is consistent with that of alfalfa anthracnose. Lignin is a complex phenolic polymer and the second most abundant component of secondary plant cell walls [42,43]. Lignin is a major factor limiting the digestibility of dry forage [44,45]. Numerous studies have reported a strong inverse relationship between lignin concentration and forage digestibility [46], while the relationship between lignin and digestion in diseased alfalfa plants has barely been reported. We found that even though the lignin content in the alfalfa leaves decreased with an increase in disease severity, the lowest content was higher than that of the general level in the alfalfa plants. It was proven that the content of lignin in alfalfa could be decreased by alfalfa *Leptosphaerulina* leaf spot. Most previous studies have shown that diseases affect the photosynthesis of alfalfa [32,47,48]. Mg plays an important role in photosynthesis, primarily by participating in chlorophyll synthesis. Mg is the central atom of chlorophyll and the chlorophyll porphyrin ring [49]. In this study, the Mg content in alfalfa decreased significantly after *Leptosphaerulina* infection, particularly in the leaves. Therefore, it can be hypothesized that *Leptosphaerulina* infection decreases photosynthesis in alfalfa by decreasing the Mg in leaves, which then affects chlorophyll synthesis. P, K and Ca are essential nutrients in plants [47]. In this study, the content of Ca and P in alfalfa infected by *Leptosphaerulina* leaf spot decreased by more than 25%, and when the severity of alfalfa anthracnose with *Colletotrichum american-borealis* was grade 4, Ca content decreased by 30% [30]. The results of the two studies were consistent. Most of the proteins in feeds are degraded in the rumen [50]. In this study, the results showed that the RUP content positively correlated with the severity of alfalfa *Leptosphaerulina* leaf spot. The increase in rumen protein over activates fermentation by anaerobic microorganisms in the rumen. The resultant flatulence of livestock reduces protein absorption in the small intestine, affecting the nutrients available to the livestock [50].

In addition, the net milk production (NEL), maintenance net energy (NEM), net weight gain (NEG), total digestible nutrients (TDN), milk production (MT) and nonfibrous carbohydrate (NFC) in this research were decreased when they were infected by *Leptosphaerulina* sp. Therefore, when alfalfa *Leptosphaerulina* disease occurs, it will affect the performance of livestock by affecting the quality of herbage. Most of the studies only measured and studied the main nutritional indexes of alfalfa diseases, such as CP, ADF and NDF [29–32], while this study comprehensively revealed the effects of alfalfa leaf spot disease on 21 conventional nutritional indexes. These results will guide the control of the disease and alfalfa production.

5. Conclusions

Alfalfa leaf spot disease has been prevalent in Inner Mongolia for a long time, and its incidence was much higher than other alfalfa leaf diseases. We suspect that this disease

will continue to be prevalent in the future. In addition, according to the quality standard of alfalfa hay, the occurrence of alfalfa *Leptosphaerulina* leaf spot could affect the quality classification and then affect the economic benefits and feeding value on alfalfa. Therefore, we must pay attention to control this disease in future work, such as with resistant cultivars.

Supplementary Materials: The following supporting information can be downloaded at: https://www.mdpi.com/article/10.3390/agriculture12091465/s1. Table S1: Fertilizer kinds and dosage in the field. Table S2: Climate information. Table S3: Survey method and investigator. Table S4: Reference methods and database for the nutriment measurement.

Author Contributions: Y.L. and L.Z. designed the study; L.Z. investigated and analyzed all data, then drew the tables and wrote the main body of the manuscript. Y.L. revised the manuscript and tables. All authors have read and agreed to the published version of the manuscript.

Funding: This study was financially supported by Gansu Provincial Science and Technology Major Projects (No. 19ZD2NA002), National Natural Science Foundation of China (32061123004), and the Earmarked Fund for CARS (CARS-34).

Institutional Review Board Statement: Not applicable.

Data Availability Statement: All data supporting the findings of this study are available within the paper and within its Supplementary Materials published online.

Acknowledgments: We thank the Gansu Yasheng Pastoral Company for providing experimental plots from 2019 to 2020. Moreover, we would like to thank the Quality Testing Laboratory of Landre Forage and Feed (China) for measuring nutritional indicators.

Conflicts of Interest: The authors declare no conflict of interest.

References

1. Radovic, J.; Sokolovic, D.; Markovic, J. Alfalfa-most important perennial forage legume in animal husbandry. *Biotechnol. Anim. Husb.* **2009**, *25*, 465–475. [CrossRef]
2. Earing, J.E.; Cassill, B.D.; Hayes, S.H.; Vanzant, E.S.; Lawrence, L.M. Comparison of in vitro digestibility estimates using the DaisyII incubator with in vivo digestibility estimates in horses. *J. Anim. Sci.* **2010**, *88*, 3954–3963. [CrossRef]
3. Potts, L.B.; Hinkson, J.J.; Graham, B.C.; Loest, C.A.; Turner, J.L. Nitrogen retention and nutrient digestibility in geldings fed grass hay, alfalfa hay, or alfalfa cubes. *J. Equine Vet. Sci.* **2010**, *30*, 330–333. [CrossRef]
4. Sturgeon, L.S.; Baker, L.A.; Pipkin, J.L.; Haliburton, J.C.; Chirase, N.K. The digestibility and mineral availability of Matua, Bermuda grass, and alfalfa hay in mature horses. *J. Equine Vet. Sci.* **2000**, *20*, 45–48. [CrossRef]
5. Woodward, A.D.; Nielsen, B.D.; Liesman, J.; Lavin, T.; Trottier, N.L. Protein quality and utilization of timothy, oat-supplement timothy, and alfalfa at differing harvest maturities in exercised Arabian horses. *J. Anim. Sci.* **2011**, *89*, 4081–4092. [CrossRef] [PubMed]
6. Guo, Z.G.; Liu, H.X.; Wang, S.M.; Tian, F.P.; Cheng, G.D. Biomass, persistence and drought resistance of nine lucerne varieties in the dry environment of west China. *Aust. J. Exp. Agric.* **2005**, *45*, 59–64. [CrossRef]
7. Le, X.H.; Franco, C.M.M.; Ballard, R.A.; Drew, E.A. Isolation and characterisation of endophytic actinobacteria and their effect on the early growth and nodulation of lucerne (*Medicago sativa* L.). *Plant Soil* **2016**, *405*, 13–24. [CrossRef]
8. Guo, T.; Bai, J.; Wang, J.G. Research on the present situation and countermeasures of alfalfa grass industry in China. *Chin. J. Grassl.* **2018**, *40*, 111–115.
9. Chen, L.L.; Yang, X.F.; Wu, Y.H.; Na, R.S.; Lv, N.; Liang, Q.W. Evaluation of production performance of 35 introduced varieties of alfalfa in Chifeng area of Inner Mongolia. *Pratacultural. Sci.* **2012**, *29*, 790–797.
10. Wang, Y.; Yuan, Q.H.; Miao, L.H.; Zhang, L.; Pan, L.Q. The major types and epidemic trends of alfalfa diseases innortheast and north China. *Acta Prataculturae Sin.* **2016**, *25*, 52–59.
11. Zhang, L.L.; Li, Y.Z. First report of alfalfa leaf spot caused by *Leptosphaerulina* australis in China. *Plant Dis.* **2021**, *105*, 2254. [CrossRef] [PubMed]
12. Liang, J.; Li, G.; Hou, L.; Zhao, M.; Cai, L. *Leptosphaerulina* species isolated from golf turfgrass in China, with description of *L. macrospora*,sp.nov. *Mycologia* **2021**, *5*, 956–967.
13. Xue, F.X. Grassland Conservation. In *Pasture Pathology*, 3rd ed.; China Agriculture Press: Beijing, China, 2008; p. 118.
14. Mitkowski, N.A.; Browning, M. *Leptosphaerulina australis* associated with intensively managed stands of *Poa annua* and *Agrostis palustris*. *Can. J. Plant Pathol.* **2004**, *26*, 193–198. [CrossRef]
15. Shurtleff, M.C.; Fermanian, T.W.; Randell, R. *Controlling Turfgrass Pest*, 3rd ed.; Prentice-Hall: Hoboken, NJ, USA, 1987.

16. Smiley, R.H.; Dernoeden, P.H.; Clarke, B.B. Compendium of turf grass diseases. In *Phytopathological Society*; Amer Phytopathological Society, APS Press: St. Paul, Minnesota, USA, 2005; p. 31.
17. Graham, J.H.; Luttrell, E.S. Species of *Leptosphaerulina* on forage plants. *Phytopathology* **1961**, *51*, 680–693.
18. Denison, W.C. Ascocarp developmentin *Leptosphaerulina argentinensis*. *J. Mitchell Soc.* **1968**, *84*, 254–257.
19. Abler, S.W. Ecology and taxonomy of *Leptosphaerulina* spp. associated with turfgrasses in the United States. Master's Thesis, Virginia State University, Ettrick, VA, USA, 2003.
20. Liu, X.P.; Jing, X.M.; Yan, H.X.; Li, G.L.; Luo, Y.H. First report of *Leptosphaerulina* leaf spot caused by *Leptosphaerulina trifolii* on alfalfa in Heilongjiang Province, China. *Plant Dis.* **2019**, *103*, 2673. [CrossRef]
21. Leath, K.T. *Leptosphaerulina briosiana* on alfalfa: Relation of lesion size to leaf age and light intensity. *Phytopathology* **1974**, *64*, 243. [CrossRef]
22. Li, M.T.; Zhu, Y.; Li, J.P.; Dai, R.H.; Liu, X.P. Investigation and correlation analysis of three leaf fungal diseases in different alfalfa varieties. *Heilongjiang Animan Sci. Vet. Med.* **2021**, 114–119.
23. Cao, S.; Liang, Q.W.; Clement, N.; LI, Y.Z. *Paraphoma* root rot of alfalfa (*Medicago sativa*) in InnerMongolia, China. *Plant Pathol.* **2020**, *69*, 231–239. [CrossRef]
24. Berkenkamp, B. Losses from foliage diseases of forage crops in central and northern Alberta in **1970**. *Can. Plant Dis. Surv.* **1971**, *51*, 96–100.
25. Hart, R.I.K.; Close, R.C. Control of leaf diseases of lucerne with benomyl. In Proceedings of the 29th New Zealand WeedPest Control Conference, Christchurch, New Zealand, 3–5 August 1976; pp. 42–45.
26. Morgan, W.C.; Parbery, D.G. Depressed fodder quality and increased oestrogenic activity of lucerne infected with *Pseudopeziza medicaginis*. *Aust. J. Agric. Res.* **1980**, *31*, 1103–1110. [CrossRef]
27. Nutter, F.W.J.; Guan, J.; Gotlieb, A.R.; Rhodes, L.H.; Grau, C.R.; Sulc, R.M. Quantifying alfalfa yield losses caused by foliar diseases in Iowa, Ohio, Wisconsin, and Vermont. *Plant Dis.* **2002**, *86*, 269–277. [CrossRef] [PubMed]
28. Hwang, S.F.; Wang, H.; Gossen, B.D.; Chang, K.F.; Turnbull, G.D.; Howard, R.J. Impact of foliar diseases on photosynthesis, protein content and seed yield of alfalfa and efficacy of fungicide application. *Eur. J. Plant Pathol.* **2006**, *115*, 389–399. [CrossRef]
29. Zeng, L.; Yuan, Q.H.; Yao, T. Study on yield loss prediction of alfalfa leaf spot. *Chin. J. Grassl.* **2009**, *31*, 40–43.
30. Zhang, L.L.; Shi, M.; Li, Y.Z. Effect of anthracnose infection on alfalfa yield and quality in the Shaerqin area. *Acta Prataculture Sin.* **2020**, *29*, 117–126.
31. Barbetti, M.J.; Nichols, P.G.H. Effect of *Phom medicaginis* and *Leptosphaerulina trifolii* on herbage and seed yield and coumestrol content of annual *Medicago* species. *Phytophylactica* **1991**, *23*, 223–227.
32. Li, Y.; Shi, J.; Cui, N.N.; Han, Y. Lucerne common leaf spot (*Pseudopeziza medicaginis*) decreases the photosynthetic performance and forage quality of *Medicago sativa*. *Acta Prataculturae Sin.* **2017**, *26*, 149–157.
33. Yuan, X.J.; Wang, Q.; Li, Z.H.; Yu, C.Q.; Xia, T.Y.J.; Shao, T. Effect of molasses addition on fermentation and nutritive quality of mixedsilage of hulless barley straw and perennial ryegrass inTibet. *Acta Pratacature Sin.* **2013**, *22*, 116–123.
34. Arinze, E.A. Simulation o fnatural and solar heated air hay drying systems. *Comput. Electron. Agric.* **1993**, *19*, 325–345. [CrossRef]
35. Sun, L.L. Effects of storage conditions and timeon the quality of alfalfa hay in Hexi Corridor. Master's Thesis, College of Pratrcultural Science Gansu Agricultural University, Lanzhou, China, 2021.
36. Butler, G.W.; Bailey, R.W. *Chemistry and Biochemistry of Herbage*; Academic Press: New York, NY, USA, 1983; pp. 134–136.
37. Moore, J.E. Forage quality indices: Development and application. *Forage Qual. Eval. Util.* **1994**, 977–998.
38. Hong, B.J.; Broderick, G.A.; Walgenbach, R.P. Effect of chemical conditioning of alfalfa on drying rate and nutrient digestion in ruminants. *J. Dairy Sci.* **1998**, *91*, 557–558. [CrossRef]
39. Pleger, L.; Weindl, P.N.; Weindl, P.A.; Carrasco, L.S.; Bellof, G.; Zhao, M.J.; Aulrich, K.; Bellof, G. Precaecal digestibility of crude protein and amino acids from alfalfa (*Medicago sativa*) and red clover (*Trifolium pratense*) leaves and silages in broilers. *Anim. Feed Sci. Technol.* **2021**, *275*, 114856. [CrossRef]
40. Sauvant, D.; Perez, J.M.; Tran, G. *Tables of Composition and Nutritional Value of Feed Materials*, 2nd ed.; Wageningen Academic Publishers, The Netherl and & INRA: Paris, France, 2004.
41. Li, F. Alfalfa wilt (*Verticillium* alfalfa) in China. Ph.D. Thesis, Lanzhou University, Lanzhou, China, 2021.
42. Grev, A.M.; Hathaway, M.R.; Sheaffer, C.C.; Scott, W.M.; Reiter, A.S.; Martinson, K.L. Apparent digestibility, fecalparticle size, and mean retention time of reduced lignin alfalfa hay fed to horses. *J. Anim. Sci.* **2021**, *7*, 7.
43. Li, X.X.; Zhang, Y.G.; Hannoufa, A.; Yu, P.Q. Transformation with TT8 and HB12 RNAi constructs in model forage (*Medicago sativa*, Alfalfa) affects carbohydrate structure and metabolic characteristics in ruminant livestock systems. *J. Agric. Food Chem.* **2015**, *63*, 9590. [CrossRef]
44. Jung, H.J.G.; Samac, D.A.; Sarath, G. Modifying crops to increase cell wall digestibility. *Plant Sci.* **2012**, *185–186*, 65–77. [CrossRef] [PubMed]
45. Reddy, M.S.S.; Chen, F.; Shadle, G.; Jackson, L.; Aljoe, H.; Dixon, R.A. Targeted down-regulation of cytochrome P450 enzymes for forage quality improvement in alfalfa (*Medicago sativa* L.). *Proc. Natl. Acad. Sci. USA* **2005**, *102*, 16573–16578. [CrossRef] [PubMed]
46. Jung, H.J.G.; Mertens, D.R.; Payne, A.J. Correlation of acid detergent lignin and klason lignin with digestibility of forage dry matter and neutral detergent fiber. *J. Dairy Sci.* **1997**, *80*, 1622. [CrossRef]
47. Fan, Q. Study on pathogenic mechanism of *Phoma medicaginis* on alfalfa. Ph.D. Thesis, Lanzhou University, Lanzhou, China, 2018.

48. Mandal, K.; Saravanan, R.; Maiti, S.; Kothari, I.K. Effect of downy mildew disease on photosynthesis and chlorophyII fluorescence in plantago ovata forsk. *J. Plant Dis. Prot.* **2009**, *116*, 164–168. [CrossRef]
49. Zhang, Q.D.; Zhang, S.P.; Zhang, Q.F. Role of magnesium Ion in plant photosynthsis. *J. Nat. Sci. Heilongjiang Univ.* **1992**, *9*, 82–88.
50. Sun, Y.Y.; Xu, M.; Hu, H.L. The research progress of cows rumen bypass protein. *Feed Ind.* **2017**, *38*, 48–50.

agriculture

MDPI

Article

Effect of Sodium Selenite Concentration and Culture Time on Extracellular and Intracellular Metabolite Profiles of *Epichloë* sp. Isolated from *Festuca sinensis* in Liquid Culture

Lianyu Zhou [1,2,3,*], Huichun Xie [1,2,3,4], Xuelan Ma [1,2,3], Jiasheng Ju [1,2,3], Qiaoyu Luo [1,2,3] and Feng Qiao [1,2,3,*]

[1] Key Laboratory of Medicinal Plant and Animal Resources of the Qinghai-Tibetan Plateau, Xining 810008, China
[2] Academy of Plateau Science and Sustainability, Qinghai Normal University, Xining 810008, China
[3] School of Life Science, Qinghai Normal University, Xining 810008, China
[4] Qinghai Ecosystem Observation and Research Station in the Southern Qilian Mountains, Haidong 810500, China
* Correspondence: 2023056@qhnu.edu.cn (L.Z.); 2025089@qhnu.edu.cn (F.Q.)

Abstract: Selenium (Se) is not only an essential trace element critical for the proper functioning of an organism, but it is also an abiotic stressor that affects an organism's growth and metabolite profile. In this study, *Epichloë* sp. from *Festuca sinensis* was exposed to increasing concentrations of Na_2SeO_3 (0, 0.1, and 0.2 mmol/L) in a liquid media for eight weeks. The mycelia and fermentation broth of *Epichloë* sp. were collected from four to eight weeks of cultivation. The mycelial biomass decreased in response to increased Se concentrations, and biomass accumulation peaked at week five. Using gas chromatography-mass spectrometry (GC-MS), approximately 157 and 197 metabolites were determined in the fermentation broth and mycelia, respectively. Diverse changes in extracellular and intracellular metabolites were observed in *Epichloë* sp. throughout the cultivation period in Se conditions. Some metabolites accumulated in the fermentation broth, while others decreased after different times of Se exposure compared to the control media. However, some metabolites were present at lower concentrations in the mycelia when cultivated with Se. The changes in metabolites under Se conditions were dynamic over the experimental period and were involved in amino acids, carbohydrates, organic acids, fatty acids, and nucleotides. Based on these results, we conclude that selenite concentrations and culture time influence the growth, extracellular and intracellular metabolite profiles of *Epichloë* sp. from *F. sinensis*.

Keywords: *Epichloë* sp. from *Festuca sinensis*; metabolomics; selenium; culture time

Citation: Zhou, L.; Xie, H.; Ma, X.; Ju, J.; Luo, Q.; Qiao, F. Effect of Sodium Selenite Concentration and Culture Time on Extracellular and Intracellular Metabolite Profiles of *Epichloë* sp. Isolated from *Festuca sinensis* in Liquid Culture. *Agriculture* **2022**, *12*, 1423. https://doi.org/10.3390/agriculture12091423

Academic Editor: Bernhard Huchzermeyer

Received: 2 July 2022
Accepted: 30 August 2022
Published: 9 September 2022

1. Introduction

Selenium (Se) is an essential metalloid element that plays a key role in the biosynthesis of important selenoenzymes, such as glutathione peroxidase, deiodinase iodothyronine, and thioredoxin reductase [1]. Though microorganisms can convert inorganic selenium into less toxic and more bio-available organic forms [2–4], variations in selenium content and availability cause differences in microbial growth and metabolic processes [5–7]. Recent studies have indicated that some fungi present metabolic mechanisms to tolerate Se, including those in lipid and amino acid metabolism [8,9]. For example, Xu et al. [10] reported that 200 mmol/L of Na_2SeO_4 inhibits endophytic bacterial growth, though the endophyte *Herbaspirillum* sp. is capable of transforming Se through reduction. Based on metabolic abilities of microbes, the application of microbial agents, including endophytic microbes, may remediate Se-polluted soils.

Microorganisms often encounter fluctuations in substrate form and availability during growth, which affect their metabolism, and subsequently, their physiology. For example, Wang et al. observed dynamic ranges of intracellular and extracellular metabolites from

Aspergillus niger in response to high and low glucose concentrations [11]. Additionally, some studies have verified that microbial cells secrete many metabolites into the extracellular medium without intracellular accumulation in response to environmental factors [12,13]. Metabolomic analysis is a commonly used approach in these and similar studies looking into phenotypical responses to environmental changes, as it can provide the most direct and "real-time" picture of cellular responses [14].

Endophytes do not only have to respond to the abiotic environment, but to the biological environment of their host plant. While each relationship is unique, many endophytes can promote plant growth and enhance their host's resilience to biotic and abiotic stresses, including to excessive Se [10,15]. The endophytic species to grasses, *Epichloë*, is no different as it also provides protection against stresses [15,16]. To date, several studies have described the *Epichloë* species based on morphology, physiology, biochemical properties, and phylogenetic analyses [17–20], as well as host specificity and the species' ability to confer resistance against stress, which has been related to host adaptability [21].

Festuca sinensis is an important perennial cool-season grass species in cool and semi-arid regions of China. This grass species is frequently infected with an asexual and beneficial *Epichloë* sp. Which has been shown to enhance host fitness against drought, waterlogging, cold, and pathogens [22–26], as well as producing alkaloids in the host tissues [27,28]. Previous studies on *Epichloë* sp. from *F. sinensis*, identified as *Epichloë sinensis*, have been confined to morphology, physiology, phylogeny, and bioactivity [25,29,30]. Our previous study found that different concentrations of sodium selenite (Na_2SeO_3) induced changes in the growth and metabolite profile of *Epichloë* sp. mycelia cultivated on potato dextrose agar [31]. The mechanism of fungal survival under Se conditions may be expressed in several ways, among which may be that of alterations in metabolite secretion.

This current study uses a metabolomics approach to identify the extracellular and intracellular metabolic changes that occurred in *Epichloë sinensis* when subjected to different Se concentrations for eight weeks. This and other works that seek to illuminate the metabolic mechanisms by which endophytes metabolize Se are critical in understanding the species' metabolic overflow, mechanisms of Se tolerance, and their relationship to their host plants.

2. Materials and Methods

2.1. Epichloë sinensis Strain

The *Epichloë* endophytic strain was maintained on Potato Dextrose (PD) Agar media (potato infusion 200 g, dextrose 20 g, agar 20 g, distilled water 1000 mL), and was obtained from Key Laboratory of Medicinal Plant and Animal Resources of the Qinghai-Tibetan Plateau, Qinghai Normal University [25].

2.2. Fungal Cultivation

Three pieces (4 mm in diameter) of mycelial agar plugs were removed from the edge of an *Epichloë sinensis* colony and placed into 250 mL Erlenmeyer flasks with 100 mL PD broth medium (potato infusion 200 g, dextrose 20 g, distilled water 1000 mL), and were cultivated with continuous shaking (130 r/min) for 15 days at 25 °C. Then, 5 mL of this culture was added to 250 mL culture flasks containing 95 mL fermentation medium (sucrose 30 g, yeast extract 2.5 g, peptone 1 g, distilled water 1000 mL, natural pH), supplemented with a final concentration of 0 (CK), 0.1, or 0.2 mmol/L Na_2SeO_3. All cultures were incubated at 25 °C, and the cultivation was carried out in triplicates for each time point. After cultivation, the cultures were centrifuged at 4000 r/min for 10 min to obtain the mycelia and fermentation broth. The mycelia were washed twice with deionized water, then immediately quenched in 200 µL pre-chilled methanol (–20 °C) and stored at –80 °C for metabolite determination.

2.3. Metabolite Extraction and Derivatization

To extract metabolites from the fermentation broth, 100 µL was aliquoted into a 1.5 mL tube, and 350 µL of pre-chilled methanol and 10 µL of an internal standard (adonitol,

0.5 mg/mL stock, Sigma-Aldrich, American) were added. Samples were vortexed for 30 s, ultrasonicated for 10 min in an ice bath, and centrifuged at 4 °C for 15 min at 10,000 r/min. Then, 100 μL of the supernatant was transferred into a fresh tube, and 30 μL was taken from each sample and pooled together to create a QC sample. All samples were dried in a vacuum concentrator without heat. The resulting pellet was resuspended in 60 μL of methoxyamine hydrochloride (TCI) (20 mg/mL in pyridine, Adamas) and incubated at 80 °C for 30 min. Afterwards, 80 μL of N,O-bis(trimethylsilyl)trifluoroacetamide (BSTFA, REGIS Technologies), containing 1% trimethylchlorosilane (TMCS, Sigma), was added to the samples and incubated at 70 °C for 1.5 h. Additionally, 5 μL of fatty acid methyl ester (FAMEs, Dr. Ehrenstorfer) (in chloroform) was added to the QC sample as it cooled to room temperature. Fermentation broth metabolites were carried out in triplicates.

For mycelium extraction, 10 mg of lyophilized mycelial material was transferred into a 2 mL tube, and 450 μL of pre-chilled 3:1 (*v/v*) methanol:chloroform was added and then vortexed for 30 s. The mixture was homogenized with a ball mill for 4 min at 35 Hz, ultrasonicated for 5 min in an ice bath, and then centrifuged at 4 °C for 15 min at 10,000 r/min. The supernatant was carefully transferred into a fresh tube, and 40 μL from each sample was taken and pooled into a QC sample. All samples were dried in a vacuum concentrator without heat. The pellet was resuspended in 30 μL methoxyamine hydrochloride (20 mg/mL in pyridine) and incubated for 30 min at 80 °C. Subsequently, 40 μL of the BSTFA regent (1% TMCS, *v/v*) was added to the samples, incubated for 1.5 h at 70 °C, and 5 μL FAMEs (in chloroform) was added to the QC sample as it cooled to room temperature. Mycelial metabolites were analyzed in duplicates.

2.4. GC-TOF-MS Analysis

The analysis was performed on an Agilent 7890 gas chromatograph system coupled with a Pegasus HT time-of-flight mass spectrometer and a DB-5MS capillary column coated with 5% diphenyl cross-linked with 95% dimethylpolysiloxane (30 m × 250 μm inner diameter, 0.25 μm film thickness, J&W Scientific, Folsom, CA, USA). A microliter of sample was injected in splitless mode. The initial temperature was kept at 50 °C for 1 min, then raised to 310 °C at a rate of 10 °C/min and maintained at 310 °C for 8 min. Helium was used as the carrier gas at a rate of 1 mL/min. The injection, transfer line, and ion source temperatures were kept at 280 °C, 280 °C, and 250 °C, respectively. Mass spectra collected in the electron impact mode with 70 eV ionization energy were recorded at 12.5 scans/s, with the m/z range of 50 to 500 after a solvent delay of 6.25 min.

2.5. Data Processing and Statistical Analysis

Chroma TOF software (4.3X, LECO) and the LECO-Fiehn Rtx5 database were used for peak extraction, baseline filtering and calibration, peak alignment, deconvolution analysis, peak identification, and integration of the peak area. Identified metabolites were verified with the help of mass spectrum and retention index. In addition, peaks detected in less than half of the quality control (QC) samples, or with >30% comparison of repeatability (RSD) in QC samples, were removed.

Internal standard for each analyzed metabolite were used to estimate relative quantifications. Multivariate analysis (MVA) was performed with the SPSS software, Version 16.0 (SPSS, Inc., Chicago, IL, USA). To assess the degree of metabolite abundance changes, and a heatmap and hierarchical clustering was constructed using Multiple Experiment Viewer (MeV) software, Version 4.9.0. Using the SPSS 16.0 software, data from mycelia or fermentation broth were compared using repeated measurement of one-way analysis of variance (ANOVA) and least significant difference (LSD) at significance levels of $p < 0.05$ or $p < 0.001$, respectively.

3. Results

3.1. Effect of Selenite Concentration on the Mycelial Dry Weight of Epichloë sinensis

Table 1 shows the growth profile of *Epichloë sinensis* in liquid media with and without Se. The growth rate of *Epichloë sinensis* decreased in the presence of increased Se concentrations. The highest biomass accumulation occurred in week 5 when the Se content in the treated group reached 0.1–0.2 mmol/L, which was 68.21–74.29% lower than that of the control group (CK).

Table 1. Effects of Na_2SeO_3 concentrations on mycelial dry weight of *Epichloë sinensis* in liquid culture.

Se Concentration (mmol/L)	Mycelial Dry Weight (mg/mL)				
	Week 4	Week 5	Week 6	Week 7	Week 8
0.0	2.14 ± 0.15^{Ba}	2.80 ± 0.14^{Aa}	2.31 ± 0.11^{Ba}	2.12 ± 0.14^{BCa}	1.87 ± 0.08^{Ca}
0.1	0.75 ± 0.05^{BCb}	0.89 ± 0.10^{Ab}	0.80 ± 0.06^{ABb}	0.67 ± 0.03^{Cb}	$0.42 \pm 0.0.04^{Db}$
0.2	0.67 ± 0.07^{Ab}	0.72 ± 0.07^{Ac}	0.57 ± 0.01^{Bc}	0.54 ± 0.04^{Bb}	0.33 ± 0.01^{Cb}

Means followed by upper case letters differ statistically under the same selenium concentration ($p < 0.05$). Means followed by lowercase letters differ statistically among a given culture time ($p < 0.05$).

3.2. Identification of Metabolites and Screening for Differential Metabolites

Extracellular and intracellular metabolites were measured by GC-MS based on mass spectrum and retention index match and the following were identified: components of amino acid metabolism, glycolysis, the citric acid (TCA) cycle, organic acids, fatty acids, sugars, and sugar alcohols were identified. A total of 380 peaks and approximately 157 identified metabolites were detected in the fermentation broth samples (Figure S1, Table S1). A total of 440 peaks and approximately 197 identified metabolites were detected in mycelial samples (Figure S2, Table S2). There was a greater number of metabolites in the mycelia than the fermentation broth, though the two shared 95 metabolites (Figure 1). There were 62 and 102 metabolites unique to the fermentation broth and mycelia of *Epichloë sinensis*, respectively (Figure 1).

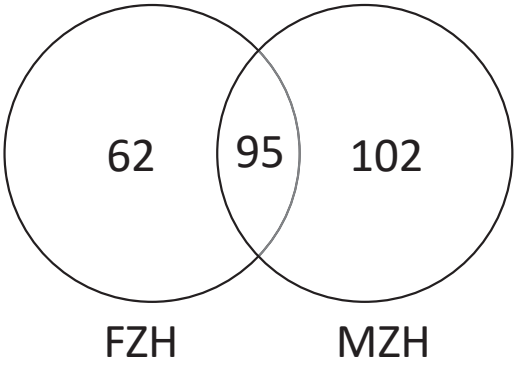

Figure 1. Venn diagram of metabolites found in the mycelia (MZH) and the fermentation broth (FZH) of *Epichloë sinensis* when cultivated in liquid culture.

3.3. Principal Component Analysis of Epichloë sinensis

The differences between Se-treated samples from the fermentation broth of *Epichloë sinensis* at different time points ware assessed using principal component analysis (PCA) (Figure 2). The first principal component produced the greatest contribution (75.79%), and the second principal component accounted for 9.84% of the total. With this method, there was a clear distinction noted between the samples under different cultivation times and Se concentrations.

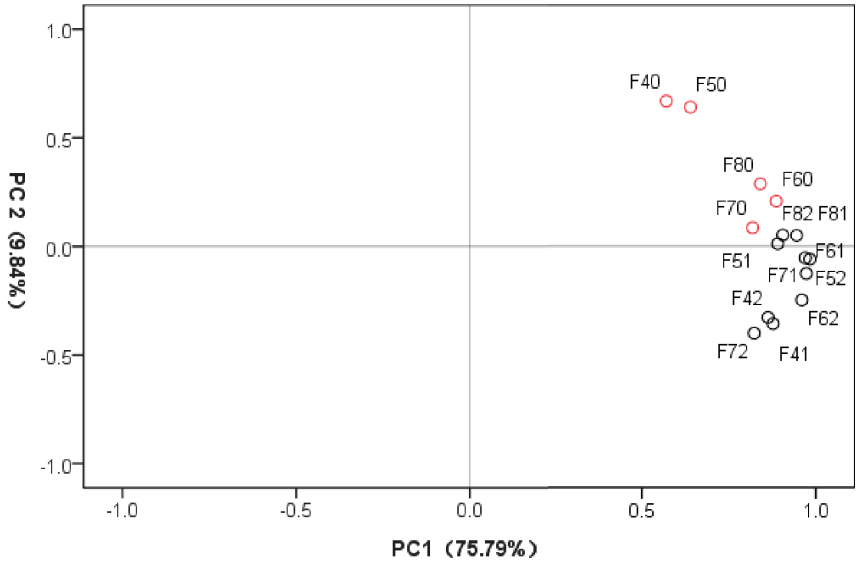

Figure 2. Principle component analysis (PCA) score plot of first and second PCs from 15 fermentation broth samples. PC1: the first principal component; PC2: the second principal component. Red and black colors represent control and Se-treated samples, respectively.

The processing of the metabolomic data with PCA revealed clustering of mycelial samples according to Se concentration and cultivation time (Figure 3). The first and second principal components accounted for 59.42% and 8.72% of the total sample variance, respectively, indicating an apparent difference between the samples under different cultivation times and Se concentrations.

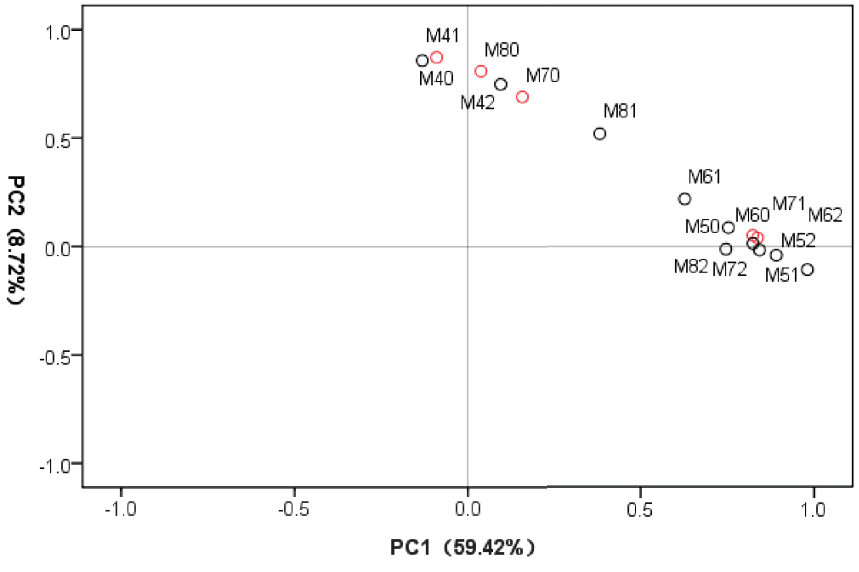

Figure 3. Principle component analysis (PCA) score plot of first and second PCs from 15 mycelial samples. PC1: the first principal component; PC2: the second principal component. Red and black colors represent control and Se-treated samples, respectively.

3.4. Heatmap and Hierarchical Cluster Analysis of Epichloë sinensis

To identify the different metabolites in the fermentation broth samples in response to Se concentrations, metabolite profiles from 15 *Epichloë sinensis* samples were assessed by heatmap and hierarchical cluster analysis (Figure 4). According to hierarchical clustering analysis of the 157 identified extracellular metabolites, a clear separation was observed between samples. The 15 fermentation broth samples were grouped into three distinct categories: the first category included two samples (the control samples for 4 and 5 weeks of cultivation), the second category included four samples (the control and 0.2 mmol/L Na_2SeO_3 treated samples for 7 weeks of cultivation, as well as the Se-treated samples from week 4), and the third category included the remaining nine samples. Additionally, 157 metabolites were divided into two clusters consisting of 74 and 83 compounds.

A similar pattern was observed with the hierarchical clustering analysis of the 197 identified intracellular metabolites from the mycelia. There was again a clear separation noted between samples. Here, the 15 samples were grouped into two distinct classes: one category consisted of 5 samples (both the control and Se-treated samples for week 4, as well as control samples between weeks 7 and 8), and the other consisted of the remaining 10 samples (both the control and treated samples between weeks 5 and 6, as well as treated samples between weeks 7 and 8) (Figure 5). Likewise, 197 metabolites were divided into two groups, consisting of 60 and 137 compounds.

3.5. Changes in the Extracellular and Intracellular Metabolite Profiles of Epichloë sinensis in Response to Selenium Conditions

The changes in identified metabolites of the fermentation broth are presented in Tables 2 and 3. Among the 157 identified metabolites, 22 metabolites displayed differential accumulation, and 17 metabolites decreased in the 0.1 mmol/L Se group compared to the 0 mmol/L Se group (CK) (0.1 mmol/L vs. CK). Additionally, in the 0.2 mmol/L group, we observed an increase in 29 metabolites and a decrease in 13 metabolites that was not found in the CK. These findings indicated that Na_2SeO_3 concentrations affected metabolite responses. Parallel to the cultivation period, 67 metabolites (~43%) increased while 70 metabolites (~45%) decreased in the 4th week in both Se-treatment groups when compared to the control group (Se vs. CK). In 5 weeks of cultivation, 87 up-regulated and 58 down-regulated metabolites were detected in Se versus CK. In week 6, there were 64 up-regulated and 38 down-regulated metabolites that were present between all Se treatments and control. There were 77 compounds that were highly accumulated, and 43 compounds were suppressed in Se versus CK during 7 weeks of cultivation. In the 8th and final week of cultivation, there were 76 accumulated and 54 depleted compounds in the Se treatment groups. Here in the fermentation broth, we discovered that the extracellular samples displayed dynamic metabolic responses in terms of cultivation time and degree of Se treatments.

Table 2. Number of increased or decreased metabolite levels among 157 identified metabolites in the fermentation broth of *Epichloë sinensis* Se-treated (0.1 and 0.2 mmol/L Na_2SeO_3) and untreated groups from 4 to 8 weeks of cultivation.

Change	Number of Metabolites		
	0.1 mmol/L vs. CK	**0.2 mmol/L vs. CK**	**0.2 mmol/L vs. 0.1 mmol/L**
Increase	22	29	11
Decrease	17	13	1

Figure 4. Heatmap and hierarchical cluster analysis for the 157 metabolites discovered in the fermentation broth of *Epichloë sinensis*. FZH40, FZH41 and FZH42 represent the treated 4-week fermentation broth samples in the presence of 0, 0.1 or 0.2 mmol/L Na_2SeO_3, respectively. FZH50, FZH51 and FZH52 represent the treated 5-week fermentation broth samples in the presence of 0, 0.1 or 0.2 mmol/L Na_2SeO_3, respectively. FZH60, FZH61 and FZH62 represent the treated 6-week fermentation broth samples in the presence of 0, 0.1 or 0.2 mmol/L Na_2SeO_3, respectively. FZH70, FZH71 and FZH72 represent the treated 7-week fermentation broth samples in the presence of 0, 0.1 or 0.2 mmol/L Na_2SeO_3, respectively. FZH80, FZH81 and FZH82 represent the treated 8-week fermentation broth samples in the presence of 0, 0.1 or 0.2 mmol/L Na_2SeO_3, respectively.

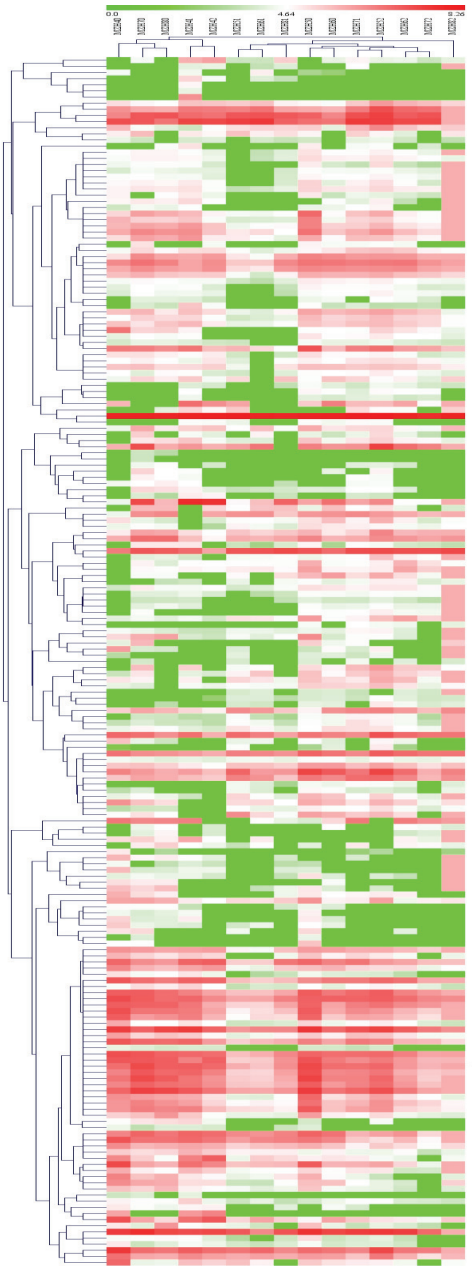

Figure 5. Heatmap and hierarchical cluster analysis for the 197 metabolites found in the mycelia of *Epichloë sinensis*. MZH40, MZH41 and MZH42 represent mycelia grown for 4 weeks in the presence of 0, 0.1, or 0.2 mmol/L Na_2SeO_3, respectively. MZH50, MZH51 and MZH52 represent mycelia grown for 5 weeks in the presence of 0, 0.1, or 0.2 mmol/L Na_2SeO_3, respectively. MZH60, MZH61 and MZH62 represent mycelia grown for 6 weeks in the presence of 0, 0.1, or 0.2 mmol/L Na_2SeO_3, respectively. MZH70, MZH71 and MZH72 represent mycelia grown for 7 weeks in the presence of 0, 0.1, or 0.2 mmol/L Na_2SeO_3, respectively. MZH80, MZH81 and MZH82 represent mycelia grown for 8 weeks in the presence of 0, 0.1, or 0.2 mmol/L Na_2SeO_3, respectively.

Table 3. Changes in metabolite profiles in the fermentation broth of *Epichloë sinensis* between Se and control groups during weeks 4–8.

Change in Se vs. CK	Number of Metabolites				
	Week 4	**Week 5**	**Week 6**	**Week 7**	**Week 8**
Increase	67	87	64	77	76
Decrease	70	58	38	43	54

Changes in metabolites from mycelia of *Epichloë sinensis* between Se and control groups are shown in Tables 4 and 5. In 0.1 mmol/L treatment group, there were 3 increased and 35 decreased metabolites compared to the control, but in the 0.2 mmol/L treatment group, there were only 2 increased and 29 decreased metabolites when compared to the control. In 4 weeks of cultivation, there were 43 up-regulated and 83 down-regulated metabolites in the Se groups when compared to the control group. In week 5, there were 21 accumulated and 98 depleted metabolites detected in Se-treated groups but not the control. In the 6th week, there were 22 up-regulated and 90 down-regulated metabolites unique to the Se-treated groups. In 7 weeks of cultivation, there were 24 up-regulated and 109 down-regulated metabolites identified in the Se-treatment groups that were not found in the control. During the last week of cultivation, there were 30 metabolites highly accumulated and 91 depleted metabolites found in the Se groups when compared to the control. The intracellular samples of *Epichloë sinensis* mycelia demonstrated metabolic complexity regarding cultivation time and varying degrees of Se exposure.

Table 4. Number of increased or decreased metabolite levels among the 197 identified metabolites in the mycelia of *Epichloë sinensis* Se-treated (0.1 and 0.2 mmo/L Na_2SeO_3) and untreated groups from 4 to 8 weeks of cultivation.

Change	Number of Metabolites		
	0.1 mmol/L vs. CK	**0.2 mmol/L vs. CK**	**0.2 mmol/L vs. 0.1 mmol/L**
Increase	3	2	0
Decrease	35	29	0

Table 5. Changes in metabolite profiles in the mycelia of *Epichloë sinensis* between Se and control groups during weeks 4–8.

Change in Se vs. CK	Number of Metabolites				
	Week 4	**Week 5**	**Week 6**	**Week 7**	**Week 8**
Increase	42	21	22	24	30
Decrease	86	98	90	109	91

3.6. Marked Metabolites Changed in Epichloë sinensis Fermentation Broth under Selenium Condition

To identify metabolite features in the fermentation broth that were significantly different between each treatment and the control, one-way ANOVA statistical analysis ($p < 0.001$) was performed. The heatmap visualized different trends of metabolite changes for each time period when exposed to Se, as well as differences when *Epichloë sinensis* was exposed to varying Se concentrations (Figures 6 and 7). There were significant metabolite differences in the fermentation broths regarding culture time and Se concentrations. For instance, there were 64, 40, 36, 49 and 30 distinct metabolites identified in the fermentation broths collected from weeks 4, 5, 6, 7, and 8, respectively (Figure 6). The 13 common metabolites among culture times were glycine, ornithine, O-methylthreonine, allose, ribose, tagatose, threitol, pyruvic acid, 2-ketoisovaleric acid, 3-hexenedioic acid, sulfuric acid, succinic acid, and α-ketoglutaric acid.

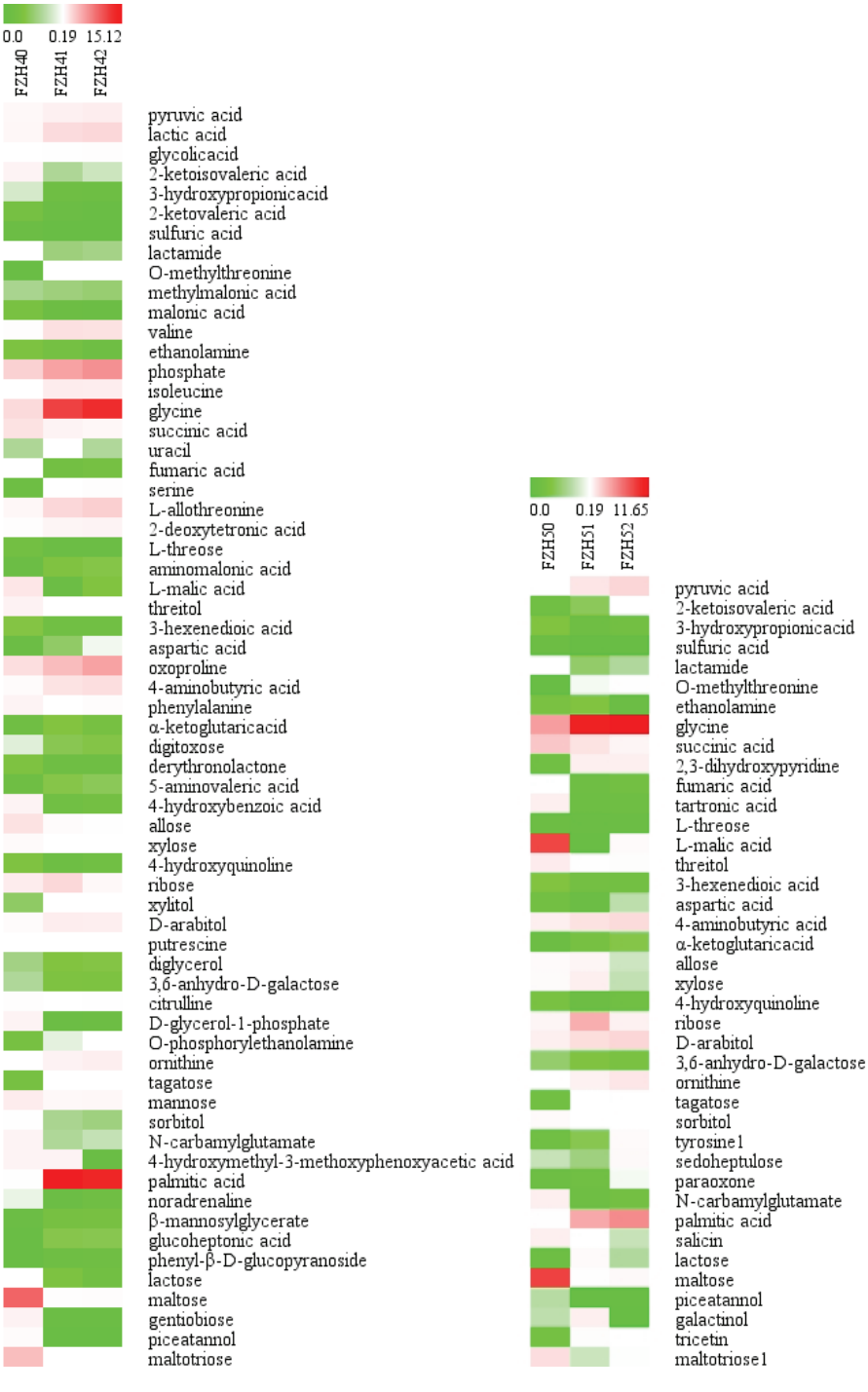

Figure 6. *Cont.*

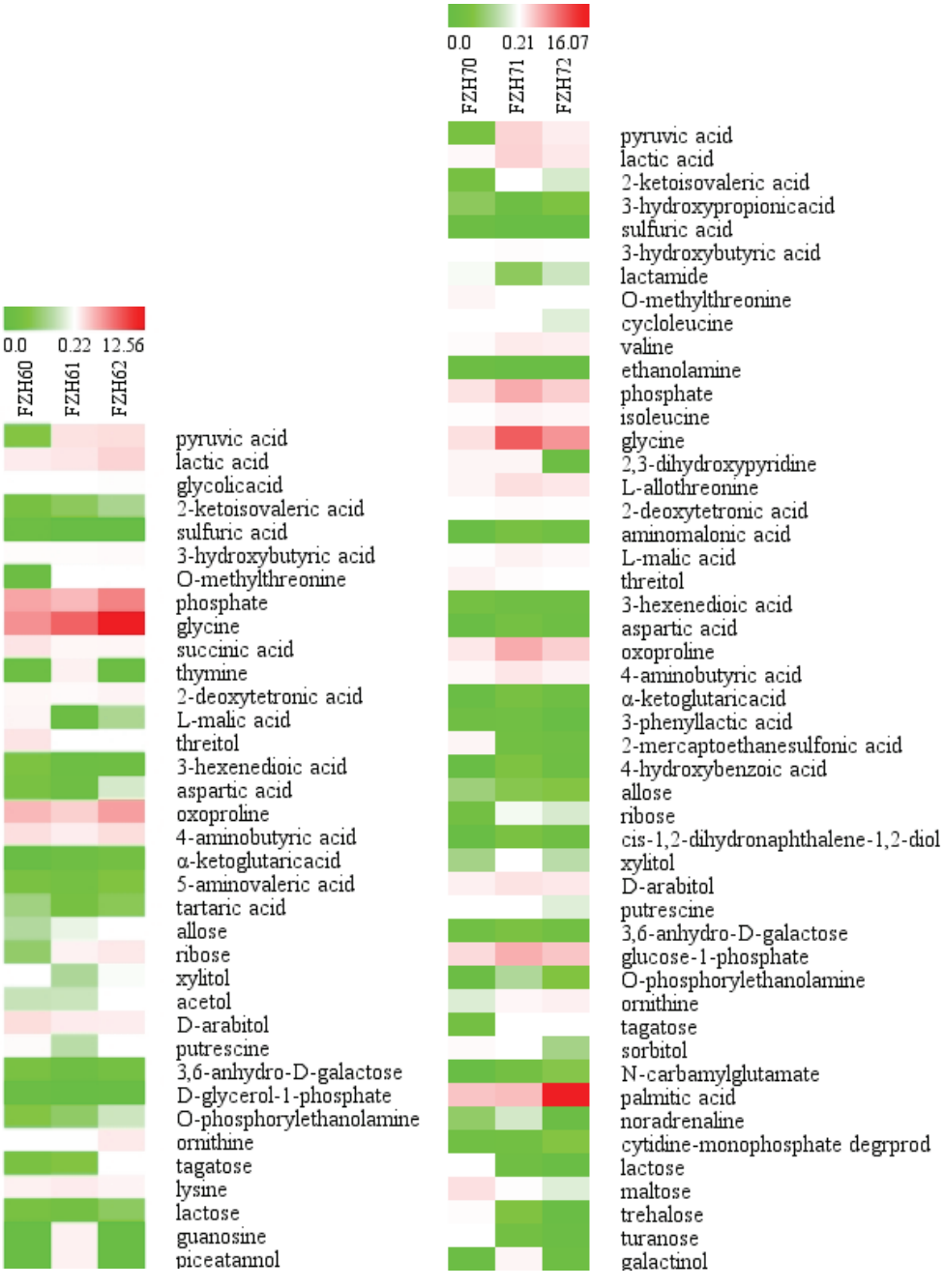

Figure 6. *Cont.*

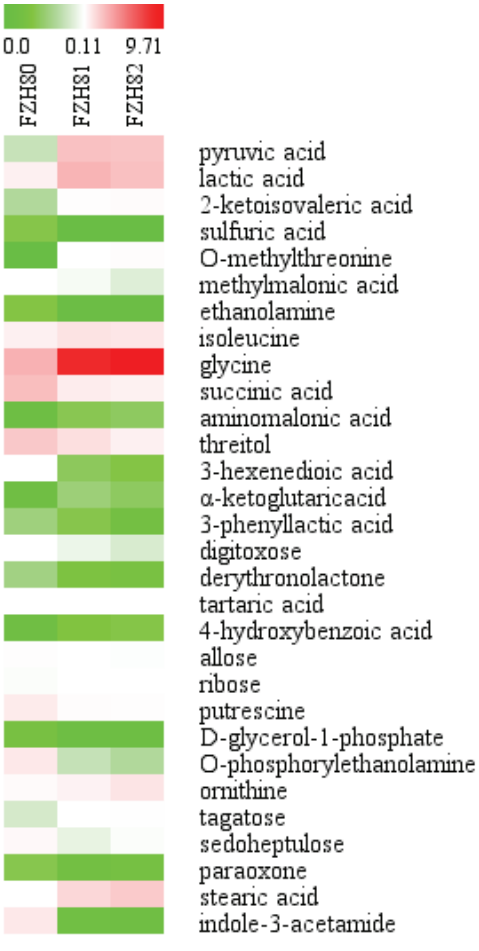

Figure 6. Heatmap of the abundance of marked metabolites in the fermentation broth of *Epichloë sinensis* when exposed to Se concentrations at a given time. Red and green blocks indicate higher and lower metabolite levels, respectively (see scale bar). FZH40, FZH41, and FZH42 represent fermentation broth for week 4 in the presence of 0, 0.1, or 0.2 mmol/L Na_2SeO_3, respectively. FZH50, FZH51, and FZH52 represent fermentation broth for week 5 in the presence of 0, 0.1, or 0.2 mmol/L Na_2SeO_3, respectively. FZH60, FZH61, and FZH62 represent fermentation broth for week 6 in the presence of 0, 0.1, or 0.2 mmol/L Na_2SeO_3, respectively. FZH70, FZH71, and FZH72 represent fermentation broth for week 7 in the presence of 0, 0.1, or 0.2 mmol/L Na_2SeO_3, respectively. FZH80, FZH81, and FZH82 represent fermentation broth for week 8 in the presence of 0, 0.1, or 0.2 mmol/L Na_2SeO_3, respectively.

At Se concentrations of 0, 0.1, and 0.2 mmol/L, we detected 67, 47 and 39 marked metabolites, respectively, in the fermentation broth using statistical analysis ($p < 0.001$) during the cultivation period (Figure 7). There were 25 common metabolites among Se concentrations, such as glycine, oxoproline, 4-aminobutyric acid, putrescine, lactamide, ethanolamine, O-phosphorylethanolamine, allose, ribose, D-arabitol, 3,6-anhydro-D-galactose, lactose, maltose, glucose-1-phosphate, threitol, xylitol, pyruvic acid, lactic acid, glycolic acid, 2-ketoisovaleric acid, sulfuric acid, phosphate, 2-deoxytetronic acid, L-malic acid, and tartaric acid.

Figure 7. Heatmap of the abundance of marked metabolites in the fermentation broth of *Epichloë sinensis* when exposed to 0, 0.1 or 0.2 mmol/L selenium. Red and green blocks indicate higher and lower metabolite levels (see scale bar). FZH40, FZH50, FZH60, FZH70, and FZH80 represent fermentation broth in absence of Se for weeks 4, 5, 6, 7, and 8, respectively. FZH41, FZH51, FZH61, FZH71, and FZH81 represent fermentation broth in the presence of 0.1 mmol/L Se between weeks 4 to 8. FZH42, FZH52, FZH62, FZH72, and FZH82 represent fermentation broth in the presence of 0.2 mmol/L Se during weeks 4 to 8.

The addition of 0.1 or 0.2 mmol/L Se in the medium significantly increased some amino acids found in the fermentation broth ($p < 0.001$). There were elevated levels of alanine and citrulline in week 4; tyrosine in week 5; serine in weeks 4 and 5; oxoproline and phenyalanine in weeks 4, 6, and 7; isoleucine in weeks 4, 7, and 8; aspartic acid in weeks 4 to 7; valine in the weeks 4, 5, 7, and 8; and glycine and ornithine throughout the course of the experiment when compared to the control. In addition to increased levels of amino acids, the concentrations of several amino acids changed with time (Figure 6). There were highly significant ($p < 0.001$) contributions of culture time detected for glutamine and O-methylthreonine in the control fermentation broth; proline, tyrosine, and serine in

the 0.1 mmol/L Se fermentation broth; ornithine, phenylalanine, and isoleucine levels of fermentation broth under control and 0.1 or 0.2 mmol/L Se, and glycine, aspartic acid, oxoproline, 4-aminobutyric acid levels of fermentation broth with all experimental media (0–0.2 mmol/L Se). In regard to the variance observed per time period, the metabolite levels of both Se-treated fermentation broths (0.1 or 0.2 mmol/L) were the highest in the 4th week (Figure 7), though the metabolite levels from the control were the highest in weeks 6 or 8.

During the cultivation period, the fermentation broth of samples exposed to Se (0.1 and 0.2 mmol/L Na_2SeO_3) had higher overall levels of pyruvic acid, 2-ketoisovaleric acid, and α-ketoglutaric acid of the fermentation broth than the control medium ($p < 0.001$). The control, however, had higher levels of succinic acid and 3-hexenedioic acid in the fermentation broth than of all the Se-treated samples ($p < 0.001$). All cultures (0, 0.1, and 0.2 mmol/L Na_2SeO_3) exhibited significant increases of 2-ketoisovaleric acid and 3-hexenedioic acid after the 8-week cultivation period. Furthermore, the identified compounds and their concentrations were dynamic and varied with time and degree of Se exposure (Figure 7). The control group had the highest levels of pyruvic acid in the 4th week, which lowered after the 5th week, but this trend took longer in the Se-treated fermentation broths. Cultures treated with 0.1 mmol/L Se had pyruvic acid levels peak in the 7th week and tapered off in the 8th week ($p < 0.001$), and cultures treated with 0.2 mmol/L Se experienced a sharp increase in pyruvic acid only in the last week of cultivation ($p < 0.001$). A significant increase of succinic acid was observed in the 5th week in media supplemented with 0 and 0.1 mmol/L Se ($p < 0.001$), and no significant trend was found in cultures treated with 0.2 mmol/L Se. The untreated and 0.1 mmol/L Se samples behaved similarly again with α-ketoglutaric acid levels increasing significantly in the 4th week ($p < 0.001$) relative to other time points, although fermentation broth supplemented with 0.2 mmol/L Se trailed behind with markedly enhanced α-ketoglutaric acid levels observed in the 5th week ($p < 0.001$). Lactic acid concentrations were the highest in week 5 for the control, weeks 7 and 8 for the 0.1 mmol/L Se cultures ($p < 0.001$), and week 7 for the 0.2 mmol/L Se cultures. Glycolic acid concentrations in the control fermentation broth were significantly elevated between the 5th and 6th weeks of cultivation relative to other weeks ($p < 0.001$). Glycolic acid levels peaked sooner with Se treatment. The highest concentrations were observed in week 4 in 0.1 mmol/L Se cultures ($p < 0.001$), and weeks 4 and 6 for 0.2 mmol/L Se cultures ($p < 0.001$). There were significant increases in 2-deoxytetronic acid observed in the 6th and 4th weeks in the control and both Se-treated samples, respectively ($p < 0.001$). The untreated fermentation broth had significantly higher L-malic acid levels in week 5 relative to other time points ($p < 0.001$), while the cultures supplemented with 0.1 mmol/L Se had much more L-malic acid later in the cultivation period during weeks 7 and 8 ($p < 0.001$), and cultures treated with 0.2 mmol/L Se did not peak until the last week of cultivation ($p < 0.001$). Levels of tartaric acid in the control and 0.2 mmol/L Se-treated fermentation broths were greater in week 8 than at the beginning of the experiment ($p < 0.001$). The 0.1 mmol/L Se-treated fermentation broth, however, demonstrated a unique trend, where tartaric acid levels reached a minimum in the 6th week ($p < 0.001$).

Many sugars and sugar alcohols of fermentation broth were significantly different across the time points ($p < 0.001$). Se-supplemented fermentation broths significantly accumulated tagatose ($p < 0.001$) in comparison to the control fermentation broth, though they had greatly reduced levels of allose, ribose, and threitol. Fermentation broth for the control and 0.2 mmol/L Se showed higher allose values in the 4th week, but lower levels after the 5th week, and 0.1 mmol/L Se treated cultures had the most allose in week 5 ($p < 0.001$). Maltose in untreated fermentation broth peaked in 4 and 5 weeks of cultivation, whereas 0.1 mmol/L Se cultures had significantly higher concentrations in the 4th and 7th weeks. In contrast, 0.2 mmol/L Se cultures had significantly less maltose in the 7th week than before treatment or in the 8th week ($p < 0.001$).

Lactose in the control fermentation broth was significantly higher in week 7 than before treatment and in the final week of cultivation, though lactose in fermentation broths

from both Se-treatments were the greatest in week 5 ($p < 0.001$). The ribose concentrations for the control, 0.1 mmol/L Se, and 0.2 mmol/L Se fermentation broths peaked in the 4th, 5th and 6th weeks, respectively ($p < 0.001$). The highest xylitol levels were found in the 6th and 8th weeks for the control fermentation broth, and the lowest levels were observed in the 6th and 7th weeks for 0.1 and 0.2 mmol/L Se cultures, respectively. The increase in D-arabitol in all fermentation broths was found to be the highest during the 8th week of cultivation.

3.7. Marked Metabolites Changed in the Mycelia of Epichloë sinensis under Selenium Conditions

As shown in Figures 8 and 9, there were significant differences in metabolites of mycelia throughout the cultivation period and varying Se concentrations. In weeks 4, 5, 6, 7, and 8 there were 17, 27, 16, 41, and 6 distinct metabolites identified, respectively, in mycelia using LSD ($p < 0.05$). At Se concentrations of 0, 0.1, and 0.2 mmol/L there were 6, 18, and 44 marked metabolites found, respectively, in the mycelia at a significance level of $p < 0.05$. There were no commonly marked metabolites across the time points ($p < 0.05$) or the different Se concentrations. Over the time course, Se promoted N-acetyl-β-D-mannosamine and glucoheptonic acid levels, but inhibited 19 metabolites, such as glycolic acid, oxalic acid, 3-hydroxybutyric acid, sulfuric acid, malonic acid, hydroxyurea, dihydroxyacetone, ethanolamine, phosphate, proline, glycine, succinic acid, uracil, 2-deoxytetronic acid, 4-aminobuyric acid, 4-hydroxyphenylethanol, conduritol b epoxide, gentiobiose, and isomaltose.

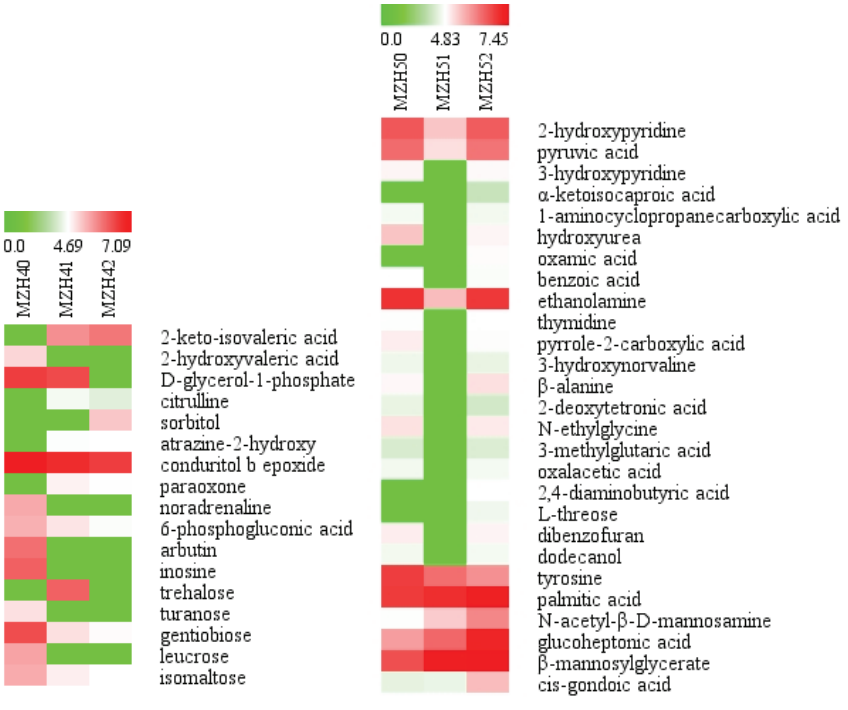

Figure 8. *Cont.*

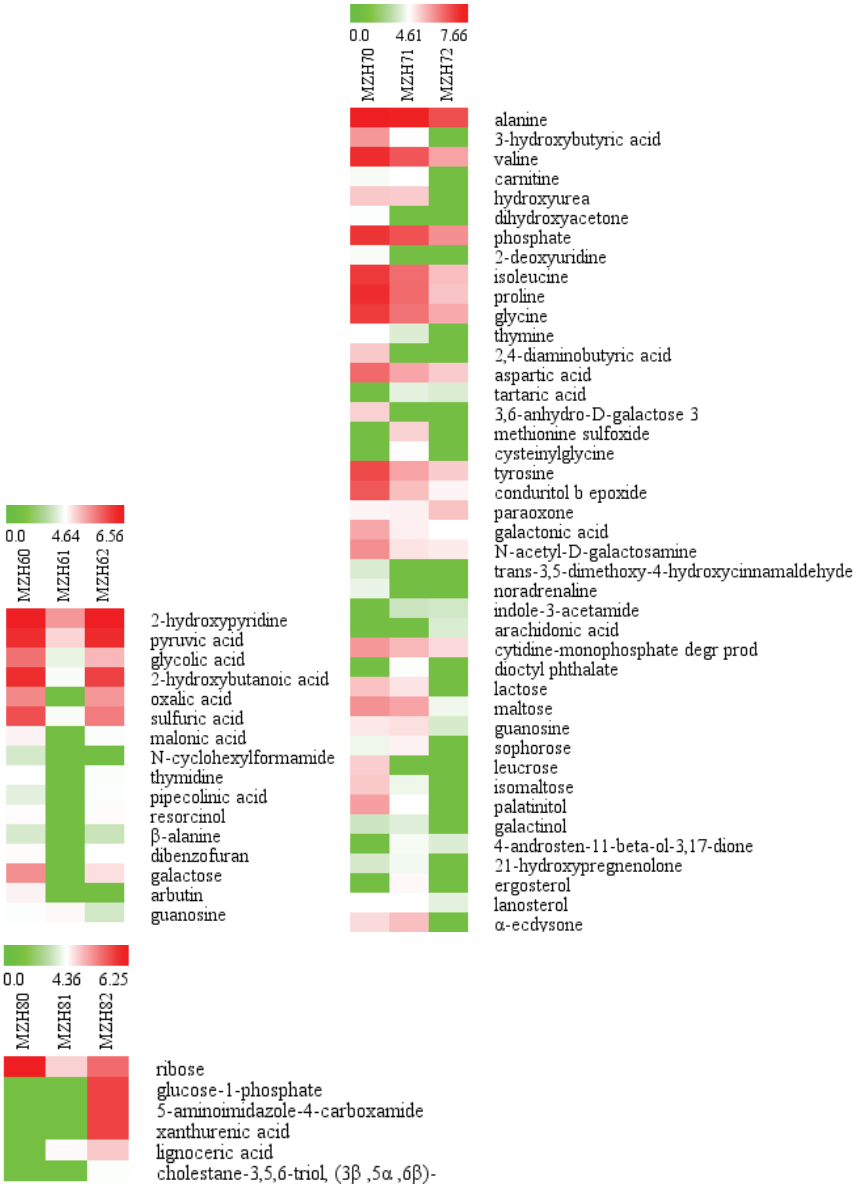

Figure 8. Heatmap of the abundance of identified metabolites in the mycelia of *Epichloë sinensis* under selenium concentrations in a given cultivation time. Red and green blocks indicate higher or lower metabolite levels (see scale bar). MZH40, MZH41, and MZH42 represent mycelia grown for 4 weeks in the presence of 0, 0.1, or 0.2 mmol/L Na_2SeO_3, respectively. MZH50, MZH51, and MZH52 represent mycelia grown for 5 weeks in the presence of 0, 0.1, or 0.2 mmol/L Na_2SeO_3, respectively. MZH60, MZH61, and MZH62 represent mycelia grown for 6 weeks in the presence of 0, 0.1, or 0.2 mmol/L Na_2SeO_3, respectively. MZH70, MZH71, and MZH72 represent mycelia grown for 7 weeks in the presence of 0, 0.1, or 0.2 mmol/L Na_2SeO_3, respectively. MZH80, MZH81, and MZH82 represent mycelia grown for 8 weeks in the presence of 0, 0.1, or 0.2 mmol/L Na_2SeO_3, respectively.

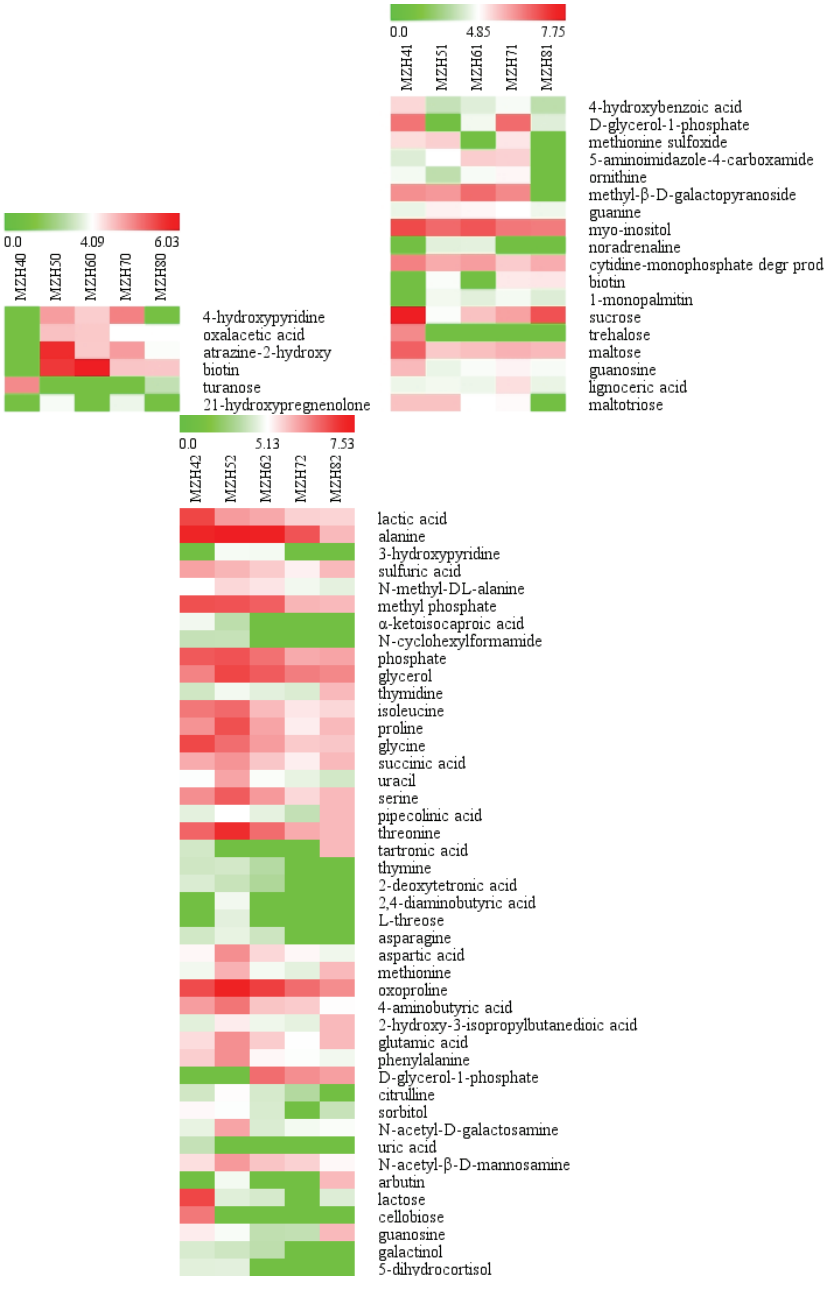

Figure 9. Heatmap of the abundance of identified metabolites in the mycelia of *Epichloë sinensis* under each selenium concentration throughout weeks 4 to 8. Red and green blocks indicate higher or lower metabolite levels (see scale bar). MZH40, MZH50, MZH60, MZH70, and MZH80 represent mycelia grown in the absence of Se for 4, 5, 6, 7, and 8 weeks, respectively. MZH41, MZH51, MZH61, MZH71, and MZH81 represent mycelia grown in the presence of 0.1 mmol/L Se during weeks 4 to 8. MZH42, MZH52, MZH62, MZH72, and MZH82 represent mycelia grown in the presence of 0.2 mmol/L Se during weeks 4 to 8.

There were no differences observed in serine, homoserine, methionine, oxoproline, glutamic acid, phenylalanine, ornithine, N-methyl-alanine, and cycloleucine levels when exposed to different Se treatments at a specific time (Figure 8). When Se concentrations were 0.1 and 0.2 mmol/L, there were significant increases in only citrulline in the 4th week, but significant decreases in N-ethylglycine in the 5th week, and in tyrosine in the 5th and 7th weeks. In week 7, the levels of alanine, valine, isoleucine, proline, and asparagine found in the mycelia treated with 0.2 mmol/L Se were significantly lower than those of 0 and 0.1 mmol/L Se. Additionally, glycine, serine, threonine, and carnitine levels for 0.2 mmol/L Se-treated mycelia were lower than those of the control group. Similarly, aspartic acid levels of mycelia treated with 0.1 mmol/L Se were lower than those of the control in week 5. Time also had significant effects on ornithine levels of mycelia treated with 0.1 mmol/L Se (Figure 9), as well as alanine, valine, isoleucine, proline, glycine, serine, threonine, asparagine, aspartic acid, methionine, oxoproline, glutamic acid, phenylalanine, and citrulline levels of mycelia treated with 0.2 mmol/L Se ($p < 0.05$). It was also noted that these amino acid levels increased in 5 weeks of cultivation, relative to the other time points.

We found that Se concentration was a significant contributor to the changes observed in some organic acids in the mycelia ($p < 0.05$) (Figure 8). In both Se conditions (0.1 and 0.2 mmol/L), there were increases in 2-ketoisovaleric acid, tartaric acid, and lignoceric acid observed in the 4th, 7th, and 8th weeks, respectively. Levels of benzoic acid, galactonic acid, and 3-hydroxybutyric acid decreased in mycelia treated with 0.1 or 0.2 mmol/L Se after weeks 5 or 7, respectively. The lowest levels of oxalacetic acid were in the control mycelia ($p < 0.05$) and 1-monopalmitin in the 0.1 mmol/L Se-treated mycelia was observed in the 4th week for their respective groups. Additionally, in this week, lactic acid, tartronic acid, 2-deoxytetronic acid, and α-ketoisocaproic acid levels began to decrease in 0.2 mmol/L Se-treated mycelia and continued to do so until the end of the experiment. Despite the decrease in α-ketoisocaproic acid in 0.2 mmol/L Se samples, its levels were still significantly greater than those of the control or 0.1 mmol/L Se-treated mycelia, as well as cis-gondoic acid, and palmitic acid ($p < 0.05$) in week 5. This week also saw the lowest levels of arachidonic acid in 0.1 mmol/L Se-treated mycelia than in any other condition. In the 6th week, there were significantly depleted levels of malonic acid and pipecolinic acid in mycelia exposed to 0.1 mmol/L Se ($p < 0.05$). In the 7th week, 0.2 mmol/L Se treatment induced higher levels of 3-methyglutaric acid, 2-deoxytetronic acid, and oxalacetic acid levels than those of other mycelia ($p < 0.05$). In this time point, lignoceric acid levels peaked in the 0.1 mmol/L Se-treated mycelia. During the last week, 0.2 mmol/L Se samples showed enhanced levels of xanthurenic acid, but also the lowest levels of succinic acid and pipecolinic acid.

The presence of selenium significantly decreased levels of gentiobiose, leucrose, and turanose during weeks 4 and 5. The concentrations of maltose, isomaltose, lactose, and trehalose for 0.1 mmol/L Se-treated mycelia were equal to, or above, levels found in the control at certain time points, though galactose and ribose were significantly lower in 0.1 mmol/L Se samples than in the control mycelia in the 6th and 8th weeks, respectively. When analyzing the effect of time in intracellular sugars, mycelia treated with 0.1 mmol/L Se had significantly lower sucrose in the 5th week than in other time points, and the lowest concentration of maltotriose at the end of the experiment ($p < 0.05$), though there was a peak in maltose and trehalose levels in week 4. In addition, the greatest lactose and cellobiose in mycelia were found in week 4 in 0.2 mmol/L Se-treated samples.

Se concentration had significant effects ($p < 0.05$) on sugar alcohols at specific time points. Sorbitol was the highest in mycelia exposed to 0.2 mmol/L Se in week 4 than in any other condition. Intracellular galactinol and lanosterol levels were lower in 0.2 mmol/L Se-treated mycelia in week 7 than in the 0 and 0.1 mmol/Se samples. Ergosterol concentration of 0.1 mmol/L Se-treated mycelia were significantly higher than in the 7th week in 0 and 0.2 mmol/L Se samples. In addition to Se concentrations, time also had a significant influence on some sugar alcohols ($p < 0.05$). Mycelia in the presence of 0.2 mmol/L Se had the highest galactinol levels in weeks 4 and 5, but decreased throughout the experiment, and had the lowest levels in 7 and 8 weeks of cultivation. Likewise, sorbitol reached a

minimum in week 7, though it increased slightly in week 8 and glycerol content peaked in the 5th and 6th weeks, but levels lowered in the subsequent weeks.

Significant effects of Se treatment were detected for some nucleotide bases and nucleosides for mycelia. While the control mycelia had an increase in inosine in the 4th week ($p < 0.05$), the Se-treated mycelia saw more dynamic responses throughout the cultivation period. Mycelia treated with 0.1 mmol/L Se had guanine levels increase slightly after the 4th week before falling again after the 6th week, and there was a small decrease in thymidine in week 5. Samples grown with 0.2 mmol/L Se had uracil and thymidine levels peak in week 5, though thymine levels began to decrease in weeks 4 and 5, and there was significantly less thymine in weeks 7 and 8 ($p < 0.05$), as well as significantly reduced levels of guanosine in week 6. In the cases of both 0.1 and 0.2 mmol/L Se culture medium, increases in guanosine were observed in week 4.

4. Discussion

The present study has shown that the changes in extracellular and intracellular metabolite profiles of *Epichloë sinensis* at different concentrations of Na_2SeO_3 during fermentation over eight weeks. Some amino acids, carbohydrates, organic acids, nucleotides, and their metabolites, especially those from the extracellular environment, were significantly changed due to selenite conditions and culture time.

Se is required for some of the normal biochemical processes in the cell, but it is known to be toxic in excess. Additionally, it is known that there are diverse fungal species that exhibit varying levels of Se tolerance [32–34]. Consistent with the literature, our data demonstrated that the mycelial dry weight of *Epichloë sinensis* decreased when exposed to increasing concentrations of Se. However, both the Se-treated and control samples experienced steady decrease in the mycelial biomass after week 5 due to insufficient energy and carbon sources. The lower biomass in Se-exposed samples, than in the control, might have been due to the stress of Se, which would also be consistent with the known toxicity of Se [34].

In the experiments described in this paper, the significant effects of Se concentration were detected in the changes of some amino acid levels of mycelia and fermentation broth of *Epichloë sinensis*. Some amino acids of mycelia, such as glycine and serine for the biosynthesis of glutathione, were significantly depressed with increase of Se concentration (Figure 8), but these amino acids were found in greater amounts in the fermentation broth (Figure 6), which could be beneficial for detoxification of the harmful metalloid. Concentrations of Se at 60 mg/L reduced the levels of only serine and tyrosine in *Cordyceps militaris* mycelia cultivated in a liquid medium, but increased other amino acids [5]. A recent study demonstrated that amino acids, such as proline, glutamine, alanine, arginine, and methionine, varied between *Candida utilis* and *Saccharomyces cerevisiae* when the culture media was enriched with 20 mg/L Se, when compared to the control [9]. Concentrations of individual amino acids depend on the presence of Se in the culture conditions, further supporting this notion [35]. In addition, our results showed that the intracellular concentrations of alanine, isoleucine, proline, glycine, serine, threonine, asparagine, aspartic acid, oxoproline, methionine, phenylalanine, citrulline, and glutamic acid found in the mycelia treated with 0.2 mmol/L Se varied markedly over time ($p < 0.05$), with the maximum levels observed in the 5th or the 4th weeks (Figure 9). Many extracellular amino acids showed highly significant dynamic response to low Se conditions as well. It is likely that Se contributes to the reductive environment for the catalytic efficiency of many enzymes, and, therefore, affects the biosynthesis of some amino acids. These findings demonstrate that the shifts in amino acid are affected by many factors, such as Se concentration, substrate, cultivation time, and microorganism species.

In this study, most of the organic acids from the fermentation broth that changed were dramatically decreased with the increase of Se concentration, with only a few exceptions. Pyruvic acid is a crucial intermediate metabolite of the central carbon metabolism that determines the carbon fluxes to the tricarboxylic acid (TCA) cycle. In this study, the

extracellular content of pyruvic acid in Se conditions was highly significant and higher than the control media ($p < 0.001$). Increased pyruvic acid could be attributed to the TCA cycle. Then, an increase in α-ketoglutaric acid might influence further transformations forming ornithine, and ultimately, reducing succinic acid. However, these organic acids of TCA in mycelia showed no significant change between Se-treated samples. Undissociated organic acids are membrane permeable and can be secreted by fungi [11], which, in turn, would favor the maintenance of the intracellular pH environment. Levels of succinic acid in the control and Se-treated fermentation broths, and 0.2 mmol/L Se-treated mycelia, were at a maximum in the 5th week. Likewise, Yang et al. [36] reported similar dynamic changes in succinic acid and other TCA organic acids from the culture broth of *Aspergillus saccharolyticus* when cultivated under different pH conditions.

The profile of fatty acids is correlated with the duration of the cultivation period and selenium concentration [6]. *C. utilis*, without Se exposure, accumulated more oleic acid (C18:1), stearic acid (C18:0), palmitoleic acid (C16:1), and myristic acid (C14:0) than cultures treated with Se culture. However, Se supplementation promoted the abundances of oleic acid, palmitoleic acid, and myristic acid in *S. cerevisiae* [9]. Similarly, the addition of Se to the culture medium caused an increase in the C-18 fatty acid contents of *S. cerevisiae* [6]. Guan et al. [33] have found 90 μg/mL Se raised the concentration of arachidonic acid (C20:4) in *Diasporangium jonesianum* but reduced the levels of myristic acid, hexadecenoic acids (C16:1), and octadecenoic (C18:1), and slightly changed the level of other fatty acids when compared to the control group. Our data suggests that selenium at 0.1 and 0.2 mmol/L significantly increased lignoceric acid (24:0) of mycelia during the last week of an 8-week cultivation period. Additionally, Se at 0.2 mmol/L significantly increased palmitic acid (C16:0) in week 5 and arachidonic acid in week 7. During the fermentation process, few long chain fatty acids were detected in the fermentation broth, implying that long chain fatty acids mainly maintain cell membranes. There were no significant differences observed in the changes for linoleic acid (C18:2), oleic acid, stearic acid, and palmitoleic acid in *Epichloë* mycelia regardless of Se treatment and culture time, which might have been due to this species' variance affecting the fluctuation of fatty acids.

Some carbohydrates are involved in maintaining the structural integrity of cells in the case of several adverse environmental conditions. Compared with the control, the carbohydrates from the mycelia are more significant in *Penicillium expansum* when cultivating with 20 mg/L Se [37]. The addition of 0.1 mmol/L Na_2SeO_3 decreases the trehalose content of *S. cerevisiae* [38]. In this respect, we observed that Se significantly decreased intracellular levels of gentiobiose, leucrose, and turanose in the 4th and 5th weeks. The dose of 0.1 mmol/L Se significantly increased trehalose levels in the 4th week of cultivation, but decreased galactose and ribose of mycelia in 6 and 8 weeks of cultivation, respectively. Moreover, Se highly and significantly promoted extracellular tagatose and ribose levels. Se might be playing a major role in the cell's sugar uptake and transport. *Lactobacillus reuteri* CRL1101 can modulate proteins and enzymes involved in sugar synthesis or degradation to adapt to Se conditions [39]. However, different species have evolved their metabolome for specific metabolites. *Trichoderma harzianum*, *Aureobasidium pullulans*, *Mortierella humilis*, and *Phoma glomerata* treated with 1 mmol/L Na_2SeO_3 had distinct exopolysaccharide levels [33].

As previous studies have noted, most fungi produce sugars and sugar alcohols to facilitate tolerance to environmental stress conditions [40,41]. In the case of the fermentations described in the present study, a dose of 0.2 mmol/L Se significantly increased intracellular sorbitol in the 4th week, but decreased galactinol and lanosterol levels of mycelia in week 7 when compared to the control samples. Sorbitol can act as an alternative energy source and can protect cells against oxidative damage by scavenging free reactive oxygen radicals [42]. Perhaps this is why sorbitol was highly accumulated in the intracellular environment of *Streptococcus thermophilus* when in stationary phase [43]. More interestingly, some studies have shown that lanosterol, found as endophytic fungal secondary metabolites, have good medicinal potential to treat cataract diseases [44,45]. In addition, our results showed that Se significantly decreased threitol levels in the fermentation broth. In this study, dynamics

of the significant changes in glycerol of mycelia under 0.2 mmol/L Se conditions over the cultivation period peaked in week 5. However, Ianutsevich et al. [46] concluded that *Rhizomucor miehei* increased levels of arabitol and glycerol when under osmotic stress, and no significant changes in glycerol between 3 h and 6 h were found. This might have been due to time variance affecting the mycelia metabolic capacity. Ergosterol, a vitamin D precursor, plays the pivotal role in membrane fluidity. The addition of Se to *Pleurotus ostreatus* and *Ganoderma lucidum* growth media resulted in lower levels of ergosterol in fruiting bodies when compared to the control group [47]. In this respect, ergosterol levels found in the mycelia with the addition of 0.1 mmol/L Se were significantly higher than those of other mycelia in the 7th week. Hence, it can be concluded that Se affected membrane fluidity and the stabilization of its structure.

Most purines and pyrimidines in the cell take part in the biosynthesis of genetic information carriers (DNA and RNA) or energy suppliers (ATP and GTP) [48]. In the present study, some intermediates of purine and pyrimidine metabolism of 0.1 or 0.2 mmol/L Se-treated mycelia, including thymine, inosine, 2-dioxyuridine, and guanosine, were down-regulated at certain times. There was also a greater thymidine amount detected in 0.1 mmol/L Se-exposed mycelia in 5 and 6 weeks of cultivation. The contents of adenosine in *C. militaris* were promoted with increase in Se concentrations [5]. Results from a study presented by Hu et al. [49] confirmed that high adenosine content was detected in *C. militaris* by Se, which regulated purine and pyrimidine metabolism. The results suggest that Se influences DNA and RNA synthesis throughout the entire growing period, thus interfering with mycelial metabolites. Overall, the marked metabolites of *Epichloë* species were affected by Se, and they were involved in the metabolic pathways, such as glycolysis, TCA cycle, amino acid, purine and pyrimidine metabolism.

5. Conclusions

In this study, we determined the dynamic intra and extracellular metabolic responses of *Epichloë sinensis* when exposed to varying concentrations of Se over an 8-week period ($p < 0.05$, $p < 0.001$). There were considerably fewer extracellular metabolites than what was found in the case of intracellular metabolites. Redox balance appears to drive the active secretion of some intracellular metabolites, which might have contributed to this finding. Additionally, we observed that the intracellular metabolites in the mycelia of *Epichloë sinensis* varied greatly when exposed to higher concentrations of Se, but the opposite was seen with extracellular metabolites, which were significantly dynamic in the absence of Se. Moreover, the results presented in this study not only deepen our knowledge of extracellular and intracellular metabolic responses of *Epichloë sinensis* throughout its growth, but also contribute to better understanding of the relationship between *Epichloë sinensis* and its host plant, *F. sinensis*. Further studies regarding metabolite variations, in addition to analysis of gene expression, selenium metabolites and related enzyme activities, are necessary to describe the detailed mechanism of selenium tolerance.

Supplementary Materials: The following supporting information can be downloaded at: https://www.mdpi.com/article/10.3390/agriculture12091423/s1, Figure S1: Total ion chromatogram of fermentation broth of *Epichloë sinensis*; Figure S2: Total ion chromatogram of mycelia of *Epichloë sinensis*; Table S1: List of the 157 metabolites from fermentation broth; Table S2: List of the 197 metabolites from mycelia.

Author Contributions: Conceptualization, L.Z. and H.X.; methodology, F.Q.; software, Q.L.; validation, X.M. and J.J.; formal analysis, L.Z.; data curation, X.M.; writing—original draft preparation, L.Z. and H.X.; writing—review and editing. All authors have read and agreed to the published version of the manuscript.

Funding: This research was funded by the National Natural Science Foundation of China (grant numbers 31760697) and the Science and Technology Program of Qinghai Province (grant numbers 2022-ZJ-740).

Institutional Review Board Statement: Not applicable.

Informed Consent Statement: Not applicable.

Data Availability Statement: The data presented in this study are available within the article.

Acknowledgments: We would like to thank Shanghai Biotree Biotech Co., Ltd. for the technical support of metabolome analysis.

Conflicts of Interest: The authors declare no conflict of interest.

References

1. Kieliszek, M.; Błażejak, S. Current knowledge on the importance of selenium in food for living organisms: A review. *Molecules* **2016**, *21*, 609. [CrossRef] [PubMed]
2. Tie, M.; Li, B.R.; Sun, T.B.; Guan, W.; Liang, Y.Q.; Li, H.W. HPLC-ICP-MS speciation of selenium in Se-cultivated *Flammulina velutipes*. *Arab. J. Chem.* **2017**, *13*, 416–422. [CrossRef]
3. Zhao, L.; Zhao, G.H.; Zhao, Z.D.; Chen, P.; Tong, J.Y.; Hu, X.S. Selenium distribution in a Se-enriched mushroom species of the genus *Ganoderma*. *J. Agric. Food Chem.* **2004**, *52*, 3954–3959. [CrossRef] [PubMed]
4. Kieliszek, M.; Błażejak, S.; Gientka, I.; Bzducha-Wróbel, A. Accumulation and metabolism of selenium by yeast cells. *Appl. Microbiol. Biotechnol.* **2015**, *99*, 5373–5382. [CrossRef]
5. Dong, J.Z.; Lei, C.; Ai, X.R.; Wang, Y. Selenium enrichment on *Cordyceps militaris* link and analysis on its main active components. *Appl. Biocham. Biotechnol.* **2012**, *166*, 1215–1224. [CrossRef] [PubMed]
6. Čertík, M.; Breierová, E.; Oláhová, M.; Šajbidor, J.; Márová, I. Effect of selenium on lipid alternations in pigment-forming yeasts. *Food Sci. Biotechnol.* **2013**, *22*, 45–51. [CrossRef]
7. Kieliszek, M.; Błażejak, S.; Bzducha-Wróbel, A.; Kot, A.M. Effect of selenium on growth and antioxidative system of yeast cells. *Mol. Biol. Rep.* **2019**, *46*, 1797–1808. [CrossRef] [PubMed]
8. Kieliszek, M.; Dourou, M. Effect of selenium on the growth and lipid accumulation of *Yarrowia lipolytica* yeast. *Biol. Trace Elem. Res.* **2021**, *199*, 1611–1622. [CrossRef]
9. Kieliszek, M.; Błażejak, S.; Bzducha-Wróbel, A.; Kot, A.M. Effect of selenium on lipid and amino acid metabolism in yeast cells. *Biol. Trace Elem. Res.* **2019**, *187*, 316–327. [CrossRef]
10. Xu, X.; Cheng, W.; Liu, X.; You, H.; Wu, G.T.; Ding, K.M.; Tu, X.L.; Yang, L.F.; Wang, Y.P.; Li, Y.D.; et al. Selenate reduction and selenium enrichment of tea by the endophytic *Herbaspirillum* sp. strain WT00C. *Curr. Microbiol.* **2020**, *77*, 588–601. [CrossRef]
11. Wang, S.; Liu, P.; Shu, W.; Li, C.; Li, H.; Liu, S.S.; Xia, J.Y.; Noorman, H. Dynamic response of *Aspergillus niger* to single pulses of glucose with high and low concentrations. *Bioresour. Bioprocess.* **2019**, *6*, 16. [CrossRef]
12. Han, T.L.; Tumanov, S.; Cannon, R.D.; Villas-Boas, S.G. Metabolic response of *Candida albicans* to phenylethyl alcohol under hyphae-inducing conditions. *PLoS ONE* **2013**, *88*, e71364. [CrossRef] [PubMed]
13. Granucci, N.; Pinu, F.R.; Han, T.L.; Villas-Boas, S.G. Can we predict the intracellular metabolic state of a cell based in extracellular metabolite data? *Mol. BioSyst.* **2015**, *11*, 3297–3304. [CrossRef]
14. Pinu, F.R.; Granucci, N.; Daniell, J.; Han, T.L.; Carneiro, S.; Rocha, I.; Nielsen, J.; Villas-Boas, S.G. Metabolite secretion in microorganisms: The theory of metabolic overflow put to the test. *Metabolomics* **2018**, *14*, 43. [CrossRef] [PubMed]
15. Johnson, L.J.; de Bonth, A.C.M.; Briggs, L.R.; Caradus, J.R.; Finch, S.C.; Fleetwood, D.J.; Fletcher, L.R.; Hume, D.E.; Johnson, R.D.; Popay, A.J.; et al. The exploitation of *epichloae* endophytes for agricultural benefit. *Fungal Divers.* **2013**, *60*, 171–188. [CrossRef]
16. Lindblom, S.D.; Wangeline, A.L.; Valdez Barillas, J.R.; Devibiss, B.; Fakra, S.C.; Pilon-Smits, E.A.H. Fungal endophyte *Alternaria tenuissima* can affect growth and selenium accumulation in its hyperaccumulator host *Astragalus bisulcatus*. *Front. Plant Sci.* **2018**, *9*, 1213. [CrossRef]
17. Li, C.J.; Nan, Z.B.; Li, F. Biological and physiological characteristics of *Neotyphodium gansuense* symbiotic with *Achnatherum inebrians*. *Microbiol. Res.* **2008**, *163*, 431–440. [CrossRef]
18. Leuchtmann, A.; Bacon, C.W.; Schardl, C.L.; White, J.F.; Tadych, M. Nomenclatural realignment of *Neotyphodium* species with genus *Epichloë*. *Mycologia* **2014**, *106*, 202–215. [CrossRef]
19. Chen, L.; Li, X.Z.; Li, C.J.; Swoboda, G.A.; Young, C.A.; Sugawara, K.; Leuchtmann, A.; Schardl, C.L. Two distinct *Epichloë* species symbiotic with *Achnatherum inebrians*, drunken horse grass. *Mycologia* **2015**, *107*, 863–873. [CrossRef]
20. Yi, M.; Hendricks, W.Q.; Kaste, J.; Charlton, N.D.; Nagabhyru, P.; Panaccione, D.G.; Young, C.A. Molecular identification and characterization of endophytes from uncultivated barley. *Mycologia* **2018**, *110*, 453–472. [CrossRef]
21. Wei, M.Y.; Yin, L.J.; Jia, T.; Zhu, M.J.; Ren, A.Z.; Gao, Y.B. Responses of three endophyte fungi species isolated from natural grass to abiotic stresses. *Bot. Res.* **2012**, *1*, 1–7. (In Chinese, with English Abstract)
22. Peng, Q.Q.; Li, C.J.; Song, M.L.; Nan, Z.B. Effects of seed hydropriming on growth of *Festuca sinensis* infected with *Neotyphodium* endophyte. *Fungal Ecol.* **2013**, *6*, 83–91. [CrossRef]
23. Wang, J.J.; Zhou, Y.P.; Lin, W.H.; Li, M.M.; Wang, M.N.; Wang, Z.G.; Kuang, Y.; Tian, P. Effect of an *Epichloë* endophyte on adaptability to water stress in *Festuca sinensis*. *Fungal Ecol.* **2017**, *30*, 39–47. [CrossRef]
24. Zhou, L.Y.; Li, C.J.; Zhang, X.X.; Johnson, R.; Bao, G.S.; Yao, X.; Chai, Q. Effects of cold shocked *Epichloë* infected *Festuca sinensis* on ergot alkaloid accumulation. *Fungal Ecol.* **2015**, *14*, 99–104. [CrossRef]

25. Zhou, L.Y.; Zhang, X.X.; Li, C.J.; Christensen, M.J.; Nan, Z.B. Antifungal activity and phytochemical investigation of the asexual endophyte of *Epichloë* sp. from *Festuca sinensis*. *Sci. China Life Sci.* **2015**, *8*, 821–826. [CrossRef]
26. Zhou, L.Y.; Li, C.J.; White, J.F.; Johnson, R.D. Synergism between calcium nitrate applications and fungal endophytes to increase sugar concentration in *Festuca sinensis* under cold stress. *Peer J.* **2021**, *9*, e10568. [CrossRef]
27. Tian, P.; Kuang, Y.; Lin, W.H.; Wang, J.J.; Nan, Z.B. Shoot morphology and alkaloid content of *Epichloë* endophyte-*Festuca sinensis* associations. *Crop Pasture Sci.* **2018**, *69*, 430–438.
28. Lin, W.H.; Kuang, Y.; Wang, J.J.; Duan, D.D.; Xu, W.B.; Tian, P.; Nzabanita, C.; Wang, M.N.; Li, M.M.; Ma, B.H. Effects of seasonal variation on the alkaloids of different ecotypes of *Epichloë* endophyte–*Festuca sinensis* associations. *Front. Microbiol.* **2019**, *10*, 1695. [CrossRef] [PubMed]
29. Jin, W.J.; Li, C.J.; Nan, Z.B. Biological and physiological characteristics of *Neotyphodium* endophyte symbiotic with *Festuca sinensis*. *Mycosystema* **2009**, *28*, 363–369. (In Chinese, with English Abstract)
30. Tian, P.; Xu, W.B.; Li, C.J.; Song, H.; Wang, M.N.; Schardl, C.L.; Nan, Z.B. Phylogenetic relationship and taxonomy of a hybrid *Epichloë* species symbiotic with *Festuca sinensis*. *Mycol. Prog.* **2020**, *19*, 1069–1081. [CrossRef]
31. Zhou, L.Y.; Jiao, L.; Ju, J.S.; Ma, X.L. Effect of sodium selenite on the metabolite profile of *Epichloë* sp. mycelia from *Festuca sinensis* in solid culture. *Biol. Trace Elem. Res.* **2022**, 1–15. [CrossRef] [PubMed]
32. Guan, X.Y.; Dai, C.C.; Xu, Y.F. Enhancement of polyunsaturated fatty acid production by selenium treatment in polyunsaturated fatty acid-producing fungus. *J. Am. Oil Cham. Soc.* **2010**, *87*, 1309–1317. [CrossRef]
33. Liang, X.J.; Marie-Jeanne Perez, M.A.; Nwoko, K.C.; Egbers, P.; Feldmann, J.; Csetenyi, L.; Gadd, G.M. Fungal formation of selenium and tellurium nanoparticles. *Appl. Microbiol. Biot.* **2019**, *103*, 7241–7259. [CrossRef] [PubMed]
34. Rehan, M.; Alsohim, A.S.; El-Fadly, G.; Tisa, L.S. Detoxification and reduction of selenite to elemental red selenium by *Frankia*. *Antonie Leeuwenhoek* **2018**, *112*, 127–139. [CrossRef]
35. Suhajda, A.; Hegóczki, J.; Janzsó, B.; Pais, I.; Vereczkey, G. Preparation of selenium yeasts I. Preparation of selenium-enriched *Saccharomyces cerevisiae*. *J. Trace Elem. Med. Biol.* **2000**, *14*, 43–47. [CrossRef]
36. Yang, L.; Lübeck, M.; Ahring, B.K.; Lübeck, P.S. Enhanced succinic acid production in *Aspergillus saccharolyticus* by heterologous expression of fumarate reductase from *Trypanosoma brucei*. *Appl. Microbiol. Biotechnol.* **2016**, *100*, 1799–1809. [CrossRef]
37. Wu, Z.L.; Yin, X.B.; Lin, Z.Q.; Bañuelos, G.S.; Yuan, L.X.; Liu, Y.; Li, M. Inhibitory effect of selenium against *Penicillium expansum* and its possible mechanisms of action. *Curr. Microbiol.* **2014**, *69*, 192–201. [CrossRef]
38. Sharma, S.C.; Anand, M.S. Role of selenium supplementation and heat stress on trehalose and glutathione content in *Saccharomyces cerevisia*. *Appl. Biocham. Biotechnol.* **2006**, *133*, 1–7. [CrossRef]
39. Gómez-Gómez, B.; Pérez-Corona, T.; Mozzi, F.; Pescuma, M.; Madrid, Y. Silac-based quantitative proteomic analysis of *Lactobacillus reuteri* CRL 1101 response to the presence of selenite and selenium nanoparticles. *J. Proteomics* **2019**, *195*, 53–65. [CrossRef]
40. Ramirez, M.L.; Chulze, S.N.; Magan, N. Impact of osmotic and matric water stress on germination, growth, mycelial water potentials and endogenous accumulation of sugars and sugar alcohols by *Fusarium graminearum*. *Mycologia* **2004**, *96*, 470–478. [CrossRef]
41. Neschi, A.; Etcheverry, M.; Magan, N. Osmotic and matric potential effects on growth and sugar alcohol and solute accumulation in *Aspergillus* section *Flavi* strains from Argentina. *J. Appl. Microbiol.* **2004**, *96*, 965–972. [CrossRef] [PubMed]
42. Santivarangkna, C.; Kulozik, U.; Foerst, P. Effect of carbohydrates on the survival of *Lactobacillus helveticus* during vacuum drying. *Lett. Appl. Microbiol.* **2006**, *42*, 271–276. [CrossRef]
43. Qiao, Y.L.; Liu, G.F.; Lv, X.P.; Fan, X.J.; Zhang, Y.J.; Meng, L.; Ai, M.Z.; Feng, Z. Metabolic pathway profiling in intracellular and extracellular environments of *Streptococcus thermophilus* during pH-controlled batch fermentations. *Front. Microbiol.* **2020**, *10*, 3144. [CrossRef] [PubMed]
44. Zhao, L.; Chen, X.J.; Zhu, J.; Xi, Y.B.; Yang, X.; Hu, L.D.; Ouyang, H.; Patel, S.H.; Jin, X.; Lin, D.N.; et al. Lanosterol reverses protein aggregation in cataracts. *Nature* **2015**, *523*, 607–611. [CrossRef] [PubMed]
45. Song, R.J.; Wang, J.L.; Sun, L.; Zhang, Y.J.; Ren, Z.H.; Zhao, B.Y.; Lu, H. The study of metabolites from fermentation culture of *Alternaria oxytropis*. *BMC Microbiol.* **2019**, *19*, 35. [CrossRef]
46. Ianutsevich, E.A.; Danilova, O.A.; Kurilov, D.V.; Zavarzin, I.V.; Tereshina, V.M. Osmolytes and membrane lipids in adaptive response of thermophilic fungus *Rhizomucor miehei* to cold, osmotic and oxidative shocks. *Extremophiles* **2020**, *24*, 391–401. [CrossRef]
47. Siwulski, M.; Budzyńska, S.; Rzymski, P.; Gąsecka, M.; Niedzielski, P.; Kalač, P.; Mleczek, M. The effects of germanium and selenium on growth, metalloid accumulation and ergosterol content in mushrooms: Experimental study in *Pleurotus ostreatus* and *Ganoderma lucidum*. *Eur. Food Res. Tech.* **2019**, *245*, 1799–1810. [CrossRef]
48. Castellanos, M.; Wilson, D.B.; Shuler, M.L. A modular minimal cell model: Purine and pyrimidine transport and metabolism. *Proc. Natl. Acad. Sci. USA* **2004**, *101*, 6681–6686. [CrossRef]
49. Hu, T.; Liang, Y.; Zhao, G.S.; Wu, W.L.; Li, H.F.; Guo, Y.B. Selenium biofortification and antioxidant activity in *Cordyceps militaris* supplied with aelenate, aelenite, or aelenomethionine. *Biol. Trace Elem. Res.* **2019**, *187*, 553–561. [CrossRef]

agriculture

MDPI

Article

Modification of Cuticular Wax Composition and Biosynthesis by *Epichloë gansuensis* in *Achnatherum inebrians* at Different Growing Periods

Zhenrui Zhao [1], Mei Tian [2], Peng Zeng [1], Michael J. Christensen [3], Mingzhu Kou [4,*], Zhibiao Nan [1] and Xingxu Zhang [1]

[1] State Key Laboratory of Grassland Agro-Ecosystems, Key Laboratory of Grassland Livestock Industry Innovation, Ministry of Agriculture and Rural Affairs, College of Pastoral Agriculture Science and Technology, Lanzhou University, Lanzhou 730020, China
[2] Institute of Horticulture, Ningxia Academy of Agricultural and Forestry Sciences, Yinchuan 750002, China
[3] Grasslands Research Centre, Private Bag 11-008, Palmerston North 4442, New Zealand
[4] Xining Center of Natural Resources Comprehensive Survey, CGS (China Geological Survey), Xining 810000, China
* Correspondence: koumzh18@lzu.edu.cn

Abstract: Cuticular wax plays a critical role as a plant protectant against various environmental stresses. We predicted that the presence of the mutualistic fungal endophyte *Epichloë gansuensis* in *Achnatherum inebrians* would change both the composition of leaf cuticular wax as plants aged during the growing season and the gene expression levels associated with the wax biosynthesis pathway. Endophyte-infected (EI) and endophyte-free (EF) *A. inebrians* plants were established for a four-month pot experiment. In agreement with our prediction, the presence of *E. gansuensis* can change the composition of leaf cuticular wax at different growing periods, particularly the proportion of esters, fatty acids and hydrocarbons. The proportion of fatty acids in EI plants was lower than that in EF plants. The proportion of hydrocarbons increased and esters decreased as plants grew. Furthermore, we found 11 DEGs coding for proteins involved in cuticular wax biosynthesis, including FabF, FAB2, ECR, FAR, CER1, ABCB1 and SEC61A. The present study highlights the significant contribution of *E. gansuensis* to leaf cuticular wax composition and biosynthesis in *A. inebrians* plants.

Keywords: *Epichloë gansuensis*; *Achnatherum inebrians*; growing periods; cuticular wax; GC–MS; transcriptome analysis

Citation: Zhao, Z.; Tian, M.; Zeng, P.; Christensen, M.J.; Kou, M.; Nan, Z.; Zhang, X. Modification of Cuticular Wax Composition and Biosynthesis by *Epichloë gansuensis* in *Achnatherum inebrians* at Different Growing Periods. *Agriculture* **2022**, *12*, 1154. https://doi.org/10.3390/agriculture12081154

Academic Editor: Rosario Nicoletti

Received: 14 June 2022
Accepted: 31 July 2022
Published: 4 August 2022

1. Introduction

Cuticular wax, as the first physical barrier, plays a crucial role in protecting all land plants from nonstomatal water loss, UV radiation, pathogens and herbivores [1–4]. Cuticular wax is a mixture of very long-chain fatty acids (VLCFAs), primary alcohols, esters, aldehydes, hydrocarbons, secondary alcohols, ketones, phenols, triterpenoids, sterols and flavonoids, with carbon chain lengths ranging from C_{20} to C_{40} [5,6]. The formation of cuticular wax is completed in two stages. The first stage is the biosynthesis of C16 and C18 fatty acyl-acyl carrier proteins (ACPs) in the plastids, which is the same as other lipid biosynthetic pathways [7]. Then, long-chain acyl-ACPs are esterified to long-chain acyl-Coenzyme As (CoAs) and translocated to the endoplasmic reticulum (ER) [8]. The second stage is the elongation of C_{16} and C_{18} acyl-CoAs and the formation of derivatives in the ER. The extension is mediated by fatty acid elongase (FAE) complexes including the condensing enzyme β-ketoacyl-CoA synthase (KCS), β-keto acyl reductase (KCR), β-hydroxyacyl-CoA dehydratase (HCD) and enoyl-CoA reductase (ECR), which add two carbons per cycle [9]. The biosynthesis of derivatives is divided into two different pathways. One pathway produces primary alcohols and esters while another synthesizes aldehydes, alkanes, secondary alcohols and ketones [10]. Finally, the wax mixture is exported from

the ER, through the plasma membrane, across the cell wall, and to the cuticle by adenosine triphosphate (ATP)-binding cassette (ABC) transporters and lipid transfer proteins (LTPs) [11].

The cuticular wax composition varies from species to species, as well as the growing periods [12]. For example, in leaves of *Arabidopsis thaliana*, alkanes were reported as the most dominant wax compound [10]. Primary alcohols were found to be the most abundant components in wheat (*Triticum aestivum*) [13], maize (*Zea mays*) [14], barley (*Hordeum vulgare*) [15] and *Poa pratensis* [16]. However, few studies have focused on the wax composition in different growing periods. Early research found that in wheat, the major components were octacosanol and β-diketone at 50 and 66 days, respectively, and the content of fatty acids and esters increased from 66 to 100 days [17]. In maize, primary alcohols were reported as the most plentiful components in young leaves, while esters were the most dominant wax components in mature leaves [18]. After leaf unfolding, a dynamic biosynthesis of wax components started, especially aldehydes and β-amyrenyl acetate [19]. Recent studies showed that in wheat the quantities of alkanes, fatty acids and aldehydes increased gradually from 50 to 230 days, while the quantity of alcohols first increased and reached a maximum at 100 days, and then continuously decreased during further leaf development [20]. As leaves developed, the cuticular wax compositions in arabidopsis were found to shift from fatty acid to alkane constituents [21]. Though the genes involved in the biosynthesis of cuticular wax are not well characterized for grasses compared with arabidopsis, progress has been recently made. *TaFAR1*, *TaFAR2*, *TaFAR3*, *TaFAR4* and *TaFAR5* genes were reported as homologs of arabidopsis *CER4* encoding active alcohol-forming fatty acyl-coenzyme A reductase (FAR), which is involved in the synthesis of primary alcohol in wheat leaf in response to environmental stresses [22–24]. At least 18 *Glossy* genes can affect the synthesis and composition of cuticular wax in maize leaves [25]. *OsGL1-1*, *OsGL1-2* and *OsGL1-3* genes, homologs of arabidopsis *CER3*, were reported to be involved in cuticular wax biosynthesis in rice (*Oryza sativa*) [26–28].

Epichloë (syn. *Neotyphodium*) endophytes that are symbiotic with many cool season grasses spend all or nearly all of their life cycles within the hosts [29,30]. In the stable symbioses of *Epichloë* endophytes with hosts, growth of both partners is fully synchronized [31]. Host grasses provide shelter, nutrition, and dissemination through seeds, while endophytes protect against herbivory, which is attributable to bioactive alkaloids of fungal origin [32–34]. Nearly 100% of *Achnatherum inebrians* plants, a widespread perennial bunchgrass, are infected by *E. gansuensis* or *E. inebrians* in the arid and semi-arid grasslands of northwest China [35–37]. *Epichloë gansuensis* can confer to *A. inebrians* plants the ability to resist various adverse environmental conditions, such as pests, pathogens, drought, heavy metals, low temperature and salt, to improve the competitive edge of hosts [38–44]. However, studies to see if endophytes can change the composition and biosynthesis of cuticular wax have not been reported yet.

Here, we predicted that the presence of the endophyte *E. gansuensis* would change the composition of leaf cuticular wax and that changes in composition would continue over the growing season. In addition, we predicted that the gene expression levels associated with the wax biosynthesis pathway in *A. inebrians* plants would also change. In order to verify these predictions, we set up endophyte-infected (EI) and endophyte-free (EF) *A. inebrians* plants for a four-month pot experiment in the greenhouse. The composition and proportion of leaf cuticular wax and the expression levels of genes related to the cuticular wax biosynthesis pathway were determined by gas chromatography−mass spectrometry (GC−MS) and transcriptome analysis, respectively.

2. Materials and Methods

2.1. Plant Materials and Treatment

EI and EF seeds originated from a single EI and EF *A. inebrians* plant in the field of the College of Pastoral Agriculture Science and Technology, Yuzhong Campus of Lanzhou University (104°39′ E, 35°89′ N, Altitude 1653 m) in 2013. The seeds were stored at 4 °C

for further study. Before sowing, the seeds were stained with aniline blue as described by Li et al. [45] to determine that the frequency of fungal endophytes of EI and EF seeds were 100% and 0%. In June 2020, a four-month pot experiment was carried out in the greenhouse (temperature: 26 ± 2 °C; moisture: 42 ± 2%) of the College of Pastoral Agriculture Science and Technology, Yuzhong Campus of Lanzhou University. The seeds were sown in 100 plastic pots (diameter: 24 cm; height: 15 cm; 50 pots for EI plants and 50 pots for EF plants) with 200 g sterilized vermiculite (180 °C sterilization for 2 h). Three seeds were sown in each pot initially, but only one plant was chosen and kept in each pot after seed germination. These pots were placed at random in different positions and watered appropriately every day. Hoagland's solution was rationed to the pots every 7 days after the second fully unfolded leaf appeared. Leaf blade samples from different growing periods were collected at 1, 2, 3 and 4 months after sowing (S1, S2, S3 and S4, respectively), which came from the same part of equal-sized *A. inebrians* plants (6 EI plants and 6 EF plants each period). After collecting, samples were instantly frozen in liquid nitrogen and then kept at −80 °C in a refrigerator until analysis.

2.2. Leaf Cuticular Wax Extraction

Leaf cuticular waxes were extracted by soaking leaf blades, which were cut into 10 cm lengths, for 45 s in 10 mL chloroform (Tianjin Guangfu Fine Chemical Research Institute, Tianjin, China) at room temperature and containing 20 μL n-tetracosane (1 μg/μL, Sigma-Aldrich Corp., St. Louis, MO, USA) as an internal standard. Then, concentrate the solution to 1 mL under a stream of nitrogen and treat it with 20 μL of N, O-bis(trimethylsilyl)-trifluoroacetamide (GC Derivatization reagent, ≥98.0%, Sigma-Aldrich Corp., St. Louis, MO, USA) and 20 μL of pyridine (Standard for GC, >99.9%, Alfa Aesar, Ward Hill, MA, USA) for 1 h at 70 °C. Through organic filtration (0.45 μm), the solution was transferred into GC sample bottles (1.5 mL), blown dry under nitrogen gas again, and redissolved in 500 μL of chloroform for GC−MS analysis.

2.3. Chemical Analysis

The composition of cuticular wax was analyzed by GC−MS (6890N-5975C, Agilent Technologies Inc., Palo Alto, CA, USA) equipped with a DB−1 MS capillary column (0.25 μm film thickness, 0.25 mm inner diameter, 30 m length, Agilent Technologies Inc., Palo Alto, CA, USA). GC was performed with temperature-programmed on-column injection and oven temperature set at 50 °C for 2 min, increased by 40 °C/min to 200 °C, maintained at 200 °C for 2 min, increased by 3 °C/min to 320 °C, and maintained at 320 °C for 30 min. Inlet temperature, MS quadrupole temperature and transfer line temperature were set at 280 °C, 150 °C and 250 °C, respectively. Helium was used as a carrier gas at a flow rate of 1.2 mL/min. Individual wax components were identified via comparing their mass spectra with data in the literature through the National Institute of Standards and Technology (NIST) 2008 library [46]. Quantification was based on comparison of peak areas with those of the internal standard.

2.4. Transcriptome Analysis

The transcriptomes were characterized by sequencing total RNAs on leaves of EI and EF plants at four months after sowing. The RNA extraction was conducted with the TRIzol reagent (Invitrogen, Carlsbad, CA, USA) and cleaned using the RNeasy Plant Mini Kit (Qiagen, Valencia, CA, USA). The integrity, purities and concentration of RNA were assessed with RNA Nano 6000 assays (Agilent Bioanalyzer 2100 system, Agilent Technologies, Palo Alto, CA, USA), NanoPhotometer® spectrophotometers (IMPLEN, Calabasas, CA, USA) and Qubit® 2.0 fluorometers (Life Technologies, Carlsbad, CA, USA), respectively. The Biomarker Technologies Company (Beijing, China) performed transcriptome analysis. Transcriptome libraries were generated by the NEBNext® Ultra™ RNA Library Prep Kit for Illumina® (NEB, Ipswich, MA, USA) and then sequenced using the Illumina HiSeq 2000 platform. The library fragments were amplified by PCR, using Phusion high-fidelity DNA

polymerases (New England Biolabs, Ipswich, MA, USA) and purified with the AMPure XP system (Beckman Coulter, Brea, CA, USA).

Annotation of gene functions was based on several databases, namely, GO (gene Ontology), KEGG (Kyoto Encyclopedia of Genes and Genomes), KOG/COG/eggNOG (Clusters of Orthologous Groups of proteins), NR (NCBI non-redundant protein sequences), Pfam (Protein family) and Swiss-Prot (a manually annotated and reviewed protein sequence database). The expression level of each annotated gene was normalized based on the transcript lengths and the library size. The normalized gene expression levels were then reported as FPKM (fragments per kilobase per million mapped fragments). Differentially expressed genes (DEGs) were assigned to unigenes using the DESeq2 package in the R software with fold change (FC) values greater than or equal to 2 and with false discovery rate (FDR) values less than 0.05.

All raw sequence data utilized in the present study were deposited in the Sequence Read Achieve (SRA) of the NCBI database and the accession number was PRJNA748183.

2.5. Statistical Analysis

The effects of the presence of *Epichloë* endophytes and the different growing periods on the wax composition of the leaves of *A. inebrians* plants were analyzed by two-way ANOVA using SPSS Statistics 22.0 software (SPSS Inc., Chicago, IL, USA). The significance of differences between EI and EF plants at different growing periods was determined by an independent samples *t*-test. The values shown in the result all correspond to means + standard errors. Statistical significance was defined at the 95% confidence level.

3. Results

3.1. Composition of Leaf Cuticular Wax

The leaf cuticular wax composition under eight treatments (S1EI, S1EF, S2EI, S2F, S3EI, S3EF, S4EI and S4EF) was identified and relatively quantified by GC−MS. A total of 47 different wax compounds were detected, with 23, 23, 24, 29, 23, 24, 16, 14 compounds in the eight treatments, respectively (Table S1 of the Supplementary Materials). The wax mixture contained six identifiable compound classes including hydrocarbons (from minimum to maximum of 69.4392.61%), esters (from minimum to maximum of 3.11–23.03%), alcohols (from minimum to maximum of 1.07–8.12%), fatty acids (from minimum to maximum of 0–10.85%), phenols (from minimum to maximum of 0–3.25%) and ketones (from minimum to maximum of 0–0.40%; Figures 1 and 2).

Two–way ANOVA analysis indicated that the status of *E. gansuensis* endophytes, the different growing periods and interaction between the two factors had significant ($p < 0.05$) effects on the proportion of fatty acids (Table 1). Fatty acids were detected in EI plants only at S2. At S4, fatty acids were not identified in either EI or EF plants. Within EF plants, the proportion of fatty acids at S3 was significantly ($p < 0.05$) higher than that at S2 (Figure 2c). In addition, the different growing periods had significant ($p < 0.05$) effects on the proportion of esters and hydrocarbons (Table 1). The proportion of esters at S4 was significantly lower than that at S1, S2 and S3 (Figure 2b). However, the proportion of hydrocarbons at S4 was significantly higher than at S1, S2 and S3 (Figure 2d). Ketones were only found in EF plants at S2 (Figure 2e).

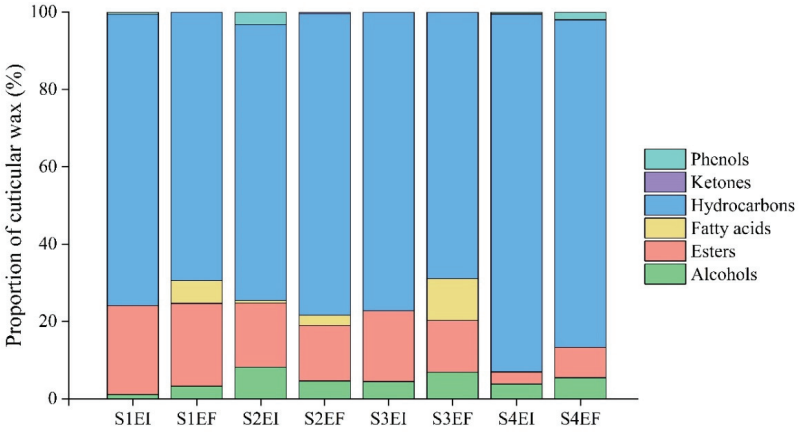

Figure 1. Composition and proportion of leaf cuticular wax in *Achnatherum inebrians* according to the status of *Epichloë gansuensis* endophytes and in different growing periods (S1: 1 month after sowing, S2: 2 months after sowing, S3: 3 months after sowing, S4: 4 months after sowing, EI: endophyte-infected and EF: endophyte-free).

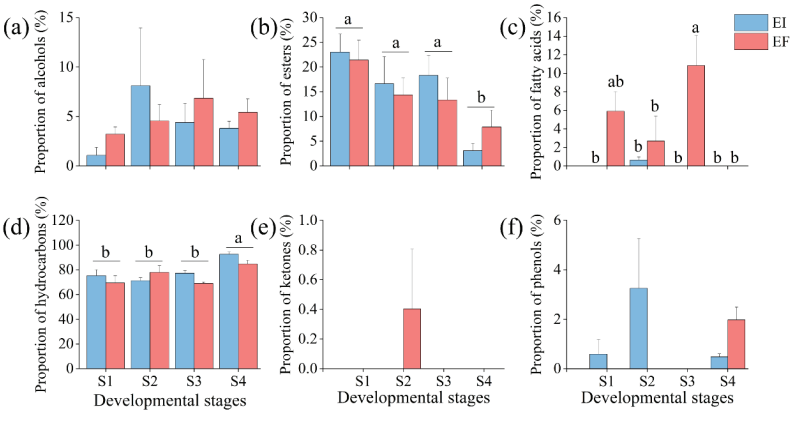

Figure 2. The proportion of alcohols (**a**), esters (**b**), fatty acids (**c**), hydrocarbons (**d**), ketones (**e**) and phenols (**f**) of leaf cuticular wax in *Achnatherum inebrians* according to the status of *Epichloë gansuensis* endophytes and in different growing periods (S1: 1 month after sowing, S2: 2 months after sowing, S3: 3 months after sowing, S4: 4 months after sowing, EI: endophyte-infected and EF: endophyte-free). Values are mean, with standard error bars (n = 3). Columns with non-matching letters indicate a significant difference at $p < 0.05$.

Table 1. Two–way ANOVA analysis showing the effects of the status of *Epichloë gansuensis* endophytes and different growing periods on the wax composition of the leaves of *Achnatherum inebrians* (E: the status of endophytes, S: developmental stages, E × S: the interaction between endophyte status and developmental stages).

		Alcohols		**Esters**		**Fatty Acids**		**Hydrocarbons**		**Ketones**		**Phenols**	
Treatment	**df**	**F**	**P**	**F**	**P**	**F**	**P**	**F**	**P**	**F**	**P**	**F**	**P**
E	1	0.12	0.734	0.137	0.716	15.812	0.001	2.158	0.161	1	0.332	1.172	0.295
S	3	0.902	0.462	6.317	0.005	3.741	0.033	8.552	0.001	1	0.418	2.007	0.154
E × S	3	0.54	0.662	0.564	0.647	4.073	0.025	1.813	0.185	1	0.418	3.372	0.045

3.2. Carbon Chain Length of Leaf Cuticular Wax

The carbon chain length distribution suggested that alcohols ranged from mannitol (C_6) to octacosanol (C_{28}), and octacosanol was the most abundant (Figure 3a, Table S1). C_{19} and C_{21} were the dominant esters (Figure 3b, Table S1). Four fatty acids were detected in this study including tetradecanoic acid (C_{14}), hexadecanoic acid (C_{16}), octadecanoic acid (C_{18}) and nordeoxycholic acid (C_{23}; Figure 3c, Table S1). The carbon chain length of hydrocarbons was the longest of all components, and ranged from 1,3,7-octatrien-5-yne (C_8) to n-heptacosane (C_{27}), and the prominent components were C_{17}, C_{21} and C_{27} (Figure 3d, Table S1). C_{10} and C_{17} were the abundant ketones—these ranged from C_6 to C_{17} (Figure 3e, Table S1). Furthermore, 2,4-di-tert-butylphenol (C_{14}) was the only phenol detected (Figure 3f, Table S1).

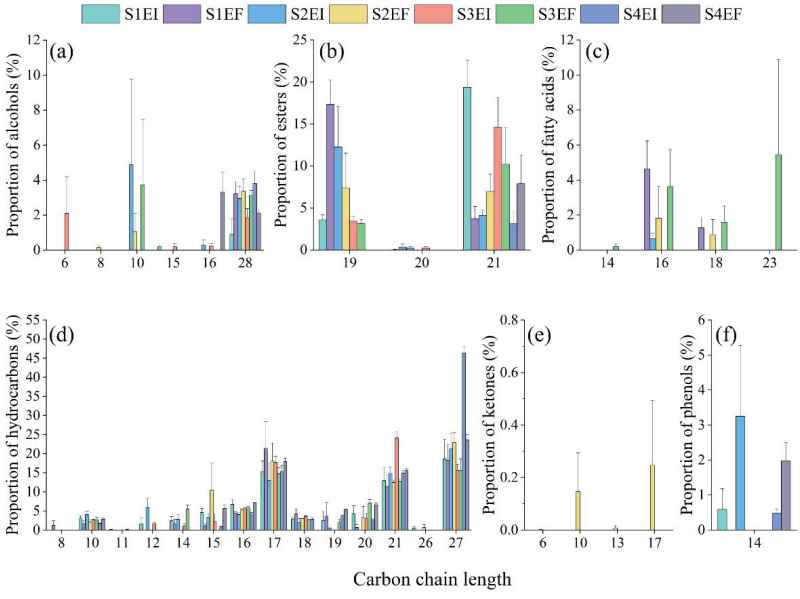

Figure 3. The carbon chain length distribution detected in the cuticular wax of *Achnatherum inebrians* according to the status of *Epichloë gansuensis* endophytes and in different growing periods: alcohols (**a**), esters (**b**), fatty acids (**c**), hydrocarbons (**d**), ketones (**e**), phenols (**f**). Values are mean, with standard error bars (n = 3, S1: 1 month after sowing, S2: 2 months after sowing, S3: 3 months after sowing, S4: 4 months after sowing, EI: endophyte-infected and EF: endophyte-free).

3.3. Differentially Expressed Gene (DEG) Analysis

Upon comparison with the EF plants, the unigenes with gene expression FC values greater than or equal to 2 and with FDR values less than 0.05 were defined as DEGs. Based on these strict criteria, we found 11 (1 upregulated and 10 downregulated) DEGs between EF plants versus EI plants.

3.4. KEGG Pathway Enrichment Analysis of the DEGs

To characterize the complex biological behavior of the transcriptome, the 11 DEGs were subjected to a KEGG pathway enrichment analysis (Figure 4). The "Fatty acid metabolism (ko01212)", "Biosynthesis of unsaturated fatty acids (ko01040)", "Fatty acid biosynthesis (ko00061)" and "Cutin, suberine and wax biosynthesis (ko00073)" categories were significantly enriched.

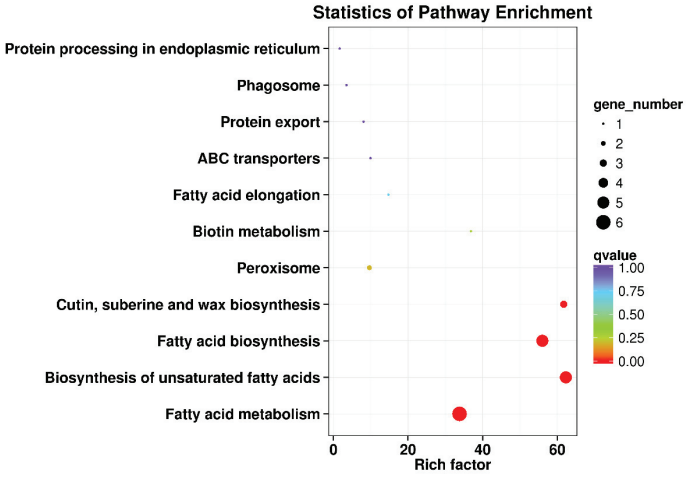

Figure 4. KEGG pathway enrichment of differentially expressed genes (DEGs) associated with *Achnatherum inebrians* according to the status of *Epichloë* endophytes and in different growing periods. The q-value ranges from 0 to 1, and a q-value closer to 0 indicates greater enrichment.

3.5. GO Functional-Enrichment Analysis of the DEGs

To clarify the functions of the detected 11 DEGs, we performed the GO annotation. A total of 22 GO categories were assigned to the 11 DEGs (Figure 5). GO term enrichment analysis was conducted to categorize the annotated sequences into three main categories: biological process, cellular component and molecular function. The most abundant subcategory under the biological process category was "metabolic process," which was followed by "single-organism process" and "cellular process". In the cellular component category, “cell” and “cell part” were the dominant groups, followed by “organelle” and “membrane”. As for the molecular function category, “catalytic activity” was the most dominant subcategory, followed by “binding” and “transporter activity”.

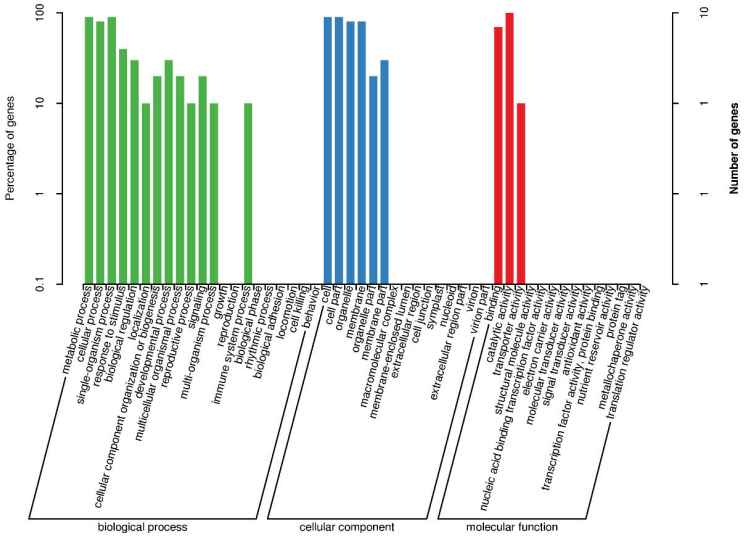

Figure 5. GO class of differentially expressed genes (DEGs) associated with *Achnatherum inebrians* according to the status of *Epichloë* endophytes and in different growing periods.

3.6. Biosynthesis Pathway of Cuticular Wax

A four-part model of cuticular wax biosynthesis pathway was proposed including fatty acid biosynthesis, fatty acid elongation, wax biosynthesis and transporters (Figure 6). Only one gene (BMK_Unigene_075090) coding for FabF protein expression level was upregulated by the *Epichloë* endophyte. The expression levels of 10 genes were downregulated by the *Epichloë* endophyte, including four genes (BMK_Unigene_074718, BMK_Unigene_074719, BMK_Unigene_099365, BMK_Unigene_103953) coding for FAB2 protein, one gene (BMK_Unigene_095289) coding for ECR protein, one gene (BMK_Unigene_094624) coding for CER1 protein, two genes (BMK_Unigene_065461, BMK_Unigene_065462) coding for FAR protein, one gene (BMK_Unigene_110117) coding for ABCB1 protein and one gene (BMK_Unigene_110042) coding for SEC61A protein.

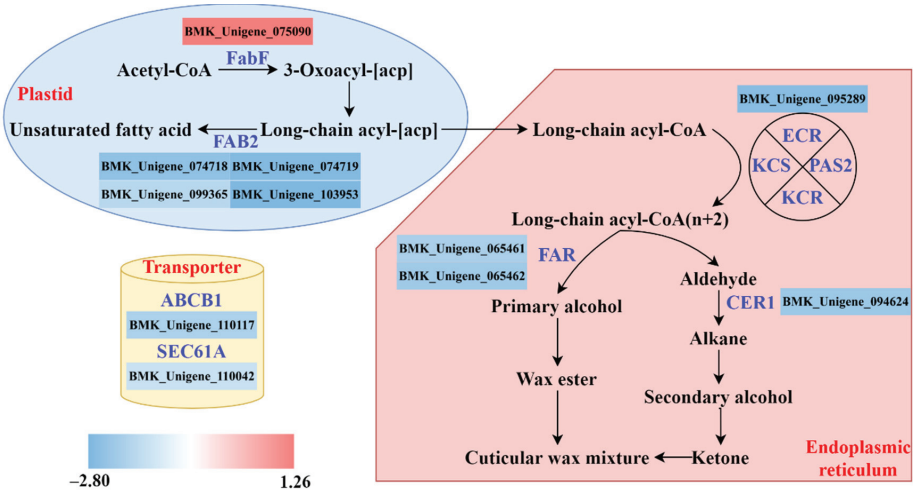

Figure 6. Proposed model for cuticular wax biosynthesis. Color bars ranging from blue to red represent downregulation and upregulation in transcript expression. Gene ID is shown.

4. Discussion

In this study, we have established a hypothesis that both the composition of leaf cuticular wax at different growing periods and the expression levels of genes related to the wax biosynthesis pathway in EI *A. inebrians* plants would change compared with that in EF plants. Our results through GC−MS indicated that hydrocarbons were the most abundant components of cuticular wax in both EI and EF plants. The proportion of esters was reduced as plants grew. By contrast, the proportion of hydrocarbons increased with plant growth. Compared with EF plants, the leaf cuticular wax of EI plants had fewer fatty acids. In agreement with our hypothesis, by transcriptome analysis, we found 11 DEGs coding for proteins involved in cuticular wax biosynthesis, including FabF, FAB2, ECR, FAR, CER1, ABCB1 and SEC61A.

Cuticular wax plays a critical role as a plant protectant against various environmental stresses [12,47]. In the present study, cuticular wax was dominated by hydrocarbons in *A. inebrians* plants. It is consistent with the results in arabidopsis [10], but different from the results in other grasses. Several studies about the leaf cuticular wax of grasses indicated that primary alcohols are the predominant components in maize [14], barley [15,48], wheat [13,49], and *Poa pratensis* [16] In addition, the composition of the cuticle changes at different growing periods [12]. In our study of *A. inebrians* plants, we found that the proportions of hydrocarbons and esters differed in reverse ways from each other. Although hydrocarbons were always the major components at different sampling times, the proportion of hydrocarbons and esters increased and decreased at 4 months after sowing,

respectively. Previous studies showed that the cuticular wax content of esters increased from 66 to 100 days in wheat [17]. Clearly, our results are inconsistent with this study, which may be a characteristic of the different species. *Epichloë* endophyte-grass associations are generally considered as mutualistic associations and almost certainly have been exposed to the selection pressures of long-term coevolution [50]. Previous studies indicated that disease symptoms caused by the powdery mildew fungus *Blumeria graminis* were reduced by the presence of endophyte *Epichloë* within *A. inebrians* plants [41]. Powdery mildew, a common fungal disease, causes serious damage to a variety of cereal crops with a broad host range including 634 species belonging to the Poaceae [51]. To cause infection, conidia of *B. graminis* produce appressoria and germ tubes that penetrate through the cuticle and walls of epidermal cells. Fatty acid biosynthesis in plants provides nutritional support to powdery mildew and promotes infection [52]. Therefore, according to the above evidence, we can infer that endophytic *Epichloë* is likely to enhance the resistance of grasses to powdery mildew by reducing the content of fatty acids. Our results showing that the proportion of fatty acids in the cuticle of EI plants was lower than in EF plants support this inference. Although advances have been made in gene characterization associated with the biosynthesis of cuticular wax in grasses, more studies are needed to obtain the understanding that is now available for arabidopsis [53]. In this study, we proposed a possible model for cuticular wax biosynthesis in mutualistic symbiosis using transcriptome analysis. The *FabF* gene encoding β-ketoacyl-ACP synthases (KAS) II enzymes has been demonstrated to regulate temperatures of fatty acid synthesis [54,55]. In the plastid, a *FabF* gene was upregulated by *Epichloë* endophyte according to our results, which may lead to the difference in the proportion of fatty acids. ECR/CER10 catalyzes the final step of VLCFA elongation required for the synthesis of all the VLCFA and plays an essential role in cell expansions [56]. We found that one DEG coding for ECR protein was downregulated in ER in the present study. In the alkane synthesis pathway, there was also a downregulated DEG coding for CER1 protein, which catalyzes the redox-dependent synthesis of alkanes from acyl-CoAs [57]. In the primary alcohol synthesis pathway, two DEGs coding for the FAR protein were downregulated. Wang et al. found that the *TaFAR5* gene, coding for FAR, contributes significantly to producing primary alcohols in wheat leaf blades [24]. Additionally, wax mixtures must be exported to the plant surface once synthesized. The mechanisms behind the transport of cuticular wax remain poorly understood. Previous studies showed that in arabidopsis, ABCG11 and CER5/ABCG12 proteins are required for wax transport [58,59]. In our study, we found one DEG coding for the ABCB1 protein was downregulated by the presence of *Epichloë* endophytes, which may play the same role as proteins of the ABCG subfamily. However, validation of the gene function still needs to be carried out in subsequent studies. In the protein export pathway, a gene belonging to the SEC61A subfamily was differentially expressed, which plays an important role in protein translocation across the ER [60].

5. Conclusions

In the present study, an objective was to investigate the contribution of the mutualistic *E. gansuensis* endophyte to leaf cuticular wax composition and the biosynthesis of *A. inebrians* plants. Our results suggested that the presence of *Epichloë* endophytes can change the composition of leaf cuticular wax at different growing periods, particularly the proportion of esters, fatty acids and hydrocarbons. In addition, we found 11 DEGs involved in wax biosynthesis, most of which were downregulated. However, validation of the gene function related to cuticular wax of endophyte-symbiotic plants is required.

Supplementary Materials: The following supporting information can be downloaded at: https://www.mdpi.com/article/10.3390/agriculture12081154/s1, Table S1: Qualitative GC-MS analysis of the leaf extract of endophyte-infected Achnatherum inebrians under different growing periods, elucidation of empirical formulas and putative identification (where possible) of the compounds (S1: 1 month after sowing, S2: 2 months after sowing, S3: 3 months after sowing, S4: 4 months after

sowing, EI: endophyte-infected and EF: endophyte-free). Data are the means of three replications. ND, not detected.

Author Contributions: Conceptualization, X.Z. and Z.N.; Methodology, M.K. and M.T.; Investigation, P.Z., M.K. and Z.Z.; Writing—Original Draft, Z.Z.; Writing—Review & Editing, M.J.C. and Z.Z.; Funding Acquisition, X.Z.; Resources, P.Z., M.K. and Z.Z.; Supervision, M.K., X.Z. and Z.N. All authors have read and agreed to the published version of the manuscript.

Funding: This work was financially supported by the National Nature Science Foundation of China (32061123004 and 31772665), the National Basic Research Program of China (2014CB138702), and the Leading Fund Project of Science and Technology Innovation of Ningxia Academy of Agricultural and Forestry Sciences (NKYG-22-03).

Institutional Review Board Statement: Not applicable.

Informed Consent Statement: Not applicable.

Data Availability Statement: All data supporting the findings of this study are available within the paper and within its Supplementary Materials published online. The RNA-seq used in this study have been deposited in the Sequence Read Achieve (SRA) of the NCBI database under the accession number PRJNA748183.

Acknowledgments: We wish to thank the editor and anonymous reviewers for their valuable comments.

Conflicts of Interest: The authors declare no competing interests.

Abbreviations

UV: ultraviolet; VLCFAs: very long-chain fatty acids; ACPs: acyl-acyl carrier proteins; CoAs: Coenzyme As; ER: endoplasmic reticulum; FAE: fatty acid elongase; KCS: β-ketoacyl-CoA synthase; KCR: β-keto acyl reductase; HCD: β-hydroxyacyl-CoA dehydratase; ECR: enoyl-CoA reductase; ABC transporters: adenosine triphosphate-binding cassette transporters; LTPs: lipid transfer proteins; FAR: fatty acyl-coenzyme A reductase; EI: endophyte-infected; EF: endophyte-free; GC−MS: gas chromatography−mass spectrometry; S1: 1 month after sowing; S2: 2 months after sowing; S3: 3 months after sowing; S4: 4 months after sowing; NIST: National Institute of Standards and Technology; NR: NCBI non-redundant protein sequences; Pfam: Protein family; KEGG: Kyoto Encyclopedia of Genes and Genomes; GO: gene Ontology; DEGs: differentially expressed genes; FC: fold change; FDR: false discovery rate; SRA: Sequence Read Achieve; ANOVA: analysis of variance; FabF: 3-oxoacyl-[acyl-carrier-protein] synthase II; FAB2: acyl-[acyl-carrier-protein] desaturase; CER1: aldehyde decarbonylase; ABCB1: ATP-binding cassette, subfamily B, member 1; SEC61A: protein transport protein SEC61 subunit alpha; KAS: β-ketoacyl-ACP synthases; ABCG: ATP-binding cassette, subfamily G.

References

1. Kosma, D.; Bourdenx, B.; Bernard, A.; Parsons, E.P.; Lü, S.; Joubès, J.; Jenks, M.A. The impact of water deficiency on leaf cuticle lipids of Arabidopsis. *Plant Physiol.* **2009**, *151*, 1918–1929. [CrossRef]
2. Krauss, P.; Markstadter, C.; Riederer, M. Attenuation of UV radiation by plant cuticles from woody species. *Plant Cell Environ.* **1997**, *20*, 1079–1085. [CrossRef]
3. Pfündel, E.E.; Agati, G.; Cerovic, Z.G. Optical properties of plant surfaces. In *Annual Plant Reviews Volume 23: Biology of the Plant Cuticle*; Riederer, M., Müller, C., Eds.; Blackwell: Oxford, UK, 2006; pp. 216–249.
4. Wink, M. Plant breeding: Importance of plant secondary metabolites for protection against pathogens and herbivores. *Theor. Appl. Genet.* **1988**, *75*, 225–233. [CrossRef]
5. Javelle, M.; Vernoud, V.; Rogowsky, P.M.; Ingram, G.C. Epidermis: The formation and functions of a fundamental plant tissue. *New Phytol.* **2011**, *189*, 17–39. [CrossRef]
6. Lemieux, B. Molecular genetics of epicuticular wax biosynthesis. *Trends Plant Sci.* **1996**, *1*, 312–318. [CrossRef]
7. Li-Beisson, Y.; Shorrosh, B.; Beisson, F.; Andersson, M.X.; Arondel, V.; Bates, P.D.; Baud, S.; Bird, D.; DeBono, A.; Durrett, T.P.; et al. *Acyl-Lipid Metabolism*; The American Society of Plant Biologists: Rockville, MD, USA, 2013; Volume 11.
8. Samuels, L.; Kunst, L.; Jetter, R. Sealing plant surfaces: Cuticular wax formation by epidermal cells. *Annu. Rev. Plant Biol.* **2008**, *59*, 683–707. [CrossRef]

9. Kunst, L.; Samuels, A.L. Biosynthesis and secretion of plant cuticular wax. *Prog. Lipid Res.* **2003**, *42*, 51–80. [CrossRef]
10. Bernard, A.; Joubès, J. Arabidopsis cuticular waxes: Advances in synthesis, export and regulation. *Prog. Lipid Res.* **2013**, *52*, 110–129. [CrossRef]
11. Kunst, L.; Samuels, L. Plant cuticles shine: Advances in wax biosynthesis and export. *Curr. Opin. Plant Biol.* **2009**, *12*, 721–727. [CrossRef]
12. Post-Beittenmiller, D. Biochemistry and molecular biology of wax production in plants. *Annu. Rev. Plant Physiol. Plant Mol. Biol.* **1996**, *47*, 405–430. [CrossRef]
13. Koch, K.; Barthlott, W.; Koch, S.; Hommes, A.; Wandelt, K.; Mamdouh, W.; De-Feyter, S.; Broekmann, P. Structural analysis of wheat wax (*Triticum aestivum*, *c.v.* 'Naturastar' L.): From the molecular level to three dimensional crystals. *Planta* **2006**, *223*, 258–270. [CrossRef] [PubMed]
14. Javelle, M.; Vernoud, V.; Depège-Fargeix, N.; Arnould, C.; Oursel, D.; Domergue, F.; Sarda, X.; Rogowsky, P.M. Overexpression of the epidermis-specific homeodomain-leucine zipper IV transcription factor OUTER CELL LAYER1 in maize identifies target genes involved in lipid metabolism and cuticle biosynthesis. *Plant Physiol.* **2010**, *154*, 273–286. [CrossRef] [PubMed]
15. Avato, P.; Mikkelsen, J.D.; Wettstein-knowles, P.V. Synthesis of epicuticular primary alcohols and intracellular fatty acids by tissue slices from *cer-j*^{59} barley leaves. *Carlsberg Res. Commun.* **1982**, *47*, 377–390. [CrossRef]
16. Yao, L.H.; Ni, Y.; Guo, N.; He, Y.J.; Gao, J.H.; Guo, Y.J. Leaf cuticular waxes in *Poa pratensis* and their responses to altitudes. *Acta Prataculturae Sin.* **2018**, *27*, 97–105.
17. Tulloch, A.P. Composition of leaf surface waxes of Triticum species: Variation with age and tissue. *Phytochemistry* **1973**, *12*, 2225–2232. [CrossRef]
18. Avato, P.; Bianchi, G.; Pogna, N. Chemosystematics of surface lipids from maize and some related species. *Phytochemistry* **1990**, *29*, 1571–1576. [CrossRef]
19. Gülz, P.-G.; Prasad, R.B.N.; Müller, E. Surface structure and chemical composition of epicuticular waxes during leaf development of *Tilia Tomentosa* moench. *Z. Nat. C* **1991**, *46*, 743–749. [CrossRef]
20. Wang, Y.; Wang, J.H.; Chai, G.Q.; Li, C.L.; Hu, Y.G.; Chen, X.H.; Wang, Z.H. Developmental changes in composition and morphology of cuticular waxes on leaves and spikes of glossy and glaucous wheat (*Triticum aestivum* L.). *PLoS ONE* **2015**, *10*, e0141239. [CrossRef]
21. Busta, L.; Hegebarth, D.; Kroc, E.; Jetter, R. Changes in cuticular wax coverage and composition on developing Arabidopsis leaves are influenced by wax biosynthesis gene expression levels and trichome density. *Planta* **2017**, *245*, 297–311. [CrossRef] [PubMed]
22. Wang, M.L.; Wang, Y.; Wu, H.Q.; Xu, J.; Li, T.T.; Hegebarth, D.; Jetter, R.; Chen, L.T.; Wang, Z.H. Three *TaFAR* genes function in the biosynthesis of primary alcohols and the response to abiotic stresses in *Triticum aestivum*. *Sci. Rep.* **2016**, *6*, 25008. [CrossRef]
23. Wang, Y.; Wang, M.L.; Sun, Y.L.; Hegebarth, D.; Li, T.T.; Jetter, R.; Wang, Z.H. Molecular characterization of *TaFAR1* involved in primary alcohol biosynthesis of cuticular wax in hexaploid wheat. *Plant Cell Physiol.* **2015**, *56*, 1944–1961. [CrossRef] [PubMed]
24. Wang, Y.; Wang, M.L.; Sun, Y.L.; Wang, Y.T.; Li, T.T.; Chai, G.Q.; Jiang, W.H.; Shan, L.W.; Li, C.L.; Xiao, E.S.; et al. FAR5, a fatty acyl-coenzyme A reductase, is involved in primary alcohol biosynthesis of the leaf blade cuticular wax in wheat (*Triticum aestivum* L.). *J. Exp. Bot.* **2015**, *66*, 1165–1178. [CrossRef] [PubMed]
25. Neuffer, M.G.; Coe, E.H.; Wessler, S.R. Mutants of maize. *Q. Rev. Biol.* **1998**, *73*, 207.
26. Islam, M.A.; Du, H.; Ning, J.; Ye, H.; Xiong, L. Characterization of *Glossy1*-homologous genes in rice involved in leaf wax accumulation and drought resistance. *Plant Mol. Biol.* **2009**, *70*, 443–456. [CrossRef]
27. Qin, B.-X.; Tang, D.; Huang, J.; Li, M.; Wu, X.-R.; Lu, L.-L.; Wang, K.-J.; Yu, H.-X.; Chen, J.-M.; Gu, M.-H.; et al. Rice *OsGL1-1* Is Involved in Leaf Cuticular Wax and Cuticle Membrane. *Mol. Plant* **2011**, *4*, 985–995. [CrossRef]
28. Zhou, X.Y.; Li, L.Z.; Xiang, J.H.; Gao, G.F.; Xu, F.X.; Liu, A.L.; Zhang, X.W.; Peng, Y.; Chen, X.B.; Wan, X.Y. OsGL1-3 is involved in cuticular wax biosynthesis and tolerance to water deficit in rice. *PLoS ONE* **2015**, *10*, e116676. [CrossRef]
29. Siegel, M.R.; Latch, G.C.M.; Johnson, M.C. Fungal endophytes of grasses. *Annu. Rev. Phytopathol.* **1987**, *25*, 293–315. [CrossRef]
30. Leuchtmann, A.; Bacon, C.W.; Schardl, C.L.; White, J.J.F.; Tadych, M. Nomenclatural realignment of *Neotyphodium* species with genus *Epichloë*. *Mycologia* **2014**, *106*, 202–215. [CrossRef]
31. Christensen, M.; Voisey, C. The biology of the endophyte/grass partnership. *NZGA Res. Pract. Ser.* **2007**, *13*, 123–133. [CrossRef]
32. Bacon, C.W.; Porter, J.K.; Robbins, J.D.; Luttrell, E.S. *Epichloë typhina* from toxic tall fescue grasses. *Appl. Environ. Microbiol.* **1977**, *34*, 576–581. [CrossRef]
33. Schardl, C.L.; Grossman, R.B.; Nagabhyru, P.; Faulkner, J.R.; Mallik, U.P. Loline alkaloids: Currencies of mutualism. *Phytochem.* **2007**, *68*, 980–996. [CrossRef] [PubMed]
34. Schardl, C.L.; Leuchtmann, A.; Spiering, M.J. Symbioses of grasses with seed borne fungal endophytes. *Annu. Rev. Plant Biol.* **2004**, *55*, 315–340. [CrossRef] [PubMed]
35. Nan, Z.B.; Li, C.J. Neotyphodium in Native Grasses in China and Observations on Endophyte/Host Interactions. In Proceedings of the 4th International Neotyphodium/Grass Interactions Symposium, Soest, Germany, 27–29 September 2000; pp. 41–50.
36. Chen, L.; Li, X.Z.; Li, C.J.; Swoboda, G.A.; Young, C.A.; Sugawara, K.; Leuchtmann, A.; Schardl, C.L. Two distinct *Epichloë* species symbiotic with *Achnatherum inebrians*, drunken horse grass. *Mycologia* **2015**, *107*, 863–873. [CrossRef]
37. Li, C.J.; Nan, Z.B.; Paul, V.H.; Dapprich, P.D.; Liu, Y. A new *Neotyphodium* species symbiotic with drunken horse grass (*Achnatherum inebrians*) in China. *Mycotaxon* **2004**, *90*, 141–147.

38. Kou, M.Z.; Bastías, D.; Christensen, M.; Zhong, R.; Nan, Z.B.; Zhang, X.X. The plant salicylic acid signalling pathway regulates the infection of a biotrophic pathogen in grasses associated with an *Epichloë* endophyte. *J. Fungi* **2021**, *7*, 633. [CrossRef] [PubMed]
39. Wang, J.; Tian, P.; Christensen, M.J.; Zhang, X.; Li, C.; Nan, Z. Effect of *Epichloë gansuensis* endophyte on the activity of enzymes of nitrogen metabolism, nitrogen use efficiency and photosynthetic ability of *Achnatherum inebrians* under various NaCl concentrations. *Plant Soil* **2018**, *435*, 57–68. [CrossRef]
40. Xia, C.; Christensen, M.J.; Zhang, X.X.; Nan, Z.B. Effect of *Epichloë* gansuensis endophyte and transgenerational effects on the water use efficiency, nutrient and biomass accumulation of *Achnatherum inebrians* under soil water deficit. *Plant Soil* **2018**, *424*, 555–571. [CrossRef]
41. Xia, C.; Li, N.N.; Zhang, X.X.; Feng, Y.; Christensen, M.J.; Nan, Z.B. An *Epichloë* endophyte improves photosynthetic ability and dry matter production of its host *Achnatherum inebrians* infected by *Blumeria graminis* under various soil water conditions. *Fungal Ecol.* **2016**, *22*, 26–34. [CrossRef]
42. Zhang, X.; Li, C.; Nan, Z. Effects of cadmium stress on growth and anti-oxidative systems in *Achnatherum inebrians* symbiotic with *Neotyphodium gansuense*. *J. Hazard. Mater.* **2010**, *175*, 703–709. [CrossRef]
43. Zhang, X.X.; Li, C.; Nan, Z.B.; Matthew, C. *Neotyphodium* endophyte increases *Achnatherum inebrians* (drunken horse grass) resistance to herbivores and seed predators. *Weed Res.* **2012**, *52*, 70–78. [CrossRef]
44. Chen, N.; He, R.L.; Chai, Q.; Li, C.J.; Nan, Z.B. Transcriptomic analyses giving insights into molecular regulation mechanisms involved in cold tolerance by *Epichloë* endophyte in seed germination of *Achnatherum inebrians*. *Plant Growth Regul.* **2016**, *80*, 367–375. [CrossRef]
45. Li, C.J.; Nan, Z.B.; Liu, Y.; Paul, V.H.; Peter, D. Methodology of Endophyte Detection of Drunken Horse Grass (*Achnatherum Inebrians*). In Proceedings of the Annual Meeting of Chinese Society for Plant Pathology, Guangzhou, China, 21–27 July 2008; pp. 129–132.
46. Linstrom, P.J.; Mallard, W.G. *NIST Chemistry WebBook, NIST Standard Reference Database Number 69*; National Institute of Standards and Technology: Gaithersburg, MD, USA, 2001. Available online: https://webbook.nist.gov/chemistry/ (accessed on 24 May 2022).
47. Lewandowska, M.; Keyl, A.; Feussner, I. Wax biosynthesis in response to danger: Its regulation upon abiotic and biotic stress. *New Phytol.* **2020**, *227*, 698–713. [CrossRef] [PubMed]
48. Wang, C.; Wang, J.H.; Wang, Y.; Wang, Z.h.; Quan, L. Analysis of cuticular wax components and crystal structures of barley. *J. Triticeae Crops* **2018**, *38*, 693–700.
49. Zhang, Y.Y.; Li, T.T.; Sun, Y.L.; Wang, Y.T.; Wang, M.L.; Wang, Y.; Shi, X.; Quan, L.; Li, C.L.; Wang, Z.H. Analysis on composition and content of leaf cuticular waxes of wheat (*Triticum Aestivum*) detected by GC-MS. *J. Triticeae Crops* **2014**, *34*, 963–968.
50. Saikkonen, K.; Wäli, P.; Helander, M.; Faeth, S.H. Evolution of endophyte-plant symbioses. *Trends Plant Sci.* **2004**, *9*, 275–280. [CrossRef]
51. Inuma, T.; Khodaparast, S.A.; Takamatsu, S. Multilocus phylogenetic analyses within *Blumeria graminis*, a powdery mildew fungus of cereals. *Mol. Phylogenetics Evol.* **2007**, *44*, 741–751. [CrossRef]
52. Jiang, Y.; Wang, W.; Xie, Q.; Liu, N.; Liu, L.; Wang, D.; Zhang, X.; Yang, C.; Chen, X.; Tang, D.; et al. Plants transfer lipids to sustain colonization by mutualistic mycorrhizal and parasitic fungi. *Science* **2017**, *356*, 1172–1175. [CrossRef]
53. Lee, S.B.; Suh, M.C. Advances in the understanding of cuticular waxes in *Arabidopsis thaliana* and crop species. *Plant Cell Rep.* **2015**, *34*, 557–572. [CrossRef]
54. Edwards, P.; Nelsen, S.J.; Metz, J.G.; Dehesh, K. Cloning of the *fabF* gene in an expression vector and in vitro characterization of recombinant *fabF* and *fabB* encoded enzymes from *Escherichia coli*. *FEBS Lett.* **1997**, *402*, 62–66. [CrossRef]
55. Magnuson, K.; Carey, M.R.; Cronan, J.E. The putative *fabJ* gene of Escherichia coli fatty acid synthesis is the *fabF* gene. *J. Bacteriol.* **1995**, *177*, 3593–3595. [CrossRef]
56. Zheng, H.Q.; Rowland, O.; Kunst, L. Disruptions of the Arabidopsis Enoyl-CoA reductase gene reveal an essential role for very-long-chain fatty acid synthesis in cell expansion during plant morphogenesis. *Plant Cell* **2005**, *17*, 1467–1481. [CrossRef]
57. Bernard, A.; Domergue, F.; Pascal, S.; Jetter, R.; Renne, C.; Faure, J.-D.; Haslam, R.P.; Napier, J.A.; Lessire, R.; Joubès, J. Reconstitution of plant alkane biosynthesis in yeast demonstrates that *Arabidopsis* ECERIFERUM1 and ECERIFERUM3 are core components of a very-long-chain alkane synthesis complex. *Plant Cell* **2012**, *24*, 3106–3118. [CrossRef] [PubMed]
58. Bird, D.; Beisson, F.; Brigham, A.; Shin, J.; Greer, S.; Jetter, R.; Kunst, L.; Wu, X.M.; Yephremov, A.; Samuels, L. Characterization of Arabidopsis ABCG11/WBC11, an ATP binding cassette (ABC) transporter that is required for cuticular lipid secretion. *Plant J.* **2007**, *52*, 485–498. [CrossRef] [PubMed]
59. Pighin, J.A.; Zheng, H.Q.; Balakshin, L.J.; Goodman, I.P.; Western, T.L.; Jetter, R.; Kunst, L.; Samuels, A.L. Plant cuticular lipid export requires an ABC transporter. *Science* **2004**, *306*, 702–704. [CrossRef] [PubMed]
60. Rapoport, T.A. Protein translocation across the eukaryotic endoplasmic reticulum and bacterial plasma membranes. *Nature* **2007**, *450*, 663–669. [CrossRef] [PubMed]

agriculture

MDPI

Article

Effects of Rust on Plant Growth and Stoichiometry of *Leymus chinensis* under Different Grazing Intensities in Hulunber Grassland

Yawen Zhang [1,2], Zhibiao Nan [1,*], Michael John Christensen [3], Xiaoping Xin [4] and Nan Zhang [2]

[1] State Key Laboratory of Grassland Agro-Ecosystems, Key Laboratory of Grassland Livestock Industry Innovation, Ministry of Agriculture and Rural Affairs, College of Pastoral Agricultural Science and Technology, Lanzhou University, Lanzhou 730020, China; zhangyawen@lzu.edu.cn
[2] School of Pharmacy, Lanzhou University, Lanzhou 730000, China; zhangnan2019@lzu.edu.cn
[3] Retired from AgResearch, Grasslands Research Centre, Private Bag 11-008, Palmerston North 4442, New Zealand; mchristensenpn4410@gmail.com
[4] National Hulunber Grassland Ecosystem Observation and Research Station, Institute of Agricultural Resources and Regional Planning, Chinese Academy of Agricultural Science, Beijing 100081, China; xinxiaoping@caas.cn
* Correspondence: zhibiao@lzu.edu.cn; Tel.: +86-931-8661047; Fax: +86-931-8910979

Abstract: Grazing is the main utilization of native grassland, and forage fungal disease is one of the limiting factors of grassland productivity. The present research in the Hulunber meadow steppe grassland was conducted to investigate the responses of the dominant plant *Leymus chinensis* (Trin.) to beef cattle grazing, rust, and their interaction influence. Six grazing intensity treatments with three replicates were established. The response of *L. chinensis* to grazing and rust was systematically studied for two consecutive years. The main findings were that grazing and rust had significant effects ($p < 0.05$) on the growth and nutrient elements content of *L. chinensis*. Compared with the 0 cattle ha^{-1} treatment, the dry matter of *L. chinensis* in the 0.42, 0.63, and 1.67 cattle ha^{-1} treatments decreased by 42.2%, 90.5%, and 339.5%, respectively. Compared with non-infected plants, dry matter of rust-infected *L. chinensis* plants decreased by 45.6%. The N:C and P:C ratios of rust-infected plants were lower than in non-infected plants, and positively correlated with their relative growth rates. Therefore, we concluded that the growth rate hypothesis still applied in *L. chinensis* under the interactive effects of grazing and disease. Additionally, grazing can alleviate the loss of dry matter caused by disease.

Keywords: dry matter; ecological stoichiometry; grazing intensity; rust; *Leymus chinensis*; Hulunber meadow steppe

Citation: Zhang, Y.; Nan, Z.; Christensen, M.J.; Xin, X.; Zhang, N. Effects of Rust on Plant Growth and Stoichiometry of *Leymus chinensis* under Different Grazing Intensities in Hulunber Grassland. *Agriculture* **2022**, *12*, 961. https://doi.org/10.3390/agriculture12070961

Academic Editor: Alessandro Vitale

Received: 29 April 2022
Accepted: 28 June 2022
Published: 5 July 2022

1. Introduction

Grasslands, about 390 million ha, cover 41% of the total land area in China [1]. The Hulunber meadow steppe, located in northeastern China, is one of the largest areas of natural temperate sub-humid meadow steppe grassland in the world, covering an area about 9.97×10^6 km^2 [2]. It plays a critical role in regional ecological balance and is also an important ecological barrier in north China [3,4]. The most dominant plant species of this grassland is *Leymus chinensis* (Trin.) [5]. *L. chinensis* is a perennial rhizomatous grass with rich nutritional content, high yield, and palatability, and lays the foundation for highly productive livestock husbandry in the Hulunber grassland [4,6].

Large herbivores are key drivers of plant communities and ecosystem functioning in many terrestrial ecosystems as they influence nutrient cycling and availability in soil and plants [7–11]. Livestock grazing is the most prevalent use of grasslands. Grazing herbivores change the vegetation cover and cause soil compaction as a result of ingestion and trampling [4,12–14]. Generally, the response of grassland ecosystems to livestock

disturbance is mediated by various factors, such as local environmental conditions, livestock species, grazing intensity, and plant diseases [9,15,16].

Fungal diseases are one of the main limiting factors affecting grassland productivity, leading to degradation, and can strongly contribute to the rate and magnitude of ecosystem function in grassland [17–19]. In addition, disease also reduces the palatability of grass for livestock [20]. Infection of grasses by some fungi can result in the accumulation of fungal toxins and secondary metabolites that are harmful to grazing animals and even humans [21–23], further restricting the productivity of animal husbandry [21]. It is worth noting that there have been some clues that conservative grazing may be one of the effective ways to control fungal disease in this grassland [24]. However, the influence of grazing on grassland diseases is not a consistent factor with plant diseases. Grazing may reduce the incidence by removing the infected tissues and pathogens on the foliage through ingestion [22], or, in contrast, promote pathogen invasion by forming wounds on plants through ingestion or trampling [25–28]. The transmission and infection of pathogens is also significantly affected by plant species diversity, plant abundance, aboveground biomass, and the functional composition of grassland ecosystems [29–33]. All the above-mentioned factors are directly or indirectly affected by grazing. Therefore, grazing should be regarded as one of the potential available methods to limit the damage caused by plant pathogens in grasslands and forage-based grazing systems.

Ecological stoichiometry describes the balance of energy and nutrients between organisms and their environment and can improve our understanding of impacts of energy and nutrient fluxes, and also balances between plants, microbes, soil, and individual organism growth [34–37]. There are two different mechanisms to explain the effect of grazing on grassland nutrient cycling [9,34,38]. One is that grazing may stimulate soil microbial activity and accelerate nutrient cycling rates by introducing fresh leaves, plant litter, and livestock waste into the soil [39,40]. The other viewpoint suggests that grazing may reduce nutrient cycling rates by increasing plant species with low palatability within the population [9,38,41,42]. Ecological stoichiometry focuses on the chemical elements necessary for all life and is easily generalizable across systems and taxa, which is extremely useful in research on multi-trophic interactions such as infectious diseases on plants [43–45]. The classical paradigm, the growth rate hypothesis, based on the relationships between the N:P in organisms and their growth rate capacity and scaling ecological consequences, has been proved in many systems [35,43]. It allows us to make predictions about the roles of specific elements in diseases, and about the linkage between infectious diseases and nutrient cycles, by uniting them with a common, multimetric currency [46].

Both grazing and disease have significant effects on the productivity of plants [2,47]. However, the mechanism of ecological stoichiometry in response to grassland diseases is rarely reported. How the interaction between grazing and disease affects the stoichiometry of the individual plant is still uncertain. Therefore, a two-year study was carried out in the Hulunber grasslands trial site. *L. chinensis*, the dominant plant species in the local area, was utilized as the experimental species. Through analyzing the growth indexes, disease incidence, and elements content in individual plants, we aimed to explore the ecological stoichiometry response strategies of *L. chinensis* to grazing and disease, as well as their interaction effects. Hopefully, our results will enhance understanding about how to use grazing as one of the methods to control diseases in natural grasslands.

2. Materials and Methods

2.1. Study Site

This study site is located at the Hulunber Grassland Ecosystem Station of the Chinese Academy of Agricultural Sciences, which is in the northeast Inner Mongolia grassland, a central part of the Hulunber meadow steppe, China (N 49°19′21″~49°20′10″, E 119°56′31″~119°57′51″; elevation varies from 666 m~680 m) [4]. The climate of this location is temperate semiarid continental, with an annual average of 110 frost-free days. The mean annual temperature range is −5 °C~−2 °C and with an annual precipitation

range of 350 mm~400 mm, with more than 80% falling from July to August [5]. The precipitation was about 280 mm~320 mm during the growing season in 2015 and 2016. The type of the soil is kastanozems according to FAO/UNESCO System of Soil Classification. The vegetation is characterized as typical meadow steppe that is dominated by *L. chinensis*, *Stipa baicalensis* (Roshev.), and *Carex duriuscula* (C.A. Mey), other species are *Galium verum* (L.), *Bupleurum scorzonerifolium* (Willd.) and *Filifolium sibiricum* (L.). The grassland usually regrows in early May and starts to wither in late September. It is suitable for cattle grazing only from June to October, limited by the short growing season.

2.2. Experimental Design

The grassland area was divided into 18 paddocks, each of 5 ha (300 m × 167 m). Six levels of cattle grazing intensity were set as follows: 0.00, 0.42, 0.63, 0.83, 1.25, and 1.67 cattle ha^{-1}, corresponding to 0, 2, 3, 4, 6, and 8 adult cattle with 500 kg of live body weight per plot, which were designated G0, G1, G2, G3, G4, and G5, respectively, in a randomized complete block design with three replicates (Appendix A Figure A1). The grazing cattle were kept in plots for 24 h a day over the grazing period and supplied with water from an outside source. This study site has been used since 2009 as summer pastures, with a grazing period from June to September each year.

2.3. Plant Sample Collection and Measurements

During the growing season, tillers of *L. chinensis* were obtained at the end of June, July, and August in 2015 and 2016. One hundred tillers were collected in each plot from rust-infected and also non-infected plants (100 tillers per plot × 6 grazing intensities × 3 replicates). Tillers that had 30–50% of the leaf area covered by uredinia and telia were collected as rust-infected samples, while tillers that were without any rust pustules were collected as the non-infected samples [48]. All of the collected tillers were cut near to the soil surface and oven-dried at 65 °C to a constant weight (at least 48 h) to obtain dry matter (DM) content. Then the weighed samples were milled to a fine powder with a particle size <0.2 mm for plant organic carbon (C), plant-total-nitrogen (N), and total phosphorus (P) analysis [48,49]. The percentage of C was analyzed by the Walkley–Black modified acid-dichromate $FeSO_4$ titration method as described by Nelson and Sommers [50]. Briefly, 0.015 g of milled plant tissue was digested with 5 mL of 1 N $K_2Cr_2O_7$ and 10 mL of concentrated sulfuric acid at 185 °C for 5 min, followed by titration of the digests with standardized $FeSO_4$. N and P were determined by a FIAstar 5000 Analyzer (Foss Tecator, Höganäs, Sweden) [9].

We surveyed *L. chinensis* monthly for the presence of rust pathogens in five assigned quadrats (1 m × 1 m) in each of the 18 (5 ha) grazing plots from June to August in 2015 and 2016. We conducted the survey using an 'X' preselected pattern, and the separation distance for adjacent quadrats was at least 100 m. The quadrats were located away from the plot fences to avoid marginal effects. In each survey, we visually examined the aboveground tissues (stems, leaves, inflorescences) of all the *L. chinensis* plants present per quadrat. We also collected 5~10 samples of rust-infected *L. chinensis* to establish the identity of the rust species in the laboratory using both the morphological methods via light microscopy (Olympus CX31, Japan) and molecular methods.

Relative growth rate (μ) was calculated as [34]:

$$\mu = \mathrm{Ln}\,(M_1/M_0)/t \quad (1)$$

where M_1 and M_0 represented the DM of *L. chinensis* at the beginning and at the end of the month, respectively, t for 30 days.

The response ratio was calculated as the ratio of non-infected tillers to rust-infected tillers. The smaller the ratio, the smaller the impact of the rust [51].

2.4. Statistical Analysis

The incidence of rust on *L. chinensis* was calculated as the percentage of rust-infected tillers in each quadrat. The data analyses were performed using the GenStat version 17.1

(VSN International Ltd., Oxford, UK) based on the 2-year (2015 and 2016) average. One way analysis of variance (ANOVA) with Tukey's tests was used to evaluate the effects of grazing intensity on dry matter, relative growth rate, C, N, and P content (%), and C:N:P stoichiometry of non-infected and rust-infected *L. chinensis*, respectively. Generalized linear mixed models were used to test the significance of variation in dry matter, relative growth rate, C, N, and P content (%), and C:N:P stoichiometry, with sample date and grazing intensity as main effects. Individual comparisons of dry matter, C, N, and P content (%), C:N:P stoichiometry and relative growth rate between non-infected and rust-infected tillers were performed using independent sample *t*-tests at $p < 0.05$.

Prior to the ANOVA, data were checked for normality and homogeneity, and were transformed whenever necessary to meet the assumption. Means are reported with standard errors. To assess the relationship between the relative growth rates of non-infected and rust-infected plants with the C:N:P stoichiometry, we constructed a series of generalized linear models. The redundancy analysis (RDA) was used to further assess the effects of grazing and rust on the DM and C, N, and P content (%). To quantify the relative importance of the grazing and rust on the DM of *L. chinensis*, we constructed the structural equation model (SEM) based on the known relationship among grazing intensity and the C, N, and P content (%) of *L. chinensis*. The RDA and the structural equation were carried out with the Canoco console 4.5 [52] and RStudio, respectively.

3. Results

3.1. Effects of Grazing Intensity on L. chinensis Rust Incidence and Growth

The rust on *L. chinensis* was predominantly caused by *Puccinia elymi* (Westend.), a species that was first reported in Jilin province of China [53]. The specific identification process and pathogenicity testing was as used in our previous studies [16]. The field survey results indicated that the rust incidence tended to significantly ($p < 0.05$) decrease with increasing grazing intensity from June to August. As compared with the G0 treatment, the incidence under the G5 treatment decreased by 89%. The rust incidence was the highest under the G0 and G1 treatments in July. Under the rest of the grazing intensities, incidence on *L. chinensis* was the highest in August (Figure 1).

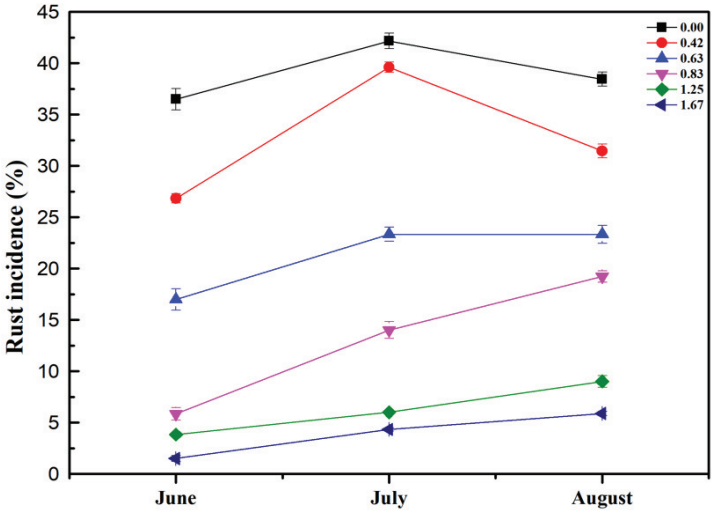

Figure 1. Rust (*Puccinia elymi*) incidence of *Leymus chinensis* under different grazing intensities from June to August based on the 2-year (2015 and 2016) average. Grazing intensities (0, 0.42, 0.63, 0.83, 1.25, and 1.67 cattle ha^{-1}) are indicated by different colors. The presented data are the mean of three replicates and the bars indicate standard errors.

During the growth season, the DM of *L. chinensis* declined significantly ($p < 0.05$) in response to increasing grazing intensities in the meadow steppe. As compared with the G0 treatment, the DM decreased by 42.2%, 90.5%, and 339.5% in the G1, G3, and G5 treatments, respectively. Compared with non-infected plants, there was a sharp decrease by 30.2% in the DM of rust-infected plants (Figure 2a) from June to August. The relative growth rate of *L. chinensis* was the highest in the G0 treatment. With the grazed treatments it increased from the G1 to the G3 treatment and decreased from the G3 to the G5 treatment in June. Over time, relative growth rate increased from the G0 to the G3 treatment in June and then declined from the G3 to the G5 treatment in July. However, the relative growth rate was negative due to the cessation of *L. chinensis* growth. The relative growth rate of rust-infected plants decreased by 57.1% compared with non-infected plants (Figure 2b).

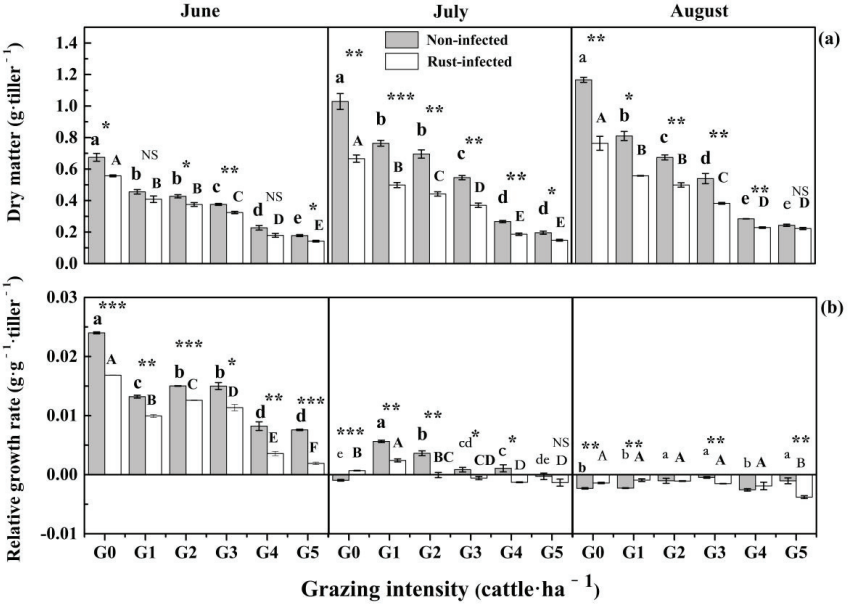

Figure 2. Influence of grazing intensity on the dry matter (**a**) and relative growth rate (**b**) of non-infected and rust-infected *Leymus chinensis* from June to August based on the 2-year (2015 and 2016) average (error bars denote standard errors). Different lower-case and upper-case indicate significant differences among grazing intensities, respectively. The asterisk (*) indicates significant differences between non-infected and rust-infected plants (***, $p < 0.001$; **, $p < 0.01$; *, $p < 0.05$; NS, $p > 0.05$).

3.2. Effects of Grazing Intensity on Stoichiometry of Non-Infected and Rust-Infected L. chinensis

For the C content, there were no significant differences ($p > 0.05$) between the G0 treatment and the G4 and G5 treatments. There was also no significant difference ($p > 0.05$) between non-infected and rust-infected plants except in the G1, G2, and G5 treatments (Figure 3a). The N content increased with the increase of grazing intensity, except for the ungrazed treatment. There was a significant ($p < 0.05$) decrease of 8.3% in the N content of rust-infected plants in July and August (Figure 3b). The P content was the lowest under the G3 treatment, and there was no significant difference ($p > 0.05$) compared with the G5 treatment. The P content of rust-infected plants decreased by 7.7% from June to August (Figure 3c).

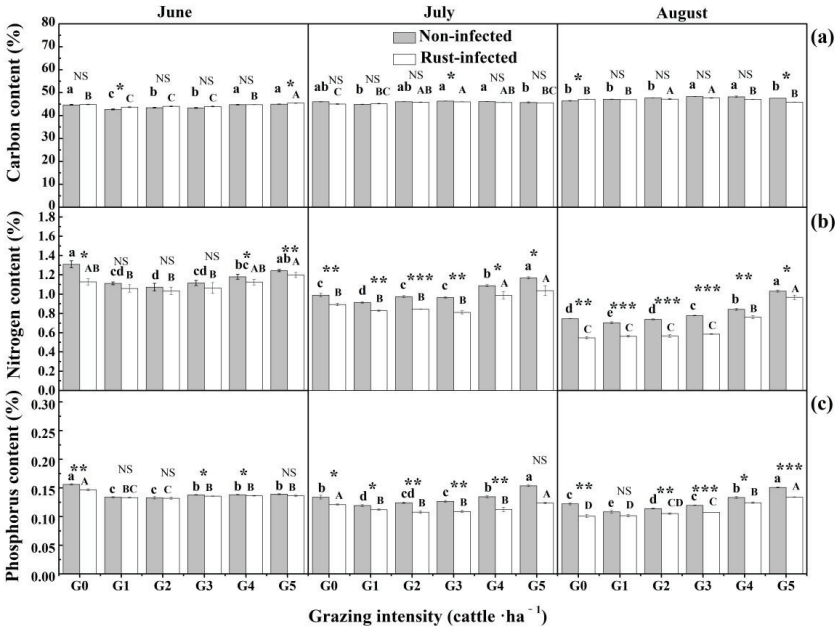

Figure 3. Influence of grazing intensity on the carbon (**a**), nitrogen (**b**) and phosphorus contents (%) (**c**) of non-infected and rust-infected *Leymus chinensis* from June to August based on the 2-year (2015 and 2016) average (error bars denote standard errors). Different lower-case and upper-case indicate significant differences among grazing intensities. The asterisk (*) indicates significant differences between non-infected and rust-infected plants (***, $p < 0.001$; **, $p < 0.01$; *, $p < 0.05$; NS, $p > 0.05$).

The C:N ratios of *L. chinensis* increased from G0 to G2, then they decreased from G3 to G5 from June to August. From G3 to G5, reduced C:N ratios were due primarily to increases in N content (Figure 4a). The C:P ratios (Figure 4b) showed similar patterns as the C:N ratios. The C:N and C:P ratios were both the highest in July. However, the N:P ratios did not show specific rules (Figure 4c). In contrast to the C, N, and P content (%) of non-infected and rust-infected plants, the C:N and C:P ratios significantly ($p < 0.05$) increased by 17.3% and 10.2%, respectively, from June to August (Figure 4a, b). There was no significant difference ($p > 0.05$) in the N:P ratios between non-infected and rust-infected plants (Figure 4c).

3.3. The Relationship between Relative Growth Rate and C:N:P Stoichiometry

For non-infected and rust-infected plants, the ratios of N:C and P:C increased with the relative growth rates. The higher growth rates correspond to a higher N:C and P:C ratios (Figure 5).

3.4. The Responses Ratios of L. chinensis to Rust

The response ratios of DM fluctuated in June and decreased with the increase of grazing intensity in July and August. The response ratios of N and P were decreased with the increase of grazing intensity in June and August. The response ratio of C was steady under various grazing intensities from June to August (Figure 6).

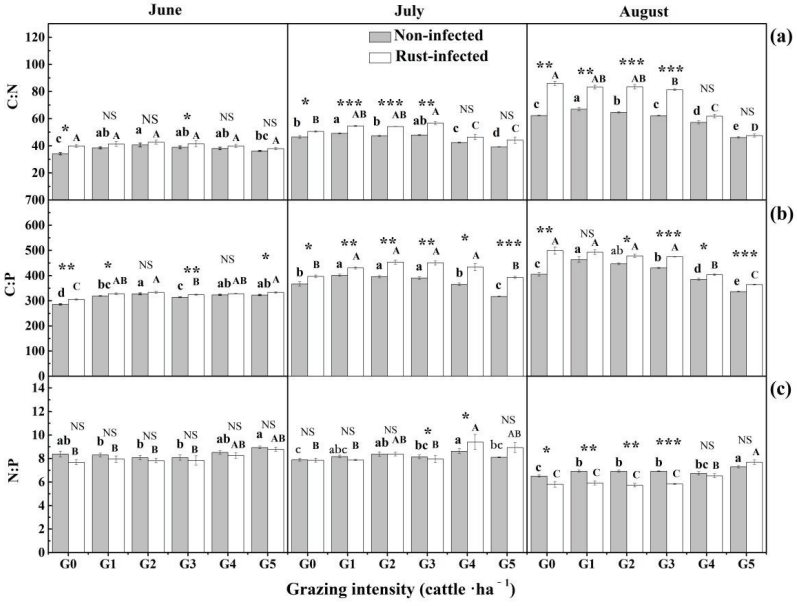

Figure 4. Influence of grazing intensity on the C:N (**a**), C:P (**b**), and N:P (**c**) ratios of non-infected and rust-infected *Leymus chinensis* from June to August based on the 2-year (2015 and 2016) average (error bars denote standard errors). Different lower-case and upper-case indicate significant differences among grazing intensities. The asterisk (*) indicates significant differences between non-infected and rust-infected plants (***, $p < 0.001$; **, $p < 0.01$; *, $p < 0.05$; NS, $p > 0.05$).

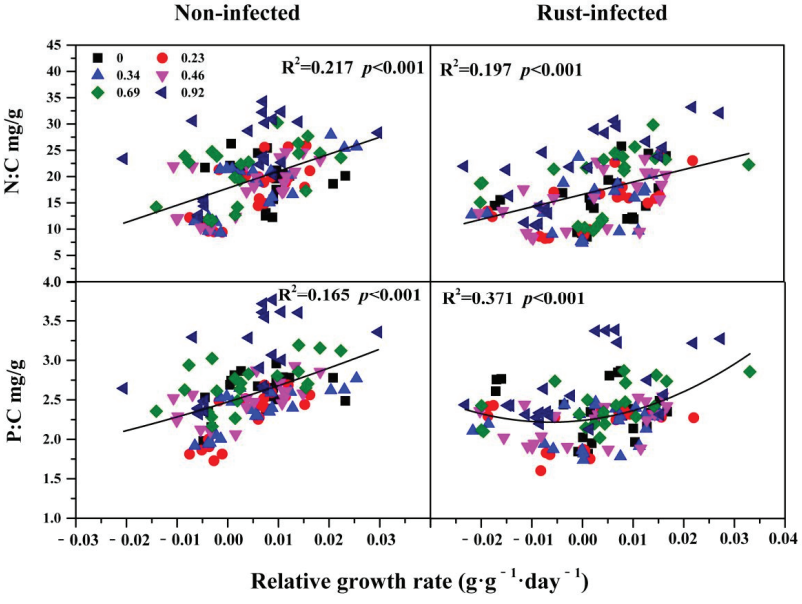

Figure 5. The relationship between relative growth rate and C:N:P stoichiometry of *Leymus chinensis* (non-infected and rust-infected plants) under different grazing intensities. Grazing intensities (0, 0.42, 0.63, 0.83, 1.25, and 1.67 cattle ha^{-1}) are indicated by different colors.

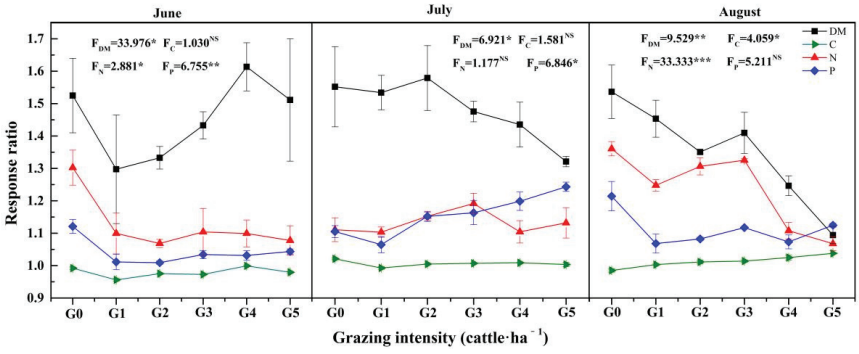

Figure 6. The differences of dry matter (DM), carbon (C), nitrogen (N), and phosphorus (P) contents response ratios between non-infected and rust-infected *Leymus chinensis* under different grazing intensities. Significant differences among grazing intensities are reported from ANOVA as ***, $p < 0.001$; **, $p < 0.01$; *, $p < 0.05$; NS, $p > 0.05$ and F-values (F) are given.

3.5. The Interactions of Grazing and Rust to L. chinensis

The DM, N, and P content (%), and the C:N and C:P ratios were significantly affected by rust ($p < 0.05$). The DM, relative growth rate, C, N, and P content (%), and the C:N and C:P ratios were significantly affected by grazing intensities ($p < 0.05$). All of the measurements were significantly affected by sample date ($p < 0.05$) and there were only three-way interaction effects of sample date, rust, and grazing intensity on the DM (Table 1).

Table 1. General linear mixed-effects model results for the effects of sample date (SD), grazing intensity (GI), and rust (RU) on dry matter (DM g·tiller^{-1}), relative growth rate (RW g g^{-1}·day^{-1}), carbon, nitrogen, and phosphorus contents (%), and C: N: P stoichiometry of *Leymus chinensis*. F-values (F) and *p*-values (*p*) are given. Significant *p*-values ($p < 0.05$) in bold.

Source	df	DM		RW		Carbon		Nitrogen		Phosphorus		C:N		C:P		N:P	
		F	*p*	F	*p*	F	*p*	F	*p*	F	*p*	F	*p*	F	*p*	F	*p*
SD	5	5.52	**0.015**	41.73	**0.023**	31.07	**0.031**	126.57	**0.008**	17.89	0.053	40.50	**0.024**	28.61	**0.034**	27.43	**0.035**
RU	1	6.71	**0.045**	3.11	0.251	0.17	0.718	24.71	**0.025**	6.38	0.111	5.05	0.138	**7.60**	0.133	0.75	0.449
GI	5	24.54	**0.002**	**61.78**	**<0.001**	4.41	0.065	35.41	**0.001**	15.54	**0.005**	15.33	**0.005**	**32.33**	**0.001**	3.60	0.093
SD × RU	4	8.35	**0.007**	7.15	**0.012**	5.50	**0.024**	3.93	0.055	12.64	**0.002**	17.72	**0.001**	6.78	**0.014**	10.74	**0.043**
SD × GI	25	3.82	**0.023**	10.76	**<0.001**	4.21	**0.016**	7.40	**0.020**	10.11	**0.001**	7.61	**0.002**	6.62	**0.003**	1.90	0.164
RU × GI	5	6.52	**0.006**	0.24	0.936	1.02	0.457	1.56	0.258	2.01	0.162	2.23	0.132	0.46	0.800	4.15	**0.027**
SD × RU × GI	20	3.05	**0.001**	0.71	0.714	0.53	0.865	0.10	1.000	0.53	0.867	0.10	1.000	0.82	0.612	0.11	1.000

3.6. Factors Influencing DM of L. chinensis

The first axis and second axis of the redundancy analysis (RDA) explained 70.1% and 30.1% of the variance, respectively. The total explained value of grazing intensity and rust to DM and the C, N, and P content (%) was 0.85, and the explained value of grazing intensity was 0.76, while the rust was 0.081. According to RDA, grazing was the most important factor to affect the DM of *L. chinensis*. The grazing intensity had a negative effect on dry matter, and a negative effect on the N content (%). The rust had a negative effect on the dry matter, and the C, N, and P content (%) (Figure 7).

The structural equation modeling (SEM) analysis revealed that grazing and rust directly altered the N and P content (%), which further influenced the DM of *L. chinensis*. In contrast, the grazing intensity and rust had no direct influences on the C content. In addition, grazing had a significant ($p < 0.05$) and direct effect on the DM of *L. chinensis* and was the most important pathway for determining the dry matter. The rust also notably affected DM directly, but less than grazing (Figure 8).

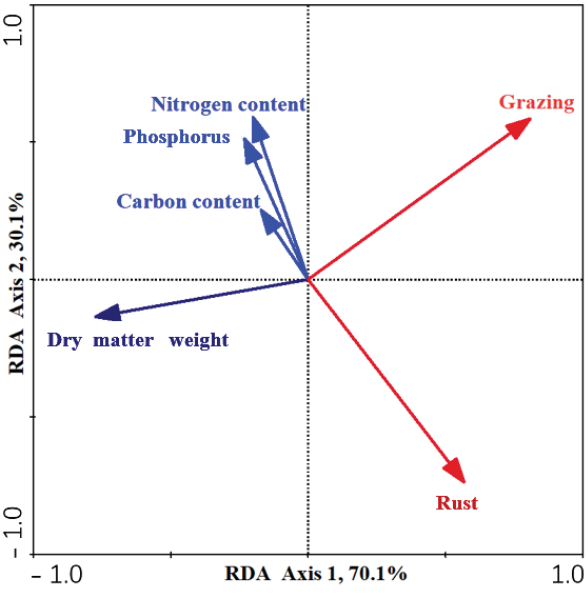

Figure 7. Redundancy analysis (RDA) of the effects of grazing and rust on dry matter, carbon, nitrogen, and phosphorus contents (%) of *Leymus chinensis*, showing the correlational relationships among grazing intensities (0, 0.42, 0.63, 0.83, 1.25, and 1.67 cattle ha^{-1}), disease (rust), dry matter of *L. chinensis*, and the content of elements (C, N, and P). Direction of arrow indicates the correlation between the parameters, and the length of the arrow indicates the magnitude of the association.

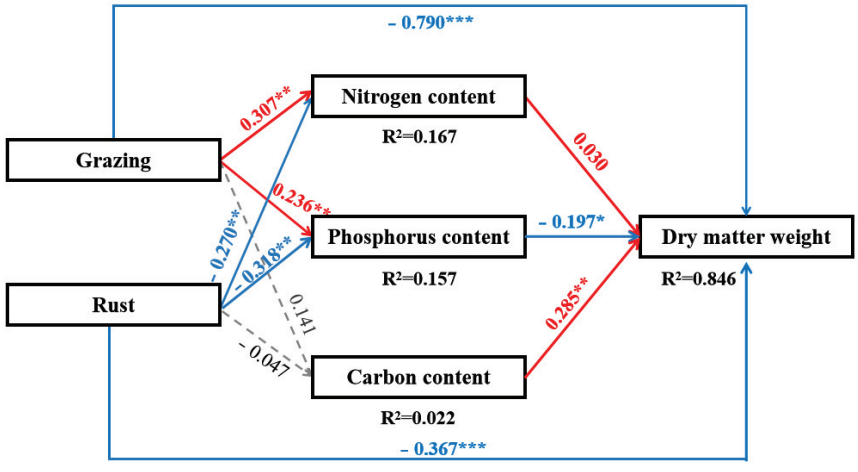

Figure 8. Final results of structural equation modeling (SEM) analysis for the effects of grazing and rust on the dry matter of *Leymus chinensis* in 2015 and 2016. Red arrows, evidence for positive relationships; blue arrows, evidence for negative relationships; gray arrows, insufficient statistical evidence for path coefficients ($p > 0.05$). Width of the arrows shows the strength of the causal relationship, and the number adjacent to arrows are standardized path coefficients, which reflect the effect size of the relationship; asterisks indicate statistical significance (***, $p < 0.001$; **, $p < 0.01$; *, $p < 0.05$). The proportion of variance explained (R^2) appears alongside each response variable in the model. The final model adequately fitted the data: $\chi^2 = 249.059$, Df = 4, $P = 0.104$, GFI = 0.955.

4. Discussion

The key findings of the present study showed that grazing intensity and rust infection could negatively affect the biomass accumulation and nutrient element content and affect the ecological stoichiometry of *L. chinensis*. The N:C and P:C ratios were still positively correlated with the relative growth rates of plants. Non-infected *L. chinensis* had higher N:C and P:C ratios than rust-infected plants, which was consistent with the growth rate hypothesis. Meanwhile, almost all response ratios of DM under various grazing intensities were smaller than that in the G0 treatment. The findings of our study indicated that the growth rate hypothesis, based on ecological stoichiometry, still applied in *L. chinensis* under the interactive effects of grazing and disease. Additionally, grazing alleviated the loss of DM caused by disease.

4.1. Effects of Grazing on Rust

Grazing could change the relationship between host plants and pathogenic fungi through direct or indirect influence, thereby affecting the occurrence of grassland diseases. According to another of our studies carried out at the same experimental site, pathogen load on plants was directly affected by grazing through ingestion, and indirectly by shifting the plant community structure and the micro-environment [54]. In the case of this study, the incidence of *L. chinensis* decreased significantly ($p < 0.05$) with increased grazing intensity. Generally, grazing would increase the population of younger tillers [55], and younger plants are generally more susceptible to disease [56]. This is the opposite of our results, which may be because grazing cattle remove not only infected tissues, but also infectious spores when they selectively graze [22]. Ingestion by cattle under higher grazing intensity treatments (G4 and G5) provided ample space for seedlings and young tillers to grow without being severely restricted by abundant surrounding plants. Additionally, grazing decreased the number of old leaves that contained a high load of rust spores. Increasing numbers of young leaves and seedlings of *L. chinensis* grew in an environment where there were fewer infectious propagules and a lower pressure imposed by pathogenic plants in this study. Therefore, the young leaves and seedlings are very likely to have a lower incidence of rust infection. This switch from a predominance of old infected leaves to young leaves is likely a main reason why the rust incidence of *L. chinensis* decreased with increased grazing intensity.

Additionally, the selective ingestion by cattle would also change the species diversity of this grassland. A previous study in this area had verified that the species diversity was increased under the G3 treatment [2]. According to the dilution effect, high plant community diversity could negatively regulate the occurrence of infection [57–59]. Thus, the increase of species diversity in grazing treatments may also have resulted in deceased incidence of *L. chinensis*. This is another potential reason why the incidence of rust is lower in grazing treatments than in non-grazing treatment.

4.2. Effects of Grazing and Disease on DM

The DM of *L. chinensis* decreased gradually with the increase of grazing intensity, which was consistent with prior research based on the community level of Yan et al. [2] carried out in the same experimental site as the present research, and also similar to most grazing experiments carried out in grasslands in other parts of the world [47,60,61]. However, according to the compensation phenomenon, plants have the ability to compensate for the loss in vegetative biomass or reproductive potential, and to alleviate the detrimental effects of herbivores [62], but the result of the present study is different. This may be because *L. chinensis* is a constructive species and is the most favored plant species for cattle grazing in the Hulunber grasslands [2]. Compensatory growth, at least above ground, cannot match the rate of ongoing ingestion of this palatable grass by livestock. As a result, the plants even have negative growth in higher grazing intensities (G4 and G5 treatments). However, a previous study [63] in the same experimental plots showed that the below-ground biomass of *L. chinensis* was the highest in the grazing treatments (G2 and G3) than in the ungrazed

treatment, which may also meet predictions of the compensatory phenomenon. In the present study, the DM of rust-infected plants was smaller than the non-infected plants. It is easy to understand that diseases always damage the plant photosynthesis system, further reducing the biomass accumulation and even resulting in plant death [18,21].

4.3. Effects of Grazing and Disease on Relative Growth Rate and Ecological Stoichiometry

Carbon is considered as a relatively stable framework element, thus grazing and disease did not significantly ($p > 0.05$) affect the C content of *L. chinensis*, which is consistent with the previous study for the above ground plants in this area [64]. N and P are the most important elements for plant growth and affect plant growth and function [65]. The N content in *L. chinensis* increased gradually with the increasing of grazing intensity. This may because outcomes of grazing livestock include the introduction of more fresh leaves, plant litter, as well as dung and urine, which promote microbial activity in soil, further increase the soil nutrients available to plants, ultimately changing the content and stoichiometry of the plant community [39,40]. On the other hand, pathogen infection would induce N metabolism and transportation [66,67]. Both N and P are acquired via roots from soil [9]. Transpiration is the main force for N and P absorption. Pathogens produce degrading enzymes to damage leaf tissues, negatively affecting photosynthesis and transpiration [20,46,68], further decreasing the absorption ability of rust-infected plants to N and P from soil. This may be the reasons why N and P content was decreased in rust-infected *L. chinensis*.

Ecological stoichiometry of living organisms has been important in the understanding of the implications of human disturbance to element cycles [34,69,70]. Previous studies demonstrated that higher N:C and P:C ratios in many heterotrophic organisms were coupled to higher relative growth rates [71,72]. According to our results, the N:C and P:C ratios were significant ($p < 0.05$) and positively correlated with the relative growth rate of *L. chinensis* in the six treatments. It was higher in the G1, G2, and G3 grazing treatments than in the G4 and G5 grazing treatments, which is consistent with the growth rate hypothesis [71,72]. Our findings showed that *L. chinensis* plants under lower grazing intensities had higher growth rates than those under higher grazing intensities. In other words, growth rate hypothesis, based on ecological stoichiometry, still applied in plants under various grazing intensities.

Some of the variation in field measurements of stoichiometric homeostasis was due to parasitism [73]. Therefore, infected hosts will display greater stoichiometric homeostatic variability than non-infected hosts [46]. In our study, the rust also had strong negative impacts on *L. chinensis* by altering the C, N, and P content (%) as well as the C:N:P stoichiometry. The N:C and P:C ratios of rust-infected plants were higher than those in non-infected plants. This finding confirmed that the stoichiometric ratio would not only reflect the plant growth rate but further reflect the health status of plants.

4.4. Grazing Alleviated the Loss of DM Caused by Disease

Grazing and rust substantially altered the DM and ecological stoichiometry of *L. chinensis* in the present study. The value of the response ratio could reflect the strength of influence of disease on DM [51]. The larger the value, the greater the impact. Almost all response ratios of DM under various grazing intensities were smaller than that in the G0 treatment, which means grazing alleviated the loss of DM caused by disease. Disease caused the primary loss in production of host plants by damaging the plant photosynthesis system, reducing the content of elements [18,21]. However, grazing increased the content of elements in plants [74]. SEM showed the same result, and this may be one of the potential reasons why grazing could alleviate the loss of DM caused by disease.

Our study provides a stoichiometric approach to understanding the interaction between grass and fungal disease under various grazing intensities, which provides new knowledge linking variation in host and livestock to patterns in the emergence and distri-

bution of fungal pathogens and provides better understanding and prediction of grazing-diseases interactions.

Author Contributions: Conceptualization, Y.Z., Z.N. and X.X.; methodology, Y.Z. and X.X.; software, Y.Z. and N.Z.; formal analysis, Y.Z.; investigation, Y.Z. and X.X.; data curation, Y.Z. and X.X.; writing—original draft preparation, Y.Z. and N.Z.; writing—review and editing, Y.Z., Z.N. and M.J.C.; visualization, Y.Z. and N.Z.; supervision, Z.N.; project administration, Z.N.; funding acquisition, Z.N. and Y.Z. All authors have read and agreed to the published version of the manuscript.

Funding: This research was financially supported by the National Public Welfare Industry of Agricultural Science and Technology Special Projects (201303057) and the Fundamental Research Funds for the Central Universities (561221001).

Institutional Review Board Statement: Not available.

Informed Consent Statement: Not available.

Data Availability Statement: Not available.

Conflicts of Interest: The authors declare no conflict of interest.

Appendix A

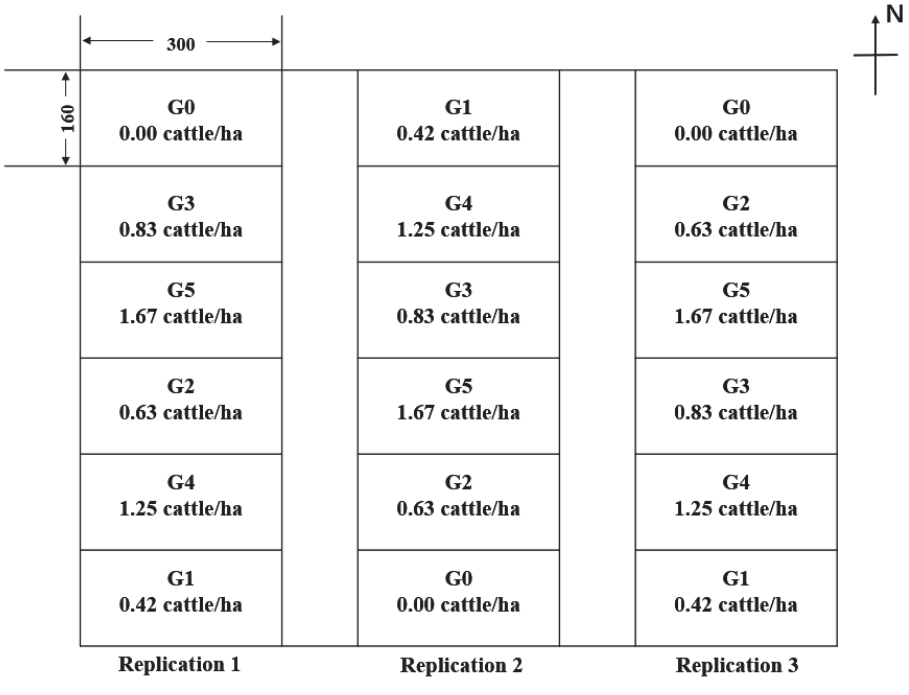

Figure A1. Sketch map of the experimental site.

References

1. Wang, D.; Wu, G.; Zhu, Y.; Shi, Z. Grazing exclusion effects on above- and below-ground C and N pools of typical grassland on the Loess Plateau (China). *Catena* **2014**, *123*, 113–120. [CrossRef]
2. Yan, R.; Xin, X.; Yan, Y.; Wang, X.; Zhang, B.; Yang, G.; Liu, S.; Deng, Y.; Li, L. Impacts of differing grazing rates on canopy structure and species composition in Hulunber Meadow Steppe. *Rangel. Ecol. Manag.* **2015**, *68*, 54–64. [CrossRef]
3. Hou, F.J.; Yang, Z.Y. Effects of grazing of livestock on grassland. *Acta Ecol. Sin.* **2006**, *26*, 244–264.
4. Xun, W.; Yan, R.; Ren, Y.; Jin, D.; Xiong, W.; Zhang, G.; Cui, Z.; Xin, X.; Zhang, R. Grazing-induced microbiome alterations drive soil organic carbon turnover and productivity in meadow steppe. *Microbiome* **2018**, *6*, 170. [CrossRef] [PubMed]

5. Yan, R.R.; Tang, H.J.; Lv, S.H.; Jin, D.Y.; Xin, X.P.; Chen, B.R.; Zhang, B.H.; Yan, Y.C.; Wang, X.; Murray, P.J.; et al. Response of ecosystem CO_2 fluxes to grazing intensities-a five-year experiment in the Hulunber meadow steppe of China. *Sci. Rep.* **2017**, *7*, 9491. [CrossRef] [PubMed]
6. Hu, X.W.; Huang, X.H.; Wang, Y.R. Hormonal and temperature regulation of seed dormancy and germination in *Leymus chinensis*. *Plant Growth Regul.* **2012**, *67*, 199–207. [CrossRef]
7. Reeder, J.D.; Schuman, G.E.; Morgan, J.A.; Lecain, D.R. Response of organic and inorganic carbon and nitrogen to long-term Grazing of the shortgrass steppe. *Environ. Manag.* **2004**, *33*, 485–495. [CrossRef]
8. Estes, J.A.; Terborgh, J.; Brashares, J.S.; Power, M.E.; Berger, J.; Bond, W.J.; Carpenter, S.R.; Essington, T.E.; Holt, R.D.; Wardle, D.A. Trophic downgrading of planet earth. *Science* **2011**, *6040*, 301–306. [CrossRef]
9. Bai, Y.; Wu, J.; Clark, C.M.; Pan, Q.; Zhang, L.; Chen, S.; Wang, Q.; Han, X. Grazing alters ecosystem functioning and C:N:P stoichiometry of grasslands along a regional precipitation gradient. *J. Appl. Ecol.* **2012**, *49*, 1204–1215. [CrossRef]
10. Sitters, J.; Bakker, E.S.; Veldhuis, M.P.; Veen, G.F.; Olde Venterink, H.; Vanni, M.J. The Stoichiometry of Nutrient Release by Terrestrial Herbivores and Its Ecosystem Consequences. *Front. Earth Sci.* **2017**, *5*, 32. [CrossRef]
11. Sitters, J.; Cherif, M.; Egelkraut, D.; Giesler, R.; Olofsson, J. Long-term heavy reindeer grazing promotes plant phosphorus limitation in arctic tundra. *Funct. Ecol.* **2019**, *33*, 1233–1242. [CrossRef]
12. Sasaki, T.; Okayasu, T.; Jamsran, U.; Takeuchi, K. Threshold changes in vegetation along a grazing gradient in Mongolian rangelands. *J. Ecol.* **2007**, *96*, 145–154. [CrossRef]
13. Hilker, T.; Natsagdorj, E.; Waring, R.H.; Lyapustin, A.; Wang, Y. Satellite observed widespread decline in Mongolian grasslands largely due to overgrazing. *Glob. Change Biol.* **2014**, *20*, 418–428. [CrossRef] [PubMed]
14. Eldridge, D.J.; Delgado-Baquerizo, M. Continental-scale impacts of livestock grazing on ecosystem supporting and regulating services. *Land Degrad. Dev.* **2016**, *28*, 1473–1481. [CrossRef]
15. Lu, X.; Kelsey, K.C.; Yan, Y.; Sun, J.; Wang, X.; Cheng, G.; Neff, J.C. Effects of grazing on ecosystem structure and function of alpine grasslands in Qinghai- Tibetan Plateau: A synthesis. *Ecosphere* **2017**, *8*, e1656. [CrossRef]
16. Zhang, Y.; Chen, T.; Nan, Z.; Christensen, M.J. Cattle grazing alters the interaction of seed-borne fungi and two foliar pathogens of *Leymus chinensis* in a meadow steppe. *Eur. J. Plant Pathol.* **2019**, *155*, 207–218. [CrossRef]
17. Nan, Z.B.; Li, C.J.; Wang, Y.W.; Wang, Y.R. Lucerne common leaf spot forage quality, photosynthesis rate and field resistance. *Acta Prataculturae Sin.* **2001**, *10*, 26–34.
18. Fisher, M.C.; Henk, D.A.; Briggs, C.J.; Brownstein, J.S.; Madoff, L.C.; Mccraw, S.L.; Gurr, S.J. Emerging fungal threats to animal, plant and ecosystem health. *Nature* **2012**, *484*, 186–194. [CrossRef]
19. Liu, X.; Ma, Z.; Cadotte, M.W.; Chen, F.; He, J.; Zhou, S. Warming affects foliar fungal diseases more than precipitation in a Tibetan alpine meadow. *New Phytol.* **2019**, *221*, 1574–1584. [CrossRef]
20. Ding, T.T.; Wang, X.Y.; Duan, T.Y. Effect of disease on photosynthesis, nutrition, and nodulation of leguminous forage. *Pratacultural Sci.* **2019**, *36*, 152–160.
21. Nan, Z.B.; Li, C.J. Forage and turfgrass disease in China and their control. In *Forage and Turfgrass Pathological Research in China*; Nan, Z.B., Li, C.J., Eds.; Ocean Press: Beijing, China, 2003; pp. 3–10.
22. Gray, F.A.; Koch, D.W. Influence of late season harvesting, fall grazing, and fungicide treatment on Verticillium Wilt incidence, plant density, and forage yield of alfalfa. *Plant Dis.* **2004**, *88*, 811–816. [CrossRef] [PubMed]
23. Aalto, S.L.; Decaestecker, E.; Pulkkinen, K. A three-way perspective of stoichiometric changes on host–parasite interactions. *Trends Parasitol.* **2015**, *31*, 333–340. [CrossRef] [PubMed]
24. Chen, T.; Zhang, Y.W.; Christensen, M.; Li, C.H.; Hou, F.J.; Nan, Z.B. Grazing intensity affects communities of culturable root-associated fungi in a semiarid grassland of northwest China. *Land Degrad. Dev.* **2017**, *29*, 361–373. [CrossRef]
25. Wennström, A.; Ericson, L. Variation in disease incidence in grazed and ungrazed sites for the system *Pulsatilla pratensis-Puccinia pulsatillae*. *Oikos* **1991**, *60*, 35–39. [CrossRef]
26. Lu, X.; Nan, Z.B. Perspectives in effects of grazing on diversity of grassland plant community and forage diseases. *Pratacultural Sci.* **2015**, *32*, 1423–1431.
27. Liu, X.; Lyu, S.; Zhou, S.; Bradshaw, C.J.A. Warming and fertilization alter the dilution effect of host diversity on disease severity. *Ecology* **2016**, *97*, 1680–1689. [CrossRef]
28. Chen, T.; Nan, Z.; Kardol, P.; Duan, T.; Song, H.; Wang, J.; Li, C.; Hou, F. Effects of interspecific competition on plant-soil feedbacks generated by long-term grazing. *Soil Biol. Biochem.* **2018**, *126*, 133–143. [CrossRef]
29. Knops, J.M.H.; Tilman, D.; Haddad, N.M.; Naeem, S.; Mitchell, C.E.; Haarstad, J.; Ritchie, M.E.; Howe, K.M.; Reich, P.B.; Siemann, E.; et al. Effects of plant species richness on invasion dynamics, disease outbreaks, insect abundances and diversity. *Ecol. Lett.* **2002**, *2*, 286–293. [CrossRef]
30. Keesing, F.; Holt, R.D.; Ostfeld, R.S. Effects of species diversity on disease risk. *Ecol. Lett.* **2006**, *9*, 485–498. [CrossRef]
31. Keesing, F.; Belden, L.K.; Daszak, P.; Dobson, A.; Harvell, C.D.; Holt, R.D.; Hudson, P.; Jolles, A.; Jones, K.E.; Mitchell, C.E.; et al. Impacts of biodiversity on the emergence and transmission of infectious diseases. *Nature* **2010**, *468*, 647–652. [CrossRef]
32. Rottstock, T.; Joshi, J.; Kummer, V.; Fischer, M. Higher plant diversity promotes higher diversity of fungal pathogens, while it decreases pathogen infection per plant. *Ecology* **2014**, *95*, 1907–1917. [CrossRef] [PubMed]
33. Bever, J.D.; Mangan, S.A.; Alexander, H.M. Maintenance of plant species diversity by pathogens. *Annu. Rev. Ecol. Evol.* **2015**, *46*, 305–325. [CrossRef]

34. Sterner, R.W.; Elser, J.J. *Ecological Stoichiometry: The Biology of Elements from Molecular to the Biosphere*; Princeton University Press: Princeton, NJ, USA, 2002.
35. Hessen, D.O.; Jensen, T.C.; Kyle, M.; Elser, J.J. RNA responses to N-and P-limitation; reciprocal regulation of stoichiometry and growth rate in Brachionus. *Funct. Ecol.* **2007**, *21*, 956–962. [CrossRef]
36. Allen, A.P.; Gillooly, J.F. Towards an integration of ecological stoichiometry and the metabolic theory of ecology to better understand nutrient cycling. *Ecol. Lett.* **2009**, *12*, 369–384. [CrossRef]
37. Van der Wal, R.; Brooker, R.W. Mosses mediate grazer impacts on grass abundance in Arctic. *Funct. Ecol.* **2004**, *18*, 77–86. [CrossRef]
38. Bardgett, R.D.; Wardle, D.A. Herbivore-mediated linkages between aboveground and belowground communities. *Ecology* **2003**, *84*, 2258–2268. [CrossRef]
39. Holland, J.N.; Cheng, W.; Crossley, D.A. Herbivore-induced changes in plant carbon allocation: Assessment of below-ground C fluxes using carbon-14. *Oecologia* **1996**, *107*, 87–94. [CrossRef]
40. Hamilton, W.E.; Frank, D.A. Can plants stimulate soil microbes and their own nutrient supply? Evidence from a grazing tolerant grass. *Ecology* **2001**, *82*, 2397–2402. [CrossRef]
41. Hobbie, S.E. Effects of plant species on nutrient cycling. *Trends Ecol. Evol.* **1992**, *7*, 336–339. [CrossRef]
42. Ritchie, M.E.; Tilman, D.; Knops, J.M.H. Herbivore effects on plant and nitrogen dynamics in Oak Savanna. *Ecology* **1998**, *79*, 165–177. [CrossRef]
43. Elser, J.J.; Dobberfuhl, D.R.; Mackay, N.A.; Schampel, J.H. Organism size, life history, and N:P stoichiometry. *Bioscience* **1996**, *46*, 674–684. [CrossRef]
44. Jensen, B.; Munk, L. Nitrogen-induced changes in colony density and spore production of Erysiphe graminis f.sp. hordei on seedlings of six spring barley cultivars. *Plant Pathol.* **1997**, *46*, 191–202. [CrossRef]
45. Frenken, T.; Wierenga, J.; Gsell, A.S.; van Donk, E.; Rohrlack, T.; Van de Waal, D.B. Changes in N:P supply ratios affect the ecological stoichiometry of a toxic Cyanobacterium and its fungal parasite. *Front. Microbiol.* **2017**, *8*, 1015. [CrossRef] [PubMed]
46. Sanders, A.J.; Taylor, B.W. Using ecological stoichiometry to understand and predict infectious diseases. *Oikos* **2018**, *127*, 1399–1409. [CrossRef]
47. Daleo, P.; Silliman, B.; Alberti, J.; Escapa, M.; Canepuccia, A.; Peña, N.; Iribarne, O. Grazer facilitation of fungal infection and the control of plant growth in south-western Atlantic salt marshes. *J. Ecol.* **2009**, *97*, 781–787. [CrossRef]
48. Li, Y.Z.; Nan, Z.B. *The Methods of Diagnose, Investigation and Loss Evaluation for Forage Diseases*; Phenix Press: Nanjing, China, 2015.
49. Wang, Q.; Li, F.; Zhao, L.; Zhang, E.; Shi, S.; Zhao, W.; Song, W.; Vance, M.M. Effects of irrigation and nitrogen application rates on nitrate nitrogen distribution and fertilizer nitrogen loss, wheat yield and nitrogen uptake on a recently reclaimed sandy farmland. *Plant Soil* **2010**, *337*, 325–339. [CrossRef]
50. Nelson, D.W.; Sommers, L.E. Total carbon, organic carbon, and organic matter. In *Methods of Soil Analysis*; Miller, R.H., Keeney, D.R., Eds.; American Society of Agronomy and Soil Science Society of American: Madison, WI, USA, 1982; pp. 1–129.
51. Lajeunesse, M.J. On the meta-analysis of response ratios for studies with correlated and multi-group designs. *Ecology* **2011**, *92*, 2049–2055. [CrossRef]
52. Lepš, J.; Petr, Š. *Multivariate Analysis of Ecological Data Using CANOCO*; Cambridge University Press: Cambridge, UK, 2003.
53. Li, Z.; Wang, X.; Wang, D.L. First report of rust disease caused by *Puccinia elymi* on *Leymus chinensis* in China. *Plant Pathol.* **2008**, *57*, 376. [CrossRef]
54. Zhang, Y.; Nan, Z.; Xin, X. Response of plant fungal diseases to beef cattle grazing intensity in Hulunber grassland. *Plant Dis.* **2020**, *104*, 2905–2913. [CrossRef]
55. Silva, L.S.; Silva, V.J.; Yasuoka, J.I.; Sollenberger, L.E.; Pedreira, C.G.S. Tillering dynamics of 'Mulato II' brachiariagrass under continuous stocking. *Crop Sci.* **2020**, *60*, 1105–1112. [CrossRef]
56. Develey-Rivière, M.P.; Galiana, E. Resistance to pathogens and host developmental stage: A multifaceted relationship within the plant kingdom. *New Phytol.* **2007**, *175*, 405–416. [CrossRef] [PubMed]
57. Dobson, A. Population dynamics of pathogens with multiple host species. *Am. Nat.* **2004**, *164*, S64–S78. [CrossRef] [PubMed]
58. Ostfeld, R.S.; Keesing, F. Effects of host diversity on infectious disease. *Annu. Rev. Ecol. Evol.* **2012**, *43*, 157–182. [CrossRef]
59. Rudolf, V.H.W.; Antonovics, J. Species coexistence and pathogens with frequency-dependent transmission. *Am. Nat.* **2005**, *166*, 112–118. [CrossRef] [PubMed]
60. Yates, C.J.; Norton, D.A.; Hobbs, R.J. Grazing effects on plant cover, soil and microclimate in fragmented woodlands in south-western Australia: Implications for restoration. *Austral Ecol.* **2000**, *25*, 36–47. [CrossRef]
61. Altesor, A.; Oesterheld, M.; Leoni, E.; Lezama, F.; Rodríguez, C. Effect of grazing on community structure and productivity of a Uruguayan grassland. *Plant Ecol.* **2005**, *179*, 83–91. [CrossRef]
62. Gao, Y.; Wang, D.; Ba, L.; Bai, Y.; Liu, B. Interactions between herbivory and resource availability on grazing tolerance of *Leymus chinensis*. *Environ. Exp. Bot.* **2008**, *63*, 113–122. [CrossRef]
63. Yan, R.R.; Tang, H.J.; Xin, X.P.; Chen, B.R.; Murray, P.J.; Yan, Y.C.; Wang, X.; Yang, G.X. Grazing intensity and driving factors affect soil nitrous oxide fluxes during the growing seasons in the Hulunber meadow steppe of China. *Environ. Res. Lett.* **2016**, *11*, 54004. [CrossRef]
64. Cao, J.; Yan, R.; Chen, X.; Wang, X.; Yu, Q.; Zhang, Y.; Ning, C.; Hou, L.; Zhang, Y.; Xin, X. Grazing affects the ecological stoichiometry of the plant–soil–microbe system on the Hulunber Steppe, China. *Sustainability* **2019**, *11*, 5226. [CrossRef]

65. McDonald, A.; Davies, W.J. Keeping in touch: Responses of the whole plant to deficits. *Adv. Bot. Res.* **1996**, *22*, 229.
66. Loper, G.M.; Hanson, C.H.; Graham, J.H. Coumestrol content of alfalfa as affected by selection for resistance to foliar disease. *Crop Sci.* **1967**, *7*, 189–192. [CrossRef]
67. Bernot, R.J. Parasite-host elemental content and the effects of a parasite on host-consumer-driven nutrient recycling. *Freshw. Sci.* **2013**, *32*, 299–308. [CrossRef]
68. Jin, Q.; Zhou, G.Y.; Liu, J.A.; He, W.H. The role of cell wall degrading enzymes in the pathogenic process of *Camellia oleifera* disease caused by *Colletotrichum gloeosporioides*. *Plant Prot.* **2016**, *43*, 97–102.
69. Ågren, G.I. The C: N: P stoichiometry of autotrophs-theory and observations. *Ecol. Lett.* **2004**, *7*, 185–191. [CrossRef]
70. Hessen, D.O.; Ågren, G.I.; Anderson, T.R.; Elser, J.J.; de Ruiter, P. Carbon sequestration in ecosystems: The role of stoichiometry. *Ecology* **2004**, *85*, 1179–1192. [CrossRef]
71. Elser, J.J.; Acharya, K.; Kyle, M.; Cotner, J.; Makino, W.; Markow, T.; Watts, T.; Hobbie, S.; Fagan, W.; Schade, J.; et al. Growth rate-stoichiometry couplings in diverse biota. *Ecol. Lett.* **2003**, *6*, 936–943. [CrossRef]
72. Makino, W.; Cotner, J.B.; Sterner, R.W.; Elser, J.J. Are bacteria more like plants or animals Growth rate and resource dependence of bacterial C: N: P stoichiometry. *Funct. Ecol.* **2003**, *17*, 121–130. [CrossRef]
73. Halvorson, H.M.; Small, G.E. Observational field studies are not appropriate tests of consumer stoichiometric homeostasis. *Freshw. Sci.* **2016**, *35*, 1103–1116. [CrossRef]
74. Zhang, T.; Weng, Y.; Yao, F.J.; Shi, Y.T.; Cui, G.W.; Hu, G.F. Effect of grazing intensity on ecological stoichiometry of Deyeuxia angustifolia and meadow soil. *Acta Prataculturae Sin.* **2014**, *23*, 20–28.

agriculture

MDPI

Article

Effects of *Epichloë* Endophyte and Transgenerational Effects on Physiology of *Achnatherum inebrians* under Drought Stress

Xuelian Cui [1], Xingxu Zhang [1], Lielie Shi [1], Michael John Christensen [2,†], Zhibiao Nan [1] and Chao Xia [1,*]

[1] State Key Laboratory of Grassland Agro-Ecosystems, Key Laboratory of Grassland Livestock Industry Innovation, Ministry of Agriculture and Rural Affairs, Engineering Research Center of Grassland Industry, Ministry of Education, College of Pastoral Agriculture Science and Technology, Lanzhou University, Lanzhou 730020, China; cuixl18@lzu.edu.cn (X.C.); xxzhang@lzu.edu.cn (X.Z.); shill19@lzu.edu.cn (L.S.); zhibiao@lzu.edu.cn (Z.N.)

[2] Grasslands Research Centre, AgResearch, Palmerston North 4442, New Zealand; mchristensenpn4410@gmail.com

* Correspondence: xiac@lzu.edu.cn; Tel.: +86-183-9433-6560

† Retired scientist.

Abstract: The present study explored the effects of an *Epichloë* endophyte on growth and physiology parameters of drunken horse grass (DHG, *Achnatherum inebrians*) under four different soil water content. The possible transgenerational effects (TGE) on the above-mentioned indicators were examined. DHG plants with (EI) and without (EF) this *Epichloë* endophyte, grown from seed of plants from the same seed line, were used. The seeds had originated in the relatively dry site at Yuzhong [YZ(D)], and also used were seed of plants from this original seed-line grown at the relatively wet site Xiahe [XH(W)]. The growth, photosynthesis, phytohormones, and elements were measured. This study showed that the endophyte increased the aboveground biomass and chlorophyll content, with the increasing of photosynthetic parameters. The presence of endophyte also significantly promoted abscisic acid and indolE−3-acetic acid content but decreased the cytokinin content. The nitrogen and phosphorus content of EI plants was significantly higher than that of EF plants, but the endophyte decreased ratios of C:N and C:P at drought condition. In addition, TGE were present, affecting host growth and the above-mentioned parameters, and which indicated that the plants grown from the seeds in YZ(D) site are more competitive than those in the XH(W) site under water deficiency conditions.

Keywords: *Achnatherum inebrians*; *Epichloë* endophyte; drought stress; growth; physiology; transgenerational effects

Citation: Cui, X.; Zhang, X.; Shi, L.; Christensen, M.J.; Nan, Z.; Xia, C. Effects of *Epichloë* Endophyte and Transgenerational Effects on Physiology of *Achnatherum inebrians* under Drought Stress. *Agriculture* **2022**, *12*, 761. https://doi.org/10.3390/agriculture12060761

Academic Editor: Matevz Likar

Received: 28 April 2022
Accepted: 24 May 2022
Published: 26 May 2022

1. Introduction

In natural conditions, plants always form beneficial symbioses with various microorganisms, such as nitrogen-fixing bacteria, mycorrhizal fungi and endophytic fungi [1–3] that enhance growth and persistence, including under adverse environments. The establishment of symbiotic relationships between microorganism and plants is an important advancement of evolution [4]. Many cool-season grasses (subfamily Pooideae) are host of the *Epichloë* endophytes [5], which are nearly all asexual interspecific hybrids, and colonize intercellular spaces of host plant aboveground tissue, and are transmitted vertically via grass seeds [6,7]. The relationship between these fungi and grasses is considered to be mutualistic [8]; the *Epichloë* endophyte utilizes photosynthates from its host to carry out metabolic processes necessary for its survival and growth. In return, their presence can enhance plants tolerance to various biotic [9,10] and abiotic [11–13] stresses via the production and induction of fungal alkaloids and other secondary metabolites.

Most studies on *Epichloë* endophytes and grass symbiotic associations involved grasses of the genera *Festuca* and *Lolium*, as these endophytes improve the fitness and productivity

of the symbiont under a variety of biotic and abiotic stresses in agricultural and grassland ecosystems [14–16], but there are fewer studies related to *Achnatherum inebrians*. *A. inebrians* is commonly known as drunken horse grass (DHG) because of its narcotic impacts on grazing livestock; it usually grows in the arid and semi-arid grassland in north and northwest China with annual precipitation from 129 to 444 mm [17]. It is the host of seed-borne *Epichloë gansuensis* [18] or *E. inebrians* [19] endophytes, and the infection rate can reach 100% in natural conditions [17]. The *Epichloë* endophytes make DHG toxic to grazing livestock as they produce abundant ergot alkaloids, including ergine and ergonovine [20,21] to grazing livestock. In addition, the presence of endophyte increases tolerance to biotic and abiotic stresses, such as fungal pathogens [22–24], insect pests [25,26], heavy metals [27], low temperature [28], salt [29,30], and drought [31].

Drought is one of the most detrimental abiotic stresses for plants. The beneficial effect of *Epichloë* endophytes on the host grass is often achieved through improving growth rates and allocating more resources to reproduction under drought stress [32]. Photosynthesis is crucial in this process, which converts atmospheric carbon dioxide (CO_2) into organic compounds in the leaves of green plants using solar energy [33]. The *Epichloë* endophyte enhanced the ability of the symbiont to use available resources for photosynthesis, further improving growth [34]. Phytohormone balance largely governed plant physiological responses to biotic and abiotic stresses [35,36]. Phytohormones play central roles in the ability of plants to adapt to changing environments, by mediating growth, nutrient allocation, and source/sink transitions [37]. *Epichloë* infection increases the accumulation of phytohormones [38] and activates certain signaling pathways to enhance host tolerance [26,39]. The ability of plant growth and development, and the balance of multiple key elements, can be reflected through the ratios of C:N, C:P, and N:P [40,41]. *Epichloë* endophyte infection affects mineral uptake, nutrient elements assimilation, and resource allocation abilities of the host [42]. However, previous studies have indicated that the positive effects of *Epichloë* to drought resistance of host grass depended on genotypes of both host plant and endophyte, and environmental conditions [43].

A transgenerational effect (TGE) is the source of phenotypic variation expressed in the progeny from plants experiencing different environmental conditions. It occurs when an abiotic or biotic environmental factor acts on a parental individual and thereby affects the phenotype of offspring [44]. On account of the importance of TGE for understanding plant evolution and ecology, and as one of the mechanisms for plants to respond to biotic and abiotic factors of stress [45], their underlying mechanisms are of general interest. A TGE can be part of a suite of fine-tuned mechanisms, which was selected over evolutionary time. It allows parental organisms to plastically match the traits of the next generation to the prevailing local ecological conditions by transferring resources and/or information to offspring [46]. Maternal plants are major contributors of TGE, as they are directly influenced by the environment where seed production occurs. Under these circumstances, the phenotype of progeny will be affected by parental characteristics to adjust to the local environmental conditions by transferring resources and/or information to offspring [46]. The *Epichloë* endophytes are an ideal system to study TGE since they are vertically transmitted through the seed. Therefore, these endophytes have high potential as carriers to transfer information from parental individual to progeny [44,47]. Some studies have suggested that *Epichloë* endophytes have transgenerational positive effects when plants undergo ozone [12,48] and drought stress [31]. However, the role of *Epichloë* fungal endophytes in mediating drought induced TGE on effect of DHG physiology has not been studied.

The aims of the present study are to determine (1) how the *Epichloë* endophyte affects photosynthesis, phytohormones and/or nutrient elements of DHG under drought stress, and (2) whether vertically transmitted *Epichloë* mediates TGEs by affecting above-mentioned indicators under limited water conditions. A pot-based study was employed to test whether the *Epichloë* endophyte improved the above-mentioned indicators in DHG to enhance the drought resistance, and if the adjustment of the parental DHG taken place at two environmentally different sites also affected these indicators.

2. Materials and Methods

2.1. Biological Material

Endophyte-free (EF) and endophyte-infected (EI) DHG seeds were prepared as described in the previously reported study [31]. In May 2014, EF and EI seeds with similar genetic background were sown at Xiahe county of Gansu province, where it is more moist (wet site, XH(W)) and at Yuzhong campus of Lanzhou University, where is drier (dry site, YZ(D)). Seeds from the two hundred of EF and from the two hundred of EI DHG at both the XH(W) and YZ(D) sites were harvested in September 2015, bulked as EF or EI, and stored at a constant temperature of 4 °C for the current study. Ten seeds were selected randomly from both EF and EI seed samples of the XH(W) and YZ(D) site to confirm the infection statues before planting.

2.2. Experimental Design

On 24 August 2016, two hundred plastic pots with 140 mm diameter and 170 mm height were prepared, and 600 g vermiculite was put into the pots. The water-holding capacity of the vermiculite, from now on referred to as soil, was measured, and when saturated, 600 g medium is able to hold 1134 g available water on average. Five corresponding seeds of YZ(D)EF, YZ(D)EI, XH(W)EF, and XH(W)EI were planted into fifty pots, respectively. After germination, only one seedling was retained in each pot, and these were watered as needed. All pots were assigned randomly to the greenhouse of Yuzhong campus of Lanzhou University. The greenhouse conditions were maintained at a temperature of 24 ± 2 °C and a photoperiod of 16/8 h (light/dark) with a moisture of 76 ± 2%. After three weeks, for DHG of each seed type XH(W) and YZ(D), eighty pots with similar growth state DHG were selected, forty with EF and forty with EI plants. A total of 160 pots were employed in the present experiment. On 9 October, according to the measured saturated water content of the soil, the water gradient was established by reducing the water content of soil. The soil water-holding capacity (SWC) of each of the 40 pots of each of the four soil treatments was established: 15% SWC (strong drought), 30% SWC (light drought), 45% SWC (normal moisture) and 60% SWC (abundant moisture) conditions. Each SWC condition was assigned to 10 pots of the YZ(D)EF, YZ(D)EI, XH(W)EF and XH(W)EI seedlings, and every afternoon of the experiment at 6 o'clock, each pot was weighed, and water was added to maintain the required SWC. After that, the position of each pot was transposed at random.

2.3. Measurement Protocols

2.3.1. Chlorophyll Content

On 8 December, the leaf in the top of each DHG plant in each different soil water condition was selected to measure its chorophyll content using a SPAD-502Plus (Konica Minolta Sensing, Inc., Tokyo, Japan), according to the method of Ye et al. [49].

2.3.2. Photosynthetic Indexes

The same day as the chlorophyll content measurement, photosynthesis in the top leaf, that is, the same leaf that chlorophyll content was measured, of each DHG in each treatment was measured according to the method of Xia et al. [31]. An LI-6400 portable photosynthesis system (LI-COR Inc., Lincoln, NE, USA) was used to measure the photosynthetic indexes between 9 o'clock and 11 o'clock in the morning. Five measurements were conducted at different points as 5 repetitions along the top leaf of each plant.

2.3.3. Biomass

After the measurement of chlorophyll content and photosynthetic, all plants were harvested and separated into shoots and roots and washed with distilled water. To determine the dry weight and elemental analysis, some of the samples were dried at 80 °C to a constant weight. The dry weight of shoot and root samples was measured.

2.3.4. Abscisic Acid (ABA), Cytokinin (CtK), and IndolE−3-acetic Acid (IAA) Content Determination

The other subsamples were wrapped with aluminum foil and immediately frozen in liquid nitrogen on 8 December. These samples were stored in a refrigerator at −80 °C for subsequent ABA, CtK, and IAA content determination by enzyme-linked immunosorbent assay (ELISA) according to the methods of Xu et al. [38].

2.3.5. Elemental Analysis

All shoot and root dried tissues were ground in an MM400 ball mill (Retsch, Germany) to obtain homogenous samples. The plant organic carbon (C) content was measured using a K_2CrO_7-H_2SO_4 oxidation method [50], and total nitrogen (N) and total phosphorus (P) content were determined by flow injection analysis (FIAstar 5000 Analyzer, FOSS Analytical, Hillerød, Denmark) [31]. The proportion of C, N, and P including C:N, C:P, and N:P was calculated.

2.4. Statistical Analysis

Data analyses were conducted using SPSS v20.0 (SPSS, Inc., Chicago, IL, USA). The effects of origin of seed, water content, and endophyte on biomass, nutrient content, photosynthetic indexes, and phytohormone content parameters were analyzed with a three-way ANOVA. An independent-sample t-test was used to determine the differences in all indictors in the present study. These included the differences between EI and EF under the same soil water content, or XH(W) and YZ(D) of EF/EI DHG, or XH(W) and YZ(D) maternal habitat type. Statistical significance was considered at p value < 0.05. Data shown in figures are means with their standard errors. Mapping was with Origin 9.0 (Origin Lab, Northampton, MA, USA).

3. Results

3.1. Biomass

Endophyte ($p < 0.001$), water content ($p < 0.001$), and the interaction between seed origin and water content ($p < 0.001$) significantly affected the shoot biomass (Table S1). At the 30% SWC, endophyte increased the shoot biomass of DHG from the YZ(D) site significantly ($p < 0.05$), with a difference of 23.09%. Importantly, the shoots biomass of YZ(D)EI plants was significantly higher than XH(W)EI ($p < 0.05$) at 30% and 60% SWC, with an increase of 29.21% and 37.65%, respectively. The shoots biomass of YZ(D)EF plants was also higher than XH(W)EF ($p < 0.05$) at the same SWC, with a relative increase of 20.53% and 26.17%, respectively. The differences of shoot biomass between the EI plants from the two sites are higher than the difference between the EF plants of the two sites at each same SWC (Figure 1).

The root biomass of seedlings was significantly affected by the seed origin ($p < 0.001$), water content ($p < 0.001$) and the interaction between seed origin and water content ($p < 0.001$) (Table S1). Endophyte increased the root biomass of DHG from XH(W) sites at 15% and 30% SWC significantly ($p < 0.05$), with a difference of 15.35% and 8.09%. Endophyte also increased the root biomass of YZ(D) DHG at 15% and 30% SWC significantly ($p < 0.05$), with a relative difference of 11.89% to 11.95%. Additionally, the root biomass of YZ(D)EI plants was higher than XH(W)EI at 15% SWC significantly ($p < 0.05$), with an increase of 9.01%, while the root biomass of YZ(D)EF plants was also higher than XH(W)EF at 15% SWC significantly, with a relative increase of 12.38% (Figure 1).

3.2. Phytohormones

ABA content of shoots was significantly affected by endophyte ($p < 0.001$), water content ($p < 0.001$), seed origin ($p < 0.001$), seed origin × water content ($p < 0.001$), and endophyte × water content ($p < 0.001$) (Table S1). Endophyte increased the ABA content of shoots of both XH(W) and YZ(D) DHG at 30% to 60% SWC significantly ($p < 0.05$), with a difference of 43.23% to 135.01%. The shoot ABA content of YZ(D) DHG was higher than

XH(W) DHG significantly ($p < 0.05$), with a relative difference of 20.54%. Importantly, the shoot ABA content of YZ(D)EI DHG was higher than XH(W)EI DHG significantly at 15% and 30% SWC ($p < 0.05$), with a difference of 27.99% and 27.08%. The shoot ABA content of YZ(D)EF plants was also higher than XH(W)EF DHG ($p < 0.05$) at 15%, 30%, and 45% SWC, with an increase of 27.96%, 28.19%, and 29.53%, respectively (Figure 2). The root ABA content was significantly affected by endophyte ($p < 0.001$), water content ($p = 0.001$), seed origin ($p < 0.001$), seed origin × water content ($p = 0.001$), and endophyte × water content ($p < 0.001$) (Table S1). Endophyte increased the ABA content of roots of DHG from the XH(W) and YZ(D) sites significantly at 15% to 60% SWC ($p < 0.05$), with a difference of 19.33% to 156.12%. The root ABA content of YZ(D) DHG was higher than XH(W) significantly ($p < 0.05$), with a relative difference of 20.18%. Importantly, the root ABA content of YZ(D)EI DHG was higher than XH(W)EI DHG significantly ($p < 0.05$) at 15% and 30% SWC, with a difference of 27.97% and 27.49%. The root ABA content of YZ(D)EF DHG was also higher than XH(W)EF DHG ($p < 0.05$) at each same SWC, with a relative increase of 28.84% and 30.99%, respectively (Figure 2).

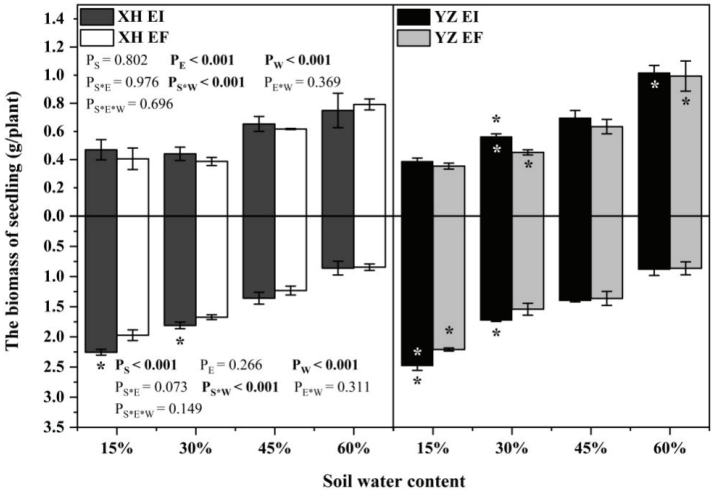

Figure 1. The biomass of *A.inebrians* seedlings shoots and roots from XH(W) and YZ(D) seeds under various soil water content (g/plant). Upwards and downwards bars represent the value of shoot and root part, respectively. The asterisk (*) above/below error bars means significant difference ($p < 0.05$) between EI and EF under the same soil water content. White/black * in the black/gray bars indicates significant difference ($p < 0.05$) between Xiahe and Yuzhong maternal habitat type of EF/EI grasses.

IAA content of shoots was only significantly affected by endophyte ($p < 0.001$) (Table S1). The shoots IAA content of XH(W)EI DHG were higher than XH(W)EF DHG significantly at 15% and 30% SWC, with a difference of 9.75% and 9.91%, respectively. Endophyte also increased the shoot IAA content of YZ(D) DHG at 15% SWC significantly ($p < 0.05$), with a difference of 18.27%. The shoots IAA content of YZ(D)EI DHG was lower than XH(W)EI significantly at 30% and 60% SWC ($p < 0.05$), with a decrease of 10.66% and 8.68%. The shoot IAA content of YZ(D)EF DHG was also lower than XH(W)EF DHG ($p < 0.05$) at 15% SWC, with a relative decrease of 13.99% (Figure 3). Endophyte ($p = 0.037$) significantly affected the root IAA content (Table S1). Endophyte increased the root IAA content of XH(W) DHG significantly ($p < 0.05$) at 15%, 30%, and 60% SWC, with a difference of 13.55%, 23.22%, and 16.48%, respectively. The root IAA content of YZ(D)EI DHG plants were higher than YZ(D)EF DHG at 30% SWC significantly, with a relative difference of 11.33%. The root IAA content of YZ(D)EI DHG was also lower than XH(W)EI DHG ($p < 0.05$) at 60% SWC, with a decrease of 15.61% (Figure 3).

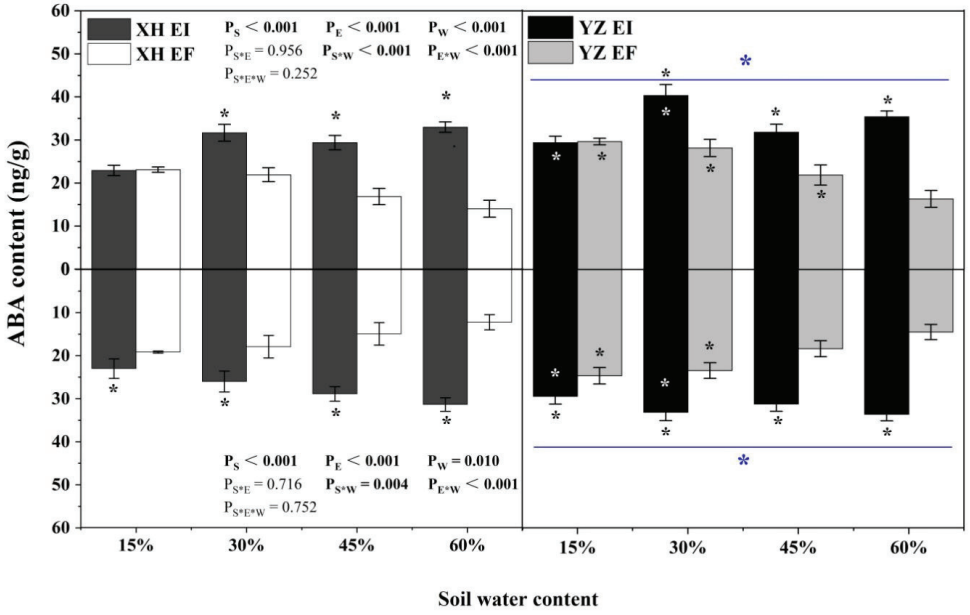

Figure 2. The ABA content of *A. inebrians* seedlings shoots and roots from XH(W) and YZ(D) seeds under various soil water content (ng/g). Upwards and downwards bars represent the value of shoot and root part, respectively. The asterisk (*) above/below error bars means significant difference ($p < 0.05$) between EI and EF under the same soil water content. White/black * in the black/gray bars indicates significant difference ($p < 0.05$) between Xiahe and Yuzhong maternal habitat type of EF/EI grasses. The blue * above/below full blue line indicates significant difference ($p < 0.05$) between Xiahe and Yuzhong maternal habitat type.

The shoot CtK content of DHG was significantly affected by endophyte ($p < 0.001$), water content ($p < 0.001$), seed origin ($p = 0.018$), endophyte × water content ($p = 0.008$), endophyte × seed origin ($p < 0.001$), and endophyte × water content × seed origin ($p = 0.028$) (Table S1). The shoot CtK content of XH(W)EI DHG was lower than XH(W)EF at significantly 15% to 45% SWC, with a difference of 11.47%, 16.60%, and 17.08%, respectively. Endophyte also decreased the shoot CtK content of YZ(D) DHG significantly ($p < 0.05$) at 15% and 30% SWC, with a relative decrease of 16.33% and 17.64%. Additionally, YZ(D) DHG had a lower CtK content of shoots than XH(W) significantly ($p < 0.05$), with a difference of 2.71%. The shoot CtK content of YZ(D)EI DHG was lower than XH(W)EI DHG significantly ($p < 0.05$) at 60% SWC, with a relative decrease of 10.04% (Figure 4). The root CtK content of DHG was significantly affected by endophyte ($p < 0.001$), water content ($p < 0.001$), seed origin ($p < 0.001$), seed origin × water content ($p = 0.027$), endophyte × water content ($p < 0.001$) and endophyte × water content × seed origin ($p = 0.002$) (Table S1). Endophyte decreased the root CtK content of XH(W) DHG ($p < 0.05$) at 15%, 30%, and 60% SWC significantly, with a decrease of 10.13%, 18.48%, and 10.66%, respectively. It also decreased the root CtK content of YZ(D) DHG significantly ($p < 0.05$) at 15%, 30%, and 45% SWC, with a relative decrease of 14.42%, 11.67%, and 4.50%, respectively. Additionally, YZ(D) DHG had higher root CtK content than XH(W) DHG significantly ($p < 0.05$). Importantly, the root CtK content of YZ(D)EI DHG was higher than XH(W)EI DHG significantly ($p < 0.05$) at 60% SWC, with a relative increase of 10.72%, respectively. The root CtK content of YZ(D)EF DHG was also higher than XH(W)EF DHG ($p < 0.05$) at 15% and 45% SWC, with an increase of 9.93% and 5.87%, respectively (Figure 4).

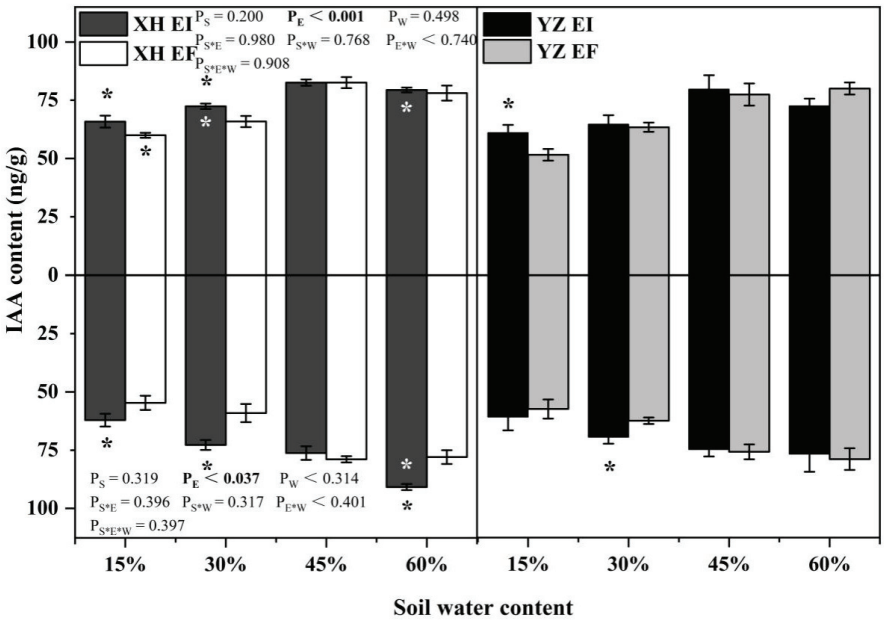

Figure 3. The IAA content of *A. inebrians* seedlings shoots and roots from XH(W) and YZ(D) seeds under various soil water content (ng/g). Upwards and downwards bars represent the value of shoot and root part, respectively. The asterisk (*) above/below error bars means significant difference ($p < 0.05$) between EI and EF under the same soil water content. White/black * in the dark gray/white bars indicates significant difference ($p < 0.05$) between Xiahe and Yuzhong maternal habitat type of EF/EI grasses.

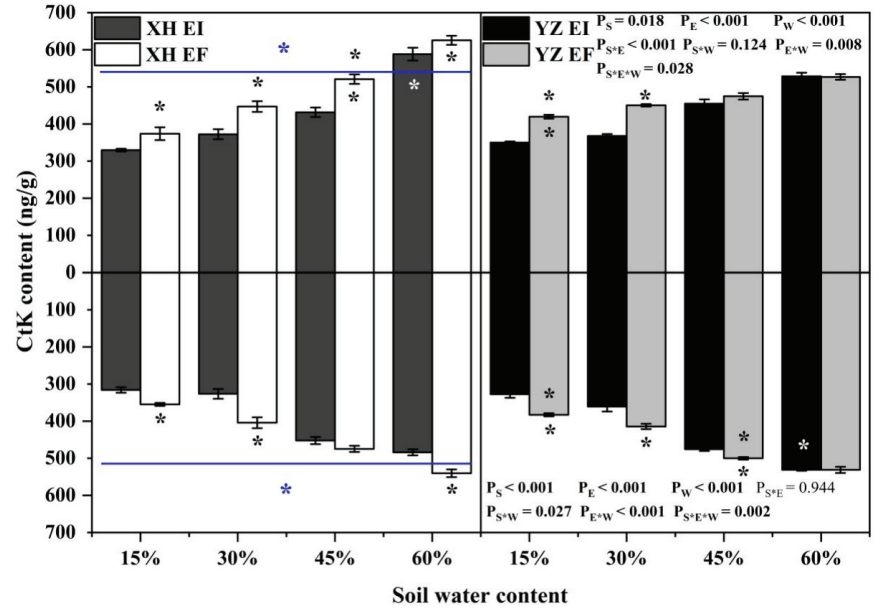

Figure 4. The CtK content of *A. inebrians* seedlings shoots and roots from XH(W) and YZ(D) seeds under various soil water content (ng/g). Upwards and downwards bars represent the value of shoot

and root part, respectively. The asterisk (*) above/below error bars means significant difference ($p < 0.05$) between EI and EF under the same soil water content. White/black * in the white, black and gray bars indicates significant difference ($p < 0.05$) between Xiahe and Yuzhong maternal habitat type of EF/EI grasses. The blue * above/below full blue line indicates significant difference ($p < 0.05$) between Xiahe and Yuzhong maternal habitat type.

3.3. Photosynthetic Indexes

Chlorophyll content was significantly affected by endophyte ($p < 0.001$), water content ($p < 0.001$), seed origin ($p < 0.001$), endophyte × water content ($p = 0.004$), endophyte × seed origin ($p = 0.013$), water content × seed origin ($p = 0.038$) (Table S2). Endophyte increased the chlorophyll content of YZ(D) DHG at the 15% to 45% SWC significantly ($p < 0.05$), with a relative difference of 12.56%, 13.12%, and 9.60%, respectively. At the 15% and 30% SWC, endophyte increased the chlorophyll content of XH(W) DHG significantly ($p < 0.05$). YZ(D) DHG had a significantly higher chlorophyll content than XH(W) DHG ($p < 0.05$). Importantly, the chlorophyll content of YZ(D)EI DHG was higher than XH(W)EI DHG significantly at 45% and 60% SWC ($p < 0.05$), with an increase of 4.84% and 10.71%, respectively (Figure 5).

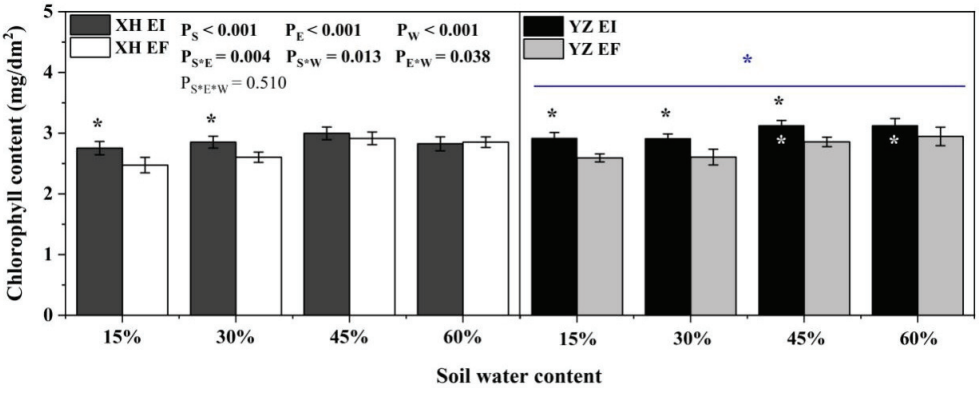

Figure 5. The chlorophyll content of *A. inebrians* seedlings shoots from XH(W) and YZ(D) seeds under various soil water content (mg/dm^2). The asterisk (*) above/below error bars means significant difference ($p < 0.05$) between EI and EF under the same soil water content. White * in the black bars indicates significant difference ($p < 0.05$) between Xiahe and Yuzhong maternal habitat type of EF/EI grasses. The blue * above/below full blue line indicates significant difference ($p < 0.05$) between Xiahe and Yuzhong maternal habitat type.

Net photosynthetic rate of DHG was significantly affected by endophyte ($p < 0.001$), water content ($p < 0.001$), seed origin ($p < 0.001$), endophyte × water content ($p < 0.001$), water content × seed origin ($p < 0.001$) and endophyte × water content × seed origin ($p < 0.001$) (Table S2). The photosynthetic rate of EI DHG was higher than EF DHG from both the XH(W) and YZ(D) site under each SWC significantly ($p < 0.05$). Importantly, YZ(D) DHG had a higher photosynthetic rate than XH(W) DHG significantly ($p < 0.05$), with an increase of 39.53%. Additionally, the photosynthetic rate of YZ(D)EI DHG was higher than those from the XH(W)EI DHG significantly ($p < 0.05$) at 30% to 60% SWC, with a relative increase of 43.16%, 40.04%, and 30.22%, respectively. The net photosynthetic rate of YZ(D)EF DHG was also higher than XH(W)EF DHG ($p < 0.05$) at each same SWC, with an increase of 31.20%, 94.50%, and 41.13%, respectively. The difference of photosynthetic rate between the EI DHG from the two sites is higher than the difference between the EF DHG of the two sites at a relative drought of 30% SWC (Figure 6A).

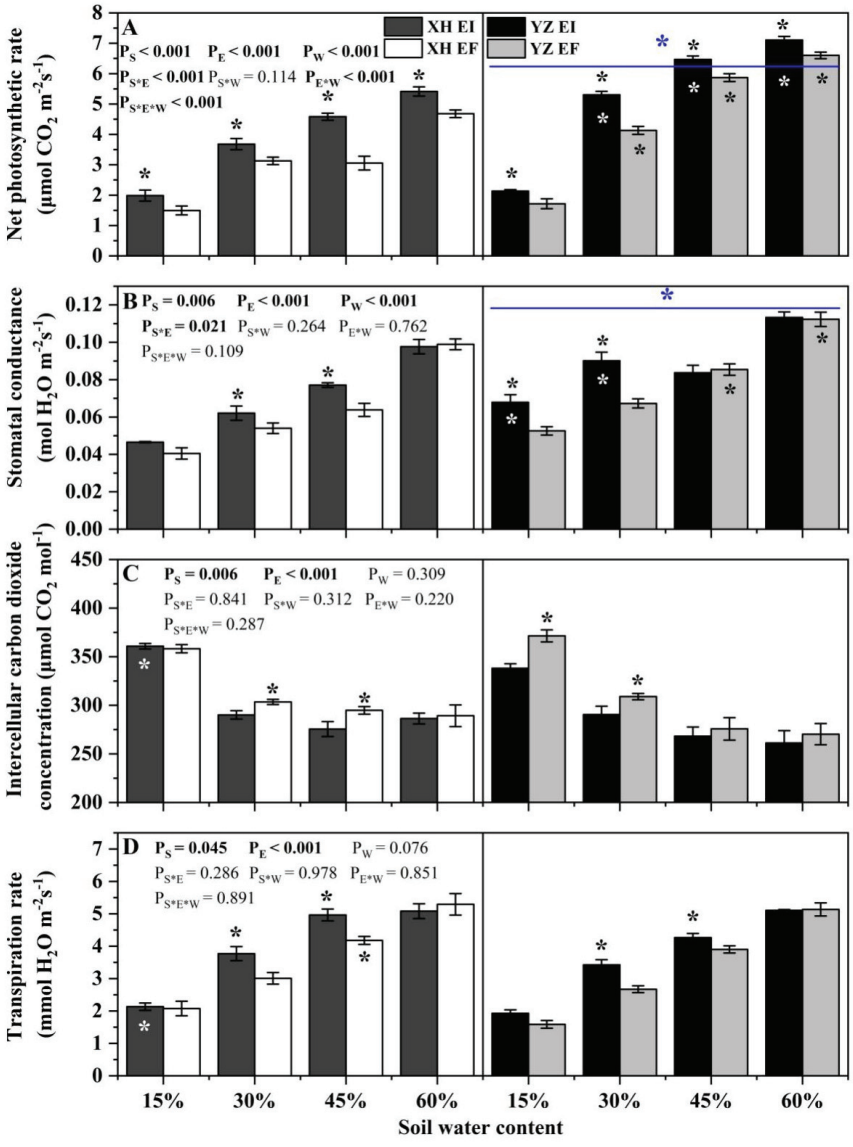

Figure 6. The photosynthetic parameters of *A. inebrians* seedlings shoots from XH(W) and YZ(D) seeds under various soil water content. (**A**) Net photosynthetic rate (μmol CO_2 $m^{-2}s^{-1}$), (**B**) Stomatal conductance (mol H_2O $m^{-2}s^{-1}$), (**C**) Intercellular carbon dioxide concentration (μmol CO_2 mol^{-1}), (**D**) Transpiration rate (mmol H_2O $m^{-2}s^{-1}$). The asterisk (*) above error bars means significant difference ($p < 0.05$) between EI and EF under the same soil water content. White/black * in the dark gray, black and gray bars indicates significant difference ($p < 0.05$) between Xiahe and Yuzhong maternal habitat type of EF/EI grasses. The blue * above/below full blue line indicates significant difference ($p < 0.05$) between Xiahe and Yuzhong maternal habitat type.

The stomatal conductance of DHG was significantly affected by endophyte ($p = 0.006$), water content ($p < 0.001$), seed origin ($p < 0.001$) and endophyte × water content ($p = 0.021$) (Table S2). Endophyte increased the stomatal conductance of XH(W) DHG under 30% and 45% SWC significantly, with a difference of 15.67% and 21.53%, respectively. At the 15% and

30% SWC, endophyte also increased the stomatal conductance of YZ(D) DHG significantly ($p < 0.05$). YZ(D) DHG had higher stomatal conductance than XH(W) DHG significantly ($p < 0.05$), with an increase of 23.87%. Additionally, the stomatal conductance of YZ(D)EI DHG was higher than XH(W)EI DHG ($p < 0.05$) at 15% and 30% SWC significantly, with a relative increase of 44.48% and 43.68%, respectively. The stomatal conductance of YZ(D)EF DHG was also higher than XH(W)EF DHG ($p < 0.05$) at 45% and 60% SWC, with an increase of 34.10% and 13.41%, respectively (Figure 6B).

Intercellular carbon dioxide concentration was significantly affected by endophyte ($p = 0.006$) and water content ($p < 0.001$) (Table S2). Endophyte decreased the intercellular carbon dioxide concentration of XH(W) DHG under 30% and 45% SWC significantly, with a difference of 4.13% and 6.32%, respectively. At the 15% and 30% SWC, endophyte also decreased the intercellular carbon dioxide concentration of YZ(D) DHG significantly ($p < 0.05$), with a difference of 9.17% and 5.80%, respectively. In addition, the intercellular carbon dioxide concentration of YZ(D)EI DHG was lower than XH(W)EI DHG ($p < 0.05$) at 15% SWC significantly, with a relative decrease of 6.02% (Figure 6C).

Transpiration rate was significantly affected by endophyte ($p = 0.045$) and water content ($p < 0.001$) (Table S2). Endophyte significantly increased the transpiration rate of XH(W) DHG at 30% and 45% SWC, with a difference of 27.72% and 18.53%, respectively. Endophyte also significantly increased the transpiration rate of YZ(D) DHG at the same SWC, with a relative difference of 29.67% and 9.17%, respectively. Additionally, the transpiration rate of YZ(D)EI DHG was significantly lower than XH(W)EI DHG ($p < 0.05$) at 15% SWC, with a relative decrease of 11.86%. The transpiration rate of YZ(D)EF DHG was also lower than XH(W)EF DHG ($p < 0.05$) at 45% SWC, with a decrease of 7.74% (Figure 6D).

3.4. Elements and Stoichiometry

The C content of shoots was significantly affected by endophyte ($p = 0.001$) and water content ($p < 0.001$) (Table S3). The root C content was affected by water content significantly ($p = 0.013$) (Table S3). XH(W)EI DHG had higher shoot C content than XH(W)EF DHG with a relative increase of 13.35% at 15% SWC significantly ($p < 0.05$) (Figure 7).

The shoot N content was affected by endophyte ($p < 0.001$), water content ($p < 0.001$), seed origin ($p < 0.001$), endophyte × water content ($p = 0.002$), water content × seed origin ($p = 0.002$) and endophyte × seed origin ($p = 0.001$) significantly (Table S3). Endophyte increased the N content of shoots of XH(W) DHG significantly ($p < 0.05$) by 12.42% and 15.47% at 15% and 30% SWC, respectively. Endophyte also increased the shoot N content of YZ(D) DHG significantly ($p < 0.05$) by 30.99% and 27.14% at 15% and 30% SWC, respectively. Further, YZ(D) DHG had significantly lower shoot N content than XH(W) DHG ($p < 0.05$) by 7.72%. The shoot N content of YZ(D)EI DHG was lower than XH(W)EI DHG ($p < 0.05$) at 60% SWC significantly, with a relative decrease of 10.71%. The shoot N content of YZ(D)EF DHG was also lower than XH(W)EF DHG ($p < 0.05$) at 15% to 60% SWC, with a decrease of 17.63% to 19.06% (Figure 8). The root N content was significantly affected by endophyte ($p < 0.001$), water content ($p < 0.001$), seed origin ($p < 0.001$), endophyte × seed origin ($p = 0.001$) and endophyte × water content × seed origin ($p < 0.001$) (Table S3). Endophyte increased the root N content of DHG significantly ($p < 0.05$) from the XH(W) site at 15% and 30% SWC, with a relative increase of 18.76% and 26.26%, respectively. Importantly, YZ(D) DHG had lower N root content than XH(W) site significantly ($p < 0.05$) by 12.40%. The root N content of YZ(D)EI DHG was significantly lower XH(W)EI DHG ($p < 0.05$) at 15% and 30% SWC, with a relative decrease of 14.37% and 15.18, respectively. The root N content of YZ(D)EF DHG was also lower than XH(W)EF DHG ($p < 0.05$) at 30% and 45% SWC, with a decrease of 17.70% and 12.64% (Figure 8).

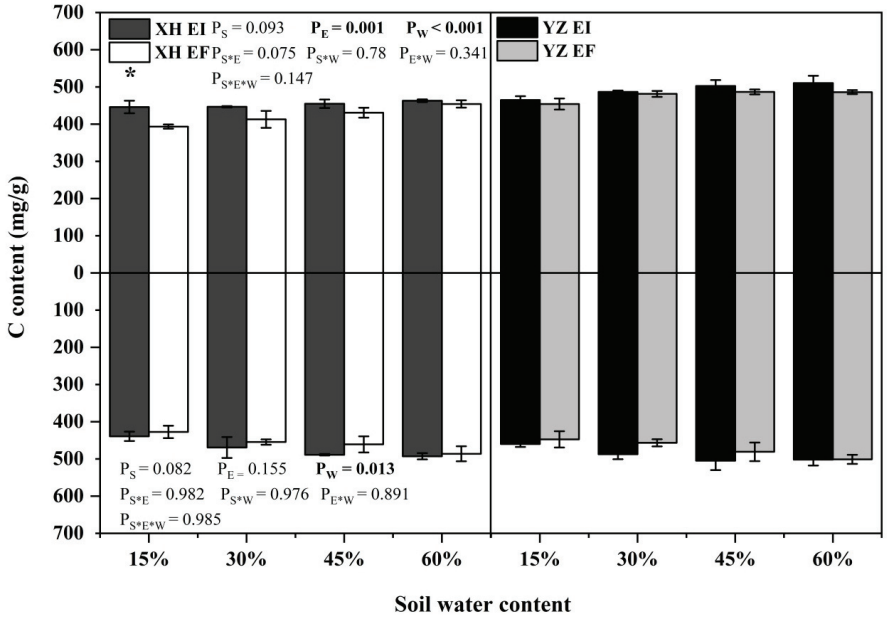

Figure 7. The C content of *A. inebrians* seedlings shoots and roots from XH(W) and YZ(D) seeds under various soil water content (mg/g). Upwards and downwards bars represent the value of shoot and root part, respectively. The asterisk (*) above error bars means significant difference ($p < 0.05$) between EI and EF under the same soil water content.

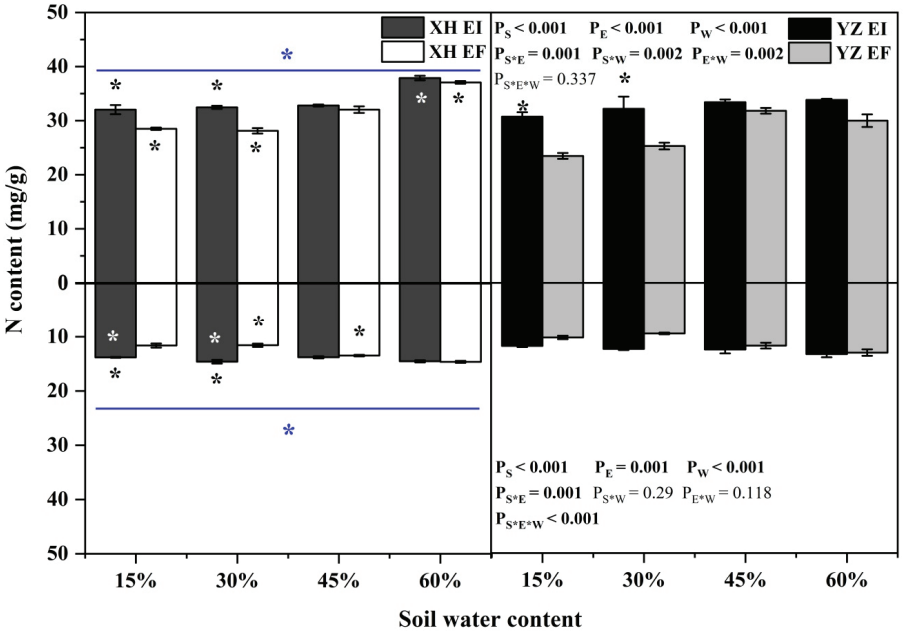

Figure 8. The N content of *A. inebrians* seedlings shoots and roots from XH(W) and YZ(D) seeds under various soil water content (mg/g). Upwards and downwards bars represent the value of shoot and root part, respectively. The asterisk (*) above/below error bars means significant difference

($p < 0.05$) between EI and EF under the same soil water content. White/black * in the dark gray/white bars indicates significant difference ($p < 0.05$) between Xiahe and Yuzhong maternal habitat type of EF/EI grasses. The blue * above/below full blue line indicates significant difference ($p < 0.05$) between Xiahe and Yuzhong maternal habitat type.

The shoot P content was significantly affected by endophyte ($p = 0.004$), seed origin ($p < 0.001$) and water content ($p < 0.001$) (Table S3). The shoot P content of both EI and EF DHG from the YZ(D) and XH(W) sites increased as the SWC increasing. Endophyte increased the shoot P content of XH(W) DHG significantly ($p < 0.05$) at 15% and 30% SWC, with an increase of 50.36% and 26.24%, respectively. The shoot P content of YZ(D)EI DHG was higher than YZ(D)EF DHG under 15% and 30% SWC significantly ($p < 0.05$) by 16.63% and 23.49%, respectively. Importantly, YZ(D) DHG had higher shoot P content than XH(W) DHG significantly ($p < 0.05$) by 90.08%. Additionally, YZ(D)EI DHG had a significantly higher shoot P content than XH(W)EI DHG at each SWC ($p < 0.05$), with a relative increase of 170.37%, 138.03%, 84.36%, and 84.29%, respectively. The shoot P content of YZ(D)EF DHG was also higher than XH(W)EF DHG ($p < 0.05$) at each same SWC, with an increase of 248.55%, 143.33%, 76.75%, and 96.57%, respectively. The differences of shoot P content between the EI from the two sites are higher than the difference between the EF of the two sites at 45% SWC (Figure 9). The root P content was significantly affected by endophyte ($p < 0.001$), water content ($p = 0.021$), and endophyte × water content ($p = 0.018$) (Table S3). Endophyte significantly increased the root P content of XH(W) DHG at 15% and 30% SWC ($p < 0.05$), with a relative increase of 30.05% and 44.69%, respectively. The root P content of YZ(D)EI DHG was higher than YZ(D)EF DHG under 15% and 30% SWC significantly ($p < 0.05$), with an increase of 7.6% and 16.94%, respectively. In addition, the root P content of YZ(D)EF DHG was also higher than XH(W)EF DHG ($p < 0.05$) at 15% and 30% SWC by 23.47% and 20.13% (Figure 9).

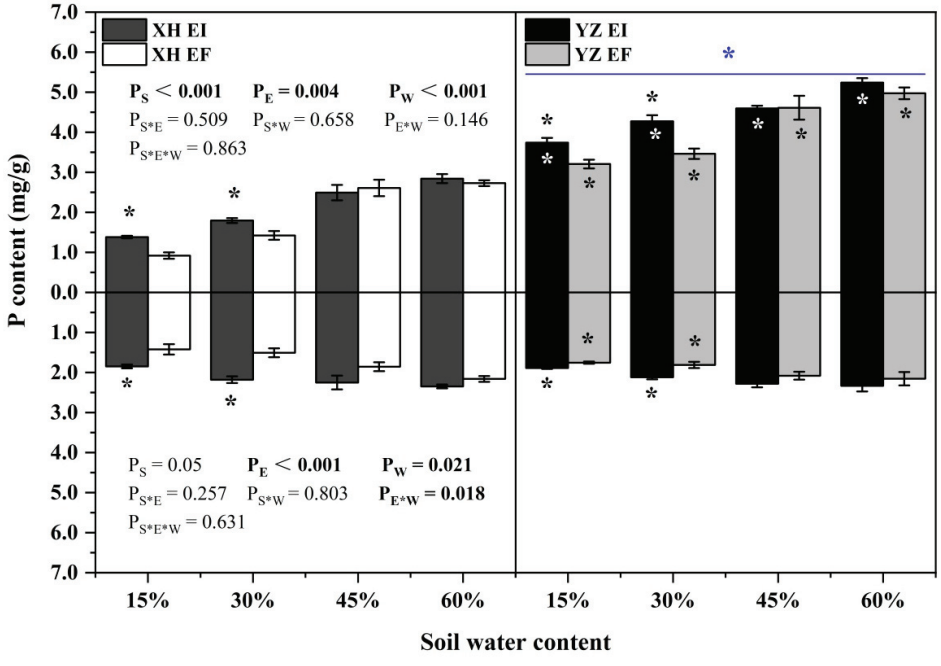

Figure 9. The P content of *A. inebrians* seedlings growth shoots and roots from XH(W) and YZ(D) seeds under various soil water content (mg/g). Upwards and downwards bars represent the value of shoot and root part, respectively. The asterisk (*) above/below error bars means significant difference

($p < 0.05$) between EI and EF under the same soil water content. White/black * in the black/gray bars indicates significant difference ($p < 0.05$) between Xiahe and Yuzhong maternal habitat type of EF/EI grasses. The blue * above/below full blue line indicates significant difference ($p < 0.05$) between Xiahe and Yuzhong maternal habitat type.

The shoot C:N ratio was significantly affected by endophyte ($p < 0.001$), water content ($p < 0.001$), seed origin × endophyte ($p < 0.001$), endophyte × water content ($p = 0.002$), seed origin × water content ($p = 0.022$) and endophyte × water content × seed origin ($p = 0.046$) (Table S4). The shoot C:N ratio of XH(W)EI DHG was lower than XH(W)EF DHG significantly ($p < 0.05$) at 30% SWC by 6.51%. Endophyte decreased the shoot C:N ratio from the YZ(D) site at 15% and 30% SWC significantly ($p < 0.05$), with a decrease of 21.83% and 19.85%, respectively. The shoot C:N ratio of YZ(D)EI DHG was higher than XH(W)EI DHG ($p < 0.05$) at 60% SWC significantly by 14.60%. The shoot C:N ratio of YZ(D)EF DHG was also higher than XH(W)EF DHG ($p < 0.05$) at 15%, 30%, and 60% SWC, with a relative increase of 30.08%, 20.00%, and 23.43% (Figure 10). The root C:N ratio was significantly affected by endophyte ($p = 0.018$), seed origin ($p = 0.005$) and endophyte × water content ($p = 0.041$) (Table S4). Endophyte decreased the C:N ratio of roots significantly ($p < 0.05$) from the XH(W) site at 15% and 30% SWC, with a decrease of 13.34% and 18.47%, respectively. The root C:N ratio of YZ(D)EI DHG was lower than YZ(D)EF DHG significantly ($p < 0.05$) at 30% SWC by 18.02%. Importantly, YZ(D) DHG had a significantly higher root C:N ratio of roots than XH(W) DHG ($p < 0.05$), with an increase of 9.86%. The root C:N ratio of YZ(D)EF DHG was also higher than XH(W)EF DHG ($p < 0.05$) at 30% SWC by 13.25% (Figure 10).

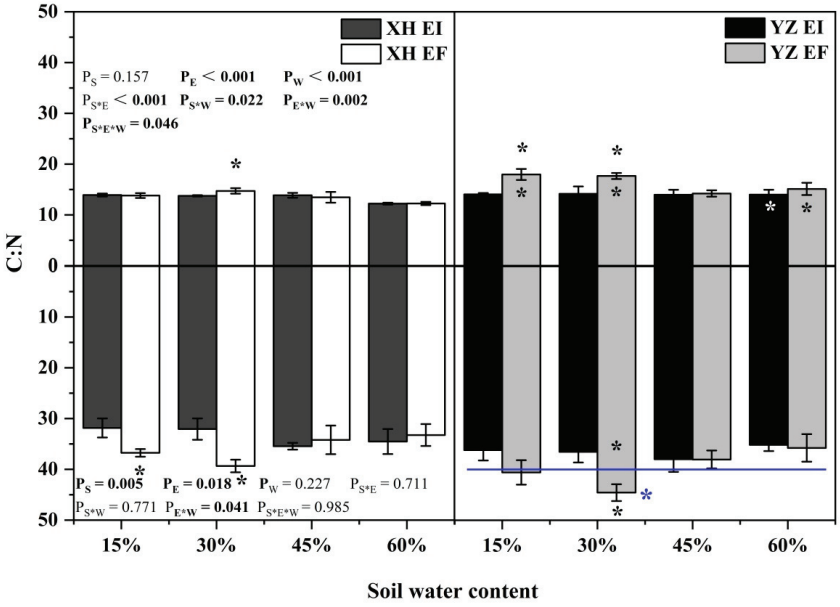

Figure 10. The C:N content of *A. inebrians* seedlings shoots and roots from XH(W) and YZ(D) seeds under various soil water content. Upwards and downwards bars represent the value of shoot and root part, respectively. The asterisk (*) above/below error bars means significant difference ($p < 0.05$) between EI and EF under the same soil water content. White/black * in the black/gray bars indicates significant difference ($p < 0.05$) between Xiahe and Yuzhong maternal habitat type of EF/EI grasses. The blue * above/below full blue line indicates significant difference ($p < 0.05$) between Xiahe and Yuzhong maternal habitat type.

The shoot C:P ratio was significantly affected by seed origin ($p < 0.001$), endophyte ($p = 0.025$), water content ($p < 0.001$), endophyte × water content ($p = 0.036$), and seed origin × water content ($p < 0.001$) (Table S4). Endophyte decreased the shoot C:P ratio from the XH(W) site at 15% SWC significantly ($p < 0.05$) by 25.05%. The shoot C:P ratio of YZ(D)EI DHG was lower than YZ(D)EF DHG at 15% and 30% SWC significantly ($p < 0.05$). Importantly, YZ(D) DHG had a lower shoot C:P ratio than XH(W) DHG significantly ($p < 0.05$), with a decrease of 57.19%. Additionally, the shoot C:P ratio of YZ(D)EI DHG was significantly lower than XH(W)EI DHG ($p < 0.05$) at each SWC, with a relative decrease of 64.31%, 59.64%, 47.65%, and 44.19%, respectively. The shoot C:P ratio of YZ(D)EF DHG was also lower than XH(W)EF DHG ($p < 0.05$) at each same SWC, with a decrease of 69.41%, 56.21%, 41.36%, and 49.91%, respectively (Figure 11). Endophyte ($p = 0.002$), seed origin ($p = 0.006$) and water content ($p = 0.024$) significantly affected the root C:P ratio (Table S4). The root C:P ratio decreased as SWC increasing. Endophyte decreased the root XH(W) DHG C:P ratio at 15% and 30% SWC significantly ($p < 0.05$) by 21.02% and 25.57%. The root C:P ratio of YZ(D)EI DHG was significantly lower than YZ(D)EF DHG at 30% SWC ($p < 0.05$). YZ(D) DHG had a lower root C:P ratio than XH(W) DHG significantly ($p < 0.05$), with a relative decrease of 10.22%. The root C:P ratio of YZ(D)EF DHG was also lower than XH(W)EF DHG ($p < 0.05$) at 15% and 30% SWC by 21.26% and 18.89% (Figure 11).

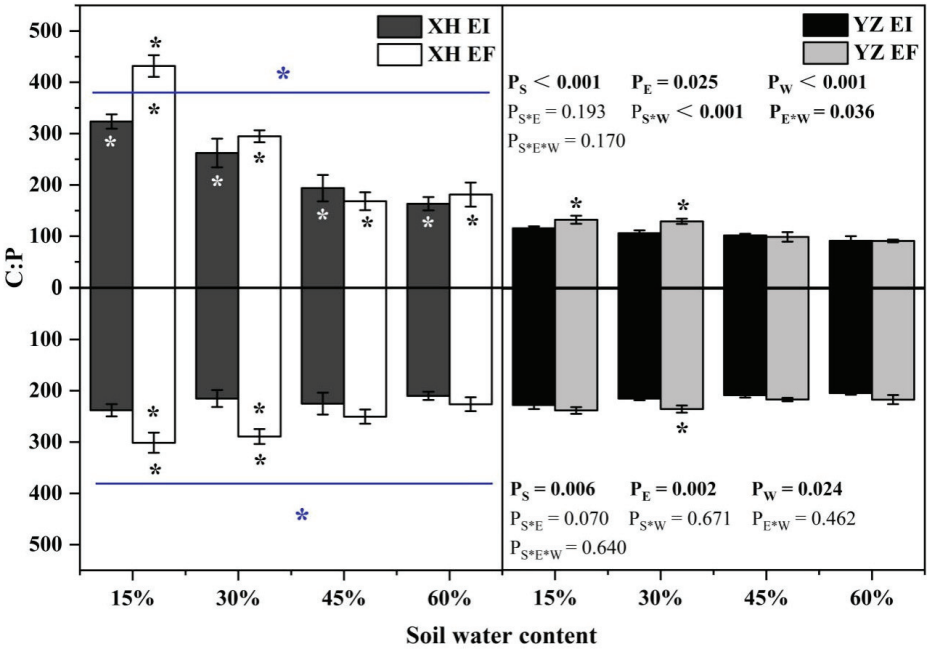

Figure 11. The C:P content of *A. inebrians* seedlings shoots and roots from XH(W) and YZ(D) seeds under various soil water content. Upwards and downwards bars represent the value of shoot and root part, respectively. The asterisk (*) above/below error bars means significant difference ($p < 0.05$) between EI and EF under the same soil water content. White/black * in the dark gray/white bars indicates significant difference ($p < 0.05$) between Xiahe and Yuzhong maternal habitat type of EF/EI grasses. The blue * above/below full blue line indicates significant difference ($p < 0.05$) between Xiahe and Yuzhong maternal habitat type.

The N:P ratio of shoots was significantly affected by seed origin ($p < 0.001$), and water content ($p < 0.001$), and the interaction between seed origin and water content ($p < 0.001$) was significantly affected (Table S4). Endophyte decreased the XH(W) DHG N:P ratio of shoots at 15% SWC significantly ($p < 0.05$). However, the shoot N:P ratio of EI DHG

was higher than EF DHG from the YZ(D) site significantly ($p < 0.05$) at 15% SWC, with an increase of 12.08%. In addition, YZ(D) DHG had a significantly lower shoot N:P ratio than XH(W) DHG ($p < 0.05$). Importantly, the N:P ratio of shoots of YZ(D)EI DHG was lower than XH(W)EI DHG at 15% and 60% SWC significantly ($p < 0.05$), with a decrease of 64.59% and 51.33%, respectively. The shoot N:P ratio of YZ(D)EF DHG was also lower than XH(W)EF DHG ($p < 0.05$) at 15% to 60% SWC, with a relative decrease of 76.55%, 64.32%, 43.94%, and 59.18%, respectively (Figure 12). Seed origin ($p < 0.001$), water content ($p = 0.024$) and seed origin × endophyte ($p = 0.028$) significantly affected the root N:P ratio (Table S4). The root N:P ratio of XH(W)EI DHG was lower than XH(W)EF DHG at 30% SWC significantly ($p < 0.05$) by 8.83%. In addition, YZ(D) DHG had a significantly lower root N:P ratio than XH(W) DHG ($p < 0.05$). Further, the root N:P ratio of YZ(D)EI DHG was lower than XH(W)EI DHG significantly ($p < 0.05$) at 15% and 30% SWC, with a decrease of 16.13% and 12.67%. The root N:P ratio of YZ(D)EF DHG was also lower than XH(W)EF DHG ($p < 0.05$) at 15% to 45% SWC, with a relative decrease of 28.59%, 28.37%, and 22.60%, respectively (Figure 12).

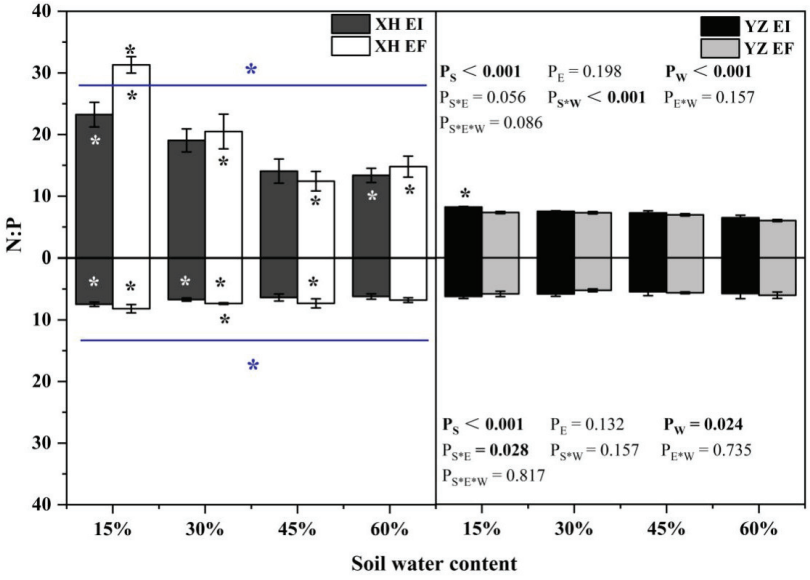

Figure 12. The N:P content of *A. inebrians* seedlings shoots and roots from XH(W) and YZ(D) seeds under various soil water content. Upwards and downwards bars represent the value of shoot and root part, respectively. The asterisk (*) above/below error bars means significant difference ($p < 0.05$) between EI and EF under the same soil water content. White/black * in the dark gray/white bars indicates significant difference ($p < 0.05$) between Xiahe and Yuzhong maternal habitat type of EF/EI grasses. The blue * above/below full blue line indicates significant difference ($p < 0.05$) between Xiahe and Yuzhong maternal habitat type.

4. Discussion

The present study showed the *Epichloë* endophyte improved the drought stress tolerance of DHG. The growth, photosynthetic efficiency, phytohormones content and C, N and P content of EI DHG was higher than the EF DHG under water deficiency conditions. Moreover, DHG from the seeds of the YZ(D) site is more competitive than from those of the XH(W) site under drought conditions. The differences of the shoots biomass, photosynthetic rate and P content of shoots between the EI plants from the seed of the two sites is higher than the differences between the EF plants of the two sites. On the contrary, the differences of the CtK content of shoots between the EI plants from the two sites are lower than the differences between the EF plants of the two sites. A positive stimulus of maternal

drought tolerance on progeny plant growth at certain conditions through the symbiotic association with *Epichloë* endophyte was found in the present study.

Previous studies have illustrated that *Epichloë* endophytes can improve the drought resistance of host plant, as revealed through the improved growth and biomass of host [51]. In the present study, EI plants had more shoot dry biomass than EF plants at drought stress, which means more photosynthetic products accumulated in plants to enhance survival through the adverse growth conditions [52]. Root mass and efficiency, as the most vital water-absorbing organ, is extremely important for maintaining plant growth, especially in arid environments [53]. Root dry biomass of EI plants was also higher than EF plants, and this is similar to several early studies that have reported that the *Epichloë* endophyte could increase root dry matter, improving water uptake from the soil to enhance drought resistance [54]. However, the results of previous studies of the effects of *Epichloë* endophytes about growth indicators were equivocal. Some studies suggest that these endophytes can promote the growth of symbionts under drought stress [55,56], while other results indicate that endophytes have no effect upon host growth [57,58], and even have a negative effect, inhibiting the growth of symbionts [59,60].

Phytohormones play central roles in integrating various environmental cues with endogenous growth programs, which can regulate various aspects of plant growth and development, as well as the responses of plants to abiotic and biotic stresses [37]. ABA is the most studied phytohormone; its synthesis is one of the fastest responses of plants to abiotic stress [61]. ABA is involved in the synthesis of stress-induced proteins to help in maintaining cellular water status and to protect other proteins, enzymes and cellular organelles from collapsing under water stress [62]. In the present experiment, the *Epichloë* endophyte significantly increased the ABA content in leaves and roots at different water contents. Therefore, it is speculated that these endophytes can improve the drought tolerance of the host by promoting the synthesis and accumulation of ABA in host grasses [38,39]. IAA participates in drought stress tolerance in various physiological activities to regulate plant growth and development [39,63]. Its content increased in various plant organs subjected to water deficit [64], which promoted water uptake into the protoplasts [65]. A previous study has found that an *Epichloë* endophyte can increase IAA content in symbionts to enhance the growth and development of host grasses under drought stress conditions [66]. In the present study, similar results were obtained, which were based on the results of growth indicators of host grasses. The upregulation of IAA content may be one of the methods that *Epichloë* endophytes improve the drought resistance of host grasses. However, these adjustments were not accomplished independently by one or two hormones but by crosstalk between the different phytohormones that resulted in synergetic or antagonistic interactions [35]. CtK could down-regulate ABA content [67,68]. The elevated drought resistance of plants may be attributed to the expression of the majority of CtK genes being down-regulated and a reduction in CtK levels when the plants were exposed to water-limiting conditions [69]. Early research has shown that *Epichloë* endophytes decreased the CtK content under drought stress [38]. This is similar to the present results.

In addition to the above-mentioned effects, phytohormones also significantly affect photosynthesis through regulating stomata, such as ABA involvement with the closure of stomata [70]. The CtK triggers responses to delay stomatal closure or stimulate stomatal opening [37,71]. Photosynthesis is a fundamental process of converting atmospheric carbon dioxide (CO_2) into organic compounds in the leaves of green plants. This process is mainly affected by light intensity, water, carbon dioxide concentration and photosynthetic pigments, which is limited by various factors such as carboxylation capacity and stomatal conductance [34]. Previous studies on the drought resistance of tall fescue (*Festuca arundinacea*) and meadow fescue (*F. pratensis*) found that endophyte can promote stomatal closure of host grasses and effectively maintain plant water. Lower stomatal conductance enables the plants to have a strong competitiveness in the process of drought tolerance [72,73]. However, stomatal closure can also negatively affect plant growth rate since it reduces carbon dioxide (CO_2) uptake, which is closely related to the efficiency of photosynthe-

sis [74]. The present research indicated the *Epichloë* endophytes significantly increased the stomatal conductance of DHG. Higher stomatal conductance is beneficial to the exchange of CO_2 and increases photosynthetic efficiency, a key determinant of plant growth under drought stress [75]. It was a possible function fulfilled by *Epichloë* endophytes to change host plant metabolism process from defense to growth and reproduction by allowing the plant to use limited resources for photosynthesis and C assimilation. The shift from defense to growth results in increasing growth rates, early flowering, and the allocation of more resources to reproduction to maximize resource use while water is available, which enables plants to finish seed production in maximize fitness [76]. The C assimilation is primarily by photosynthesis [77]. The *Epichloë* endophyte increased the photosynthetic capacity of the host grass under different conditions [31,38], thereby increasing the C concentration of the host. Comparing EI and EF DHG in the present study, the significant difference of C concentration only appeared at severe drought stress condition (15% SWC), but EI DHG had a higher C concentration than EF DHG at the other SWC. Although the *Epichloë* endophyte did not significantly increase the C concentration, the EI DHG had a greater biomass than EF DHG. Therefore, EI plants generally contained more C content, a consequence of the increase in the photosynthetic capacity from the presence of the *Epichloë* endophyte. N and P assimilation occurs by nutrient uptake in soil, which is different from C. The ability of plants to absorb and transport nutrients through the root system was positive correlated with plant transpiration [40,78]. Plants reduce water loss after the sensing of soil water deficit through changed stomatal conductance by the control of stomatal behavior [70]; this occurrence then leads to a decrease in the absorption of N and P from soil. The present experimental results confirmed these inferences that drought stress significantly inhibited the N and P assimilation of DHG by significantly reducing the transpiration of DHG. The presence of the *Epichloë* endophyte increased the photosynthetic ability and transpiration rate under water deficit stress, which provided energy for the uptake and transportation of N and P [40,78]. Moreover, previous research has indicated that EI plants had more phosphate-solubilizing fungal (PSF) diversity in their rhizosphere soil [79] or secreted more acid phosphatase by roots than of EF plants [80]. The positive association between a higher PSF diversity and acid phosphatase secretion by roots, and P-solubilization activity in the soil would generate an increase in P available for plant assimilation [81]. Thus, the *Epichloë* endophyte also makes a contribution for host plant P absorption by improving the P pool in the rhizosphere indirectly, making P available to the host plant [82]. This could be another reason why EI DHG had higher P concentration than EF DHG in the present study.

The element N is an important component of alkaloids [83–85]. The increase in N concentration may be related to the alkaloid synthesis of the host. *Epichloë* endophytes confer protection for the host grass against various stresses from the production of alkaloids [86]. Higher ergonovine alkaloids and ergine alkaloids levels were recorded for DHG under drought stress [87]. Previous research has also indicated that proline in the symbionts can be converted into precursor compounds of ergot alkaloids or loline under drought stress [88,89]. Therefore, changes in the content of alkaloid can also be regarded as an effective way of osmotic regulation to protect plants under water deficit stress [90]. P is an essential element for plant growth [91]. As we know, rRNA is needed to satisfy the demand of protein synthesis for enhancing the growth ability or/and improving various stress resistances [92,93]. Varying P levels in organisms may be partly caused by the allocation of P to the rRNA. Thus, increased N and P content may be one of the causes why the *Epichloë* endophyte enhanced the growth ability of host plants under water deficient condition.

Plant growth rate has intrinsic linkage with tissue elemental stoichiometry [40]. The growth rate hypothesis (GRH) indicates that higher growth rates are related to lower C:N and C:P ratios [94]. The health and growth status of plants could be reflected by the ratio of C:N and C:P [93]. The present study indicated that the ratios of C:N and C:P of plants were significantly higher under drought stress, and EF DHG had higher ratios of C:N and C:P. These results could explain why drought stress significantly reduced the growth rate of plants, and the *Epichloë* endophyte effectively alleviated the effect of drought on the growth

of the host plant. Additionally, it is possible that the lower C:N ratio was caused by the increased synthesis of N-containing metabolites under drought stress. It may be one of the adaptive strategies of host plants to the drought conditions [95]. The N:P ratio is a vital indicator to identify limiting nutrients during the growth process [94]. In the present study, N:P increased with the decrease in soil water content, which indicated that plant growth is more susceptible to P deficiency under drought stress, and the *Epichloë* endophyte alleviated the growth restriction caused by P deficiency. This is associated with the *Epichloë* endophyte indirectly contributing to plant nutrition absorption through increasing P available to plants by increasing the diversity of phosphate-solubilizing fungi [79].

Previous research had indicated that the effects of *Epichloë* endophytes upon the drought resistance of host plants were uncertain, sometimes dependent on the genotype of both host plant and endophyte and environmental conditions [43]. In the present study, although all the experimental DHG plants were originally from the same population, after their maternal plants were grown for two years in different environmental conditions, the drought resistance of their progeny started to be different. All of the growth and photosynthetic indexes of YZ(D) DHG were better under each treatment than XH(W) DHG. Additionally, a lower CtK content and higher ABA content of YZ(D) DHG indicated a faster response to water deficit and a stronger sensitivity level than XH(W) DHG [72]. TGE, as a mechanism for plants to cope with abiotic and biotic factors of stress, has been intensively reviewed [45]. The differences of the shoot biomass, photosynthetic rate and shoot P content between the EI plants from the two sites is higher than the differences between the EF plants of the two sites, while the CtK content is the opposite. All of these are evidence of a TGE in response to the different SWC of parental plants to stress resulting from the previous experience of water deficit [45]. These results indicated the *Epichloë* endophyte may be involved in host plant TGE by regulating the above-mentioned parameters due to its vertical transmission by seeds [47]. The *Epichloë* endophyte may be a carrier to transfer information and/or some substances from maternal plants to progeny to mediate the TGEs.

5. Conclusions

The present study found that the presence of an *Epichloë* endophyte improved the drought stress of host plants by maintaining the growth of the plant, improving photosynthesis, promoting nutrient absorption, and adjusting the metabolism of phytohormones. The results also indicated that the DHG grown from the seeds of plants in the relatively dry site are more competitive under water deficiency conditions than those from seeds of plants from the relatively wet site. Importantly, the difference of EI DHG from the two sites is higher than the differences between the EF plants of the two sites, which confirms the presence of TGEs in DHG, and the vertically transmitted endophyte mediates TGEs via above-mentioned indicators. Nonetheless, more studies are needed to totally identify and understand the mechanisms underlying the *Epichloë* endophyte mediated TGEs in plants, particularly in relation to whether they are widening the capacity of plants to deal with more than one factor of stress at once. All the present and prospective findings would help to understand the mechanisms why EI DHG has selective advantage in arid grassland ecosystems, and how to make more use of *Epichloë* endophyte attributes to breeding new drought-resistant forage germplasms for arid and semiarid regions.

Supplementary Materials: The following are available online at https://www.mdpi.com/article/10.3390/agriculture12060761/s1, Table S1: Results of univariate analysis of variance for the interaction effects of habitat type of Parent (H), endophyte (E) and water stress (W) on Biomass, ABA, CtK and IAA content of *A. inebrians.* Table S2: Results of univariate analysis of variance for the interaction effects of habitat type of Parent (H), endophyte (E) and water stress (W) on Chlorophyll content, Net photosynthetic rate, Stomatal conductance, Intercellular carbon dioxide concentration and Transpiration rate of *A. inebrians.* Table S3: Results of univariate analysis of variance for the interaction effects of habitat type of Parent (H), endophyte (E) and water stress (W) on C, N and P content of *A. inebrians.* Table S4: Results of univariate analysis of variance for the interaction effects of habitat type of Parent (H), endophyte (E) and water stress (W) on C:N, C:P and N:P of *A. inebrians.*

Author Contributions: Conceptualization, X.Z., Z.N. and C.X.; Formal analysis, C.X.; Funding acquisition, X.Z., Z.N. and C.X.; Methodology, X.C., L.S. and C.X.; Project administration, Z.N.; Software, X.C.; Writing—original draft, X.C. and L.S.; Writing—review and editing, X.C., X.Z., M.J.C., Z.N. and C.X. All authors have read and agreed to the published version of the manuscript.

Funding: This research was financially supported by the National Nature Science Foundation of China (32001387 and 31772665), the National Basic Research Program of China (2014CB138702), Lanzhou University "Double First-Class" guiding special project-team construction fund-scientific research start-up fee standard (561119208).

Institutional Review Board Statement: Not applicable.

Informed Consent Statement: Not applicable.

Data Availability Statement: Not applicable.

Conflicts of Interest: The authors declare no conflict of interest.

References

1. Brundrett, M.C. Coevolution of roots and mycorrhizas of land plants. *New Phytol.* **2002**, *154*, 275–304. [CrossRef] [PubMed]
2. Lowman, S.; Kim-Dura, S.; Mei, C.; Nowak, J. Strategies for enhancement of switchgrass (*Panicum virgatum* L.) performance under limited nitrogen supply based on utilization of N-fixing bacterial endophytes. *Plant Soil* **2016**, *405*, 47–63. [CrossRef]
3. Malinowski, D.P.; Belesky, D.P. *Epichloë* (formerly *Neotyphodium*) fungal endophytes increase adaptation of cool-season perennial grasses to environmental stresses. *Acta Agrobot.* **2019**, *72*, 1767. [CrossRef]
4. Hallasgo, A.M.; Spangl, B.; Steinkellner, S.; Hage-Ahmed, K. The fungal endophyte Serendipita williamsii does not affect phosphorus status but carbon and nitrogen dynamics in arbuscular mycorrhizal tomato plants. *J. Fungi* **2020**, *6*, 233. [CrossRef]
5. Leuchtmann, A.; Bacon, C.W.; Schardl, C.L.; White, J.F.; Tadych, M. Nomenclatural realignment of *Neotyphodium* speices with genus *Epichloë*. *Mycologia* **2014**, *106*, 202–215. [CrossRef]
6. Schardl, C.L.; Grossman, R.B.; Nagabhyru, P.; Faulkner, J.R.; Mallik, U.P. Loline alkaloids: Currencies of mutualism. *Phytochemistry* **2007**, *68*, 980–996. [CrossRef]
7. Christensen, M.J.; Bennett, R.J.; Ansari, H.A.; Koga, H.; Johnson, R.D.; Bryan, G.T.; Simpson, W.R.; Koolaard, J.P.; Nickless, E.M.; Voisey, C.R. *Epichloë* endophytes grow by intercalary hyphal extension in elongating grass leaves. *Fungal Genet. Biol.* **2008**, *45*, 84–93. [CrossRef]
8. Müller, C.B.; Krauss, J. Symbiosis between grasses and asexual fungal endophytes. *Curr. Opin. Plant Biol.* **2005**, *8*, 450–456. [CrossRef]
9. Xia, C.; Li, N.N.; Zhang, Y.W.; Li, C.J.; Zhang, X.X.; Nan, Z.B. Role of *Epichloë* endophytes in defense responses of cool-season grasses to pathogens: A review. *Plant Dis.* **2018**, *102*, 2061–2073. [CrossRef]
10. Hennessy, L.M.; Popay, A.J.; Glare, T.R.; Finch, S.C.; Cave, V.M.; Rostás, M. Olfactory responses of Argentine stem weevil to herbivory and endophyte-colonisation in perennial ryegrass. *J. Pest Sci.* **2022**, *95*, 263–277. [CrossRef]
11. Wang, J.F.; Hou, W.P.; Christensen, M.J.; Li, X.Z.; Nan, Z.B. Role of *Epichloë* endophytes in improving host grass resistance ability and soil properties. *J. Agric. Food Chem.* **2020**, *68*, 6944–6955. [CrossRef] [PubMed]
12. Ueno, A.C.; Gundel, P.E.; Molina-Montenegro, M.A.; Ramos, P.; Ghersa, C.M. Getting ready for the ozone battle: Vertically transmitted fungal endophytes have transgenerational positive effects in plants. *Plant Cell Environ.* **2021**, *44*, 2716–2728. [CrossRef] [PubMed]
13. Saedi, T.; Mosaddeghi, M.R.; Sabzalian, M.R.; Zarebanadkouki, M. Effect of *Epichloë* fungal endophyte symbiosis on tall fescue to cope with flooding-derived oxygen-limited conditions depends on the host genotype. *Plant Soil* **2021**, *468*, 353–373. [CrossRef]
14. Johnson, L.J.; Briggs, L.R.; Caradus, J.R.; Finch, S.C.; Fleetwood, D.J.; Fletcher, L.R.; Hume, D.E.; Johnson, R.D.; Popay, A.J.; Tapper, B.A. The exploitation of *epichloae* endophytes for agricultural benefit. *Fungal Divers.* **2013**, *60*, 171–188. [CrossRef]
15. Becker, M.; Becker, Y.; Green, K.; Scott, B. The endophytic symbiont *Epichloë* festucae establishes an epiphyllous net on the surface of *Lolium perenne* leaves by development of an expressorium, an appressoriumdophytic syexit structure. *New Phytol.* **2016**, *211*, 240–254. [CrossRef]
16. Soto-Barajas, M.C.; Zabalgogeazcoa, I.; Gómez-Fuertes, J.; GonzálezBlanco, V.; Vázquez-De-Aldana, B.R. *Epichloë* endophytes affect the nutrient and fiber content of *Lolium perenne*, regardless of plant genotype. *Plant Soil.* **2016**, *405*, 65–277. [CrossRef]
17. Nan, Z.B.; Li, C.J. Neotyphodium in native grasses in China and observations on endophyte/host interactions. In Proceedings of the 4th International Neotyphodium/Grass Interactions Symposium, Soest, Germany, 27–29 September 2000.
18. Li, C.J.; Nan, Z.B.; Liu, Y. Methodology of endophyte detection of drunken horse grass. *Edible Fungi China* **2008**, *27*, 16–19.
19. Chen, L.; Li, X.Z.; Li, C.J.; Swoboda, G.A.; Schardl, C.L. Two distinct *Epichloë* species symbiotic with *Achnatherum inebrians*, drunken horse grass. *Mycologia* **2015**, *107*, 863–873. [CrossRef]
20. Zhang, X.X.; Nan, Z.B.; Li, C.J.; Gao, K. Cytotoxic effect of ergot alkaloids in *Achnatherum inebrians* infected by the *Neotyphodium gansuense* endophyte. *J. Agric. Food Chem.* **2014**, *62*, 7419–7422. [CrossRef]

21. Liang, Y.; Wang, H.C.; Li, C.J.; Nan, Z.B.; Li, F.D. Effects of feeding drunken horse grass infected with *Epichloë gansuensis* endophyte on animal performance, clinical symptoms and physiological parameters in sheep. *BMC Vet. Res.* **2017**, *13*, 223. [CrossRef]
22. Xia, C.; Zhang, X.X.; Christensen, M.J.; Nan, Z.B.; Li, C.J. *Epichloë* endophyte affects the ability of powdery mildew (*Blumeria graminis*) to colonise drunken horse grass (*Achnatherum inebrians*). *Fungal Ecol.* **2015**, *16*, 26–33. [CrossRef]
23. Kou, M.Z.; Bastías, D.A.; Christensen, M.J.; Zhong, R.; Nan, Z.B.; Zhang, X.X. The plant salicylic acid signalling pathway regulates the infection of a biotrophic pathogen in grasses associated with an *Epichloë* endophyte. *J. Fungi* **2021**, *7*, 633. [CrossRef] [PubMed]
24. Zhang, H.J.; Li, X.Z.; White, J.F.; Wei, X.K.; Li, C.J. *Epichloë* endophyte improves ergot disease resistance of host (*Achnatherum inebrians*) by regulating leaf senescence and photosynthetic capacity. *J. Plant Growth Regul.* **2021**, *41*, 808–817. [CrossRef]
25. Zhang, X.X.; Li, C.J.; Nan, Z.B.; Matthew, C. *Neotyphodium* endophyte increases *Achnatherum inebrians* (drunken horse grass) resistance to herbivores and seed predators. *Weed Res.* **2012**, *52*, 70–78. [CrossRef]
26. He, Y.L.; Chen, T.X.; Zhang, H.J.; White, J.F.; Li, C.J. Fungal endophytes help grasses to tolerate sap-sucking herbivores through a hormone-signaling system. *J. Plant Growth Regul.* **2022**. [CrossRef]
27. Zhang, X.X.; Li, C.J.; Nan, Z.B. Effects of cadmium stress on growth and anti-oxidative systems in *Achnatherum inebrians* symbiotic with *Neotyphodium gansuense*. *J. Hazard. Mater.* **2010**, *175*, 703–709. [CrossRef] [PubMed]
28. Chen, N.; He, R.L.; Chai, Q.; Li, C.J.; Nan, Z.B. Transcriptomic analyses giving insights into molecular regulation mechanisms involved in cold tolerance by *Epichloë* endophyte in seed germination of *Achnatherum inebrians*. *Plant Growth Regul.* **2016**, *80*, 367–375. [CrossRef]
29. Cheng, C.; Wang, J.F.; Hou, W.P.; Malik, K.; Zhao, C.Z.; Niu, X.L.; Liu, Y.L.; Huang, R.; Li, C.J.; Nan, Z.B. Elucidating the molecular mechanisms by which seed-borne endophytic fungi, *Epichloë gansuensis*, increases the tolerance of *Achnatherum inebrians* to NaCl stress. *Int. J. Mol. Sci.* **2021**, *22*, 13191. [CrossRef]
30. Wang, J.F.; Hou, W.P.; Christensen, M.J.; Xia, C.; Chen, T.; Zhang, X.X.; Nan, Z.B. The fungal endophyte *Epichloë gansuensi*s increases NaCl-tolerance in *Achnatherum inebrians* through enhancing the activity of plasma membrane H+-ATPase and glucose-6-phosphate dehydrogenase. *Sci. China Life Sci.* **2021**, *64*, 452–465. [CrossRef]
31. Xia, C.; Christensen, M.J.; Zhang, X.X.; Nan, Z.B. Effect of *Epichloë gansuensis* endophyte and transgenerational effects on the water use efficiency, nutrient and biomass accumulation of *Achnatherum inebrians* under soil water deficit. *Plant Soil* **2018**, *424*, 555–571. [CrossRef]
32. Lee, K.; Missaoui, A.; Mahmud, K.; Presley, H.; Lonnee, M. Interaction between grasses and *Epichloë* endophytes and its significance to biotic and abiotic stress tolerance and the rhizosphere. *Microorganisms* **2021**, *9*, 2186. [CrossRef] [PubMed]
33. Xu, L.X.; Yu, J.J.; Han, L.B.; Huang, B.R. Photosynthetic enzyme activities and gene expression associated with drought tolerance and post-drought recovery in Kentucky bluegrass. *Environ. Exp. Bot.* **2013**, *89*, 28–35. [CrossRef]
34. Rozpądek, P.; Wężowicz, K.; Nosek, M.; Ważny, R.; Tokarz, K.; Lembicz, M.; Miszalski, Z.; Turnau, K. The fungal endophyte *Epichloë* typhina improves photosynthesis efficiency of its host orchard grass (*Dactylis glomerata*). *Planta* **2015**, *242*, 1025–1035. [CrossRef] [PubMed]
35. Berens, M.L.; Wolinska, K.W.; Spaepen, S.; Tsuda, K.; Affiliations, A.I. Balancing trade-offs between biotic and abiotic stress responses through leaf age-dependent variation in stress hormone cross-talk. *Proc. Natl. Acad. Sci. USA* **2019**, *116*, 2364–2373. [CrossRef]
36. Manghwar, H.; Hussain, A.; Ali, Q.; Liu, F. Brassinosteroids (BRs) role in plant development and coping with different stresses. *Int. J. Mol. Sci.* **2022**, *23*, 1012. [CrossRef]
37. Peleg, Z.; Blumwald, E. Hormone balance and abiotic stress tolerance in crop plants. *Curr. Opin. Plant Biol.* **2011**, *14*, 290–295. [CrossRef]
38. Xu, W.B.; Li, M.M.; Lin, W.H.; Nan, Z.B.; Tian, P. Effects of *Epichloë sinensis* endophyte and host ecotype on physiology of festuca sinensis under different soil moisture conditions. *Plants* **2021**, *10*, 1649. [CrossRef]
39. Zhao, Z.R.; Kou, M.Z.; Zhong, R.; Xia, C.; Christensen, M.J.; Zhang, X.X. Transcriptome analysis revealed plant hormone biosynthesis and response pathway modification by *Epichloë gansuensis* in *Achnatherum inebrians* under different soil moisture availability. *J. Fungi* **2021**, *7*, 640. [CrossRef]
40. Song, M.L.; Li, X.Z.; Saikkonen, K.; Li, C.J.; Nan, Z.B. An asexual *Epichloë* endophyte enhances waterlogging tolerance of *Hordeum brevisubulatum*. *Fungal Ecol.* **2015**, *13*, 44–52. [CrossRef]
41. Luo, Y.; Peng, Q.; Li, K.; Liu, Y.; Gong, Y.; Han, W. Patterns of nitrogen and phosphorus stoichiometry among leaf, stem and root of desert plants and responses to climate and soil factors in Xinjiang, China. *Catena* **2021**, *199*, 105100. [CrossRef]
42. Hamilton, C.E.; Gundel, P.E.; Helander, M.; Saikkonen, K. Endophytic mediation of reactive oxygen species and antioxidant activity in plants: A review. *Fungal Divers.* **2012**, *54*, 1–10. [CrossRef]
43. Saikkonen, K.; Lehtonen, P.; Helander, M.; Koricheva, J.; Faeth, S.H. Model systems in ecology: Dissecting the endophyte grass literature. *Trends Plant Sci.* **2006**, *11*, 428–433. [CrossRef] [PubMed]
44. Gundel, P.E.; Rudgers, J.A.; Whitney, K.D. Vertically transmitted symbionts as mechanisms of transgenerational effects. *Am. J. Bot.* **2017**, *104*, 787–792. [CrossRef] [PubMed]
45. Yin, J.; Zhou, M.; Lin, Z.; Li, Q.Q.; Zhang, Y.Y. Transgenerational effects benefit offspring across diverse environments: A meta-analysis in plants and animals. *Ecol. Lett.* **2019**, *22*, 1976–1986. [CrossRef] [PubMed]

46. Herman, J.J.; Sultan, S.E. Adaptive transgenerational plasticity in plants: Case studies, mechanisms, and implications for natural populations. *Front. Plant Sci.* **2011**, *2*, 102. [CrossRef]
47. Gundel, P.E.; Rudgers, J.A.; Ghersa, C.M. Incorporating the process of vertical transmission into understanding of host-symbiont dynamics. *Oikos* **2011**, *120*, 1121–1128. [CrossRef]
48. Gundel, P.E.; Sorzoli, N.; Ueno, A.C.; Ghersa, C.M.; Seal, C.E.; Bastías, D.A.; Martínez-Ghersa, M.A. Impact of ozone on the viability and antioxidant content of grass seeds is affected by a vertically transmitted symbiotic fungus. *Environ. Exp. Bot.* **2015**, *113*, 40–46. [CrossRef]
49. Ye, W.; Hu, S.; Wu, L.; Ge, C.; Cui, Y.; Chen, P.; Xu, J.; Dong, G.; Guo, L.; Qian, Q. Fine mapping a major QTL qFCC7L for chlorophyll content in rice (*Oryza sativa* L.) cv. PA64s. *Plant Growth Regul.* **2017**, *81*, 81–90. [CrossRef]
50. Tanveer, S.K.; Zhang, J.L.; Lu, X.L.; Wen, X.X.; Wei, W.; Yang, L.; Liao, Y.C. Effect of corn residue mulch and N fertilizer application on nitrous oxide (N_2O) emission and wheat crop productivity under rain-fed condition of loess plateau China. *Int. J. Agric. Biol.* **2014**, *16*, 505–512.
51. Gundel, P.E.; Irisarri, J.G.N.; Fazio, L.; Casas, C.; Pérez, L.I. Inferring field performance from drought experiments can be misleading: The case of symbiosis between grasses and *Epichloë* fungal endophytes. *J. Arid Environ.* **2016**, *132*, 60–62. [CrossRef]
52. Ren, A.Z.; Gao, Y.B.; Wang, W.; Wang, J.L. Photosynthetic pigments and photosynthetic products of endophyte-infected and endophyte-free *Lolium perenne* L. under drought stress conditions. *Front. Biol. China* **2006**, *1*, 168–173. [CrossRef]
53. Inukai, Y.; Sakamoto, T.; Ueguchi-Tanaka, M.; Shibata, Y.; Gomi, K.; Umemura, I.; Hasegawa, Y.; Ashikari, M.; Kitano, H.; Matsuoka, M. Crown rootless1, which is essential for crown root formation in rice, is a target of an auxin response factor in auxin signaling. *Plant Cell* **2005**, *17*, 1387–1396. [CrossRef] [PubMed]
54. Malinowski, D.P.; Belesky, D.P. Adaptations of endophyte-infected cool-season grasses to environmental stresses: Mechanisms of drought and mineral stress tolerance. *Crop Sci.* **2000**, *40*, 923–940. [CrossRef]
55. West, C.P.; Izekor, E.; Turner, K.E.; Elmi, A.A. Endophyte effects on growth and persistence of tall fescue along a water-supply gradient. *Agron. J.* **1993**, *85*, 264–270. [CrossRef]
56. Elmi, A.A.; West, C.P. Endophyte infection affects on stomatal conductance, osmotic adjustment and drought recovery of tall fescue. *New Phytol.* **1995**, *131*, 61–67. [CrossRef]
57. Belesky, D.P.; Stringer, W.C.; Plattner, R.D. Influence of endophyte and water regime upon tall fescue accessions. *Ann. Bot.* **1989**, *64*, 343–349. [CrossRef]
58. Belesky, D.P.; Fedders, J.M. Tall fescue development in response to *Acremonium coenophialum* and soil acidity. *Crop Sci.* **1995**, *35*, 529–533. [CrossRef]
59. Assuero, S.G.; Matthew, C.; Kemp, P.D.; Latch, G.C.M.; Barker, D.J.; Haslett, S.J. Morphological and physiological effects of water deficit and endophyte infection on contrasting tall fescue cultivars. *N. Z. J. Agron. Res.* **2000**, *43*, 49–61. [CrossRef]
60. Faeth, S.H.; Sullivan, T.J. Mutualistic asexual endophytes in a native grass are usually parasitic. *Am. Nat.* **2003**, *161*, 310–325. [CrossRef]
61. Sreenivasulu, N.; Harshavardhan, V.T.; Govind, G.; Seiler, C.; Kohli, A. Contrapuntal role of ABA: Does it mediate stress tolerance or plant growth retardation under long-term drought stress? *Gene* **2012**, *506*, 265–273. [CrossRef]
62. Kishor, P.B.K.; Sangam, S.; Amrutha, R.N.; Laxmi, P.S.; Naidu, K.R.; Rao, K.R.S.S.; Rao, S.; Reddy, K.J.; Theriappan, P.; Sreenivasulu, N. Regulation of proline biosynthesis, degradation, uptake and transport in higher plants: Its implications in plant growth and abiotic stress tolerance. *Curr. Sci.* **2005**, *88*, 424–438.
63. Defez, R.; Andreozzi, A.; Dickinson, M.; Charlton, A.; Tadini, L.; Pesaresi, P.; Bianco, C. Improved drought stress response in alfalfa plants nodulated by an IAA over-producing rhizobium strain. *Front. Microbiol.* **2017**, *8*, 2466. [CrossRef] [PubMed]
64. Pustovoitova, T.N.; Zhdanova, N.E.; Zholkevich, V.N. Changes in the Levels of IAA and ABA in Cucumber Leaves under Progressive Soil Drought. *Russ. J. Plant Physiol.* **2004**, *51*, 513–517. [CrossRef]
65. Zholkevich, V.N.; Gusev, N.A.; Kaplya, A.V.; Pakhomova, T.I.; Pil'shikova, N.V.; Samuiliv, F.D.; Slavnii, P.S.; Shmat'ko, I.G. *Water Metabolism in Plants*; Tarchevskii, I.A., Zholkevich, V.N., Eds.; Nauka: Moscow, Russia, 1989.
66. De Battista, J.P.; Bouton, J.H.; Bacon, C.W.; Siegel, M.R. Rhizome and herbage production of endophyte-removed tall fescue clones and populations. *Agron. J.* **1990**, *82*, 651–654. [CrossRef]
67. Tran, L.S.P.; Urao, T.; Qin, F.; Maruyama, K.; Kakimoto, T.; Shinozaki, K.; Yamaguchi-Shinozaki, K. Functional analysis of AHK1/ATHK1 and cytokinin receptor histidine kinases in response to abscisic acid, drought, and salt stress in Arabidopsis. *Proc. Natl. Acad. Sci. USA* **2007**, *104*, 20623–20628. [CrossRef]
68. Werner, T.; Nehnevajova, E.; Köllmer, I.; Novák, O.; Strnad, M.; Krämer, U.; Schmülling, T. Root-specific reduction of cytokinin causes enhanced root growth, drought tolerance, and leaf mineral enrichment in Arabidopsis and tobacco. *Plant Cell* **2010**, *22*, 3905–3920. [CrossRef]
69. Nishiyama, R.; Watanabe, Y.; Fujita, Y.; Le, D.T.; Kojima, M.; Werner, T.; Vankova, R.; Yamaguchi-Shinozaki, K.; Shinozaki, K.; Kakimoto, T. Analysis of cytokinin mutants and regulation of cytokinin metabolic genes reveals important regulatory roles of cytokinins in drought, salt and abscisic acid responses, and abscisic acid biosynthesis. *Plant Cell* **2011**, *23*, 2169–2183. [CrossRef]
70. Wilkinson, S.; Davies, W.J. Drought, ozone, ABA and ethylene: New insights from cell to plant to community. *Plant Cell Environ.* **2010**, *33*, 510–525. [CrossRef]
71. Acharya, B.R.; Assmann, S.M. Hormone interactions in stomatal function. *Plant Mol. Biol.* **2009**, *69*, 451–462. [CrossRef]

72. Elbersen, W.W.; West, C.P. Growth and water relations of field-grown tall fescue as influenced by drought and endophytes. *Grass Forage Sci.* **1996**, *51*, 333–342. [CrossRef]
73. Malinowski, D.P.; Leuchtmann, A.; Schmidt, D.; Nösberger, J. Symbiosis with *Neotyphodium uncinatum* endophyte may increase the competitive ability of meadow fescue. *Agron. J.* **1997**, *89*, 833–839. [CrossRef]
74. Manzur, M.E.; Garello, F.A.; Omacini, M.; Schnyder, H.; Sutka, M.R.; García-Parisi, P.A. Endophytic fungi and drought tolerance: Ecophysiological adjustment in shoot and root of an annual mesophytic host grass. *Funct. Plant Biol.* **2022**, *49*, 272–282. [CrossRef] [PubMed]
75. Blum, A. Effective use of water (EUW) and not water-use efficiency (WUE) is the target of crop yield improvement under drought stress. *Field Crops Res.* **2009**, *112*, 119–123. [CrossRef]
76. Davitt, A.J.; Chen, C.; Rudgers, J.A. Understanding context-dependency in plant–microbe symbiosis: The influence of abiotic and biotic contexts on host fitness and the rate of symbiont transmission. *Environ. Exp. Bot.* **2011**, *71*, 137–145. [CrossRef]
77. Fatichi, S.; Leuzinger, S.; Körner, C. Moving beyond photosynthesis: From carbon source to sink-driven vegetation modeling. *New Phytol.* **2014**, *201*, 1086–1095. [CrossRef] [PubMed]
78. Sardans, J.; Rivas-Ubach, A.; Peñuelas, J. The C:N:P stoichiometry of organisms and ecosystems in changing world: A review and perspectives. *Perspect. Plant Ecol.* **2012**, *14*, 33–47. [CrossRef]
79. Arrieta, A.M.; Iannone, L.J.; Scervino, J.M.; Vignale, M.V.; Novas, M.V. A foliar endophyte increases the diversity of phosphorus-solubilizing rhizospheric fungi and mycorrhizal colonization in the wild grass *Bromus auleticus*. *Fungal. Ecol.* **2015**, *17*, 146–154. [CrossRef]
80. Hou, W.P.; Wang, J.F.; Nan, Z.B.; Christensen, M.J.; Xia, C.; Chen, T.; Zhang, X.X.; Niu, X.L. *Epichloë* gansuensis endophyte-infection alters soil enzymes activity and soil nutrients at different growth stages of *Achnatherum inebrians*. *Plant Soil* **2020**, *455*, 227–240. [CrossRef]
81. Li, X.; Ren, A.Z.; Han, R.; Yin, L.J.; Wei, M.Y.; Gao, Y.B. Endophyte mediated effects on the growth and physiology of *Achnatherum sibiricum* are conditional on both N and P availability. *PLoS ONE* **2012**, *7*, e48010.
82. Zaidi, A.; Khan, M.S. Stimulatory effects of dual inoculation with phosphate solubilising microorganisms and arbuscular mycorrhizal fungus on chickpea. *Aust. J. Exp. Agric.* **2007**, *47*, 1016–1022. [CrossRef]
83. Faeth, S.H.; Fagan, W.F. Fungal endophytes: Common host plant symbionts but uncommonmutualists. *Integr. Comp. Biol.* **2002**, *42*, 360–368. [CrossRef] [PubMed]
84. Nagabhyru, P.; Dinkins, R.D.; Wood, C.L.; Bacon, C.W.; Schardl, C.L. Tall fescue endophyte effects on tolerance to water-deficit stress. *BMC Plant Biol.* **2013**, *13*, 127. [CrossRef] [PubMed]
85. Vázquez-de-Aldana, B.R.; García-Ciudad, A.; García-Criado, B.; Vicente-Tavera, S.; Zabalgogeazcoa, I. Fungal endophyte (*Epichloë* festucae) alters the nutrient content of Festuca rubra regardless of water availability. *PLoS ONE* **2013**, *8*, e84539. [CrossRef] [PubMed]
86. Schardl, C.L.; Leuchtmann, A.; Spiering, M.J. Symbioses grasses with seedborne fungal endophytes. *Annu. Rev. Plant Biol.* **2004**, *55*, 315–340. [CrossRef]
87. Zhang, X.X.; Li, C.J.; Nan, Z.B. Effects of salt and drought stress on alkaloid production in endophyte-infected drunken horse grass (*Achnatherum inebrians*). *Biochem. Syst. Ecol.* **2011**, *39*, 471–476. [CrossRef]
88. Schardl, C.; Young, C.; Hesse, U.; Amyotte, S.G.; Andreeva, K.; Calie, P.J.; Fleetwood, D.J.; Haws, D.C.; Moore, N.; Oeser, B.; et al. Plant-symbiotic fungi as chemical engineers: Multi-genome analysis of the *clavicipitaceae* reveals dynamics of alkaloid loci. *PLoS Genet.* **2013**, *9*, e1003323. [CrossRef] [PubMed]
89. Blankenship, J.D.; Houseknecht, J.B.; Pal, S.; Bush, L.P.; Grossman, R.B.; Schardl, C.L. Biosynthetic precursors of fungal pyrrolizidines, the loline alkaloids. *ChemBioChem* **2005**, *6*, 1016–1022. [CrossRef]
90. Bacon, C.W. Abiotic stress tolerances (moisture, nutrients) and photosynthesis in endophyte-infected tall fescue. *Agric. Ecosyst. Environ.* **1993**, *44*, 123–141. [CrossRef]
91. Smith, S.E.; Jakobsen, I.; Grønlund, M.; Smish, A. Roles of arbuscular mycorrhizas in plant phosphorus nutrition: Interactions between pathways of phosphorus uptake in arbuscular mycorrhizal roots have important implications for understanding and manipulating plant phosphorus acquisition. *Plant Physiol.* **2011**, *156*, 1050–1057. [CrossRef]
92. Elser, J.J.; Sterner, R.; Gorokhova, E.; Fagan, W.; Markow, T.; Cotner, J.; Harrison, J.; Hobbie, S.; Odell, G.; Weider, L. Biological stoichiometry from genes to ecosystems. *Ecol. Lett.* **2000**, *3*, 540–550. [CrossRef]
93. Hessen, D.O.; Jensen, T.C.; Kyle, M.; Elser, J.J. RNA responses to N- and P-limitation; reciprocal regulation of stoichiometry and growth rate in Brachionus. *Funct. Ecol.* **2007**, *21*, 956–962. [CrossRef]
94. Elser, J.J.; Hamilton, A. Stoichiometry and the new biology: The future is now. *PLoS Biol.* **2007**, *5*, e181. [CrossRef] [PubMed]
95. Chen, T.X.; Richard, J.; Chen, S.H.; Lv, H.; Zhou, J.L.; Li, C.J. Infection by the fungal endophyte *Epichloë bromicola* enhances the tolerance of wild barley (*Hordeum brevisubulatum*) to salt and alkali stresses. *Plant Soil* **2018**, *428*, 353–370. [CrossRef]

agriculture

MDPI

Article

Changes in Soil Bacterial Community Structure in Bermudagrass Turf under Short-Term Traffic Stress

Hongjian Wei [1,2], Yongqi Wang [1,2], Juming Zhang [1,2], Liangfa Ge [1,2] and Tianzeng Liu [1,2,*]

[1] College of Forestry and Landscape Architecture, South China Agricultural University, Guangzhou 510642, China; weihongjian@stu.scau.edu.cn (H.W.); 20202036001@stu.scau.edu.cn (Y.W.); jimmzh@scau.edu.cn (J.Z.); lge@scau.edu.cn (L.G.)

[2] Guangdong Engineering Research Center for Grassland Science, South China Agricultural University, Guangzhou 510642, China

* Correspondence: liutianzeng@scau.edu.cn

Abstract: Bermudagrass (*Cynodon dactylon* (L.) Pers.) is an extensively utilized turf grass for football fields and golf courses. Traffic stress is one of the most important stresses affecting the life of turf, which leads to a decrease in turf quality and changes in the soil microbial community structure. The structural change in soil bacterial community is an important reference for turf growth, maintenance, and restoration. Tifgreen bermudagrass turf and Common bermudagrass turf were applied with traffic treatment by a traffic simulator with moderate intensity to explore soil bacterial community structural changes in turf under traffic stress. The environmental factors including turf quality indicators and soil properties were measured, and the association of the soil bacterial community diversity with the environment factors was analyzed. As a result, traffic treatments significantly changed the soil properties and bacterial community composition in two bermudagrass species at the phylum and genus level. *Actinobacteria*, *Chloroflexi*, and *Verrucomicrobia* showed significantly high abundance in turf soils under traffic stress. The soil bacterial ACE, Chaol, and Shannon indexes of two bermudagrass species under traffic stress were significantly lower than non-traffic stress. The bacterial community structure was highly correlated with some turf quality indicators and soil properties under traffic stress. Our results illustrate that compared to Common bermudagrass, Tifgreen bermudagrass had better turf quality under traffic stress and less changes in its bacterial community structure, perhaps Tifgreen bermudagrass is a better choice of grass for sports turf as opposed to Common bermudagrass.

Keywords: traffic stress; bermudagrass; turf quality; soil bacteria; diversity; soil property

Citation: Wei, H.; Wang, Y.; Zhang, J.; Ge, L.; Liu, T. Changes in Soil Bacterial Community Structure in Bermudagrass Turf under Short-Term Traffic Stress. *Agriculture* **2022**, *12*, 668. https://doi.org/10.3390/agriculture12050668

Academic Editor: Mario Licata

Received: 11 April 2022
Accepted: 3 May 2022
Published: 6 May 2022

1. Introduction

Traffic is frequently seen as a harmful stress to turfs [1]. The traffic directly causes turf wear and reduces the photosynthesis of turf leaves, resulting in the slow growth of turf plants [2]. In addition, it changes the soil properties, causing soil compaction [3], reducing water, nutrients, and oxygen in the soil, affecting the growth of turf roots [4]. It indirectly affects turfgrass development and thus reduces the turf's quality [5]. In general, Traffic can affect the physicochemical characters of grassland soils [6], and it generally affects the soil physical properties more than the chemical properties [7]. It acts directly on the soil's surface, changing its water content, capacity, firmness, and permeability [8]. Moreover, grassland soils' physicochemical characters interact and influence each other [9]. Traffic intensities have different functions in grassland physicochemical properties, which are essential drivers of change in the nutrient content of grassland. Currently, there is no consensus on the effect of traffic on soil chemistry, and limited specific research has been conducted.

Soil lays the foundation for terrestrial ecosystems, which contains plant roots, soil animals, and microorganisms, of which soil microorganisms are the most active, having

critical functions in the maintenance of ecosystem functions and the regulation of biogeochemical cycles [10,11]. Soil bacteria are one of the most abundant and diverse organisms on earth [12,13]. The dynamics of soil bacterial communities determine a variety of ecological processes, for instance, litter decomposition and nitrogen (N) fixation [14]. Therefore, understanding the drivers of soil bacterial diversity and composition is essential to maintain ecosystem function. Abiotic conditions are highly correlated with the dynamics and activity of soil microbes [15]. Soil physicochemical characteristics are important factors affecting soil bacteria community composition. For example, the soil pH is a key driver for microbial catabolic activities and nutrient utilization [16]. In addition, other factors such as the soil organic matter (SOM) [17], soil moisture [18], and nitrogen and phosphorus content, which are indispensable sources of nutrients and energy for soil bacteria development and metabolism [19,20], may affect soil bacteria community spatial structures directly or indirectly. Moreover, the vegetation type is the critical driving factor for soil microbial distribution patterns [21].

Some scholars believe that traffic directly leads to decreased vegetation cover, increased water capacity, and reduced air content and water transfer capacity of the soil, with a consequent reduction in nitrogen mineralization rates, thus affecting microbial activity [22]. In addition, some articles indicated that soil bacteria communities typically play a vital function in plant development [23,24]. As the sensitive indicator of grassland ecosystems, soil bacteria community structural alterations may be an early indicator of grassland ecosystem function and health. Moreover, soil bacteria community alteration influences the soil nutrient effectiveness and cycling, affecting the grassland plant productivity [25]. Currently, there is limited information on how traffic affects soil microorganisms in grassland, and most of them focus on natural grassland ecosystems with spatial and temporal limitations. Fewer studies on how human traffic affects sports or recreational turfgrass and little research on how traffic alone affects the soil bacteria community in grassland are available. Most recreational and sports turf are often over-trampled, and soil bacteria community structural alterations are the key reference for turf growth maintenance and recovery.

Bermudagrass (*Cynodon dactylon* (L.) Pers.) has the advantages of quick establishment and high recovery capacity. It is an extensively utilized turf grass for football fields and golf courses in tropical and subtropical regions [26]. Bermudagrass is used as a cover crop in vineyards to improve physical and chemical soil properties, enhance biodiversity and help control weeds and pests [27]. The present work focused on investigating how the soil bacteria community and soil respiration responded to Bermudagrass turf under traffic stress to clarify how traffic affected the soil properties and subsurface microorganisms in turf ecosystems. In addition, it offers a theoretical foundation for the healthy management of urban recreation and sports turfs.

2. Materials and Methods

2.1. Site of Experiments

This work was performed in the Teaching and Research Base in South China Agricultural University, Guangzhou, China (lat.23.30° N, long.113°81 E). The native soil type of Guangzhou was Lateritic red clay soil, with an organic matter of 14.5 $g \cdot kg^{-1}$ and an average pH of 6.3. The sand used for this research varied in particle size, ranging from very coarse (9.6%), coarse (19.5%), medium (34.9%), and fine (19.7%) sand sizes. The region experiences a subtropical monsoon climate, and the annual mean evaporation, temperature, and precipitation were 1450.5 mm, 23.4 °C, and 1786.8 mm, respectively, with snowfall and frost-free periods of 365 days. Weekly average minimum and maximum air temperatures and weekly rainfall during the experimental periods of year 2020 are reported in Figure 1.

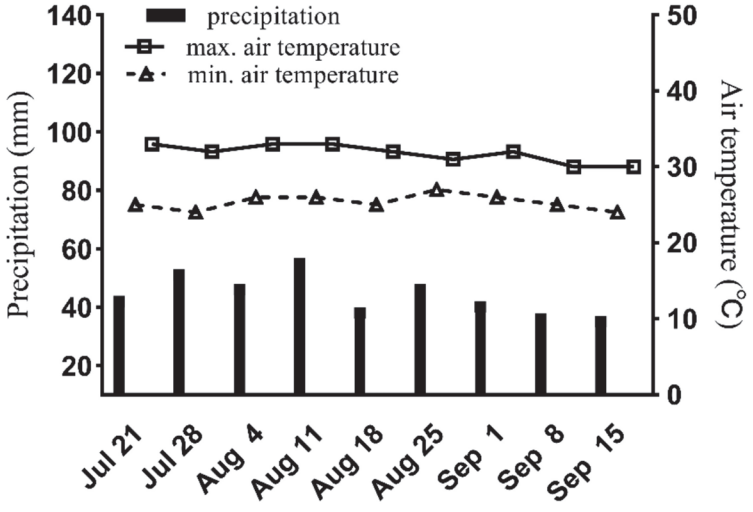

Figure 1. Weekly average minimum and maximum air temperatures and weekly rainfall during experiment: year 2020.

2.2. Experimental Design

Common Bermudagrass (*Cynodon dactylon* sp.) and Tifgreen Bermudagrass (*C. dactylon* × *C. transvaalensis* cv. Tifgreen) were used. The main regional factor in this experiment was traffic stress divided into traffic and non-traffic treatment, while different species were used as secondary factors. There were four treatments: Tifgreen Bermudagrass with traffic treatment (Tif.TS), Tifgreen Bermudagrass with non-traffic treatment (Tif.NT); Common Bermudagrass with traffic treatment (Com.TS) and Common Bermudagrass with non-traffic treatment (Com.NT). All treatments were carried out with three replicates. Traffic treatments were employed as a strip in replicates with the Selfmake Traffic Simulator (STS). STS has 5 parts: roller, steel plate, spike, bearing, and frame, all of which are steel. The steel plate and spikes are removable and easy to replace. The dimension of the drum is 21 cm diameter, 100 cm length, 1.2 cm thickness, and 80 kg weight, with a bearing in the middle of the drum of 5 cm diameter and 104 cm length, and the frame outside the drum is connected to an SR1Z-80 microtiller (Xinyuan Inc., Guangzhou, China) to drive the traffic simulator for the traffic, with a maximum engine power of 4.2 kW. The unit pressure of STS was 1.91 MPa. There were three respective replicates for all treatments, resulting in 12 plots (2 m × 10 m each), with 0.5 m protection rows between plots and 1 m open space around the experimental plots (Figure 2). The self-made traffic simulator was used for traffic treatment, with six rounds each time. The experiment began on 21 July 2020 and ended on Sep 15. The traffic treatment was carried out on Monday and Thursday every week. The experiment lasted for eight weeks.

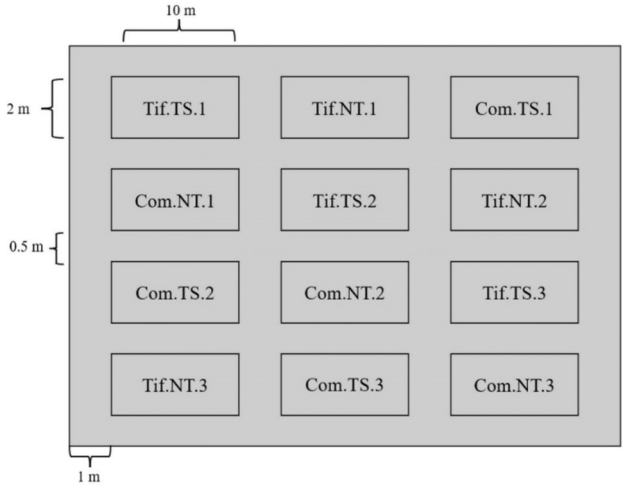

Figure 2. Sketch map of treatments. Tif.TS, Tifgreen bermudagrass with traffic treatment; Tif.NT, Tifgreen bermudagrass with non-traffic treatment; Com.TS, Common bermudagrass with traffic treatment; Com.NT, Common bermudagrass with non-traffic treatment.

2.3. Measurement of Turf Quality Indicators, Soli Physical Properties and Soil Respiration Rate

Cover degree (CD): a 50 × 50 cm sample frame composed of 100 small grids was placed randomly on the community's turf. The turf proportion in each grid was measured visually. After statistics, the cover degree of the turfgrass was calculated and expressed as a percentage.

Biomass: a self-made cylindrical soil drill sampler (diameter, 5 cm) was used to take a straw column with a 15 cm depth, placed in a sampling bag, and brought back to the laboratory. The aboveground biomass (AB) and the under-ground biomass (UB) were separated, washed with water, and then dried in an oven under 80 °C until the dry weight of the sample no longer decreased. The sample dry weight was calculated and recorded.

Turf density (TD): The number of branches of turf plants in 10 cm × 10 cm quadrat was measured and repeated thrice in each plot.

After the test, the soil impact instrument measured the surface hardness (Clegg 083, SD instrument, London, UK). A measuring hammer with a 5 cm diameter and a 2.25 kg mass fell freely from the pipe with a 30 cm diameter, and the values were recorded in the GM unit [28]. Three test points were randomized in every test plot during the measurement, and the average test results were recorded. The soil respiration (SR) rate was measured using an open-circuit soil carbon flux measurement system LI-8100A (Li-Cor, Inc., Lincoln, NE, USA). Three selected points from every plot were randomized; later, one soil respiration ring (inner diameter 22 cm, height 3.5 cm) was placed at each point. During the soil respiration measuring process, the soil respiration leaf chamber was placed onto the PVC tube base to achieve a closed state to reduce the soil surface's interference. To eliminate the plant autotrophic respiration's influence on the soil respiration, turfgrass on the soil surface of the ring was mowed before measurement.

2.4. Soil Sample Collection and Analysis

Fresh soils were collected in the 15 cm soil layer using a 5 cm auger; five soil cores (15 cm deep, 5 cm diameter) were randomly collected from each plot and combined into one composite sample in October 2020, resulting in a total of 12 samples. Alcohol (75% v/v) was utilized for auger sterilization before collecting another soil sample to avoid cross-contamination of microorganisms. Later, those collected soil samples were pooled, and one part was subjected to air-drying and manual removal of rocks and roots. Soil samples

were filtered using the 2 or 5 mm sieve to conduct different measurements. One part of the sample was preserved at 4 °C to determine the soil physicochemical properties, while the remaining fresh soil was preserved at −80 °C to extract the genomic DNA (gDNA).

A pH meter (PHS-2F, jingke Inc., Shanghai, China) was utilized to measure the pH of the suspension of soil: distilled water (1:5). Later, soils were heated for 48 h in the oven at 105 °C (101-0, jinpin instrument Inc., Shanghai, China) to determine the soil water content (SWC). The soil total phosphorus (TP) was analyzed by $HClO_4$-H_2SO_4 digestion and measured using the molybdate-blue colorimetric method. $NaHCO_3$ (0.5 M) was adopted to extract the available phosphorus (AP) and measured using spectrophotometry (UV-5200, Metash Inc., Shanghai, China) at 700 nm [29]. Meanwhile, the Kjeldahl digestion method was utilized to analyze the total nitrogen (TN). The KCl extraction–indophenol blue colorimetry was adopted for determining AN [30]. In addition, 1 M NH_4OAc was utilized to extract the available potassium (AK), followed by quantification by flame atomic absorption spectroscopy (FP6432, jingke Inc., Shanghai, China), and $K_2Cr_2O_7$ + H_2SO_4 digestion was applied to determine the soil organic carbon (SOC), with the addition of $HgSO_4$ to prevent Cl^- interference [31].

2.5. gDNA Collection and PCR Amplification

First, 1 g rhizospheric soil was collected to extract gDNA for high-throughput sequencing (HTS) using the E.Z.N.A.® Soil DNA Kit (Omega Bio-Tek, Norcross, GA, USA) in line with specific instructions. AGE (1%) was performed to qualitatively detect soil gDNA, whereas the Nanodrop 2000 spectrophotometer (Thermo Scientific, Wilmington, DE, USA) was employed to detect the DNA content and purity. The bacterial primer sequences of the v3–v4 region were utilized to carry out PCR amplification, (5′-ACTCCTACGGGAGG CAGCA-3′) and (5′-GGACTACHVGGGTWTCTAAT-3′). After recovery and purification of the amplified products, a sequencing library was prepared following fluorescence measurement. The Illumina MiSeq platform was employed for sequencing in Magigene Technology Co., Ltd. (Guangzhou, China).

2.6. Bioinformatics and Statistical Analysis

This study adopted the Quantitative Insights into Microbial Ecology package (QIIME 2 v.2010.10) [32] to analyze bacterial community patterns. For Illumina amplicon sequences, sequence variants and chimeras were removed using deblur plugin. In contrast, the remaining sequences were adopted to determine the heterogeneities of bacterial communities between symptomatic and asymptomatic samples. Later, sequences were clustered into operational taxonomic units (OTUs) by the 97% similarity threshold. Then, the obtained OTUs were compared with the bacterial taxonomic classes in the full-length SILVA 138 database. Bioconductor v.3.0 and R v.3.5.1 [33] were utilized for exploratory analysis.

After collating the data in Microsoft Excel 2019, Statistical Product and Service Solutions 22.0 (SPSS Inc., Chicago, IL, USA) was used to statistically analyze the environmental factors (turf quality indicators and soil indexes) of Tifgreen Bermudagrass and Common Bermudagrass with traffic and non-traffic treatments. One-way ANOVA was used to test the significance of differences in environmental factors under traffic and non-traffic treatment (Fisher's LSD test, $p < 0.05$). Relative abundance maps of bacterial phyla and order with average relative abundances greater than 1% were plotted in the Magigene Technology online analysis platform (http://www.magichand.online/h5-BioCloud-site/ accessed on 20 February 2021). In brief, Shannon and Simpson's indexes were calculated to represent richness and evenness through plot_anova_diversity function in the microbiome Seq package [34]. Principal coordinate analysis (PCoA) was produced using the Bray–Curtis distance metric by adopting ggplot2 package in R (v4.1.3), and phyloseq packages were used to visualize β-diversity [35]. DESeq2 R package [36] was employed to obtain differential abundance analyses of two groups, and ggplot2 package was employed to normalize taxonomical counts and visualize taxa with significantly differential abundances using the adjusted $p < 0.05$ threshold using MOTHUR software [37]. Using the Galaxy

online analysis platform (http://huttenhower.sph.harvard.edu/galaxy/ accessed on 24 February 2021), the relative abundance matrix at the phyla to order level was submitted for LEfSe analysis. The vegan and ggplot2 packages in R were used to take the environmental factors as explanatory variables and the bacteria with significant differences between treatments as species variables to perform a redundancy analysis (RDA) and draw RDA diagrams. The autocorrelation between environmental factors and bacterial phyla and order level was calculated by Pearson's test (two-tailed) at two significance levels, $p < 0.05$ and $p < 0.01$, and shown in the form of a correlation heat map by using the Hiplot online platform (https://hiplot.com.cn/ accessed on 25 February 2021).

3. Results

3.1. Effects of Traffic Stress on Turf Quality Indicators

Figure 3 presents the turf quality changes. According to Student's *t*-test, diverse treatments of two bermudagrass species showed significant differences. The turf density (TD) of Tifgreen bermudagrass under traffic treatment increased remarkably relative to common bermudagrass ($p < 0.05$) (Figure 3a). The aboveground biomass in Tifgreen bermudagrass and common bermudagrass decreased by 36.53% and 39.54%, respectively. The CD under non-traffic treatment of two bermudagrass species was more than 85.00%, while under traffic treatment, Tifgreen and common bermudagrass decreased to 74.33% and 70.67%, respectively (Figure 3b), which were significantly lower than the non-traffic treatment ($p < 0.05$). The aboveground and underground biomass of two bermudagrass species decreased remarkably after traffic ($p < 0.05$): aboveground biomass in Tifgreen bermudagrass and common bermudagrass under traffic treatment decreased by 31.25% and 60.00%, respectively, compared with non-traffic treatment (Figure 3c). In contrast, the underground biomass of Tifgreen and common bermudagrass decreased by 44.44% and 77.78%, respectively (Figure 3d). Compared with non-traffic treatment, TD, CD, AB, and UB of traffic treatment in the two bermudagrass species significantly decreased ($p < 0.05$).

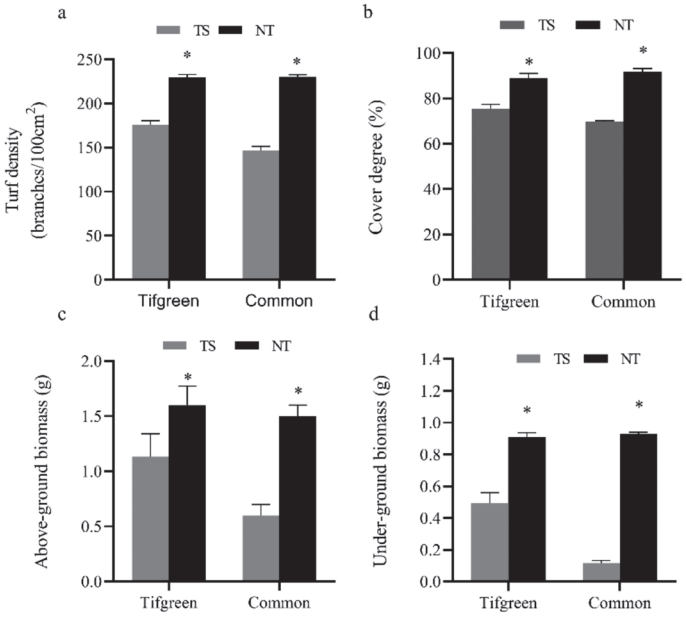

Figure 3. Turf quality indicators under traffic stress. (**a**) turf density, (**b**) cover degree, (**c**) aboveground biomass, (**d**) under-ground biomass. Note: * $p < 0.05$ under diverse treatments. TS: traffic stress; NT: non-traffic stress.

3.2. Effects of Traffic Stress on Soil Physicochemical Properties

Traffic and non-traffic treatment on two bermudagrasses altered the soil physicochemical (Table 1). The soil surface hardness (SSH) of Tifgreen and common bermudagrass increased by 45.75% and 80.93%, while the soil bulk density (SBD) increased by 26.49% and 27.90%, respectively. The soil water content (SWC) of Tifgreen and common bermudagrass decreased by 15.39% and 25.26%. The TN, TP, SOC, and available nutrients (such as AK, AN, AP) increased in Tif.NT and Com.NT compared with Tif.TS and Com.TS. The two bermudagrass species differed significantly ($p < 0.05$) in SR under non-traffic (CK) conditions. The soil respiration (SR) rate of Tifgreen and common bermudagrass decreased by 33.13% and 41.80%, respectively.

Table 1. Soil physicochemical properties under traffic stress.

Soil Properties	Tif.TS	Tif.NT	Com.TS	Com.NT
SSH (g)	120.67 ± 1.45 b	87.67 ± 1.45 c	142.33 ± 2.33 a	78.67 ± 2.62 d
SBD (g/cm^3)	1.62 ± 0.26 a	1.28 ± 0.23 b	1.73 ± 0.18 a	1.35 ± 0.14 b
SWC (%)	55.93 ± 1.36 b	66.10 ± 1.11 a	50.76 ± 1.52 c	67.92 ± 1.18 a
pH	6.83 ± 0.17 a	6.35 ± 0.21 b	6.79 ± 0.14 a	6.07 ± 0.12 c
TN ($g \cdot kg^{-1}$)	1.50 ± 0.06 a	1.53 ± 0.13 a	1.48 ± 0.03 a	1.57 ± 0.14 a
TP ($g \cdot kg^{-1}$)	0.82 ± 0.03 b	0.87 ± 0.01 a	0.83 ± 0.02 b	0.88 ± 0.05 a
AN ($mg \cdot kg^{-1}$)	11.28 ± 0.20 b	12.14 ± 0.16 a	11.12 ± 0.13 b	12.05 ± 0.22 a
AP ($mg \cdot kg^{-1}$)	45.39 ± 0.58 b	49.08 ± 0.31 a	44.28 ± 0.57 b	49.15 ± 0.58 a
AK ($mg \cdot kg^{-1}$)	240.33 ± 0.95 b	250.47 ± 1.25 a	240.48 ± 1.72 b	249.12 ± 0.90 a
SOC ($g \cdot kg^{-1}$)	15.76 ± 0.06 b	16.21 ± 0.16 a	15.61 ± 0.15 b	16.23 ± 0.08 a
SR ($\mu mol \cdot m^{-2} \cdot s^{-1}$)	4.58 ± 0.83 c	6.85 ± 0.82 a	3.78 ± 0.48 d	6.50 ± 0.73 b

Note: The data are expressed as mean ± SD. In each row of the above table, diverse letters suggest significant differences across diverse treatments ($p < 0.05$). SBD, soil bulk density; SSH, soil surface hardness; SWC, soil water content; TP, total phosphorus; TN, total nitrogen; AK, available potassium; AP, available phosphorus; AN, available nitrogen; SOC, soil organic carbon; SR, soil respiration; Tif.TS, Tifgreen bermudagrass with traffic treatment; Tif.NT, Tifgreen bermudagrass with non-traffic treatment; Com.TS, Common bermudagrass with traffic treatment; Com.NT, Common bermudagrass with non-traffic treatment.

3.3. The Composition of Bacterial Communities

Sequences were affiliated with the highest abundances of phyla Acidobacteria (29.45%–35.89% of the overall relative abundance) as well as Proteobacteria (19.22%–23.97%) in the four treatments (Figure 4a). The relative abundances of phyla Acidobacteria, Proteobacteria, Patescibacteria, Chlamydiae, Spirochaetes and Elusimicrobia in Tif.TS decreased remarkably ($p < 0.05$) relative to Tif.NT, while phyla Chloroflexi, Actinobacteria, Nitrospirae, Planctomycetes, Bacteroidetes, Gemmatimonadetes and Firmicutes in Tif.TS were significantly higher than Tif.NT ($p < 0.05$). Furthermore, in common bermudagrass, the relative abundances of phyla Acidobacteria, Patescibacteria, Chlamydiae, Spirochaetes and Elusimicrobia in Com.TS decreased dramatically ($p < 0.05$) compared with Com.NT, while the relative abundances of phyla Actinobacteria, Nitrospirae, Verrucomicrobia, Bacteroidetes, Gemmatimonadetes and Firmicutes in Com.TS increased remarkably ($p < 0.05$) relative to Com.NT (Table S1).

Order Acidobacteriales with the highest abundances in the four treatments (Figure 4b). Relative abundances of order Acidobacteriales, Betaproteobacteriales, Xanthomonadales, Chlamydiales and Elsterales in Tif.TS were significantly lower than Tif.NT at the bacterial order level ($p < 0.05$), while the relative abundances of the order Ktedonobacterales, Pedosphaerales, Rhizobiales, Anaerolineales, Gemmatales and Frankiales in Tif.TS increased remarkably ($p < 0.05$) than Tif.NT. Furthermore, in common bermudagrass, the relative abundances of the order Acidobacteriales, Ktedonobacterales, Betaproteobacteriales, Chlamydiales, Gemmatales and Elsterales in Com.TS decreased remarkably more than Com.NT ($p < 0.05$), while those of the order Pedosphaerales, Rhizobiales, Anaerolineales, Xanthomonadales and Frankiales in Com.TS increased significantly more than Com.NT ($p < 0.05$) (Table S2).

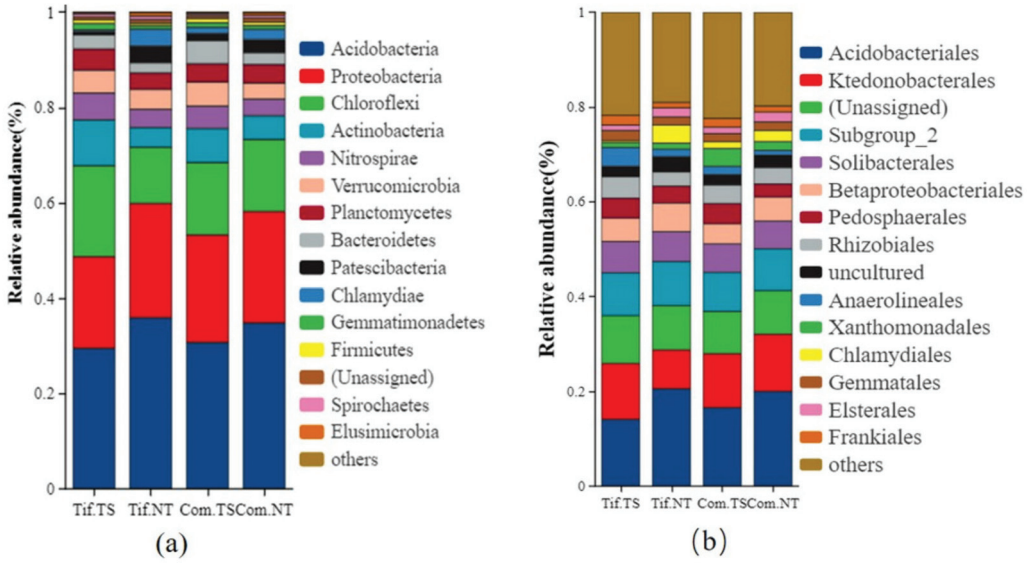

Figure 4. Difference in bacterial community relative abundances at phylum (**a**) and order (**b**) levels. Note: Tif.TS, Tifgreen bermudagrass with traffic treatment; Tif.NT, Tifgreen bermudagrass with non-traffic treatment; Com.TS, Common bermudagrass with traffic treatment; Com.NT, Common bermudagrass with non-traffic treatment.

3.4. Analysis of Bacterial Alpha- and Beta-Diversities and Their Relations with Environmental Factors

The alpha diversity index results (Figure 5) showed that the order of ACE and Chaol indexes of the four samples was Tif.NT > Com.NT > Tif.TS > Com.TS (Figure 5a,b). In conclusion, the soil bacterial community species richness was highest in Tif.NT and lowest in Com.TS. The Shannon index of soil bacteria under traffic stress was significantly lower than non-traffic stress (Figure 5c), but the Simpson index exhibited a different result, and its descending order was Com.NT < Tif.NT < Tif.TS < Com.TS (Figure 5d). The high Simpson index indicated a low soil bacterial community species diversity. Based on these four indexes, the ACE index, Chaol index and Shannon index in two species of bermudagrass under traffic stress were significantly lower than non-traffic stress ($p < 0.05$). The Simpson index increased to different degrees, indicating that traffic stress significantly reduced the richness of soil bacterial species in bermudagrass and its diversity. From the perspective of different turfgrass varieties, the ACE and Chao1 indexes of Tifgreen bermudagrass increased remarkably relative to common bermudagrass under normal growth conditions and traffic stress ($p < 0.05$) (Table S3) and the difference between Shannon and Simpson indexes was insignificant, which indicated an increased soil bacterial diversity in Tifgreen bermudagrass compared with common bermudagrass under normal growth conditions and traffic stress.

PCoA ordination was adopted to reveal distinct changes between various treatments for bacterial communities, PCoA1, and PCoA2 (the first and second principal components made 53.1% and 15.6% contributions, respectively) (Figure 6). Traffic stress significantly affected soil microbial communities according to Bray–Curtis distances.

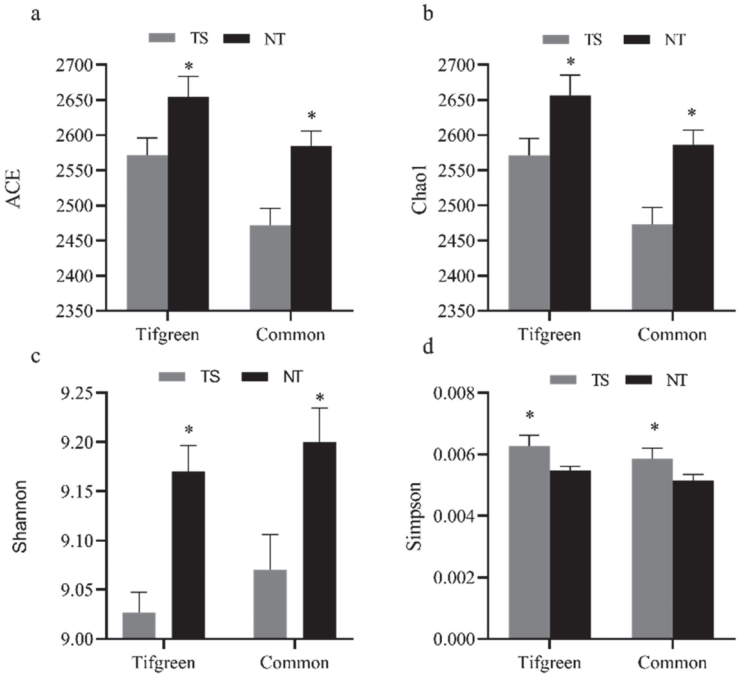

Figure 5. Alpha diversity index of soil bacterial community structure under traffic stress. (**a**) ACE index, (**b**) Chaol index, (**c**) Shannon index, (**d**) Simpson index. Note: * $p < 0.05$ under diverse treatments. TS: traffic stress; NT: non-traffic stress.

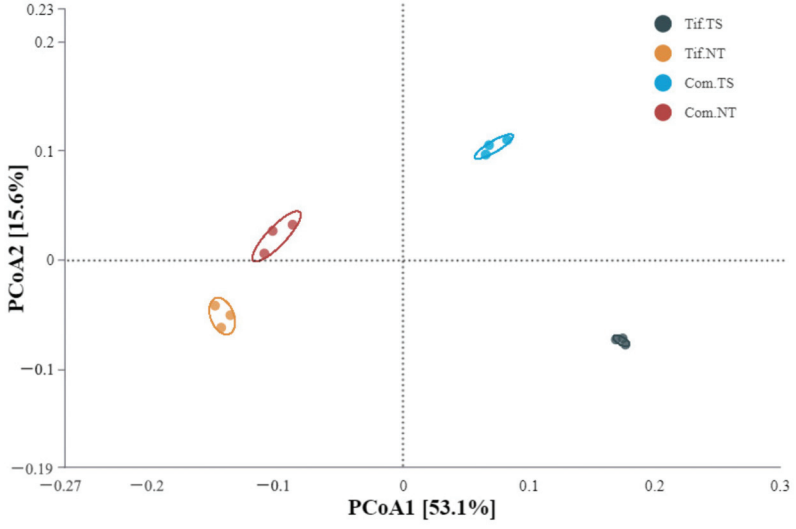

Figure 6. PCoA on structures of soil bacterial communities under traffic stress. Note: Tif.TS, Tifgreen bermudagrass with traffic treatment; Tif.NT, Tifgreen bermudagrass with non-traffic treatment; Com.TS, Common bermudagrass with traffic treatment; Com.NT, Common bermudagrass with non-traffic treatment.

3.5. LefSe

LEfSe analysis was conducted to examine the effects of traffic treatment on Tifgreen bermudagrass (Figure 7a) and Common bermudagrass (Figure 7b) (from phylum to order); the LDA scores of them were greater than 3.8. The longer the length of the column, the more apparent the differences between the species. Deltaproteobacteria, Gammaproteobacteria, Chlamyliae, Chlamydiales, Chlamydiae, Acidobacteria, Proteobacteria, Acidobacteriales, and Acidobacteriia of Tif.NT and Chloroflexi, Actinobacteria, Ktedonobacteria, Ktedonobacterales, Actinobacteria, Anaerolineae, Anaerolineales, Thermoleophilia, Rhizobiales, and Planctomycetes of Tif.TS; Actinobacteria Bacteroidetes, Xanthomonadale, Bacteroidia, Verrucomicrobiae, Sphingobacteriale, Actinobacteria, Verrucomicrobia, and Pedosphaerale of Com.NT, and Acidobacteriia, Acidobacteria, and Acidobacteriales of Com.TS.

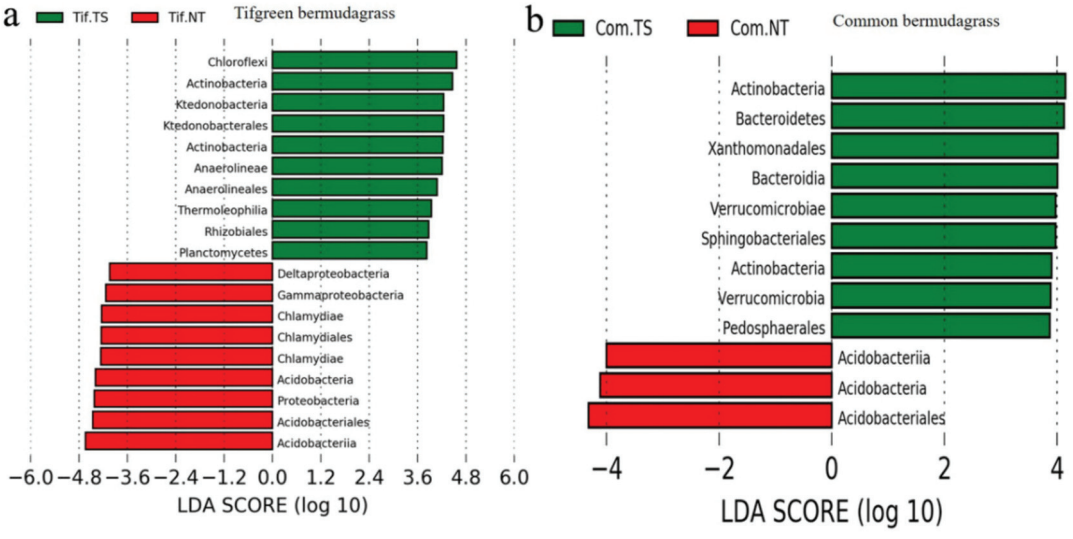

Figure 7. LDA effect size (LEfSe) analysis on soil bacteria under traffic stress in Tifgreen Bermudagrass (**a**) and Common bermudagrass (**b**). Note: Tif.TS, Tifgreen bermudagrass with traffic treatment; Tif.NT, Tifgreen bermudagrass with non-traffic treatment; Com.TS, Common bermudagrass with traffic treatment; Com.NT, Common bermudagrass with non-traffic treatment.

As revealed by redundancy analysis (RDA), alterations in the turf quality and soil physicochemical properties play a crucial function in forming the microbial community structure and composition. Changes in TD, UB, AB, CD, SR, SBD, SSH, SWC, and pH significantly affected the bacterial structural and compositional changes in diverse turf soil samples, but alterations of TN, TP, AK, AN, AP, and SOC showed less influence (Figure 8). The RDA diagram in Figure 8a showed that 61.44% of the total bacterial community variation could be explained by turf quality indicators and soil physical factors; RDA1 explained 36.81% of the total variation, and RDA2 explained 24.63% of the total variation. The RDA diagram in Figure 8b showed that 68.48% of the bacterial community variation could be explained by the soil chemical factors; RDA1 explained 40.12% of the total bacterial community variation, and RDA2 explained 28.63% of the total bacterial community variation.

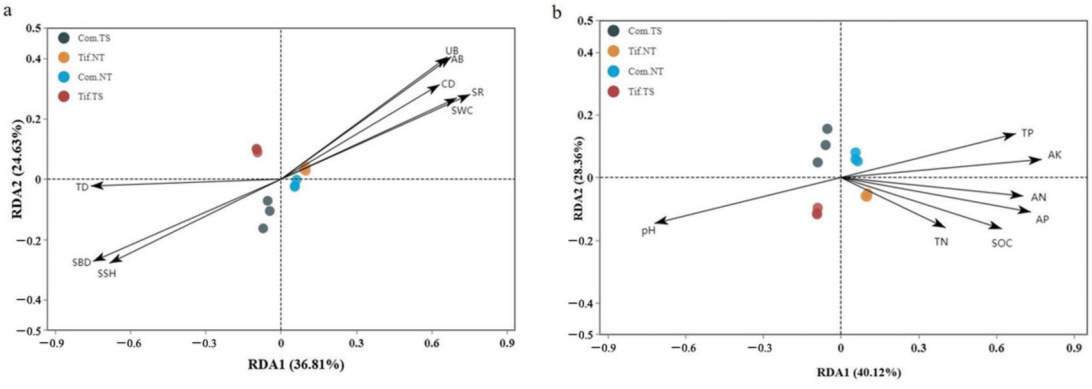

Figure 8. RDA of bacterial communities and environmental factors (**a**) RDA of turf quality indicators (TD, CD, AB, UB), soil physical properties (SBD, SSH, SWC, SR) and bacterial communities. (**b**) The RDA of soil chemical properties (TP, AP, TN, AN, AK, SOC, pH) and bacterial communities. Tif.TS, Tifgreen bermudagrass with traffic treatment; Tif.NT, Tifgreen bermudagrass with non-traffic treatment; Com.TS, Common bermudagrass with traffic treatment; Com.NT, Common bermudagrass with non-traffic treatment.

3.6. Spearman Correlation Analysis

At the bacterial phylum level, based on Spearman correlation analysis (Figure 9a), Gemmatimonadetes, Nitrospirae and Actinobacteria were strongly positively correlated to pH and TD ($p < 0.01$), while Elusimicrobia, Acidobacteria and Patescibacteria were strongly negatively associated. Additionally, Gemmatimonadetes, Nitrospirae and Actinobacteria revealed a strong negative association with AK ($p < 0.01$), while Elusimicrobia, Acidobacteria, Patescibacteria and Chloroflexi were strongly positively associated ($p < 0.01$). Elusimicrobia, Acidobacteria and Patescibacteria showed a strong direct correlation to AK, SOC, TP, SWC, AP, SR, CD, AB ($p < 0.01$).

At the bacterial order level, Frankiales showed a strong direct proportion to SSH, SBD, TD, and pH ($p < 0.01$), while in strong indirect proportion to TP, AK, SOC, CD, UB, AB, AP, SR, SWC, and AN ($p < 0.01$) (Figure 9b). Elsterales and Acidobacteriales were in strong direct proportion to SSH, SBD, TD, and pH ($p < 0.01$) and revealed a strong positive association with TP, AK, AP, SR, SWC, and AN ($p < 0.01$). Betaproteobacteriales and Elsterales revealed a strong negative association with UB, AB, AP, SR ($p < 0.01$).

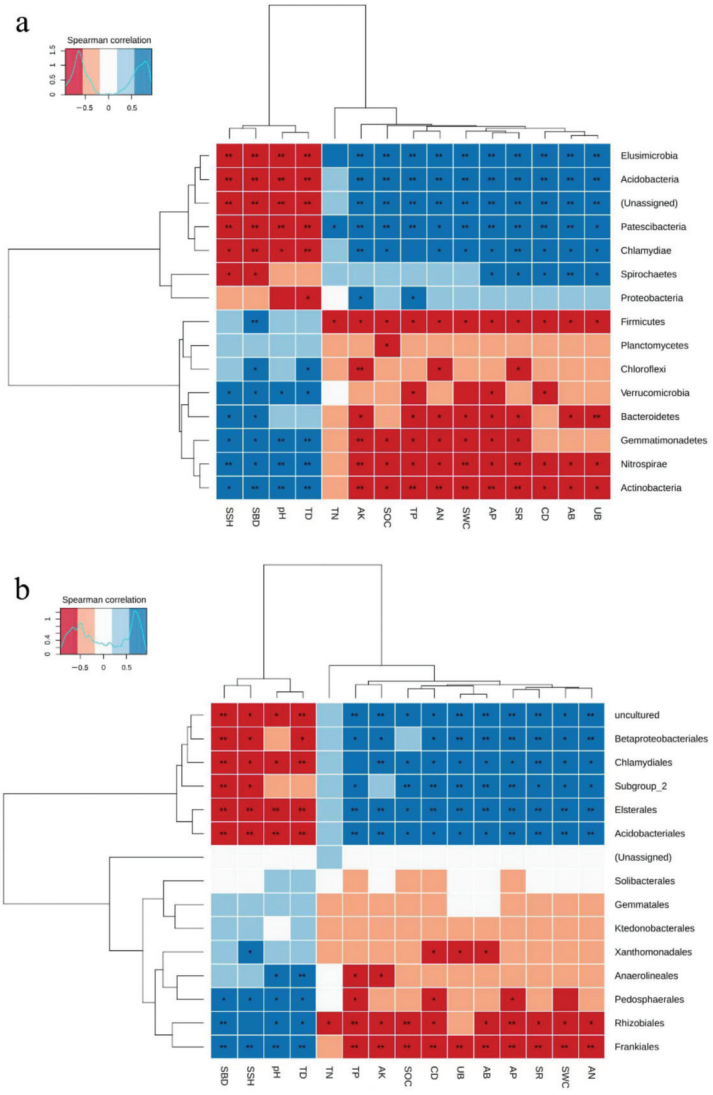

Figure 9. Spearman correlation analysis of phylum (**a**) and order (**b**) levels and environmental factors. Note: * $p < 0.05$ under diverse treatments. ** $p < 0.01$ under diverse treatments.

4. Discussion

4.1. Changes in Turf Quality, Bacterial Community Diversity, and Soil Physicochemical Characters under Traffic Stress

Traffic stress causes narrowing and curving of leaves, smaller plant size, and in severe cases, direct tearing damage or death of stem tissue in some plants [38,39], resulting in a decrease in TD, CD, AB, and UB (Figure 3). Plants can affect the soil bacterial community around the root systems via rhizosphere resources (e.g., root exudates, allelochemicals and soil nutrients) [40]. Traffic changes the soil nutrient composition and physical structure. It increased SSH, and SBD while decreasing SWC, TN, TP, AN, AP, AK, and SOC (Table 1). Traffic causes soil compaction, which destroys the soil particle distribution, and increases SSH and SBD (Table 1), which means the mechanical resistance of soil increases [41]. Thus,

it compresses the space for turfgrass roots to grow, limits the range of root activity, and reduces the roots' vigor and resistance, resulting in reduced turf quality. In this environment of low soil oxygen and high mechanical resistance, the plant root system exudes a large amount of root fluid specifically designed to alter the soil bacteria composition, which is supported by Jaqueth et al. [42]. Aboveground vegetation species may restrict specific soil microbial community growth [43]. Alpha diversity revealed that the Tif-NT soil sample had the highest bacterial community abundance, and its diversity was better than Com-NT. The bacterial community structure was different between common and Tifgreen bermudagrass (Figure 5). The PCoA results showed (Figure 6) that both species and traffic had a specific effect on soil bacterial community structures, while traffic had a stronger impact. Similarly, their soil bacterial communities changed differently due to the difference in the degree of damage and impact of traffic stress on the two bermudagrass turfs. LefSe revealed that the abundance of soil bacterial types in bermudagrass turfs traffic compared to non-traffic treatments was significantly different, mainly by Chloroflexi, Actinobacteria, and Ktedonobacteria in Tif.TS, and Proteobacteria, Acidobacteriales, and Acidobacteria in Tif.NT. Bermudagrass turf traffic compared to non-traffic treatments was significantly different, mainly by Actinobacteria, Bacteroidetes, and Xanthomonadale in Com.TS, and Acidobacteriia, Acidobacteria, and Acidobacteriales in Com.NT (Figure 7). Plant species showed great differences concerning little decomposition ability [44], which impacts their soil microbial structure [45]. Traffic directly causes damage to turfgrass stems and leaves, and some leaves fall off and become litter [46]. The material composition and structure of the stem and leaf parts of the two species of bermudagrass differ, and traffic on the aboveground part of the bermudagrass causes part of its contents to exude and flow into the soil, which we speculate may cause the change in soil bacterial communities in the two species of bermudagrass under different treatments.

The aboveground biota can provide resources such as organic carbon necessary for organic matter decomposition by belowground biota. Afterward, the products obtained from organic decomposition are adopted by aboveground biota as nutrients, particularly plants [47]. The soil bacterial ACE and Chaol indexes in both bermudagrass turf under traffic conditions remarkably decreased compared with non-traffic treatment. At the same time, the Shannon index also showed different degrees of reduction (Figure 5), indicating that traffic stress significantly reduced the number of soil bacterial species in bermudagrass and its diversity. Turf abrasion in traffic stress directly damages the rhizome part of the turfgrass on the surface, reducing the quality of the turf [48]. It also reduces the photosynthesis of turf leaves, leading to slow growth of turf plants, resulting in a decrease in the aboveground biomass of the turf [49]. The aboveground part of bermudagrass turf under traffic stress was damaged, and the aboveground biomass was significantly reduced, resulting in a decrease in the supply of organic carbon and nutrients from the aboveground to the belowground part, which to some extent affected the activity of the soil bacterial community while reducing the bacterial diversity. Alterations to the soil physicochemical properties greatly affect microbial composition and structure [50]. Under the traffic conditions of the self-made traffic simulator, with increased soil compaction, there was a corresponding increase in SBD, decrease in SWC, and decrease in respiration (Table 1).

Traffic reduced, to varying degrees, the N, P, K, and SOC contents of bermudagrass turf soils (Table 1.). On the one hand, it may be due to traffic stress reducing the cover degree of bermudagrass turf, increasing the exposed surface area and decomposition of SOC, combined with wind and water erosion, resulting in the loss of soil nutrients and decrease in soil pH. On the other hand, traffic stress increases the compaction of soil, reducing its aeration and permeability, leading to increased competition between underground parts of plants and accelerating the absorption and utilization of nutrients [51]. These factors affect the soil microbial living conditions, decreasing the soil bacterial diversity and richness. The carbon commission by soil respiration (SR) includes soil hetero-trophic respiration and root respiration, and soil heterotrophic respiration is closely related to the content of soil

organic carbon (SOC). Traffic stress causes abrasion and compression of the aboveground portion of Bermudagrass turf, which affects root growth and leads to a decrease in the belowground biomass of the grass (Figure 3) and the respiration intensity of the root system. The soil heterotrophic respiration is positively correlated with the soil organic carbon content [52]. The decrease in SR accompanied by a decrease in SOC reflected a decrease in the activity of soil microorganisms [53]. Our work demonstrated that under moderate traffic conditions, the TD, CD and AB, UB of Tifgreen bermudagrass decreased less than common bermudagrass. Traffic stress directly damaged some of the stem and leaf tissues on turfgrass, causing a 36% to 39% decrease in the aboveground biomass magnitude of the two turfgrasses due to leaf damage, decreased turfgrass photosynthetic capacity, decreased organic carbon content flowing from the aboveground part to the underground part, and a lack of nutrient content, respiratory substrate and energy supply, leading to a decrease in the soil respiration rate [54]. The belowground biomass of Tifgreen was significantly higher than common bermudagrass, resulting in a much lower respiration intensity of the root system of common bermudagrass, which was primarily related to lower soil bacterial diversity and abundance in common bermudagrass turf than Tifgreen bermudagrass under traffic stress.

4.2. Bacterial Community Structure Correlation with Soil Properties under Traffic Stress

Several species of soil bacteria exist at low levels, whereas a low portion of species exists at high levels [55]. Proteobacteria and Acidobacteria are the predominant soil bacteria at the phylum level globally [56]. We found that Acidobacteria and Proteobacteria were the predominant bacterial species at phylum levels in soil samples from all four treatments (Figure 4). Their pooled relative abundance was 50% of the overall bacterial species in the entire sample soil specimens. Proteobacteria participate in recycling nutrients and increase plant development and soil fertility [57]. Acidobacteria are ubiquitous, and among the most abundant bacterial phyla in acidic soil [58]. The pH of all treatments in our research was less than 7, belonging to an acidic environment (Table 1). The experiment site is located in a subtropical area, with high temperatures and rain in summer, an average temperature over 30 degrees, and monthly precipitation of more than 200 mm (Figure 1). Therefore, the soil weathering and soil formation were strong, the plant material cycle was rapid, and the salt base was highly unsaturated, leading to acidic soil [59]. At the same time, the plant growth is vigorous in summer, the root secretion is more than that in other seasons, and the soil organic carbon content is higher [60]. Therefore, Proteobacteria and Acidobacteria were the predominant soil bacteria at the phylum level during this experiment. Dai et al. considered that soil organic C availability is likely to preferentially support the growth of copiotrophic bacteria (e.g., some Proteobacteria) due to their preference for living in nutrient-sufficient or nutrient-limited environments [61]. We found that traffic decreased the SOC content (Table 1), which resulted in less support for the growth of Proteobacteria. The pH has been identified as the key factor distinguishing the overall bacterial species [62]. However, Proteobacteria were not significantly related to pH in a previous study [63]. Proteobacteria were significantly associated with TD, AK, and TP ($p < 0.05$). In contrast, 10 of the 15 bacterial species, such as Acidobacteria, were related to pH (Figure 9), concordant with molecular-study-derived data that Acidobacteria accounts for the main part of the soil microbial community, the greatest abundance in acidic soil [64]. At present, Acidobacteria are suggested to a play role in particular biopolymer decomposition as well as global carbon, hydrogen, and iron cycles in the natural ecosystem [65]. Moreover, Acidobacteria possessed a strong positive association with AK, SOC, TP, SWC, AP, SR, CD, and AB ($p < 0.01$). We observed that the phylum Chloroflexi, Verrucomicrobia, and Actinobacteria showed higher abundances in turf soils under traffic stress, conforming with the copiotroph/oligotroph hypothesis by Fierer et al. that bacterial phyla with oligotrophic properties are more abundant in a nutrient-poor environment [66]. In addition, it conforms with recent results that oligotrophic taxa have reduced abundances (such as Planctomycetes and Verrucomicrobia) in cultured fertilized soils [67]. In addition, Actinomycetes may ex-

hibit remarkable desiccation resistance and survive in resource-depleting soils for a long time [68]. Under traffic stress, SOC, SWC, and the content of nutrients such as N, P, K of bermudagrass turf soil showed different degrees of decrease (Table 1). Thus, bacterial phyla with oligotrophic properties such as actinomycetes and Chloroflexi were more suitable to grow in this soil environment. According to RDA, the SOC level showed a positive correlation with bacterial diversities (Figure 8) since SOC offered energy for bacteria [69]. Acidobacteriia is ecologically well adapted in dry, sandy soil characterized by a lack of organic matter [70]. Therefore, the difference in the content of Acidobacteriia was greater in common bermudagrass soils, where the decrease in turf quality and soil organic carbon content was higher under traffic conditions.

Microbial communities adapt to altering environmental conditions [71]. Such alterations in functional bacteria detected in the present work might be due to traffic-stress-induced adaptation of turfgrass. Further studies are warranted to elucidate the biological adaptation mechanism, allowing us to select the best turf management options.

5. Conclusions

Under traffic stress, both the common bermudagrass and Tifgreen bermudagrass lawn turf quality decreased, the soil physicochemical properties changed, the SSH and SBD increased, and the pH, SR, SOC, and nutrient content decreased. Traffic was the main factor affecting the soil microbial structure. Both the soil bacterial abundance and diversity decreased under trampling stress. The RDA showed that changes in the TD, UB, AB, CD, SR, SBD, SSH, SWC, and pH significantly affected the bacterial structural and compositional changes in diverse turf soils. Acidobacteria showed a significant positive association with AK, SOC, TP, SWC, AP, SR, CD, and AB. Proteobacteria were significantly associated with TD, AK, and TP. Chloroflexi, Verrucomicrobia, and Actinobacteria showed significantly increased abundances in turf soils under traffic stress. Thus, this will lay a certain theoretical foundation for the healthy treatment of urban recreation and sports turfs.

Supplementary Materials: The following supporting information can be downloaded at: https://www.mdpi.com/article/10.3390/agriculture12050668/s1, Table S1. Difference in bacterial community relative abundances at phylum level (%). Table S2. Difference in bacterial community relative abundances at order level (%). Table S3. Alpha diversity (ACE, Chaol, Shannon and Simpson indexes) index of soil bacterial community structure under traffic stress.

Author Contributions: All authors contributed to the study conception and design. J.Z. and T.L. conceived and initiated the project. All the experiments were performed by H.W. and Y.W. The material preparation and data collection were performed by Y.W. The bioinformatic analysis was conducted by L.G. The first draft of the manuscript was written by H.W. and all authors commented on previous versions of the manuscript. All authors have read and agreed to the published version of the manuscript.

Funding: This study was supported by the Natural Science Foundation of Guangdong Province (Grant No. 2020A1515011261) and Key Research and Development Program of Guangzhou (No. 202103000066).

Institutional Review Board Statement: Not applicable.

Informed Consent Statement: Not applicable.

Data Availability Statement: The data will be provided individually by contacting the corresponding author.

Conflicts of Interest: The authors declare that they have no known competing financial interests.

References

1. Gląb, T.; Szewczyk, W.; Dubas, E.; Kowalik, K.; Jezierski, T. Anatomical and Morphological Factors Affecting Wear Tolerance of Turfgrass. *Sci. Horticul.* **2015**, *185*, 1–13. [CrossRef]
2. Martiniello, P. Effect of Traffic Stress on Cool-Season Turfgrass under A Mediterranean Climate. *Agron. Sust. Dev.* **2007**, *27*, 293–301. [CrossRef]
3. Wei, H.; Yang, W.; Wang, Y.; Ding, J.; Ge, L.; Richardson, M.; Liu, T.; Zhang, J. Correlations among Soil, Leaf Morphology, and Physiological Factors with Wear Tolerance of Four Warm-season Turfgrass Species. *HortScience* **2022**, *57*, 571–580. [CrossRef]
4. Gląb, T.; Szewczyk, W. The Effect of Traffic on Turfgrass Root Morphological Features. *Sci. Horticul.* **2015**, *197*, 542–554. [CrossRef]
5. Antille, D.L.; Peets, S.; Galambošová, J.; Botta, G.F.; Rataj, V.; Macák, M.; Tullberg, J.N.; Chamen, W.C.; White, D.R.; Misiewicz, P.A.; et al. Soil Compaction and Controlled Traffic Farming in Arable and Grass Cropping Systems. *Agron. Res.* **2019**, *17*, 653–682. [CrossRef]
6. Hiernaux, P.; Bielders, C.L.; Valentin, C.; Bationo, A.; Fernandez-Rivera, S. Effects of Livestock Grazing on Physical and Chemical Properties of Sandy Soils in Sahelian Rangelands. *J. Arid Environ.* **1999**, *41*, 231–245. [CrossRef]
7. Liu, T.; Wang, X.; Zhang, J. Development of A Novel Traffic Simulator and Evaluation of Warm-Season Turfgrass Traffic Tolerance in Field Experiments. *Acta Pratacul. Sin.* **2019**, *28*, 41–52. [CrossRef]
8. Carman, K. Compaction Characteristics of Towed Wheels on Clay Loam in a Soil Bin. *Soil Till. Res.* **2002**, *65*, 37–43. [CrossRef]
9. Franzluebbers, A.; Stuedemann, J.; Schomberg, H. Spatial Distribution of Soil Carbon and Nitrogen Pools under Grazed Tall Fescue. *Soil Sci. Soc. Am. J.* **2000**, *64*, 635–639. [CrossRef]
10. Chen, Y.L.; Deng, Y.; Ding, J.Z.; Hu, H.W.; Xu, T.L.; Li, F.; Yang, G.B.; Yang, Y.H. Distinct Microbial Communities in The Active and Permafrost Layers on The Tibetan Plateau. *Mol. Ecol.* **2017**, *26*, 6608–6620. [CrossRef]
11. Singh, J.S.; Raghubanshi, A.S.; Singh, R.S.; Srivastava, S. Microbial Biomass Acts as A Source of Plant Nutrients in Dry Tropical Forest and Savanna. *Nature* **1989**, *338*, 499–500. [CrossRef]
12. Bardgett, R.D.; Van Der Putten, W.H. Belowground Biodiversity and Ecosystem Functioning. *Nature* **2014**, *515*, 505–511. [CrossRef] [PubMed]
13. Delgado-Baquerizo, M.; Oliverio, A.M.; Brewer, T.E.; Benavent-González, A.; Eldridge, D.J.; Bardgett, R.D.; Maestre, F.T.; Singh, B.K.; Fierer, N. A Global Atlas of the Dominant Bacteria Found in Soil. *Science* **2018**, *359*, 320–325. [CrossRef] [PubMed]
14. Wu, S.H.; Huang, B.H.; Huang, C.L.; Li, G.; Liao, P.C. The Aboveground Vegetation Type and Underground Soil Property Mediate the Divergence of Soil Microbiomes and The Biological Interactions. *Microb. Ecol.* **2018**, *75*, 434–446. [CrossRef] [PubMed]
15. Bissett, A.; Brown, M.V.; Siciliano, S.D.; Thrall, P.H. Microbial Community Responses to Anthropogenically Induced Environmental Change: Towards A Systems Approach. *Ecol. Lett.* **2013**, *16*, 128–139. [CrossRef] [PubMed]
16. Klimek, B.; Niklińska, M.; Jaźwa, M.; Tarasek, A.; Tekielak, I.; Musielok, Ł. Covariation of Soil Bacteria Functional Diversity and Vegetation Diversity Along an Altitudinal Climatic Gradient in The Western Carpathians. *Pedobiologia* **2015**, *58*, 105–112. [CrossRef]
17. Bukar, M.; Sodipo, O.; Dawkins, K.; Ramirez, R.; Kaldapa, J.T.; Tarfa, M.; Esiobu, M. Microbiomes of Top and Sub-Layers of Semi-Arid Soils in North-Eastern Nigeria Are Rich in Firmicutes and Proteobacteria with Surprisingly High Diversity of Rare Species. *Adv. Microbiol.* **2019**, *9*, 102–118. [CrossRef]
18. Brockett, B.F.; Prescott, C.E.; Grayston, S.J. Soil Moisture is the Major Factor Influencing Microbial Community Structure and Enzyme Activities across Seven Biogeoclimatic Zones in Western Canada. *Soil Biol. Biochem.* **2012**, *44*, 9–20. [CrossRef]
19. Cederlund, H.; Wessén, E.; Enwall, K.; Jones, C.M.; Juhanson, J.; Pell, M.; Philippot, L.; Hallin, S. Soil Carbon Quality and Nitrogen Fertilization Structure Bacterial Communities with Predictable Responses of Major Bacterial Phyla. *Appl. Soil Ecol.* **2014**, *84*, 62–68. [CrossRef]
20. He, W.; Zhang, M.; Jin, G.; Sui, X.; Zhang, T.; Song, F. Effects of Nitrogen Deposition on Nitrogen-Mineralizing Enzyme Activity and Soil Microbial Community Structure in A Korean Pine Plantation. *Microb. Ecol.* **2021**, *81*, 410–424. [CrossRef]
21. Li, J.; Shen, Z.; Li, C.; Kou, Y.; Wang, Y.; Tu, B.; Zhang, S.; Li, X. Stair-Step Pattern of Soil Bacterial Diversity Mainly Driven by pH and Vegetation Types Along the Elevational Gradients of Gongga Mountain, China. *Front. Microbiol.* **2018**, *9*, 569. [CrossRef] [PubMed]
22. Martınez, L.; Zinck, J. Temporal Variation of Soil Compaction and Deterioration of Soil Quality in Pasture Areas of Colombian Amazonia. *Soil Till. Res.* **2004**, *75*, 3–18. [CrossRef]
23. Patkowska, E. Biostimulants Managed Fungal Phytopathogens and Enhanced Activity of Beneficial Microorganisms in Rhizosphere of Scorzonera (*Scorzonera hispanica* L.). *Agriculture* **2021**, *11*, 347. [CrossRef]
24. Van Wyk, D.A.; Adeleke, R.; Rhode, O.H.; Bezuidenhout, C.C.; Mienie, C. Ecological Guild and Enzyme Activities of Rhizosphere Soil Microbial Communities Associated with Bt-Maize Cultivation Under Field Conditions in North West Province of South Africa. *J. Basic Microbiol.* **2017**, *57*, 781–792. [CrossRef]
25. Cheng, H.; Wu, B.; Wei, M.; Wang, S.; Rong, X.; Du, D.; Wang, C. Changes in Community Structure and Metabolic Function of Soil Bacteria Depending on The Type Restoration Processing in The Degraded Alpine Grassland Ecosystems in Northern Tibet. *Sci. Total Environ.* **2020**, *755*, 142619. [CrossRef]
26. Zhang, J.; Richardson, M.; Karcher, D.; McCalla, J.; Mai, J.; Luo, H. Dormant Sprigging of Bermudagrass and Zoysiagrass. *HortTechnology* **2021**, *31*, 395–404. [CrossRef]

27. Magni, S.; Sportelli, M.; Grossi, N.; Volterrani, M.; Minelli, A.; Pirchio, M.; Fontanelli, M.; Frasconi, C.; Gaetani, M.; Martelloni, L.; et al. Autonomous Mowing and Turf-Type Bermudagrass as Innovations for an Environment-Friendly Floor Management of a Vineyard in Coastal Tuscany. *Agriculture* **2020**, *10*, 189. [CrossRef]
28. Wei, H.; Ding, J.; Zhang, J.; Yang, W.; Wang, Y.; Liu, T. Changes in Soil Fungal Community Structure Under Bermudagrass Turf in Response to Traffic Stress. *Acta Pratacul. Sin.* **2022**, *31*, 102–112. [CrossRef]
29. Olsen, S.R. *Estimation of Available Phosphorus in Soils by Extraction with Sodium Bicarbonate*; US Department of Agriculture: Washington, DC, USA, 1954.
30. Wu, W.; Tang, X.P.; Yang, C.; Liu, H.B.; Guo, N.J. Investigation of Ecological Factors Controlling Quality of Flue-Cured Tobacco (*Nicotiana tabacum* L.) Using Classification Methods. *Ecol. Inform.* **2013**, *16*, 53–61. [CrossRef]
31. Walkley, A. An Examination of Methods for Determining Organic Carbon and Nitrogen in Soils. (With One Text-figure.). *J. Agric. Sci.* **1935**, *25*, 598–609. [CrossRef]
32. Caporaso, J.G.; Kuczynski, J.; Stombaugh, J.; Bittinger, K.; Bushman, F.D.; Costello, E.K.; Fierer, N.; Peña, A.G.; Goodrich, J.K.; Gordon, J.I.; et al. QIIME Allows Analysis of High-Throughput Community Sequencing Data. *Nat. Methods* **2010**, *7*, 335–336. [CrossRef] [PubMed]
33. Yilmaz, P.; Parfrey, L.W.; Yarza, P.; Gerken, J.; Pruesse, E.; Quast, C.; Schweer, T.; Peplies, J.; Ludwig, W.; Glöckner, F.O. The SILVA and "All-Species Living Tree Project (LTP)" Taxonomic Frameworks. *Nucl. Acids Res.* **2014**, *42*, D643–D648. [CrossRef] [PubMed]
34. Heruth, D.; Xiong, M.; Jiang, X. Microbiome-seq data analysis. In *Big Data Analysis for Bioinformatics and Biomedical Discoveries*; CRC Press: Boca Raton, FL, USA, 2016; Volume 97, p. 114.
35. Oksanen, J.; Kindt, R.; Legendre, P.; O'Hara, B.; Stevens, M.H.H.; Oksanen, M.J.; Simpson, G.L.; Solymos, P.; Wagner, H. The vegan package. *Comm. Ecol. Pack.* **2007**, *10*, 719. Available online: http://www.R-project.org (accessed on 24 February 2021).
36. Love, M.I.; Huber, W.; Anders, S. Moderated Estimation of Fold Change and Dispersion for RNA-seq Data with DESeq2. *Genome Biol.* **2014**, *15*, 550. [CrossRef]
37. White, J.R.; Nagarajan, N.; Pop, M. Statistical Methods for Detecting Differentially Abundant Features in Clinical Metagenomic Samples. *PLoS Comput. Biol.* **2009**, *5*, e1000352. [CrossRef]
38. Menneer, J.; Ledgard, S.; McLay, C.; Silvester, W. The Effects of Treading by Dairy Cows during Wet Soil Conditions on White Clover Productivity, Growth and Morphology in a White Clover–Perennial Ryegrass Pasture. *Grass Forage Sci.* **2005**, *60*, 46–58. [CrossRef]
39. Malleshaiah, S.; Govindaswamy, V.; Murugaiah, J.; Ganga, M.; Surakshitha, N. Influence of Traffic Stress on Warm Season Turfgrass Species under Simulated Traffic. *Indian J. Agric. Sci.* **2017**, *87*, 62–68.
40. Eilers, K.G.; Lauber, C.L.; Knight, R.; Fierer, N. Shifts in Bacterial Community Structure Associated with Inputs of Low Molecular Weight Carbon Compounds to Soil. *Soil Biol. Biochem.* **2010**, *42*, 896–903. [CrossRef]
41. Hamza, M.; Anderson, W. Soil Compaction in Cropping Systems: A Review of The Nature, Causes and Possible Solutions. *Soil Till. Res.* **2005**, *82*, 121–145. [CrossRef]
42. Jaqueth, A.L.; Turner, T.R.; Iwaniuk, M.E.; McIntosh, B.J.; Burk, A.O. Relative Traffic Tolerance of Warm-Season Grasses and Suitability for Grazing by Equine. *J. Equine Vet. Sci.* **2019**, *103*, 103244. [CrossRef]
43. Zhang, Y.; Cao, C.; Peng, M.; Xu, X.; Zhang, P.; Yu, Q.; Sun, T. Diversity of Nitrogen-Fixing, Ammonia-Oxidizing, And Denitrifying Bacteria in Biological Soil Crusts of A Revegetation Area In Horqin Sandy Land, Northeast China. *Ecol. Eng.* **2014**, *71*, 71–79. [CrossRef]
44. Cornwell, W.K.; Cornelissen, J.H.; Amatangelo, K.; Dorrepaal, E.; Eviner, V.T.; Godoy, O.; Hobbie, S.E.; Hoorens, B.; Kurokawa, H.; Pérez-Harguindeguy, N.; et al. Plant Species Traits Are the Predominant Control on Litter Decomposition Rates within Biomes Worldwide. *Ecol. Lett.* **2008**, *11*, 1065–1071. [CrossRef] [PubMed]
45. Hossain, M.Z.; Okubo, A.; Sugiyama, S.I. Effects of Grassland Species on Decomposition of Litter and Soil Microbial Communities. *Ecol. Res.* **2010**, *25*, 255–261. [CrossRef]
46. Pornaro, C.; Barolo, E.; Rimi, F.; Macolino, S.; Richardson, M. Performance of Various Cool-Season Turfgrasses as Influenced by Simulated Traffic in Northeastern Italy. *Eur. J. Hortic. Sci.* **2016**, *81*, 27–36. [CrossRef]
47. Wardle, D.A.; Bardgett, R.D.; Klironomos, J.N.; Setälä, H.; Van Der Putten, W.H.; Wall, D.H. Ecological Linkages between Aboveground and Belowground Biota. *Science* **2004**, *304*, 1629–1633. [CrossRef] [PubMed]
48. Trenholm, L.; Carrow, R.; Duncan, R. Mechanisms of Wear Tolerance in Seashore Paspalum and Bermudagrass. *Crop Sci.* **2000**, *40*, 1350–1357. [CrossRef]
49. Frank, D.A.; McNaughton, S. The Ecology of Plants, Large Mammalian Herbivores, and Drought in Yellowstone National Park. *Ecology* **1992**, *73*, 2043–2058. [CrossRef]
50. Ezeokoli, O.T.; Mashigo, S.K.; Paterson, D.G.; Bezuidenhout, C.C.; Adeleke, R.A. Microbial Community Structure and Relationship with Physicochemical Properties of Soil Stockpiles in Selected South African Opencast Coal Mines. *Soil Sci. Plant Nutr.* **2019**, *65*, 332–341. [CrossRef]
51. Cao, J.; Gong, Y.; Yeh, E.T.; Holden, N.M.; Adamowski, J.F.; Deo, R.C.; Liu, M.; Zhou, J.; Zhang, J.; Zhang, W.; et al. Impact of grassland contract policy on soil organic carbon losses from alpine grassland on the Qinghai-Tibetan Plateau. *Soil Use Manag.* **2017**, *33*, 663–671. [CrossRef]
52. Papp, M.; Fóti, S.; Nagy, Z.; Pintér, K.; Posta, K.; Fekete, S.; Csintalan, Z.; Balogh, J. Rhizospheric, Mycorrhizal and Heterotrophic Respiration in Dry Grasslands. *Eur. J. Soil Biol.* **2018**, *85*, 43–52. [CrossRef]

53. Wang, Y.; Wang, D.; Shi, B.; Sun, W. Differential Effects of Grazing, Water, And Nitrogen Addition on Soil Respiration and Its Components in a Meadow Steppe. *Plant Soil.* **2020**, *447*, 581–598. [CrossRef]
54. Gong, J.; Ge, Z.; An, R.; Duan, Q.; You, X.; Huang, Y. Soil Respiration in Poplar Plantations in Northern China at Different Forest Ages. *Plant Soil* **2012**, *360*, 109–122. [CrossRef]
55. Sogin, M.L.; Morrison, H.G.; Huber, J.A.; Welch, D.M.; Huse, S.M.; Neal, P.R.; Arrieta, J.M.; Herndl, G.J. Microbial diversity in the deep sea and the underexplored "rare biosphere". *Proc. Natl. Acad. Sci. USA* **2006**, *103*, 12115–12120. [CrossRef] [PubMed]
56. Tripathi, B.M.; Kim, M.; Singh, D.; Lee-Cruz, L.; Lai-Hoe, A.; Ainuddin, A.; Raha Abdul Rahim, R.; Husni, M.H.A.; Chun, J.; Adams, J.M. Tropical Soil Bacterial Communities in Malaysia: pH Dominates in The Equatorial Tropics Too. *Microb. Ecol.* **2012**, *64*, 474–484. [CrossRef] [PubMed]
57. Bulgarelli, D.; Schlaeppi, K.; Spaepen, S.; Van, T.; Emiel, V.L.; Schulze-Lefert, P. Structure and Functions of the Bacterial Microbiota of Plants. *Annu. Rev. Plant. Biol.* **2013**, *64*, 807–838. [CrossRef] [PubMed]
58. Eichorst, S.A.; Trojan, D.; Roux, S.; Herbold, C.; Rattei, T.; Woebken, D. Genomic Insights into The Acidobacteria Reveal Strategies for Their Success in Terrestrial Environments. *Environ. Microbiol.* **2018**, *20*, 1041–1063. [CrossRef]
59. Da, W.; Rd, B.; Jn, K. Ecological linkages between above ground and below ground biota. *Science* **2004**, *304*, 1629–1633. [CrossRef]
60. Neina, D. The Role of Soil pH in Plant Nutrition and Soil Remediation. *Appl. Environ. Soil Sci.* **2019**, *2019*, 1–9. [CrossRef]
61. Dai, Z.; Su, W.; Chen, H.; Barberán, A.; Zhao, H.; Yu, M.; Yu, L.; Brookes, P.C.; Schadt, C.W.; Chang, X.S.; et al. Long-term Nitrogen Fertilization Decreases Bacterial Diversity and Favors the Growth of Actinobacteria and Proteobacteria in Agro-Ecosystems Across the Globe. *Glob. Change Biol.* **2018**, *24*, 3452–3461. [CrossRef]
62. Jiao, S.; Lu, Y. Soil pH and Temperature Regulate Assembly Processes of Abundant and Rare Bacterial Communities in Agricultural Ecosystems. *Environ. Microbiol.* **2020**, *22*, 1052–1065. [CrossRef]
63. Lauber, C.L.; Mady, M.; Knight, R.; Fierer, N. Pyrosequencing-Based Assessment of Soil pH as A Predictor of Soil Bacterial Community Structure at The Continental Scale. *Appl. Environ. Microbiol.* **2009**, *75*, 5111–5120. [CrossRef] [PubMed]
64. Foesel, B.U.; Nägele, V.; Naether, A.; Wüst, P.K.; Weinert, J.; Bonkowski, M.; Lohaus, G.; Polle, A.; Alt, F.; Oelmann, Y.; et al. Determinants of Acidobacteria Activity Inferred from The Relative Abundances of 16S RRNA Transcripts in German Grassland and Forest Soils. *Environ. Microbiol.* **2014**, *16*, 658–675. [CrossRef] [PubMed]
65. Jones, R.T.; Robeson, M.S.; Lauber, C.L.; Hamady, M.; Knight, R.; Fierer, N. A Comprehensive Survey of Soil Acidobacterial Diversity Using Pyrosequencing and Clone Library Analyses. *ISME J.* **2009**, *3*, 442–453. [CrossRef]
66. Fierer, N.; Bradford, M.A.; Jackson, R.B. Toward an Ecological Classification of Soil Bacteria. *Ecology* **2007**, *88*, 1354–1364. [CrossRef]
67. Bledsoe, R.B.; Goodwillie, C.; Peralta, A.L. Long-term Nutrient Enrichment of an Oligotroph-Dominated Wetland Increases Bacterial Diversity in Bulk Soils and Plant Rhizospheres. *Msphere* **2020**, *5*, e00035-20. [CrossRef]
68. Radajewski, S.; Duxbury, T. Motility Responses and Desiccation Survival of Zoospores from the Actinomycete *Kineosporia* sp. Strain SR11. *Microb. Ecol.* **2001**, *41*, 233–244. [CrossRef] [PubMed]
69. Wang, Y.; Hu, N.; Ge, T.; Kuzyakov, Y.; Wang, Z.L.; Li, Z.; Tang, Z.; Chen, Y.; Wu, C.; Lou, Y. Soil Aggregation Regulates Distributions of Carbon, Microbial Community and Enzyme Activities after 23-Year Manure Amendment. *Appl. Soil Ecol.* **2017**, *111*, 65–72. [CrossRef]
70. Ivanova, A.A.; Zhelezova, A.D.; Chernov, T.I.; Dedysh, S.N. Linking Ecology and Systematics of Acidobacteria: Distinct Habitat Preferences of the Acidobacteriia and Blastocatellia in Tundra Soils. *PLoS ONE* **2020**, *15*, e0230157. [CrossRef]
71. Goldford, J.E.; Lu, N.; Bajic, D.; Estrela, S.; Tikhonov, M.; Sanchez-Gorostiaga, A.; Segrè, D.; Mehta, P.; Sanchez, A. Emergent Simplicity in Microbial Community Assembly. *Science* **2018**, *361*, 469–474. [CrossRef]

agriculture

MDPI

Article

Physicochemical Variables Better Explain Changes in Microbial Community Structure and Abundance under Alternate Wetting and Drying Events

Abbas Ali Abid [1,2], Xiang Zou [1,2], Longda Gong [1,2], Antonio Castellano-Hinojosa [3], Muhammad Afzal [2], Hongjie Di [1,2] and Qichun Zhang [1,2,*]

[1] Zhejiang Provincial Key Laboratory of Agricultural Resources and Environment, Key Laboratory of Environment Remediation and Ecological Health, Ministry of Education, Zhejiang University, Hangzhou 310058, China; abbas.ali.abid@gmail.com (A.A.A.); 0621182@zju.edu.cn (X.Z.); 21914103@zju.edu.cn (L.G.); hjdi@zju.edu.cn (H.D.)

[2] College of Environmental and Resource Sciences, Zhejiang University, Hangzhou 310058, China; mafzal.kust@gmail.com

[3] Department of Soil and Water Sciences, Southwest Florida Research and Education Center, Institute of Food and Agricultural Sciences, University of Florida, Immokalee, FL 34142, USA; ach@ugs.es

* Correspondence: qczhang@zju.edu.cn; Tel.: +86-571-8898-2413

Abstract: Soil microbial communities play an important role in nutrient cycling; however, their response under repeated long-term fertilization has attracted little attention and needs further appraisal. A 14-day incubation study compared the relative abundance, diversity, and composition of bacterial and fungal microbial communities in soils treated with long-term applications of chemical fertilizer (CF), pig manure plus chemical fertilizer (PMCF), and rice straw plus chemical fertilizer (SRCF) in a paddy field. A high-throughput sequencing approach was applied to assess the diversity and composition of microbial community. Results revealed the Shannon index of the bacterial community decreased with fertilizer addition but increased in case of fungal community. The abundance of the *Actinobacteria* was higher in the PMCF, while *Proteobacteria* were higher in the CF and SRCF treatments than those in the unamended control under alternate wetting and drying (AWD) and permanent flooding (PF). In addition, chemical fertilizer history increased the abundance of *Firmicutes* under AWD. Initially, *Nitrospira* were found higher in the unamended control than in the amended treatments, but an increase was observed with time in fertilized treatments. Among all genera, *Proteobacteria* were the most abundant bacterial genus. The main properties that markedly affected the bacterial communities were SOC ($R^2 = 0.4037$, $p < 0.02$), available P ($R^2 = 0.3273$, $p < 0.05$), and NO_3^- ($R^2 = 0.3096$, $p < 0.08$). Soil physicochemical factors and biogenic factors explained a variation of 46.27% and 29.35%, respectively. At the same time, 4.59% was the combined effect of physicochemical and biogenic factors. Our results suggested that the physicochemical properties had a more significant impact on bacterial activities than water regime by increasing N and organic matter concentrations in the soils.

Keywords: microbial diversity; wetting; drying; N-fertilization; Hi-throughput sequencing

Citation: Abid, A.A.; Zou, X.; Gong, L.; Castellano-Hinojosa, A.; Afzal, M.; Di, H.; Zhang, Q. Physicochemical Variables Better Explain Changes in Microbial Community Structure and Abundance under Alternate Wetting and Drying Events. *Agriculture* **2022**, *12*, 762. https://doi.org/10.3390/agriculture12060762

Academic Editors: Xingxu Zhang, Tingyu Duan, Gaowen Yang and Xiangling Fang

Received: 1 April 2022
Accepted: 2 May 2022
Published: 27 May 2022

1. Introduction

Nitrogen fertilization is an important practice for rice productivity. However, excessive fertilization of the paddy soils results in significant N_2O emissions [1], contributing to about 13–24% of annual emissions of N_2O [2]. About half of the world's population uses rice as a staple food. The annual production of rice is recorded at 480 million tons [3]. In paddy soils, moisture contents and fertilizers can change microbial physiology and activities, directly and indirectly, respectively, by changing soil properties [4]. For example, an increase in moisture content may lead to a shift in the community structure of microorganisms [5].

Soil microbial communities influence the biogeochemical cycling and structure of the soil, and thus play a vital role in the sustainability of the agroecosystem [6–8]. Until now, a plethora of studies have revealed that microbial composition and diversity in different agroecosystems are significantly influenced by manure application. A former study on dry land with a 33-year history of long-term fertilization confirmed that pig manure (PM) significantly promoted alpha diversity and microbial biomass [9]. Additionally, Zhang et al. [10] found that microbial diversity in paddy fields significantly enhanced after PM application. Alternatively, a significant decline in microbial diversity with excessive manure has also been observed [11]. This divergence needs further study in terms of microbial responses to excessive PM application. Additionally, it is more important to investigate the ecology under the application of repeated long-term pig manure and chemical fertilization because repeated fertilization influences soil microbial community by changing the physicochemical and biological properties of the soil [12].

The functionality of a complex and dynamic soil ecosystem depends on the connection of its physical, chemical, biological parameters, and harboring microbes [13]. The balance between maximum microbial activity and diversity explains soil quality [14]. Environment protection can be achieved in a better way by managing soil quality by preserving biodiversity and good agricultural practices [15]. Both crop growth and quality directly or indirectly depend on soil microbial activities, influenced by organic matter (OM) decomposition, mineralization, and nutrient cycling. However, soil quality is not only the subject of biological properties, i.e., the microbial composition of the soil, but physical, chemical, and biochemical properties of soil are also responsible for soil quality [16]. Water-management practices, pore-size distribution, pH, OM, total carbon, nitrogen, microbial enzymatic activity, microbial biomass carbon, and nitrogen also contribute to soil quality [17].

Alternating wetting and drying (AWD) to save water is common practice in many countries such as Japan [18], the Philippines [19], and China [20]. The AWD practice is commonly adopted because of no sacrifice of yield. Zhang et al. [21] revealed that there is no loss in the rice yield compared to continuous flooding (conventional practice) but found this practice a great source of N_2O production [22,23]. Although the effect of AWD on soil microbial community was studied previously, its effect under long-term inorganic and organic fertilization is largely unknown. In addition, no study is available related to the response of microbial communities under different water management and long-term manure and chemical application, especially in eastern China.

The linkage of the effect of manure and AWD on the shift of bacterial and fungal communities is expected to provide a better understating of microbial-mediated processes in paddy soils. Additionally, the pooled outcome of enduring fertilization and AWD on bacterial and fungal microbial structure and diversity is still inconclusive. Moreover, the focus of former long-term studies was on long-term mineral fertilizer rates. Still, the effect of fertilizer types on the soil microbial community structures is largely unknown. Hence, the objectives of the present study were: (1) to compare the effects of long-term organic (PMCF, SRCF) and inorganic (CF) fertilizers on bacterial and fungal microbial community structure and diversity under dry–wet conditions, and (2) to evaluate the most dominant factor influencing bacterial and fungal microbial structure, abundance, and diversity. We hypothesized that "bacterial and fungal soil microbial communities could be changed under long-term fertilization" under an AWD scheme.

2. Materials and Methods

2.1. Soil Sampling Site

The soil samples were collected from a long-term fertilized experiment that was in Jintan county, Jiangsu province of China (120°0′41″ E, 29°57′9″ N) (Figure 1). The study area's annual mean temperature and precipitation are 16.27 °C and 1452.5 mm, respectively. The experiment site had five years of canola-rice rotation history. The four treatments of the soil samples were grouped, with no fertilization (CK/Control), 100% chemical fertilization (CF:N 314 kg ha^{-1}, P 13.77 kg ha^{-1}, K 127 kg ha^{-1}), pig manure compost

plus 50% chemical fertilization (PMCF: Pig manure 6000 kg ha^{-1} + N 157 kg hm^{-2}, P 13.77 kg ha^{-1}, K 127 kg ha^{-1}), and rice straw plus 50% chemical fertilization (SRCF: rice straw 6000 kg ha^{-1} + N 157 kg ha^{-1}, P 13.77 kg ha^{-1}, K 127 kg ha^{-1}). After harvesting rice in 2014, five soil cores from each treatment were collected after the (three replicates). The soil cores were transported to the laboratory after packing in sterile zipped plastic bags and stored at 4 °C. All samples were air-dried after sieving through a 2.0 mm mesh and divided into sub-samples before incubation experiment. Sub-samples were used for soil chemical analysis.

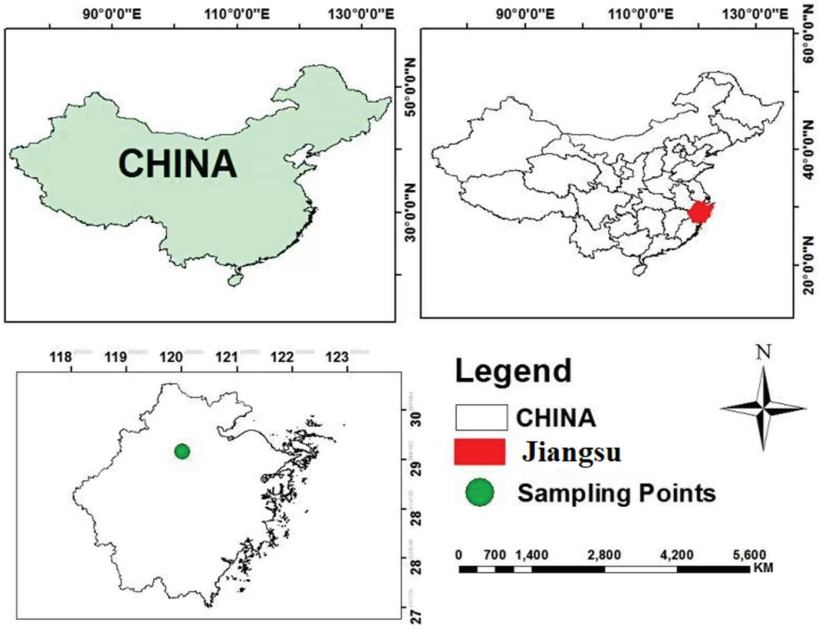

Figure 1. Sample collection point at Jiangsu Province, China.

2.2. Incubation Experimental Design

An incubation experiment was set up for two water regimes: (a) alternate wetting and drying (AWD), consisting of alternating seven days of continuous flooding followed by seven days of air-drying (AWD); (b) permanent flooding for 14 days (PF) at 25 °C. The incubation experiment complete method was described as the 200 g of soil collected from CK, CF, PMCF, and SRCF treatments (with three replicates each) were weighed in 1000 mL glass pots, and flooding conditions were created by adding distilled water up to 3 cm [4,5]. For AWD, flooded incubation was continued for seven days, and gas and soil samples were collected after 1 and 7 days of flooding incubation (100% FC, 1 d; 100% FC, 7 days). Then, the water was removed from pots to reach field capacity of 80% after 10 days (80% FC, 10 d) and 60% field capacity after 14 days (60% FC, 14 days); samples were also collected at 80% FC, 10d, and 60% FC, 14 d. For PF, incubated the soil under flooded conditions by keeping water level 3 cm for 14 d under same fertilizer treatment and soil samples were collected after 1, 7, 10, and 14 d.

2.3. 16S rRNA Gene Sequencing (Illumina-Based)

The DNA of the soil samples was extracted from 0.5 g sampled soil according to the manufacturer's instructions (TAKARA DNA Extraction Kit). The DNA was quantified by Nanodrop technology (NanoDrop Technologies, Wilmington, DE, USA). For bacterial community, V3–V4 region of 16S rRNA gene was amplified using the primers set provided. The bacterial 16S rRNA genes were amplified with the primer 319F (5′-ACTCCTACGGGAGGCAGCAG-

3′) and primer 806R (5′-GGACTACHVGGGTWTCTAAT-3′). The ITS region was targeted with the ITS1F primer (5′-CTTGGTCATTTAGAGGAAGTAA-3′) and ITS2R primer (5′-GCTGCGTTCTTCATCGATGC-3′) [5].

The PCR reaction was performed with an initial melting step for the 30 s at 98 °C, followed by 30 cycles of denaturation at 98 °C for 15 s, annealing at 58 °C for 15 s and elongation at 72 °C for 1 min. After purification, the PCR products were sent to the Illumina Mi-Seq platform for sequencing (www.majorbio.com, accessed on 5 December 2021). Bacterial 16S rRNA gene average length of 435 bp was used for sequencing analysis. The raw data were processed with QIIME 1.8.0 [24]. Sequences were analyzed according to the method described by Edgar [25]. Mi-Seq sequencing analysis was performed using R-Studio 3.5.3, phyloseq 1.26.1 version. High-quality putative bacterial 16S rRNA and fungal gene sequences were confirmed by the BLAST search engine and GenBank database (https://blast.ncbi.nlm.nih.gov/Blast.cgi, accessed on 5 December 2021). The operational taxonomic unit (OTU) was approved with a 97% 16S rRNA gene sequence.

2.4. Statistical Analysis

To examine the significance of treatments, we performed one-way analysis of variance (ANOVA) and Tukey's HSD tests to identify significant differences among the treatments, followed by Duncan's Multiple Range Test (DMRT) to separate treatment means. The vegan package of R studio was used to perform the Mantel test, redundancy analysis (RDA), and variation portioning analysis (VPA). QIIME was used to calculate alpha and beta diversity. Linear discriminant effect size analysis (LEfSe) was performed to recognize the specific bacterial taxa from the phylum to the genus level separately. Bacterial taxa with linear discriminant analysis (LDA) scores of 2.5 or more were considered significant with AWD and PF. All statistical analyses were performed by SPSS 16.0 package (SPSS, Chicago, IL, USA). The results were accepted as significant at 0.05 probability.

3. Results and Discussions

3.1. Soil Chemical Properties

The additions of chemical fertilizer alone and combined with organic amendments significantly decreased soil pH ($p = 0.001$), while this decrease was observed as higher in SRCF treatment (Table 1). Fertilized treatments significantly increased the concentrations of soil organic C ($p < 0.05$), NO_3^--N ($p < 0.01$), and available P ($p < 0.01$), and relatively higher values were observed in the PMCF treatment.

Table 1. Chemical properties of soils collected from long-term experiment plots of the unamended control (Control), chemical fertilizers (CF), pig manure plus chemical fertilizer (PMCF), and rice straw plus chemical fertilizer (SRCF). Values are mean + standard error of three replicates.

	Treatment	pH	SOC (g kg^{-1})	Total N (g kg^{-1})	NO3$^-$-N (mg kg^{-1})	NH4$^+$-N (mg kg^{-1})	Available K (mg kg^{-1})	Available P (mg kg^{-1})
	Control	6.76 ± 0.08 a	14.02 ± 1.03 a	2.37 ± 0.16 a	11.17 ± 0.65 b	16.94 ± 1.80 b	80.50 ± 12.15 a	9.61 ± 1.47 c
	CF	6.25 ± 0.07 b	18.38 ± 2.17 ab	2.64 ± 0.09 a	20.31 ± 1.73 a	20.27 ± 2.49 ab	69.20 ± 6.69 a	16.98 ± 3.09 ab
	PMCF	6.22 ± 0.04 b	24.63 ± 2.08 a	2.78 ± 0.26 a	19.91 ± 0.29 a	21.08 ± 1.42 a	74.85 ± 8.14 a	22.59 ± 1.31 a
	SRCF	5.54 ± 0.29 c	21.93 ± 2.31 a	2.90 ± 0.29 a	19.80 ± 4.00 a	21.48 ± 2.64 a	86.75 ± 8.94 a	13.04 ± 1.73 bc
		**	*	ns	**	ns	ns	**
F-value		17.76	5.51	1.57	8.13	3.04	0.69	8.44
p-value		0.0007	0.024	0.27	0.008	0.09	0.58	0.007

SOC; soil organic carbon. Values are mean + standard error of the replicates ($n = 3$). The identical letters inside a column show that there is no significant difference 95% probability. Ns—the relationship between treatment and water condition is insignificant. * Significant interaction between treatment and water condition at $p \leq 0.05$ level. ** Highly significant interaction between treatment and water condition at $p \leq 0.01$ level.

3.2. Microbial Biodiversity

The current results showed that fertilizer treatments changed the microbial diversity. Generally, the Shannon and Simpson indices of bacterial community declined with fertilizer addition (Table 2). However, the Shannon indices of the fungal community were promoted

by fertilizer addition, while Simpson indices declined (Table 2). While comparing fertilizer treatments, SRCF promoted Shannon and Simpson indices in the bacterial community. In addition, the Chao 1 index declined in fertilizer treatments. PMCF promoted the Shannon index more during PF than AWD, but not in other treatments. The highest Shannon index was found in PMCF during AWD for the fungal community. For a certain period, the Shannon and Simpson indices of the bacterial community increased and then started to decrease. The goods coverage for the samples was observed as higher than 0.99, which showed that the obtained sequence libraries covered almost all microbial diversity.

Table 2. Changes over time in α-biodiversity indices of nitrifying and denitrifying bacteria and fungi based on 16S rRNA gene in soils collected from long-term experiment plots of the unamended control (Control), chemical fertilizers (CF), pig manure plus chemical fertilizer (PMCF), and rice straw plus chemical fertilizer (SRCF) under alternate wet–dry conditions (AWD) or permanent flooding (PF).

			AWD				PF			
	Treatment	**Time (d)**	**Shannon Index**	**Simpson Index**	**Chao Index**	**Coverage**	**Shannon Index**	**Simpson Index**	**Chao Index**	**Coverage**
Bacterial	CK	1	6.55	0.004	2824	0.98	6.54	0.004	2824	0.98
		7	6.92	0.003	3175	0.97	6.92	0.002	3175	0.97
		10	6.9	0.002	2949	0.97	6.77	0.002	2979	0.97
		14	6.75	0.004	3080	0.97	6.75	0.003	3041	0.96
	CF	1	5.77	0.023	2613	0.98	5.77	0.022	2613	0.98
		7	6.54	0.005	2704	0.97	6.54	0.004	2704	0.97
		10	6.42	0.005	2696	0.97	6.35	0.004	2536	0.97
		14	6.39	0.008	2645	0.97	6.62	0.002	2671	0.96
	PMCF	1	6.23	0.006	2433	0.98	6.22	0.006	2433	0.98
		7	6.61	0.003	2439	0.97	6.6	0.002	2439	0.97
		10	6.53	0.004	2489	0.97	6.69	0.003	2669	0.96
		14	6.12	0.014	2397	0.97	6.35	0.005	2467	0.96
	SRCF	1	6.45	0.007	2807	0.98	6.44	0.007	2807	0.98
		7	6.38	0.012	2995	0.97	6.37	0.012	2995	0.97
		10	6.87	0.002	3002	0.98	6.72	0.003	2923	0.96
		14	6.67	0.004	2928	0.97	6.68	0.003	2716	0.96
			ns	ns	**	ns	ns	ns	*	ns
Fungal	CK	1	2.99	0.15	450	0.99	2.99	0.15	450	0.99
		7	2.63	0.27	431	0.99	2.63	0.27	431	0.99
		10	2.54	0.23	418	0.99	2.11	0.24	275	0.99
		14	2.21	0.27	359	0.99	1.97	0.35	427	0.99
	CF	1	3.3	0.07	443	0.99	3.31	0.07	443	0.99
		7	3.12	0.09	505	0.99	3.12	0.09	505	0.99
		10	3.22	0.09	441	0.99	2.38	0.17	352	0.99
		14	2.4	0.15	383	0.99	2.62	0.13	321	0.99
	PMCF	1	3.75	0.05	476	0.99	3.75	0.05	476	0.99
		7	3.5	0.06	497	0.99	3.51	0.06	497	0.99
		10	3.89	0.05	512	0.99	2.38	0.21	348	0.99
		14	2.83	0.14	396	0.99	3.28	0.07	505	0.99
	SRCF	1	3.75	0.05	508	0.99	3.75	0.05	508	0.99
		7	3.21	0.04	421	0.99	0.05	0.98	94.6	0.99
		10	1.74	0.42	351	0.99	2.37	0.2	388	0.99
		14	2.42	0.16	284	0.99	2.81	0.14	383	0.99
			ns	ns	ns	ns	ns	ns	ns	ns

Ns—the relationship between treatment and water condition is insignificant. * Significant interaction between treatment and water condition at $p \leq 0.05$ level. ** Highly significant interaction between treatment and water condition at $p \leq 0.01$ level.

3.3. Community Structure and Potential Influencing Factors

The bacterial community structure in fertilized treatments was different with respect to time and different water events. The PCoA results showed the bacterial community

structure of PMCF and SRCF was different from CK and CF (Figure 2), which explained 34.22% of the variation during AWD (Figure 2A) and 32.6% during PF (Figure 2B). Additionally, CF was separated from all treatments during AWD, along with the first component (PC1), which explained 18.29% of the variation. These results suggested that the fertilizer treatments and different water conditions significantly affected microbial community structure, especially bacterial community.

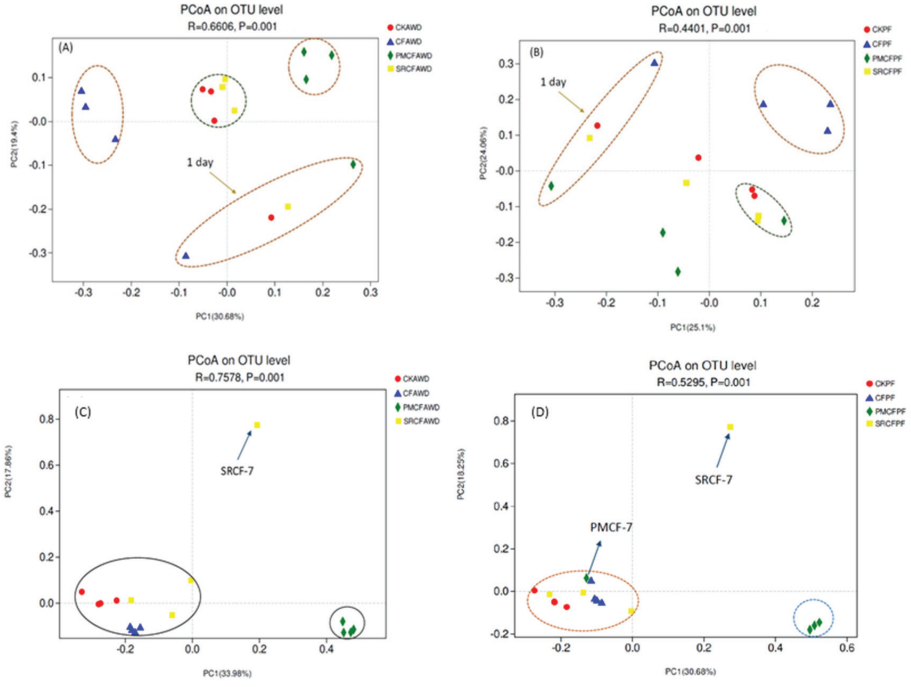

Figure 2. Principal component analysis (PCoA) of bacterial community compositions based on the Bray–Curtis distance for soils collected from long-term experiment plots of the unamended control (CK), chemical fertilizers (CF), pig manure plus chemical fertilizer (PMCF), and rice straw plus chemical fertilizer (SRCF) under alternate wet–dry (AWD) or permanent flooding (PF) conditions at 1, 7, 10, and 14 days after incubation. The PCoA of bacterial community compositions based on the Bray–Curtis distance under AWD and PF is represented by (**A**,**B**), while for fungal community compositions by (**C**,**D**) under AWD and PF, respectively.

The fungal community structure was found to be different from the bacterial community. The PMCF was separated from all treatments along with the first component (PC1), which explained 17.59% variations during AWD (Figure 2C). Meanwhile, SRCF was separated from other fertilizer treatments along with the second component (PC2), which explained the 13.62% variations. The same trends were observed during PF, which showed that moisture contents have no significant effect on fungal community structure (Figure 2D).

The bacterial community was highly diverse compared to the fungal community. For further study of the bacterial community, redundancy analysis (RDA) was conducted to examine the associations between environmental properties (Figure 3). The soil physicochemical properties, including pH, TN, NH_4^+, NO_3^-, SOC, P, and K, explained 57.11% variations during AWD and 55.70% variations during PF. Axis 1 explained 38.79% of the total variability separating CF from PMCF and CK from SRCF-1 (after one-day addition of SRCF) and SRCF-10 (after 10 days of SRCF addition) during AWD. In comparison, Axis 2 explained 17.32% of the total variability, and CK and SRCF were separated from CF and PMCF (Figure 4A). Additionally, during PF, axis 1 explained 44.43% variations and

separated the first day of all treatment applications from later days of all treatment applications, and axis 2 explained 11.27% variations, separating SRCF from all other treatments (Figure 3B). During PF, RDA1 represents TN, NH_4^+, NO_3^-, and SOC of the soils, which were positively related to the bacterial community. At the same time, pH had a negative effect, showing that bacterial community activity is favored by high TN, NH_4^+, NO_3^-, and SOC, and low pH.

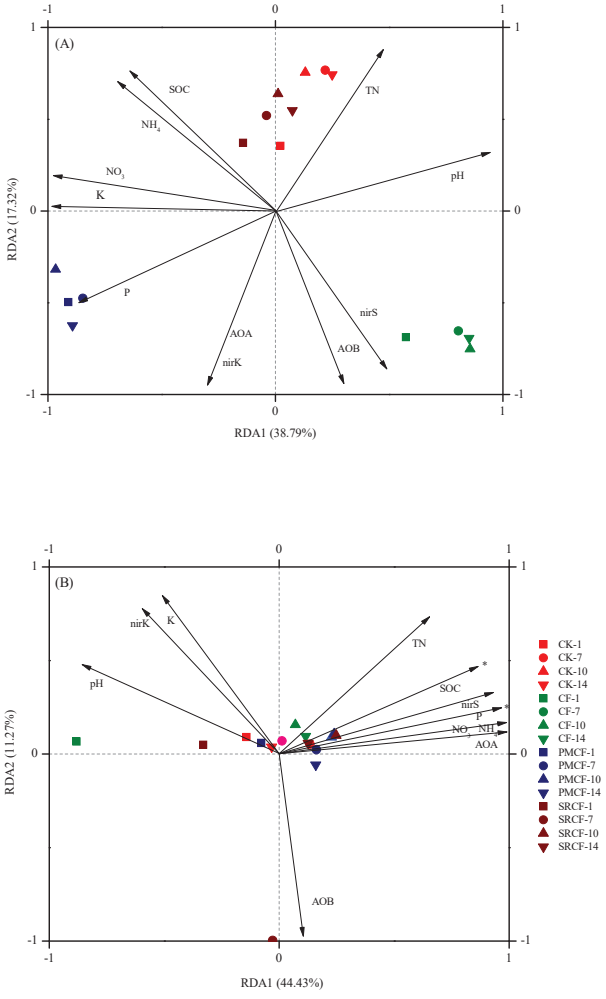

Figure 3. Redundancy analysis (RDA) performed between soil physicochemical characteristics and relative abundance of bacterial communities based on the Bray–Curtis distance at 1, 7, 10, and 14 days after incubation in soils collected from long-term experiment plots of the unamended control (CK), chemical fertilizers (CF), pig manure plus chemical fertilizer (PMCF), and rice straw plus chemical fertilizer (SRCF) under alternate wet–dry (**A**) or permanent flooding (**B**) conditions.

3.4. Species Composition

The overall abundance of the *Actinobacteria* was found to be higher after PMCF addition, while *Proteobacteria* were higher after CF and SRCF additions than those in the CK during AWD and PF (Figure 4A,B). Additionally, *Firmicutes* were higher with CF addition during AWD (Figure 4A). During the early days of the experiment, the *Nitrospira* was

found to be higher in CK treatment but started to increase in fertilized treatments with time. Among all genera, *Proteobacteria* were found to be the most abundant bacterial phylum.

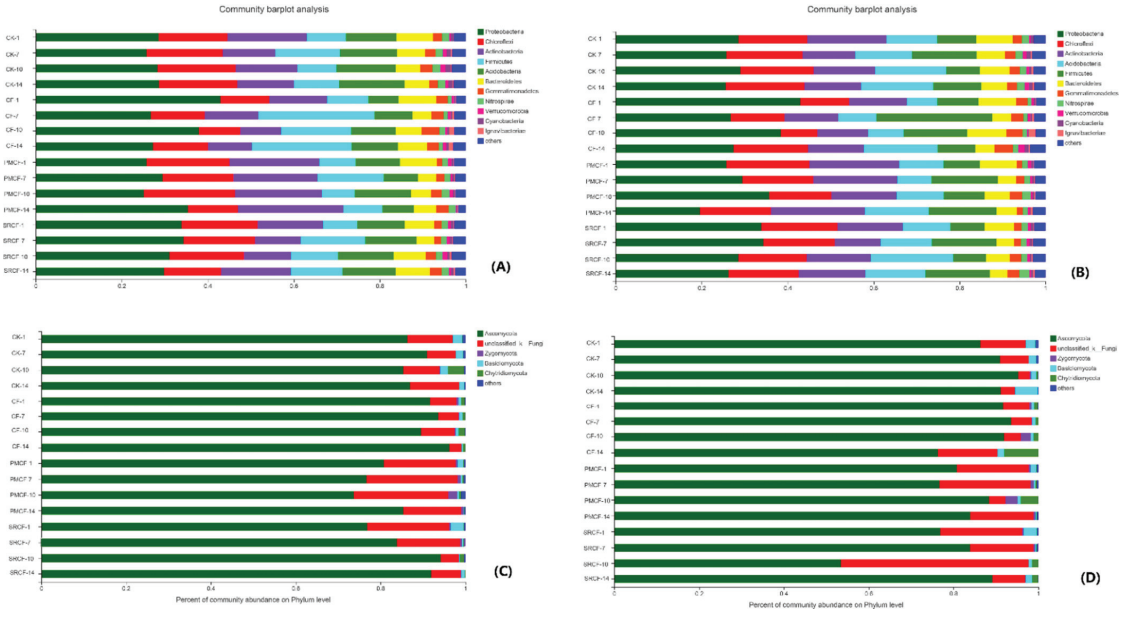

Figure 4. Relative abundance (%) of bacterial community at 1, 7, 10, and 14 days after incubation in soils collected from long-term experiment plots of the unamended control (CK), chemical fertilizers (CF), pig manure plus chemical fertilizer (PMCF), and rice straw plus chemical fertilizer (SRCF) under alternate wet–dry conditions (**A**) or permanent flooding (**B**). Relative abundance of bacterial community under AWD and PF is represented by (**A**,**B**), while for fungal community relative abundance by (**C**,**D**) under AWD and PF, respectively.

The *Ascomycota* was the dominant fungal community in all treatments during both water events (Figure 4C,D). CK promoted *Ascomycota* and *Basidiomycota* compared to the other fertilizer treatments, and *Basidiomycota* increment was five times higher after 14 days of PF compared to AWD. Among fertilizer treatments, CF promoted *Ascomycota* during AWD than PF (20.64% after 14 days), while PMCF inhibited *Ascomycota* abundance until 10 days and then started to improve. CF treatment promoted *Chytridiomycota* during both water events but was four times higher after 14 days of PF (Figure 4D). At the same time, PMCF promoted *Zygomycota* until ten days of fertilizer addition and then started to reduce during AWD. Additionally, SRCF promoted *Ascomycota* by 18.38% and 16.37% after 10 and 14 days of AWD compared to the first day of AWD (Figure 4C).

To explore the effects of WC (AWD and PF), soil physicochemical properties (including pH, available P, available K, TN, SOC, NH_4^+, and NO_3^-), and fertilizers (including CK, CF, PMCF, and SRCF) on bacterial community abundance, a variation partitioning analysis (VPA) was constructed (Figure 5). A Mantel test was conducted to observe the effects of different organic and inorganic sources. The main soil physiochemical properties which markedly affected the communities were SOC ($R^2 = 0.4037$, $p < 0.02$), available p ($R^2 = 0.3273$, $p < 0.05$), and NO_3^- ($R^2 = 0.3096$, $p < 0.08$). A total of 64.46% of the variance could be explained by WC, physicochemical properties, and fertilizer, explaining 3.96%, 29.59%, and 15.52%, respectively (Figure 5). It has also been analyzed that the dominant combined factors which affected the bacterial communities were the interactions between physicochemical properties and fertilizer, explaining 11.84% of the total variance in all the

soils. The physicochemical properties were found to be the dominant factor and affected bacterial community more than water conditions and fertilizers.

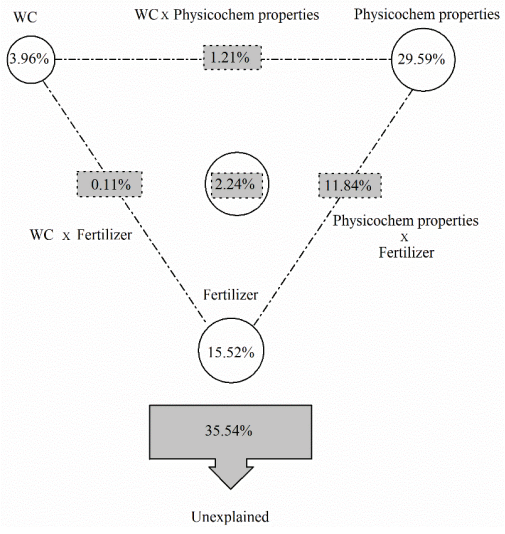

Figure 5. Mantel test and variation partitioning (VPA) analysis of soil physicochemical factors and biogenic factors and the interaction between them and soil water regimes, physicochemical properties, and fertilizer treatments and their interactions. WC—water contents; physicochem properties—physicochemical properties.

3.5. Specific Bacterial Taxa

The LEfSe was constructed to determine the specific bacterial taxa from phylum to genus level separately, affected by the different fertilizer treatments, under AWD and PF (Figures 6 and 7). AWD and PF were separated into two LEfSe figures: microbial populations were grouped as fertilizer treatments and control (Figures 6 and 7). During AWD, we detected 170 clades up to family level from phylum and 28 enriched clades in CF, 83 in the PMCF group, 17 in SRCF, and 42 clades in CK with LDA scores more than 2.5 (Figure 6). The abundance of *Actinobacteria* was found to be higher in PMCF and *Flavobacteria* in CF treatment compared to control, whereas *Acidobacteria* and *Cyanobacteria* remained abundant in CK. Fascinatingly, no significant change was observed at the phylum level in the CK. During PF, only 61 bacterial taxa were identified to have a LDA score higher than 2.5, from phylum up to family level (Figure 7). Only *Actinobacteria* were enriched in PMCF, while *Deltaproteobacteria* were found to be more abundant in CF treatment than in control.

3.6. Long-Term Fertilization and Responses of the Soil Microbiome

The present study showed that long-term fertilization (chemical and organic) application significantly influenced the bacterial and fungal community structures. Bacterial diversity and richness were not significantly changed; however, a decrease in Simpson and Shannon indices of the bacterial community in fertilization treatments was observed. A decrease in fungal diversity was observed with organic fertilizer application, which is highly sensitive to fertilization (Table 2). Previous studies [26–28] of long-term fertilizer application, even for 113 years [29], reported different responses of bacterial and fungal communities, which might be due to the different soil properties and condition. Opposite to our assumption, organic fertilizer applied long term did not change the diversity of the fungal community.

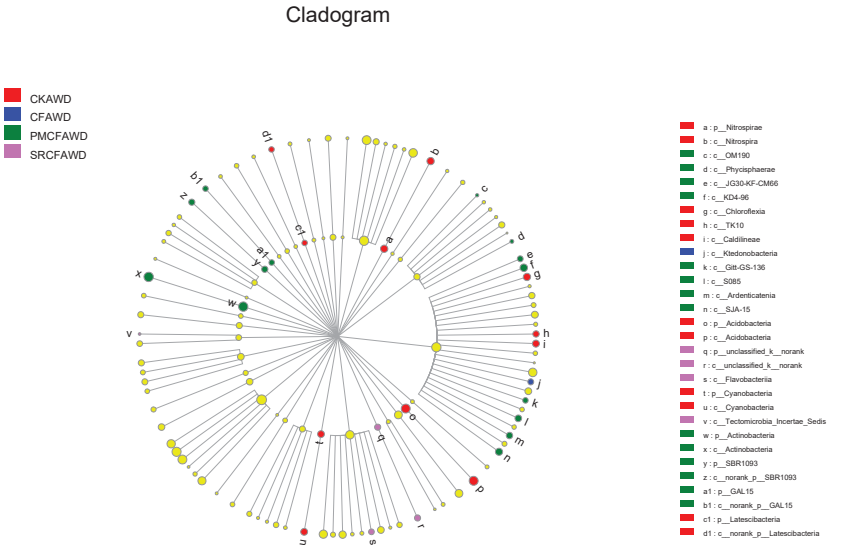

Figure 6. Linear discriminant effect size analysis cladogram of comparison between the unamended control (CK), chemical fertilizers (CF), pig manure plus chemical fertilizer (PMCF), and rice straw plus chemical fertilizer (SRCF) under alternate wet–dry (AWD) conditions. The subsequent colors stand for the abundance of individual taxa. Only taxa meeting a linear discriminant analysis significance threshold of 2.5 were shown. The domain of the cladogram is phylum and class. CKAWD showed CK treatment under AWD condition and so on.

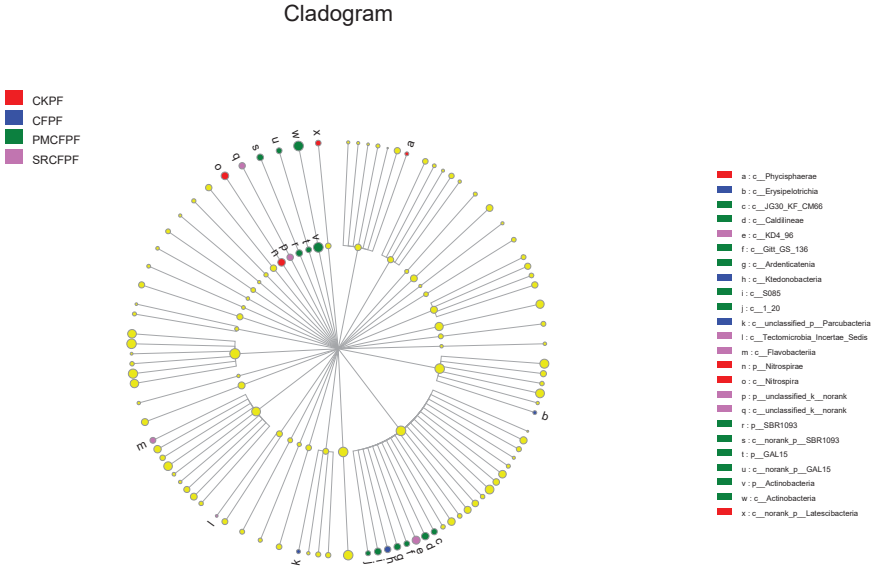

Figure 7. Linear discriminant effect size analysis cladogram of comparison between the unamended control (CK), chemical fertilizers (CF), pig manure plus chemical fertilizer (PMCF), and rice straw plus chemical fertilizer (SRCF) under permanent flooding (PF) conditions. The subsequent colors stand for the abundance of individual taxa. Only taxa meeting a linear discriminant analysis significance threshold of 2.5 were shown. The domain of the cladogram is phylum and class. CKPF showed CK treatment under PF condition and so on.

3.7. Microbial Community Structure under Different Fertilizer Applications and Water Regimes

The current results confirmed that water events and fertilizer treatments changed the relative abundance of the bacterial community, which could further affect the bacterial activities and structure. Some bacterial genera displayed a decrease in relative abundance with different water events and fertilizer treatments [30], which could pertain to this reduction in waterlogging/drought stresses. *Proteobacteria, Bacteroidetes, Chloroflexi, Firmicutes, Actinobacteria,* and *Verrucomicrobia* were abundantly represented phyla during both water events (Figure 4A,B). Of those, *Proteobacteria* and *Firmicutes* were the most abundant Gram-negative bacteria in all fertilizer treatments, consistent with Zhang et al. [30]. Generally, both these phyla members are fast-growing bacteria that prefer a C-rich environment, called copiotrophic bacteria [31,32]. In addition, soil microbial composition might change due to the application of pig manure, which adds external community to the soil, such as *Proteobacteria* and *Firmicutes,* which are common in fecal matter [33]. *Actinobacteria*, an organic matter decomposer, was the dominant phylum in all treatments, especially in NPK treatment, significantly promoting soil quality [34]. The higher level of Gram-negative bacteria was due to the presence of available C. In contrast, Gram-positive bacteria utilize organic C, which needs a more complex set of processes to obtain energy due to its more complex nature [35]. Furthermore, *Nitrospira* was reduced with fertilizer addition because *Nitrospira* is classified as K-strategist that is slow-growing and oligotrophic with a low affinity for N substrates. This result was supported by previous studies of long-term fertilization of 27 years in grasses and eight years in agricultural soils [36].

No significant changes in the fungal community were observed with different water events. *Ascomycota* and *Basidiomycota* were dominant during both water events (Figure 4C,D), consistent with Afzal et al. [5]. These results might be because *Ascomycota* and *Basidiomycota* are the main degraders of the rice straws [6,7]. These results may assume that high and low moisture contents may reduce the fungal community but only favor *Ascomycota* and *Basidiomycota* growth.

RDA results of the bacterial community representing TN, NH_4^+, NO_3^-, and SOC of the soils was positively correlated to the bacterial community (Figure 3). Furthermore, we observed the negative impact of high pH on bacterial growth. However, low pH, an environment rich in SOC, NO_3^-, NH_4^+, and TN, is responsible for promoting bacterial activities. Pig manure and rice straw addition promoted inorganic N and SOC contents; that is why their influence on the bacterial community was high. The input of N either directly influences soil microbiota by altering the inorganic N content of the soil, or indirectly by changing pH, C:N ratio, and SOC availability [37,38]. In addition, soil microbial growth can be enhanced by N fertilizer, which can promote the microbial ability to utilize C sources, and thereby an increase in microbial biomass [39]. A positive correlation between TN and bacteria biomass was found (Figure 3), showing N fertilizer promoted bacterial growth.

In total, 64.46% explained variance, WC, physicochemical properties, and fertilizer explained 3.96%, 29.59%, and 15.52%, variation, respectively (Figure 5). It has also been analyzed that the dominant combined factors affecting the bacterial communities were the interactions between physicochemical properties and fertilizer, explaining 11.84% of the total variance in all the soils. The fertilizer treatments improved the soil's chemical properties and N contents and affected the activities of bacterial communities. Interestingly, physicochemical properties influence the N cycle more than water contents.

4. Conclusions

Verrucomicrobia, Actinobacteria, Firmicutes, Chloroflexi, Bacteroidete, and Proteobacteria were abundantly represented phyla during both water events. No significant changes in the fungal community were observed with different water events. *Ascomycota* and *Basidiomycota* were found dominant during both water events. TN, NH_4^+, NO_3^-, and SOC of the soils were positively correlated to the bacterial community, while pH had a negative effect on the bacterial community. The fertilizer treatments and chemical properties had a more significant impact on the activities of bacteria than moisture conditions. Moreover, in

future studies, underlying mechanisms should be evaluated. Additionally, it is necessary to take more soil biogeochemical processes into consideration in order to better understand the effects of long-term fertilization on the soil.

Author Contributions: Conceptualization, A.A.A. and Q.Z.; methodology, A.A.A. and Q.Z.; software, A.A.A., A.C.-H. and L.G.; validation, A.A.A., M.A. and X.Z.; formal analysis, A.A.A., M.A., L.G. and X.Z.; investigation, A.A.A.; resources, Q.Z.; data curation, A.A.A.; writing—original draft preparation, A.A.A.; writing—review and editing, Q.Z., H.D. and A.C.-H.; visualization, Q.Z.; supervision, Q.Z.; project administration, Q.Z.; funding acquisition, Q.Z. All authors have read and agreed to the published version of the manuscript.

Funding: The funding is supported by the Natural Science Foundation of Zhejiang Province (LZ21C030002, LGN21C200017), the National Natural Science Foundation of China (41877044), and the Development Program of China (2016YFD0801103, 2021YFD1700803).

Informed Consent Statement: Not applicable.

Data Availability Statement: Not applicable.

Acknowledgments: The authors gratefully acknowledge the financial support of the Natural Science Foundation of Zhejiang Province (LZ21C030002, LGN21C200017), the National Natural Science Foundation of China (41877044), and the Development Program of China (2016YFD0801103, 2021YFD1700803).

Conflicts of Interest: The authors declare no conflict of interest.

References

1. Antonio, C.H.; Jesús, G.L.; Eulogio, J.B. Effect of nitrogen fertilization on nitrous oxide emission and the abundance of microbial nitrifiers and denitrifiers in the bulk and rhizosphere soil of Solanum lycopersicum and Phaseolus vulgaris. *Plant Soil* **2020**, *451*, 107–120.
2. IPCC. *Climate Change 2007: The Physical Science Basis. Contribution of Working Group I to the Fourth Assessment Report of the Intergovernmental Panel on Climate Change*; Cambridge University Press: Cambridge, UK, 2007.
3. Muthayya, S.; Sugimoto, J.D.; Montgomery, S.; Maberly, G.F. An overview of global rice production, supply, trade, and consumption. *Ann. N. Y. Acad. Sci.* **2014**, *1324*, 7–14. [CrossRef] [PubMed]
4. Abid, A.A.; Zhang, Q.C.; Wang, J.W.; Di, H.J. Nitrous Oxide fluxes and nitrifier and denitrifier communities as affected by dry-wet cycles in long term fertilized paddy soils. *Appl. Soil. Ecol.* **2018**, *125*, 81–87. [CrossRef]
5. Afzal, M.; Yu, M.; Tang, C.; Zhang, L.; Muhammad, N.; Zhao, H.; Feng, J.; Yu, L.; Xu, J. The negative impact of cadmium on nitrogen transformation processes in a paddy soil is greater under non-flooding than flooding conditions. *Environ. Int.* **2019**, *129*, 451–460. [CrossRef]
6. Chen, D.; Xing, W.; Lan, Z.C.; Saleem, M.; Wu, Y.; Hu, S.J.; Bai, Y.F. Direct and indirect effects of nitrogen enrichment on soil organisms and carbon and nitrogen mineralization in a semi-arid grassland. *Funct. Ecol.* **2019**, *33*, 175–187. [CrossRef]
7. Chen, Q.L.; Ding, J.; Zhu, D.; Hu, H.W.; Delgado-Baquerizo, M.; Ma, Y.B.; He, J.Z.; Zhu, Y.G. Rare microbial taxa as the major drivers of ecosystem multifunctionality in long-term fertilized soils. *Soil. Biol. Biochem.* **2019**, *141*, 107686. [CrossRef]
8. Saleem, M.; Hu, J.; Jousset, A. More than the sum of its parts: Microbiome biodiversity as a driver of plant growth and soil health. *Annu. Rev. Ecol. Evol.* **2019**, *50*, 61–62. [CrossRef]
9. Luo, P.; Han, X.; Wang, Y.; Han, M.; Shi, H.; Liu, N.; Bai, H. Influence of long-term fertilization on soil microbial biomass, dehydrogenase activity, and bacterial and fungal community structure in a brown soil of northeast China. *Ann. Microbial.* **2015**, *65*, 533–542. [CrossRef]
10. Zhang, Q.C.; Shamsi, I.H.; Xu, D.T.; Wang, G.H.; Lin, X.Y.; Jilani, G.; Hussain, N.; Chaudhry, A.N. Chemical fertilizer and organic manure inputs in soil exhibit a vice versa pattern of microbial community structure. *Appl. Soil. Ecol.* **2012**, *57*, 1–8. [CrossRef]
11. Sun, J.; Zhang, Q.; Zhou, J.; Wei, Q. Pyrosequencing technology reveals the impact of different manure doses on the bacterial community in apple rhizosphere soil. *Appl. Soil. Ecol.* **2014**, *78*, 28–36. [CrossRef]
12. Beauregard, M.; Hamel, C.; St-Arnaud, M. Long-term phosphorus fertilization impacts soil fungal and bacterial diversity but not AM fungal community in alfalfa. *Microb. Ecol.* **2010**, *59*, 379–389. [CrossRef] [PubMed]
13. Furtak, K.; Grzadziel, J.; Galazka, A.; Niedzwiecki, J. Analysis of Soil Properties, Bacterial Community Composition, and Metabolic Diversity in Fluvisols of a Floodplain Area. *Sustainability* **2019**, *11*, 3929. [CrossRef]
14. Li, P.; Zhang, T.; Wang, X.; Yu, D. Development of biological soil quality indicator system for subtropical China. *Soil Tillage Res.* **2013**, *126*, 112–118. [CrossRef]
15. Lemaire, G.; Franzluebbers, A.; Carvalho, P.C.; Dedieu, B. Integrated crop-livestock system: Strategies to achieve synergy between agricultural production and environmental quality. *Agric. Ecosyst. Environ.* **2014**, *190*, 4–8. [CrossRef]

16. Furtak, K.; Gajda, A.M. Biochemical methods for the evaluation of the functional and structural diversity of microorganisms in the soil environment. *Postępy Mikrobiol.-Adv. Microbiol.* **2018**, *57*, 194–202. [CrossRef]
17. Gajda, A.M.; Furtak, K. Measuring the Effects of Farming Systems on Physical, Chemical and Microbiological Parameters of Soil Quality. In *Novel Methods and Results of Landscape Research in Europe, Central Asia and Siberia Vol. 1, Landscapes in the 21th Century: Status Analyses. Basic Processes and Research Concepts*; Sychev, V.G., Mueller, L., Eds.; Publishing House FSBSI "Pryanishnikov Institute of Agrochemistry": Moscow, Russia, 2018; pp. 212–217.
18. Chapagain, T.; Yamaji, E. The effects of irrigation method, age of seedling and spacing on crop performance, productivity and water-wise rice production in Japan. *Paddy Water Environ.* **2010**, *8*, 81–90. [CrossRef]
19. Belder, P.; Bouman, B.A.M.; Cabangon, R.; Guoan, L.; Quilang, E.J.P.; Yuanhua, L.; Spiertz, J.H.J.; Tuong, T.P. Effect of water-saving irrigation on rice yield and water use in typical lowland conditions in Asia. *Agric. Water Manag.* **2004**, *65*, 193–210. [CrossRef]
20. Cabangon, R.J.; Tuong, T.P.; Castillo, E.G.; Bao, L.X.; Lu, G.; Wang, G.; Cui, Y.; Bouman, B.A.M.; Li, Y.; Chen, C.; et al. Effect of irrigation method and N-fertilizer management on rice yield, water productivity and nutrient-use efficiencies in typical lowland rice conditions in China. *Paddy Water Environ.* **2004**, *2*, 195–206. [CrossRef]
21. Zhang, X.; Wong, M.; Feng, X.; Wang, K. Identification of soil heavy metal sources from anthropogenic activities and pollution assessment off fuyang County, China. *Environ. Monit. Assess* **2009**, *154*, 439–449. [CrossRef]
22. Peng, S.Z.; Hou, H.J.; Xu, J.Z.; Mao, Z.; Abudu, S.; Luo, Y.F. Nitrous oxide emissions from paddy fields under different water managements in southeast China. *Paddy Water Environ.* **2011**, *9*, 403–411. [CrossRef]
23. Abid, A.A.; Zhang, Q.C.; Afzal, M.; Di, H.J. Nitrous oxide emission and production pathways under alternate wetting-drying conditions in rice paddy soils. *Appl. Ecol. Environ. Res.* **2019**, *17*, 13777–13792. [CrossRef]
24. Caporaso, J.G.; Kuczynski, J.; Stombaugh, J.; Bittinger, K.; Bushman, F.D.; Costello, E.K.; Fierer, N.; Peña, A.G.; Goodrich, J.K.; Gordon, J.I.; et al. QIIME allows analysis of highthroughput community sequencing data. *Nat. Methods* **2010**, *7*, 335–336. [CrossRef] [PubMed]
25. Edgar, R.C. UPARSE: Highly accurate OTU sequences from microbial amplicon reads. *Nat. Methods* **2013**, *10*, 996–998. [CrossRef] [PubMed]
26. Lentendu, G.; Wubet, T.; Chatzinotas, A.; Wilhelm, C.; Buscot, F.; Schlegel, M. Effects of long-term differential fertilization on eukaryotic microbial communities in an arable soil: A multiple barcoding approach. *Mol. Ecol.* **2014**, *23*, 3341–3355. [CrossRef]
27. Hartmann, M.; Frey, B.; Mayer, J.; Mader, P.; Widmer, F. Distinct soil microbial diversity under long-term organic and conventional farming. *ISME J.* **2015**, *9*, 1177–1194. [CrossRef]
28. Eo, J.; Park, K.C. Long-term effects of imbalanced fertilization on the composition and diversity of soil bacterial community. *Agric. Ecosyst. Environ.* **2016**, *231*, 176–182. [CrossRef]
29. Francioli, D.; Schulz, E.; Lentendu, G.; Wubet, T.; Buscot, F.; Reitz, T. Mineral vs. organic amendments: Microbial community structure, activity and abundance of agriculturally relevant microbes are driven by long-term fertilization strategies. *Front. Microbiol.* **2016**, *7*, 1446. [CrossRef]
30. Zhang, S.; Pang, S.; Wang, P.; Wang, C.; Guo, C.; Gyawu Addo, F.; Li, Y. Responses of bacterial community structure and denitrifying bacteria in biofilm to submerged macrophytes and nitrate. *Sci. Rep.* **2016**, *6*, 36178. [CrossRef]
31. Fierer, N.; Bradford, M.A.; Jackson, R.B. Toward an ecological classification of soil bacteria. *Ecology* **2007**, *88*, 1354–1364. [CrossRef]
32. Lienhard, P.; Terrat, S.; Prévost-Bouré, N.C.; Nowak, V.; Régnier, T.; Sayphoummie, S.; Panyasiri, K.; Tivet, F.; Mathieu, O.; Levêque, J.; et al. Pyrosequencing evidences the impact of cropping on soil bacterial and fungal diversity in Laos tropical grassland. *Agron. Sustain. Dev.* **2014**, *34*, 525–533. [CrossRef]
33. Shanks, O.C.; Kelty, C.A.; Archibeque, S.; Jenkins, M.; Newton, R.J.; Mclellan, S.L. Community structures of fecal bacteria in cattle from different animal feeding operations. *Appl. Environ. Microbiol.* **2011**, *77*, 2992–3001. [CrossRef] [PubMed]
34. Strap, J.L. Actinobacteria–plant interactions: A boon to agriculture. In *Bacteria in Agrobiology: Plant Growth Responses*; Springer: Berlin/Heidelberg, Germany, 2011; pp. 285–307.
35. Morugán-Coronado, A.; García-Orenes, F.; McMillan, M.; Pereg, L. The effect of moisture on soil microbial properties and nitrogen cyclers in Mediterranean sweet orange orchards under organic and inorganic fertilization. *Sci. Total. Environ.* **2019**, *655*, 158–167. [CrossRef] [PubMed]
36. Ramirez, K.S.; Lauber, C.L.; Knight, R.; Bradford, M.A.; Fierer, N. Consistent effects of N fertilization on soil bacterial communities in contrasting systems. *Ecology* **2010**, *91*, 3463–3470. [CrossRef] [PubMed]
37. Treseder, K.K. Nitrogen additions and microbial biomass: A meta-analysis of ecosystem studies. *Ecol. Lett.* **2008**, *11*, 1111–1120. [CrossRef]
38. Serna-Chavez, H.M.; Fierer, N.; van Bodegom, P.M. Global drivers and patterns of microbial abundance in soil. *Glob. Ecol. Biogeogr.* **2013**, *22*, 1162–1172. [CrossRef]
39. Demoling, F.; Ola Nilsson, L.; Bååth, E. Bacterial and fungal response to nitrogen fertilization in three coniferous forest soils. *Soil. Biol. Biochem.* **2008**, *40*, 370–379. [CrossRef]

MDPI
St. Alban-Anlage 66
4052 Basel
Switzerland
www.mdpi.com

Agriculture Editorial Office
E-mail: agriculture@mdpi.com
www.mdpi.com/journal/agriculture

Academic Open
Access Publishing

mdpi.com

ISBN 978-3-7258-1232-5